ROBUST OPTIMAL DESIGN OF DISTRICT COOLING SYSTEMS AND INDIVIDUAL COOLING SYSTEMS CONSIDERING UNCERTAINTY AND RELIABILITY

GANG WENJIE

Ph.D

The Hong Kong Polytechnic University

2016

The Hong Kong Polytechnic University

Department of Building Services Engineering

Robust Optimal Design of District Cooling Systems and Individual Cooling Systems Considering Uncertainty and Reliability

GANG WENJIE

A thesis submitted in partial fulfillment of the requirements

for the Degree of Doctor of Philosophy

September, 2015

CERTIFICATE OF ORIGINALITY

I hereby declare that this thesis is my own work and that, to the best of my knowledge and belief, it reproduces no materials previously published or written, nor material that has been accepted for the award of any other degree or diploma, except where due acknowledgement has been made in the text.

I also declare that the intellectual content of this thesis is the product of my own work, except to the extent that assistance from others in the project's design and conception or in style, presentation and linguistic expression is acknowledged.

_____(Signature)

GANG Wenjie (Name of student)

Department of Building Services Engineering

The Hong Kong Polytechnic University

Hong Kong, P.R. China

September, 2015

ABSTRACT

Abstract of thesis entitled: Robust optimal design of district cooling systems and individual cooling systems considering uncertainty and reliability

Submitted by: GANG Wenjie

For the degree of: Doctor of Philosophy

at The Hong Kong Polytechnic University in September, 2015

This thesis attempts to answer the following questions which are not well answered in existing studies:

- Are district cooling systems energy efficient when compared with conventional individual cooling systems and what is the performance of district cooling systems coupled with different technologies in subtropical areas?
- How to obtain a cooling system (either district cooling system or individual cooling system) that can offer the best performance under uncertainty?
- How to obtain a cooling system (either district cooling system or individual cooling system) that can offer the best performance when uncertainty or failures of equipment arise?

District cooling system is widely used but its performance is rarely reported. The system performance compared with the individual cooling system determines its future application. Performance assessment of district cooling systems is conducted by comparing with individual cooling systems in subtropical areas. Characteristics of district cooling systems are summarized after quantitative energy performance

analysis. Measures to handle the additional peak electricity load due to developing a new area and using district cooling systems are assessed. Application of ice storage systems in the district cooling system is evaluated under different tariffs and design strategies. The performance of the district cooling system integrated with PHES is analyzed. The operation costs of the district cooling system with and without combined cooling, heating and power system are compared. Comments and suggestions are summarized for the application of district cooling systems in the subtropical area.

Information or data used in the system design at planning and design stages are often very different from that when the system is in operation. Such difference is taken as uncertainty. Uncertainty exists widely in the design process of district cooling systems and individual cooling systems. It will affect the design options but is not sufficiently investigated yet. To ensure that the cooling systems perform well in operation eventually, uncertainty-based optimal design methods are proposed. The performance of the cooling systems using the proposed methods is compared with that using the conventional design method.

An optimal design method concerning uncertainty is developed based on mini-max regret theory. It achieves the optimal design considering uncertainty. Without the needs of probability distribution assumptions and introducing new models, this method can determine the uncertainty-based optimal cooling systems very effectively. By comparing the regrets of each design option, the uncertainty-based optimal cooling system can be identified, which is associated with the minimum maximum regret. The method is demonstrated in the design of the chiller plant and chilled water system of a building.

By quantifying the uncertainty at planning and design stages, an uncertainty-based optimal design method is proposed and its application steps are introduced. Uncertainties in the outdoor weather, building design/construction and indoor conditions are concerned. Strategies to deal with the variables containing uncertainties are introduced. Based on the peak cooling load distribution, the capacity of the cooling systems can be determined with quantified risks. Based on the distribution of the annual energy consumption or cost, the configuration of the cooling systems can be selected with quantified confidence. The uncertainty-based optimal method is implemented in a district cooling system and an individual cooling system in Hong Kong respectively. By using the uncertainty-based optimal design method, stake holders can make decisions with quantified confidence.

The components or sub-systems in a cooling system cannot be always available due to failures or maintenance. A robust optimal design method considering both uncertainty and reliability is proposed. The robust optimal design can maintain the good performance under uncertainty or failures of components in the cooling system. Steps to realize the robust optimal design method are presented. The availability risk cost is introduced to account for the losses caused by the unmet cooling load. By taking the total annual cost including the capital cost, operation cost and availability risk cost as the objective, the robust optimal cooling system can be achieved. The proposed method is demonstrated in both the district cooling system and individual cooling system. Performance of the cooling systems using the robust optimal design is compared with that using the conventional design method, uncertainty-based design method and reliability-based design method.

The impacts of uncertainty on the design of district cooling systems and individual cooling system are compared. The influential factors for cooling loads of the district cooling system and individual cooling system are identified. Similarities and differences are summarized. Then the impacts of both uncertainty and reliability on the design of the district cooling system and individual cooling system are also assessed and compared.

PUBLICATIONS ARISING FROM THIS THESIS

Journal papers published

[1] **Wenjie Gang**, Shengwei Wang, Dian-ce Gao, Fu Xiao. Performance assessment of district cooling systems for a new development district at planning stage. Applied Energy 2015; 140: 33-43.

[2] **Wenjie Gang**, Shengwei Wang, Kui Shan, Dian-ce Gao. Impacts of cooling load calculation uncertainties on the design optimization of building cooling systems. Energy and Buildings 2015; 94:1-9.

[3] **Wenjie Gang**, Shengwei Wang, Chengchu Yan, Fu Xiao. Robust optimal design of building cooling systems concerning uncertainties using mini-max regret theory. Science and Technology for the Built Environment 2015; 21(6): 789-799.

[4] **Wenjie Gang**, Shengwei Wang, Fu Xiao, Dian-ce Gao. Robust optimal design of building cooling systems considering cooling load uncertainty and equipment reliability. Applied Energy 2015; 159: 265-275.

[5] **Wenjie Gang**, Shengwei Wang, Fu Xiao, Dian-ce Gao. District cooling systems: technology integration, system optimization, challenges and opportunities for applications. Renewable & Sustainable Energy Reviews 2016; 53: 253-264.

[6] **Wenjie Gang**, Godfried Augenbroe, Shengwei Wang, Cheng Fan, Fu Xiao. An uncertainty-based design optimization method for district cooling systems. Energy. (Accepted).

[7] **Wenjie Gang**, Shengwei Wang, Godfried Augenbroe, Fu Xiao. Robust

optimal design of district cooling systems and the impacts of uncertainty and reliability. Energy and Buildings. (Under review).

[8] **Wenjie Gang**, Shengwei Wang, Dian-ce Gao, Fu Xiao. Energy and economic analysis of district cooling system with sustainable energy technologies in subtropical areas. Applied Energy. (Under review).

Journal papers in preparation

[1] Wenjie Gang, Shengwei Wang, Godfried Augenbroe, Fu Xiao. Robust optimal design of district cooling systems and the impacts of uncertainty and reliability in comparison with individual cooling systems. To be submitted to Energy and Buildings.

Conference papers

[1] **Wenjie Gang**, Shengwei Wang, Dian-ce Gao. Impact of Uncertainties on the Application of District Cooling Systems and Individual Cooling Systems. The 9th International Symposium on Heating Ventilation and Air Conditioning-the 3nd International Conference on Building Energy and Environment. July 12-15 2015, Tianjin, China.

[2] **Wenjie Gang**, Shengwei Wang, Fu Xiao, Dian-ce Gao. Performance Assessment of District Cooling System Coupled with Different Energy Technologies in Subtropical Area. The 7th International Conference on Applied Energy. March 28-31 2015, Abu Dhabi, United Arab Emirates.

[3] **Wenjie Gang**, Shengwei Wang, Fu Xiao, Dian-ce Gao, Chengchu Yan. Performance Assessment of District Cooling Systems Based on Uncertainty Analysis at Plan and Design Stage. The 2nd International Conference on

Sustainable Urbanization. January 7-9 2015, Hong Kong.

[4] Dian-ce Gao, Shengwei Wang, Kui Shan, **Wenjie Gang**. On-site evaluation of fault-tolerant control approaches for enhanced operation and energy performance of building HVAC systems. The 2nd International Conference on Sustainable Urbanization. January 7-9 2015, Hong Kong.

[5] **Wenjie Gang**, Shengwei Wang, Fu Xiao, Dian-ce Gao. Feasibility study of the application of district cooling system in subtropical area with various energy resources. The 13th International Conference on Sustainable Energy Technologies. August 25-28 2014, Geneva, Switzerland.

ACKNOWLEDGEMETNS

This thesis would have been not completed timely without help and support from many people.

First and foremost, I want to express my deepest thanks to my supervisor, Professor Shengwei Wang, for his patient guidance and continuous help during my PhD study. He sets a very good model for me in my future career by being earnest, foresighted and smart-working. I am very grateful to my co-supervisor, Dr. Fu Xiao. I learn a lot from her to own a successful career and a happy family simultaneously as a young female scholar.

My sincerest gratitude also goes to Professor Godfried Augenbroe, who is so nice and offers me generous help, patient and valuable instructions during my exchange study in Georgia Institute of Technology. Weekly meeting and discussing with him is joyful and benefits me a lot.

I want to thank all my colleagues in IB&BA group. Specially, Dr. Gao Dian-ce always gives me very useful suggestions. Dr. Zhao Yang, Dr. Shan Kui, Dr. Yan Chengchu and Dr. Xue Xue provide very good ideas.

I want to express my heartfelt appreciation to my friends. Ms. Zhang Xuedan always encourages me when I am not confident about my study and life. Ms. Luo Yimo is always ready to help and shares experiences. Miss Zhang Yuna is so caring and friendly during my study in USA.

In addition, I would like to thank the Hong Kong Polytechnic University and Hong Kong SAR government, funding me with the Hong Kong PhD Fellowship. Without their financial support, I cannot complete my study and attend the attachment program.

Finally, I would like to express my gratitude to my family. Thank my parents so much for their love and support. They always give me the best with whatever they have. Thank my brother and sister for care and encouragement. I would like to give my special thanks to my boyfriend. His suffering from my complaint and stress can almost win him a PhD degree. Thank him for accompanying, understanding and supporting in the past five years.

TABLE OF CONTENTS

Page

LIST OF FIGURES

Page

LIST OF TABLES

Page

NOMENCLATURE

A	transition intensity matrix
a_{ij}	transition intensity from state i to state j
AHU	air handling unit
$ARPR$	availability risk price ratio
C_a	capacity flowrate of air (kW/K)
C_{ar}	availability risk cost of a cooling system ($)
C_c	overall thermal capacity of the coil (kW/K)
C_{cpt}	annual capital cost of a cooling system ($)
C_{op}	annual operation cost of a cooling system ($)
C_{total}	total annual cost of the life cycle ($)
C_w	capacity flowrate of water (kW/K)
CAP	capacity of a cooling system (kW)
$CAP_{a,}$	available capacity of a cooling system (kW)
$CCHP$	combined cooling, heat and power
CDF	cumulative distribution function
CHP	combined heat and power
COP	coefficient of performance
COP_{abs}	COP of absorption chillers
COP_b	COP of normal electrical chillers
COP_{ice}	COP of ice storage system
COP_{tes}	COP of thermal storage system
$Cost_{CAP}$	capital cost of a CCHP system
$Cost_{CCHP}$	annual operation cost of DCS with CCHP system

$Cost_{grid}$	annual operation cost of DCS fully depending on the grid
CP	chilled water system with constant primary-only flowrate
CPVS	chilled water system with constant primary & variable secondary flowrate
DCHS	district cooling and heating system
DCS	district cooling system
DHS	district heating system
E_{cool}	energy percent for absorption chillers in a CCHP system
E_{ele}	energy percent for electricity generation in a CCHP system
E_{grid}	efficiency of electricity generation for the grid
E_{heat}	energy percent for heating/hot water in a CCHP system
E_{loss}	energy loss percent in a CCHP system
E_{∞}	mean steady-state performance of the system
EC_{total}	total electricity charge ($)
EC_{demand}	electricity charge for the electricity demand
EC_{energy}	electricity charge for the electricity usage
EC_{fuel}	electricity charge for the fuel clause
F^1_{opt}, F^2_{opt},...F^j_{opt}	optimal results at each uncertainty factor (1,2,…j)
f	frequency
G	distribution for samples
g	gravitational acceleration (m/s^2)
H	hydraulic head of pumps (m)
HVAC	heating, ventilation and air conditioning
ICS	individual cooling system
k	number of states for a system

LHS	Latin Hypercube Sampling
Load	annual cooling demand (kW)
MTTF	mean time to failure
MTTR	mean time to repair
N	pump power (kW)
P_{ar}	availability risk price ($/kWh)
P_{gas}	price of natural gas
Pb	payback period of CCHP system
PCM	phase change material
PHE	plate heat exchangers
PHES	pumped hydro energy storage
PID	proportional-integral-derivative
$P(P_1,P_2,....P_i)$	available design plans
$PR(t)$	probability vector of system states at time t
pr_i	probability of a system at state *i*
Q	water flowrate (m^3/s)
R^2	coefficient of determination
R_1	overall heat transfer resistance at air side (K/kW)
R_2	overall heat transfer resistance at water side (K/kW)
R_{ij}	regrets of plan *i* at uncertainty factor *j*
R^i_{max}	maximum regret of plan *i* under every uncertainty factor
R_{minmax}	minimum maximum regret
SI	sensitivity index
SSE	sum of squared error
SSR	sum of squared regression

SST	sum of squared total
$t_{a,in}$	inlet temperature of air to the AHU (℃)
$t_{a,out}$	outlet temperature of air from the AHU (℃)
t_c	mean temperature of the coil (℃)
$t_{w,in}$	inlet temperature of chilled water to AHU (℃)
$t_{w,out}$	outlet temperature of chilled water from the AHU (℃)
TMY	typical meteorological year
VP	chilled water system with variable primary flowrate
WWR	window wall ratio
x_1, a	pre-assumed design condition and noise for it
x_1,x_2,x_3…x_n	inputs for the cooling load
Y	output of modelling
y_i	system performance at state i
yr	number of years of a life cycle
λ	failure rate
μ	repair rate
ρ	water density (kg/m^3)
η	pump efficiency
η_{ele}	electricity generation efficiency from the primary energy
η_{PHES}	efficiency of the pumped hydro energy storage
η_{tran}	electricity transportation efficiency
η_{dist}	electricity distribution efficiency

CHAPTER 1 INTRODUCTION

1.1 Motivation

Electricity used by buildings occupies about 90% of the total electricity usage in Hong Kong. Space air conditioning systems contribute about 40% of the total electricity consumption of buildings (EMSD 2014). Effective measures to reduce the energy consumption of air conditioning systems are vital for alleviating the energy shortage and reducing the greenhouse gas emissions.

Two ways can be used to reduce the energy consumption of the air conditioning systems. One is to decrease the cooling demand by improving the building designs or adjusting the indoor conditions such as the temperature set-points. The other is to use energy-efficient air conditioning systems which can meet the thermal comfort requirement with less energy usage. District cooling system (DCS) is introduced for areas with a high density of buildings due to high efficiency and easy integration with local energy resources. The DCS is defined as a system that distributes thermal energy in the form of chilled water from a central source to residential, commercial, institutional, and/or industrial consumers for use in space cooling and dehumidification (ASHRAE 2013).

Performance assessment of DCSs is necessary for a new district at planning and design stages, especially before the choice is made between the DCS and individual cooling system (ICS) which refers to the ‘one-building-one-cooling-plant’ system. A district cooling and heating system (DCHS) was compared with the coal-fired heating system & conventional air conditioning system (Li et al. 2007; Shu et al. 2010). Results show

that the DCHS has a lower annual cost, considerable energy saving and environmental benefits. A feasibility study of a DCS in Hong Kong was conducted by Chow et al. (2004; 2004) and results show that the DCS has a good potential. Although DCSs are widely used, very limited studies can be found to compare the performance of DCSs and ICSs. The operation characteristics, energy consumption and costs of these two systems in subtropical areas are still not studied in detail. Comprehensive study on the performance of DCSs at different working conditions is essentially needed.

Developing a new district and installing a new DCS will increase the peak electricity load of the entire city/area and the existing power stations. Measures to deal with the peak electricity load need to be evaluated. The performance of a DCS with ice storage system in subtropical areas was studied and results show that the cost saving is not attractive (Chan et al. 2006). However, the conclusion highly depends on that how the DCS with ice storage system is designed and controlled under the local tariff. In available studies, DCSs integrated with combined heating and power (CHP) systems are usually used in the heating dominated areas and DCSs serve as supplemental systems to meet the cooling demand of the area. In the cooling dominated areas, application of the integrated system is rarely reported. Further research is necessary to study the performance of DCSs in subtropical areas with different technologies such as thermal storage systems, pumped hydro energy storage (PHES) and combined cooling, heating and power (CCHP) systems.

Design optimization of DCSs needs to be investigated after performance assessment and feasibility study. Appropriate design of cooling systems is significant because it does not only relate to the capital cost, but also will affect the operation cost throughout the life cycle. Three methods are often used to calculate the cooling load

and determine the size and configuration of the cooling system (ASHRAE 2009; Lu 2008; Rudoy and Cuba 1979):

1) The simplest way is to estimate the cooling load based on an index for a typical building in typical climate zones. With the gross floor area and the index, the maximum cooling load can be determined and the capacity of the cooling system can be obtained.
2) The cooling load of one design day or one hour is calculated, where the outdoor weather data are selected based on the statistic outdoor weather condition and maximum values are assigned for variables representing the internal heat sources such as the occupants, lighting, plug-in equipment, etc.
3) Professional platforms are employed like EnergyPlus (2015), DOE-2 (2009), TRNSYS (2015), DeST (2011), etc., to get the annual cooling load based on typical meteorological year (TMY) data and schedules of the occupants, lighting and plug-in equipment. TMY data for typical regions are used. Based on the peak cooling load and the partial load distribution, the capacity and configuration of the cooling system can be determined.

The cooling loads obtained from the above three methods are all deterministic. Even for the third method, parameters used in the calculation are constants for each time step, like the density of the occupants and lighting, etc. However, these parameters in the operation of the cooling system will differ from those used in the design calculation, which will cause the cooling load to deviate from the expected values. To accommodate the uncertainties and ensure the system to supply sufficient cooling, the conventional method is to multiply the peak cooling load by a safety factor as the capacity of the cooling system. Such a method may be reasonable but not necessarily efficient. Without quantifying the uncertainty, the cooling system cannot be

appropriately sized or configured. The problems of system oversizing have been reported in literature (Djunaedy et al. 2011; Woradechjumroen et al. 2014).

Reliability is another important issue in the design of DCSs and ICSs besides uncertainty. In the conventional design optimization method, the components or subsystems in DCSs and ICSs are assumed to be always available. However, they can be unavailable due to maintenance or failures. Failure of one component may result in malfunction or damage of other components and bring losses to users. The common way is to install backup systems in addition to the basic working systems to ensure sufficient cooling/heating supply in case of equipment failure or performance deterioration (ASHRAE 2012). Such a method is reasonable but not necessarily optimal. Without quantifying the uncertainty and reliability, the empirical method may result in large performance deviation and/or serious oversize problem.

Uncertainties in the cooling load of ICSs are investigated widely but few studies use the results to improve the design of central cooling plants. For DCSs, uncertainties in the cooling load are not studied yet and corresponding design optimization is far from sufficient. The reliability is important for the design of both systems but is not quantified and involved in the design process. It is therefore necessary to develop a new design method, considering uncertainty and reliability, to obtain the appropriately sized and configured cooling systems (DCSs or ICSs). The system can always achieve good performance even when the working conditions change largely from that used at planning and design stages or some component fails in operation. That is called "robust optimal cooling system". The impacts of uncertainty and reliability on the design of DCSs and ICSs need to be investigated and compared.

1.2 Aim and objectives

The aim of this study is to investigate the application of DCSs in subtropical areas and, particularly, to develop robust optimal design methods for DCSs and ICSs. The new methods should render the cooling systems to maintain good performance when uncertainty or failures occur in operation.

The objectives of this study can be summarized as follows:

1) To assess the performance of the DCS compared with the ICS. Energy consumption of both systems for a new district will be evaluated. Operational characteristics of the DCSs and the ICS will be analyzed. Primary factors affecting the comparative performance will be identified.

2) To investigate the performance of DCSs coupled with different energy technologies in subtropical areas, aiming to deal with the peak electricity demand. The economic and energy performance of DCSs with thermal storage systems, PHES and CCHP is evaluated.

3) To quantify the uncertainty of the cooling loads for both DCSs and ICSs. Factors that contain uncertainty are classified and quantified. The peak cooling load distribution and annual cooling load profile are analyzed.

4) To develop and evaluate optimized design methods considering uncertainty at planning and design stages. By using the proposed design methods, the capacity and configuration of cooling systems can be determined based on quantified risk and benefit analysis.

5) To develop a robust optimal design method considering both uncertainty at design stage and reliability of subsystems in operation. This will obtain a cooling system that is robust to uncertainty of information used in design and failures in operation.

6) To compare the impacts of uncertainty and reliability on the design of DCSs and ICSs. Similarities and differences will be summarized by analyzing the performance distributions of DCSs and ICSs under similar uncertainty and reliability.

1.3 Organization of this thesis

The outline of this study and primary contents are illustrated as Fig. 1.1 on the basis of an ongoing project in Hong Kong. According to the planning information of the government, the DCS is designed. The performance of the DCS is assessed and compared with that of ICSs. Feasibility study on the DCS with different technologies is also conducted. By considering uncertainty, the uncertainty-based optimal design methods for DCSs and ICSs are developed. By considering both uncertainty and reliability, the performance of the robust optimal designs for DCSs and ICSs is assessed. Then the impacts of uncertainty and reliability on the design optimization of DCSs and ICSs are compared.

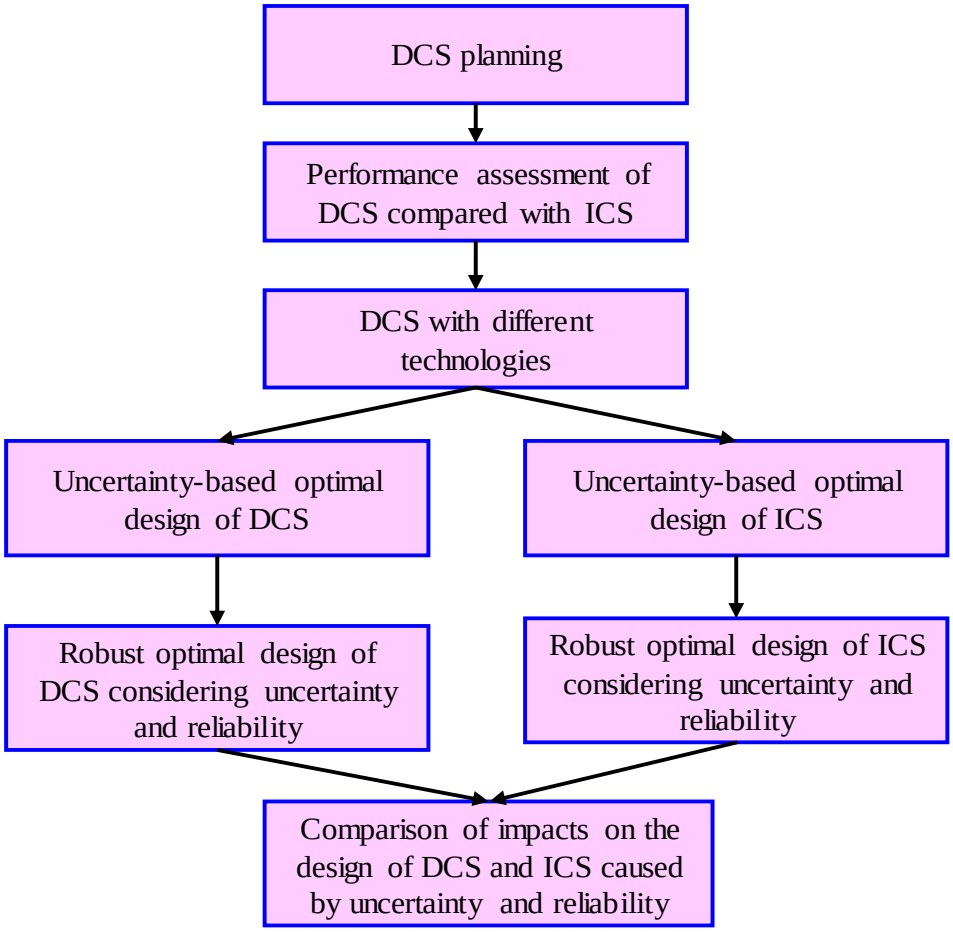

Fig. 1.1 Outline of this study

The organization of this thesis is as follows:

Chapter 1: The motivation of this study is presented, which is to optimize the design of DCSs and ICSs considering uncertainty and reliability after assessing and comparing their performance. To implement the new methods, uncertainty study and reliability assessment are conducted on DCSs and ICSs. The aim/objectives and thesis organization are presented.

Chapter 2: Studies and applications of DCSs are reviewed and categorized. Applications of uncertainty study and reliability assessment in building energy systems are summarized. Studies that involve uncertainty and reliability in the design

process of building energy systems are presented. Problems and research gaps are then summarized.

Chapter 3: A DCS in a new development area in Hong Kong is introduced. The project and planning information is described. Feasibility study on the DCS with different technologies is presented. Costs of the DCS with ice storage systems using different design methods are evaluated. Performance of the DCS with PHES is also evaluated and compared with that using thermal storage. Energy and economic performance of the DCS with and without CCHP is presented.

Chapter 4: Performance of the DCS in the new district is analyzed and compared with ICSs. The DCS and ICSs are designed based on planning information from the government. Energy and economic performance of both systems with different chilled water systems is analyzed from different viewpoints. The operational characteristics of the DCS are analyzed.

Chapter 5: The concept of robust optimal design used in cooling systems is presented, when only uncertainty is concerned, and both uncertainty and reliability are considered. The optimal design method based on mini-max regret theory is presented which does not need to quantify the uncertainty. Then the uncertainty-based optimal design method based on uncertainty quantification is introduced. The robust optimal design method is then introduced concerning and quantifying both uncertainty and reliability. Steps and main technologies of the methods are explained.

Chapter 6: Considering uncertainty, the optimal design method based on mini-max regret theory is investigated. By implementing this method in an ICS, the design of the ICS can be optimized. Two issues are considered: the combination of chillers with different numbers and capacities, and the configuration of chilled water system.

Uncertainties in cooling loads and chilled water network resistance are considered. Performance of the cooling system using the proposed method is compared with that using conventional design method.

Chapter 7: Uncertainties in the cooling load of an ICS are quantified. Capacity and configuration of the ICS is optimized based on the performance distribution at different risks. Performance of the ICS using the uncertainty-based optimal design method is analyzed and compared with that using the conventional method. Robust optimal design of the ICS considering both uncertainty and reliability is achieved by minimizing the total annual cost. Performance of the ICS designed using the robust optimal design method is analyzed and compared with that using the conventional method, the method concerning uncertainty only and the design method concerning reliability only.

Chapter 8: Cooling load distributions of the DCSs are analyzed considering uncertainty at planning and design stages. Uncertainties in the outdoor weather, building design/construction and indoor conditions are considered. Application of the uncertainty-based optimal design method in the DCS is investigated. The robust optimal design of the DCS is obtained considering both uncertainty and reliability. Performance of the DCS designed using the robust optimal method is compared with that using other methods.

Chapter 9: Impacts of uncertainties on the cooling load distribution of DCSs and ICSs are evaluated and compared. Sensitivity analysis is conducted to identify important variables for the cooling loads. Impacts of implementing the robust optimal design method in DCSs and ICSs are also assessed and compared.

Chapter 10: Main conclusions and contributions are summarized. Shortcomings of this study and recommendations for the future study are presented.

CHAPTER 2 LITERATURE REVIEW

2.1 Overview

Since this study attempts to assess the performance of DCSs, quantify uncertainties in the design of DCSs and ICSs and develop robust optimal design methods considering uncertainty and reliability, previous research efforts on DCSs, uncertainty study and reliability assessment in building energy systems are reviewed.

Section 2.2 presents the history and development of DCSs. Existing studies on DCSs are presented by classifying them into several categories: the integration of DCSs with different technologies, the design optimization and control optimization of DCSs. In Section 2.3, applications of uncertainty analysis in building energy systems are reviewed, especially in the system design. In Section 2.4, reliability assessment and its application in building energy systems are reviewed. In Section 2.5, research on the above three sections is summarized. Limitations of existing studies and challenges for future work are also presented.

2.2 District cooling systems

2.2.1 History and development

DCS is defined as a system that distributes thermal energy in the form of chilled water from a central source to residential, commercial, institutional, and/or industrial consumers for use in space cooling and dehumidification (ASHRAE 2013). It typically consists of four parts: the heat rejection system, the central chiller plant, the distribution system and the end users as shown in Fig. 2.1

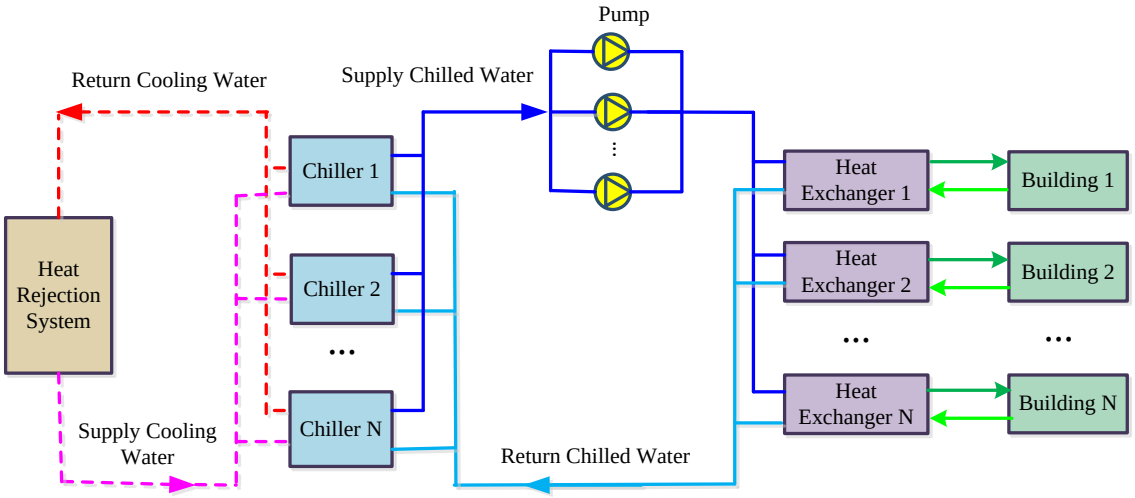

Fig. 2.1 Schematic diagram of a typical DCS

The first known DCS began to work at Denver's Colorado Automatic Refrigerator Company in 1889. In 1930s, large DCSs were used for Rockefeller Centre in New York City (Empower 2014). Approximately 20 cities and towns adopted DCSs till 1996 in US (Seeley 1996). The earliest DCS in Europe appeared in Paris in 1960s. After that it began to be widely used in Germany, Italy, Sweden, Finland, etc. DCS began to be used in Japan since 1970 and then it has been developing very fast. The Japanese government encourages the development of DCS for its high efficiency and low pollution emissions. More than 154 DCHSs in Japan had been in use by 2005 (Ma and Long 2009). The DCS was introduced in United Arab Emirates in 1999 and now it accounts for 10% of the cooling market (Hilotin 2011). In China, the DCS is a relatively new system. The first well-known DCS located in Beijing and began to work since 2004. After that, several large DCSs began to appear such as the DCS in Guangzhou University Town. A general introduction of the DCS including its advantage and disadvantage, subsystems, classifications, environment and economic effects can be found in the references (ASHRAE 2013; Booz & Company 2012; EMSD 2011; Rezaie and Rosen 2012; Shimoda et al. 2008).

2.2.2 Integration with sustainable energy technologies

1) Integration with renewable energy resources and use of waste cold energy

Usually the renewable energy resources include the energy from the surface water (such as the sea, river and lake), geothermal energy, solar energy, wind energy, biomass, etc. (Dincer I. 2000; Panwar et al. 2011). The integration of DCSs with renewable energy resources is summarized as follows.

Energy from surface water is frequently used in DCSs among all the renewable energy resources. A DCHS using seawater heat pumps was installed in the north of China (Li et al. 2007). Another DCHS with seawater heat pumps was studied and the results indicate that the economic performance of the system highly depends on the local tariff and policy (Shu et al. 2010). A DCS using seawater was installed in Hong Kong to supply cooling for a new development area (Chow et al. 2004; Chow et al. 2004; Yik et al. 2001). The DCS in Stockholm of Sweden is one of the largest DCSs in the world. The fast development of this project is encouraged by the political decision to phase out CFC and HCFC-based products, which were used as refrigerants and extremely aggressive to the ozone layer (IEA DHC|CHP 2013). By sending the cold seawater from the Baltic Sea to the heat pump units, the DCS can supply cooling to the users. Up to 2009, the cooling system serves over 600 buildings including offices, hospitals and universities, etc. (GNS Science 2009). Cold energy stored in the riverwater can also be used in DCSs. For a DCS in Paris, seven chiller plants are used, of which four plants use cooling towers and the other three use water from Seine to produce cooling. When the water temperature is below 8℃, water from the Seine is used directly for cooling (Poeuf et al. 2010).

Geothermal energy is another important cold source for the cooling system (Ampofo et al. 2006; Rybach and Sanner 2000), which mainly refers to energy from aquifer or groundwater. It is regarded to conserve about 90%~95% of energy for a DCS (Paksoy et al. 2000). One of the largest groundwater reservoirs in Norway is used to serve the Gardermoen Airport as a complemental heat sink and source for the DCHS (Eggen and Vangsnes 2006). During cooling period, chilled water is pre-cooled by the groundwater with a cooling capacity of 3 MW. It is then post-cooled by a combined heat pump/refrigeration plant with a cooling capacity of 6 MW.

Solar energy can be used in DCSs. A DCS using solar energy in a hospital district was studied in Italy (Buonomano et al. 2014). The solar energy is collected by thermal collectors and converted into hot water. The hot water exchanges heat with circulating water from the absorption chillers for cooling and district heating network for heating.

A DCS driven by thermal heat from municipal solid waste-fired power plant was studied in Thailand (Udomsri et al. 2011) . Instead of landfilling, the waste incineration is coupled with the power plant and heat is recovered for absorption chillers. The system offers a great opportunity for primary energy saving, greenhouse gas reduction and contributions to biomass-based energy production. Rentizelas et al. (2009) presented an optimization study for a place with multi-biomass. The optimization was condcuted to get the optimal bioenergy supply chain and conversion facility with a financial aim. Where, the biomass was used for a trigeneration plant which connected with a DCHS.

By coupling with renewable energy resources, the DCHS can achieve energy saving and greengas emission reduction (Ortiga et al. 2013). The renewable energy has been widely used in the district heating system (DHS). Solar energy is widely used in DHSs

(Buoro et al. 2014; Hassine and Eicker 2013; Lindenberger et al. 2000) and the benefit is promising. Geothermal energy is used by DHSs to supply the users heating by pumping hot fluid from the underground (Ozgener et al. 2005; Ozgener et al. 2006). Biamass is often used as a heating source in DHSs (Wetterlund and Söderström 2010). 14 % of gross energy consumption is met by straw in 2003 in Denmark. The biamass is used as the energy resource of a CHP plant, where the electricity and heat are supplied to surounding households (Euroheat and Power 2007). However, the application of solar energy, geothermal energy and biomass in DCSs is not as popular as that in DHSs. The main reason may be that all the above energy resources can be used for heating with high efficiency. For cooling purpose, however, the renewable energy has to be converted into heat firstly and the heat is then transferred into electricity. Alternatively, the heat energy is convered into cold energy by absorption chillers. The efficiency for cooling applications is much lower compared with the heating applications, due to the heat loss and conversion efficiency.

2) Integration with CCHP systems

DCSs are often combined with CCHP systems as shown in Fig. 2.2, which supply cooling, heating and power simultaneously to users. Wu and Wang (2006) presented a literature review on CCHP systems. The work on the system configuration, operation and performance of DCSs integrated with CCHP is summarized in this section.

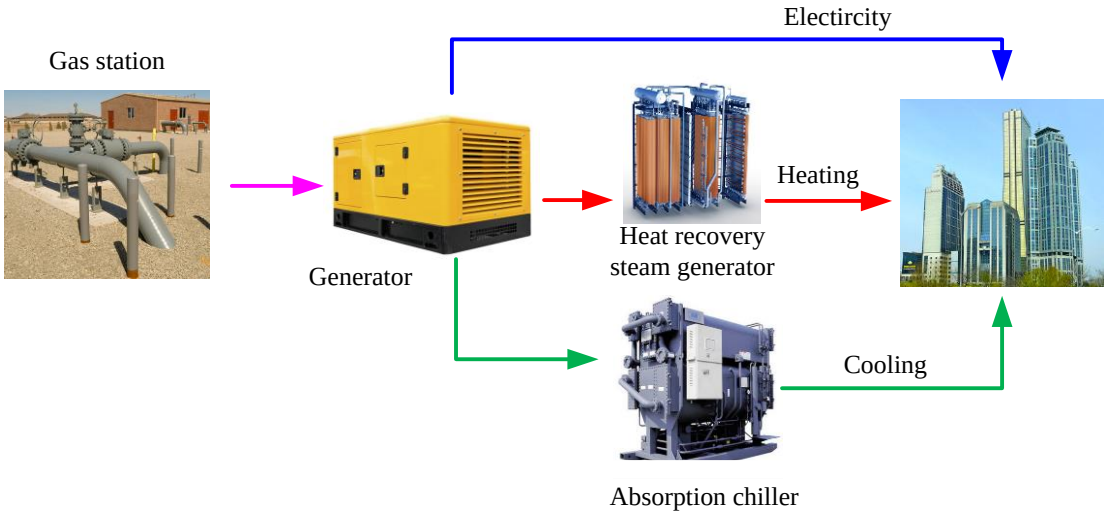

Fig. 2.2 Schematic diagram of DCS integrated with CCHP system

For DCSs integrated with CCHP, thermal driven chillers are usually employed to use the low grade heat from the CCHP system. Detailed review about the chillers can be found in the paper (Deng et al. 2011). Lozano et al. (2010) studied a CCHP system connected with a DCS in Spain, which aimed to optimize the design of the system. The system serves 500 apartments in a district. Mixed integer linear programming method was used to find the optimal design of CCHP with thermal storage system. The integrated DCS and CCHP system using absorption chillers only may not be able to meet the cooling demand and electricity demand simultaneously. When the cooling demand is very high, the cooling produced by absorption chillers may be not sufficient and electrical (compression) chillers are required. Rodriguez-Aumente et al. (2013) studied the economic performance of a DCHS coupled with a tri-generation plant under different pricing and using patterns. Absorption chillers are used as the basic units and back up with compression chillers and boilers. In CCHP systems, absorption chillers can only use saturated steam with the pressure of 0.4 MPa~0.8 MPa (Zhang et al. 2012). However, the steam produced by the power generator is usually superheated. A DCS integrated with CCHP was studied by Zhang et al. (2012), which uses an

industrial turbine, driving the compression chillers, to cool down the superheated steam. Where, a combined compression refrigeration and absorption refrigeration system is adopted, which saves a large amount of steam consumption to meet the same amount of cooling demand.

For the hot water supplied to absorption chillers in the DCS with CCHP, there is optimal supply and return temperatures with the objective of the lowest primary energy consumption of the chillers and pumps (Fu et al. 2001). Nagae et al. (2011) pointed out that the energy efficiency of DCSs integrated with CCHP systems could be improved by increasing the maximum chilled water flow rate of absorption chillers and compression chillers, decreasing the chilled water flow rate through the bypass between the supply and return pipes, and increasing the return chilled water temperature. Energy recovered from a coal-fired power plant can be used by DCHSs as reported by Erdem et al. (2010). The authors also evaluated the energy saving potentials of using the heat from the condenser, stack gases, extracted steams for feed water heater and low-pressure turbine inlet steam.

Both energy and exergy efficiency were used to assess the performance of DCSs with CCHP systems (Pak and Suzuki 1997; Rosen et al. 2005). Three DCSs integrated with CCHP systems were compared, which use electrical chillers, single-effect absorption chillers and double-effect absorption chillers respectively. Results show that it is necessary to conduct exergy analysis to assess and compare the three options since the electricity, heating and cooling produced from three systems have different natures and qualities. Hart and Rosen (1996) compared the health and environment effects caused by the DCHS integrated with CCHP system.

From the above studies, it can be observed that DCSs integrated with CCHP systems usually couple with DHSs to meet the heating and cooling demand of the users. The integrated system is often used in the heating dominated areas, while the DCS serves as a supplemental system to meet the cooling demand of the area (Li et al. 2007; Shu et al. 2010). In the cooling dominated areas, the application of DCSs with CCHP systems is rarely reported. One reason might be that the energy efficiency of CCHP systems is not high when the primary aim is to meet the cooling demand. However, there is limited quantitative and detailed study in the performance of DCSs integrated with CCHP system in cooling dominated areas. Further study on this aspect is necessary.

3) Integration with thermal storage system

To reduce the operation cost and limit the power demand of the system at peak hours, DCSs are integrated with thermal storage systems. The integrated systems with different configurations are shown in Fig. 2.3. The concept of cool storage systems is defined by the *Design Guide for Cool Thermal Storage*: Cool storage systems store cold energy during periods of low cooling demand. The stored cooling is later used to meet the air-conditioning cooling load (ASHRAE 1993). By using the thermal storage system, the power utilities benefit from the reduction of the peak electricity generation and consumers benefit from lower electricity bills, by taking advantage of the lower off-peak rates and reducing peak demand billing charges (Chan et al. 2006).

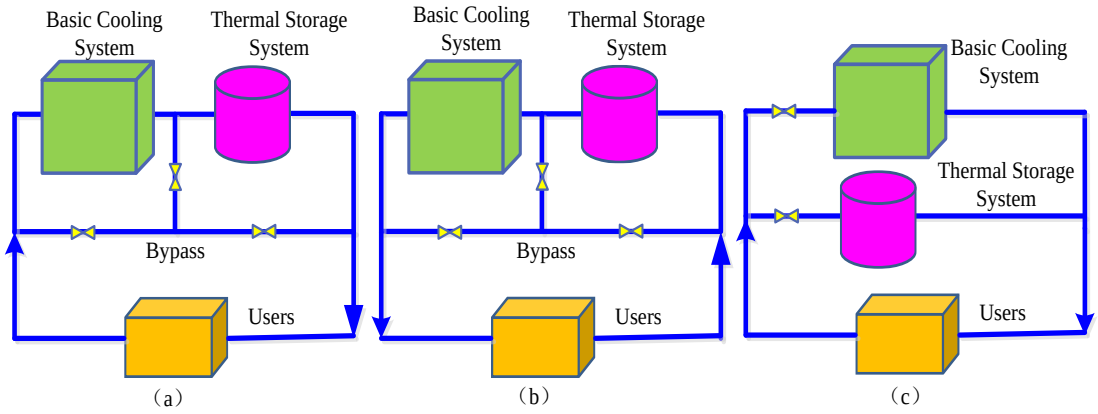

(a) serial connection with chillers upstream; (b) serial connection with chillers downstream; (c) parallel connection

Fig. 2.3 Schematic diagram of DCS integrated with thermal storage system

Water is used for thermal storage due to its low cost and high thermal capacity. The temperature of the water storage system is compatible with evaporation temperature of conventional chillers, making it easier to be connected with DCSs. Typical water-storage tanks stratify to a water temperature of 4℃ (Seeley 1996), at which the water density is at its maximum. Majid and Waluyo (2010) studied the temperature distribution at different depths of the stratified thermal energy storage tank during charging process. Thermocline thickness was evaluated for two cases with different water flow rates. Tanaka et al. (2000) investigated a DCHS using water tanks for daily thermal storage and seasonal water thermal storage. Where, the daily heat and cold storage charges were realized by a heat pump. One DCS with aquifer thermal energy storage was studied by Andersson (2007). The storage system was used to increase the capacity of the DCS plant aiming to connect more customers. It stores cooling at night and recovers during the daytime. Results show that the aquifer storage system has very good economic performance.

Ice stores cooling in the form of latent heat. It fits best in tight downtown areas because it requires smaller storage volume. The DCS with ice storage system has been used in

many projects, which are summarized in the reference (ASHRAE 2013). A DCS in Paris uses both water and ice storage systems (Poeuf et al. 2010). Three cold storage units having a capacity of 140 MWh are used, of which two are ice storage units and one is chilled water storage unit. In China, most of the DCS projects are integrated with ice storage systems. Chan et al. (2006) conducted a parametric study to evaluate the performance of a DCS with ice storage system at different partial storage capacities, control strategies, and tariff structures in Hong Kong. Results show that the DCS with ice storage system is not economic feasible because the local tariff has trivial electricity price difference between the peak time and off-peak time.

Phase change material (PCM) is another popular group of cool storage medium. Most of PCMs for cool storage are inorganic salt hydrates or mixtures of them. They are used due to their high latent heat during phase change, high density and low cost. A commercial salt hydrate PCM is used in a DCS with a phase change temperature of 13℃ (Chiu et al. 2009). The performance of the storage system was compared with systems with auxiliary chillers and stratified chilled water storage system. Results show that the latent heat thermal storage system is more economically viable. The major problem in using salt hydrates is that most of them melt incongruently. It is because they have poor nucleating properties resulting in super cooling of the liquid salt hydrate prior to freezing. Another problem is corrosion, which leads to short service life, high packing and maintenance costs. Paraffin wax can also be used for cool storage for DCS application. Bo et al. (1999) attempted to determine the thermal properties of paraffin waxes and their binary mixtures to demonstrate the potential of using these materials for cool storage. The experimental results indicate that laboratory-scale tetradecane and hexadecane and their mixtures could be used as PCMs for cool storage.

The use of thermal storage system is based on electricity price policy, i.e. different electricity prices at different time of the day. For example, the current tariff structure in Hong Kong is not so advantageous for using thermal storage system. To reduce the peak electricity demand and connect more users, promotion of appropriate electricity price is necessary. The existing literature only mentioned the use of thermal storage system in DCSs but few addressed the design and control optimization of the integrated system. Problems including the sequence control of the basic load chillers and the storage system, the optimal design of the storage system, the amount of energy to be stored, etc., need to be further investigated.

2.2.3 Optimization of DCS in planning, design and operation

DCSs can perform well only when the system is well planned, designed and operated. The work in the planning, design and operation of DCSs is categorized in Fig. 2.4 and reviewed in this section.

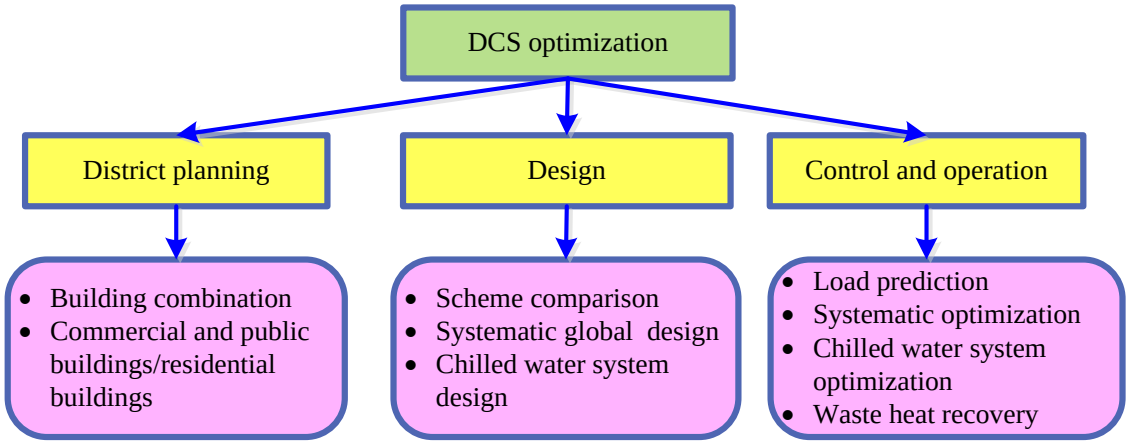

Fig. 2.4 DCS optimization in system planning, design, control and operation

A. Planning of buildings in a district

Generally, DCSs are financially beneficial for densely populated urban areas, high-density building clusters and industrial complexes. For low-density areas, the

economic advantage is less apparent because of the cold transportation loss (Rezaie and Rosen 2012). Buildings served by a DCS may have different functions, as shown in Fig. 2.5. The combination of different types of buildings in a district will affect the performance of the DCS. A more uniform cooling load profile was regarded to be suitable for DCSs because it would minimize the start and stop counts of chillers and ensure the system to work with a high stability. Chow et al. (2004) conducted a study to find the optimal percentage shares of different types of buildings in a DCS, aiming to get the most uniform cooling load profile. The performance of DCSs is not only related to the load profile but also the system design. The optimal combination should be obtained by taking the efficiency of the DCS as the objective, especially when compared with the ICSs at planning stage.

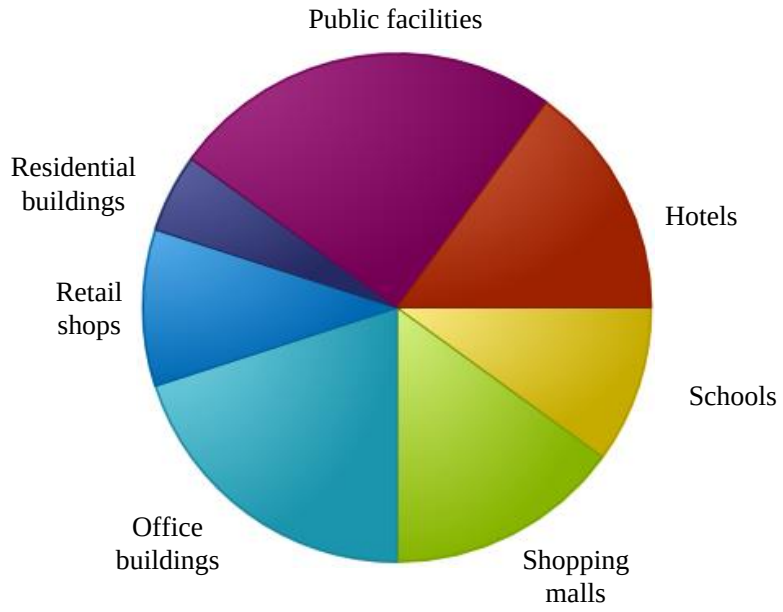

Fig. 2.5 Combination of buildings with different functions in a DCS

In Eastern Asian countries like China and Japan, most users of DCSs are commercial and public buildings. In Middle East, residential buildings are included because DCSs usually serve entire resort areas (Zafar 2014; Qatar cool 2010). For European countries

and US, both commercial buildings and residential buildings are involved as the users and DCSs couple with DHSs to supply both cooling and heating to the entire districts or cities. Actually residential buildings and commercial buildings can complement each other and combination of these two types of buildings may achieve better performance. The performance of DCSs with and without the residential buildings needs to be assessed and compared. The main barriers and corresponding solutions to include the residential buildings need to be figured out. It is easy to understand that DCSs can be used in the areas where the climate is hot and the cooling load is dominated, especially in tropical and subtropical areas. However, many well-known DCSs are developed in European countries where the climate is cold. The performance of DCSs in different climate areas needs to be studied and compared with the traditional cooling systems.

B. DCS design

The design optimization of DCSs is reviewed in this section from two viewpoints: the global system design optimization and the subsystem optimization. The global optimization aims to optimize the DCS overall system configuration. The subsystem optimization aims to improve the performance of some component or subsystem.

Global system design optimization

For the system selection, Li et al. (2007) conducted performance comparisons of cooling and heating systems using different energy resources. A DCHS using seawater heat pumps was compared with the coal-fired heating system and conventional air conditioning system in the north of China. After the system scheme is determined, design optimization of the subsystems needs to be done to get the optimal global performance. Söderman et al. (2006; 2007) used a mixed integer linear programming

model to optimize the DCS design in an urban area. The concerned issues included the location of cooling plants, the cooling capacity of the plants, the cold storage location, the storage capacity, the routing of distribution pipe-lines to individual consumers, optimal operation of cooling plants in different periods of the year, the charge and discharge of the storages and the cold medium flow rates in the district cooling pipelines.

Subsystem design optimization

Most existing studies on DCS subsystem design optimization address chilled water distribution networks. The central plants and the users are connected by the chilled water networks. The connection can be direct or indirect by isolating with heat exchangers (Skagestad and Mildenstein 2002). For systems using direct connection, chilled water is pumped from the central plant to the in-building air-conditioning systems. The direct connection is more economic efficient due to the elimination of heat exchangers and associated equipment, water treatment systems and equipment maintenance (ASHRAE 2013). The main limitation is that it is easy to get cross-contamination between different users. For systems using indirect connection, the cross-contamination can be avoided and the responsibilities of different parties are clear. However, the efficiency becomes lower and the capital cost is increased because of the heat exchangers.

The chilled water network can be organized in radial and/or tree shaped networks, as illustrated in Fig. 2.6. Genetic algorithm is frequently used to get the optimal layout and size of the chilled water network (Chan et al 2007; Feng and Long 2008; Li et al. 2010). The objective can be the piping cost plus pumping energy cost (Chan et al. 2007), or annual equivalent cost including the overall investment, annual operating

cost, maintenance and amortization expense, and annual cooling loss cost (Feng and Long 2008; Li et al. 2010). Sometimes the depreciation cost of the pumps and pipes is also included (Liu et al. 2004; Liu et al. 2006). The selection of pipe material should consider the pipe strength, durability, corrosion resistance and cost (Chow et al. 2004). The placement of the pipes was studied by Babus'Haq et al. (1986; 1987; 1990). The recommended configuration for both the DCS and DHS is to place the two pipelines one above the other in the trench with the hotter pipe being the upper one. This differs radically from the traditional arrangement (the pipes being placed side by side) and leads to at least 4% additional energy saving. Narrower trenches would be required and the cost would also be lower eventually.

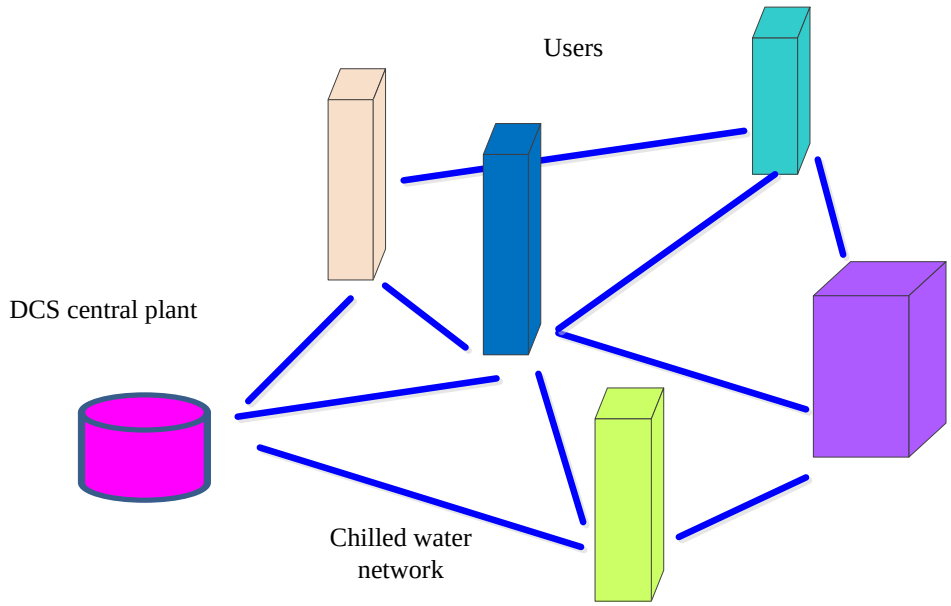

Fig. 2.6 Layout of a chilled water system connecting the DCS plant and users

The design of DCSs is important because it affects the performance of DCSs over the entire life cycle. The study on DCS design optimization is not sufficient yet, such as the chiller capacity and combinations considering partial cooling load, pump connection, the number and location of the chiller plants, etc. In addition, the DCS

installation is usually separated into several stages. Corresponding design considering multiple stages should be further studied.

C. DCS operation and control

The operation and control of DCSs is more complicated compared with ICSs. The considerable energy consumption requires stricter management and better operation.

Operation and optimization of DCS plants

To improve the energy performance of DCSs, many efforts have been paid on various aspects of DCSs, including the cooling load prediction, the optimization of system operation, the waste heat recovery, the optimization of chilled water systems etc.

Cooling load prediction is necessary for the control of DCSs, especially for the systems with thermal storage. Artificial neural networks were used to predict the cooling load of the buildings by Sakawa et al. (2001), where a three-layer artificial neural network model was used to predict the cooling load of next day using latest data available. Results show that this method can predict the cooling load accurately. Several types of buildings were surveyed including the office buildings, retail shops, restaurants and hotels (Yik et al. 2001). The surveying ratios of occupancy, lighting and fresh air supply at different time of a day were obtained, which were used in cooling load perdition using HKDLC, HTB2 and BECON as the tool. Results show that the sum of loads for each type of buildings can be predicted accurately but for each individual building, the prediction is not accurate.

Many optimization techniques have been used in DCHSs, which was reviewed by Ortiga et al. (2007). The common approaches used for DCHSs were mathematical programming, genetic algorithms, neural networks and fuzzy logic systems. Multi-

criteria optimization was used because of conflicting and non-comparable criteria existed in optimization. Sakawa et al. have done a lot of work on the optimization of DCSs. In their early work, the operational planning problem of district cooling and heating plants was regarded as a mixed 0–1 linear programming problem and it involved hundreds of variables (Sakawa et al. 2001; Sakawa et al. 2002). Genetic algorithm was adopted to get the optimal result. In their later work, the operation optimization was regarded as nonlinear 0-1 programming problems (Sakawa et al. 2003). An interactive fuzzy satisfying method through genetic algorithms was adopted. Considering the state of the components in DCHSs as continuous operating ratio instead of just on-off, the operation problem of an actual district cooling and heating plant was taken as a nonlinear programming problem in their latest work (Sakawa and Matsui 2013). To reduce the energy consumption and minimize the operation cost, a multi-objective nonlinear programming formulation was used. An interactive fuzzy satisfying method through particle swarm optimization was introduced. The feasibility and efficiency of the proposed method was tested on an actual district cooling and heating plant in Tokyo.

The use of energy efficiency measures helps to improve the benefits to the operators of DCSs when the users pay fixed amount of money for the cooling received (Uno and Shimoda 2012). Results show the following measures are effective for reducing the energy consumption of DCSs: 1) to circulate the chilled water with a large differential temperature; 2) to use the outdoor air directly for free cooling when the outdoor temperature is even lower; 3) to reduce the outdoor air intake based on ventilation demand; 4) to reset the indoor temperature set-point.

Operation and control optimization of chilled water distribution systems

Cold loss is a very important factor resulting in bad performance of the DCS. It consists of two parts: the transportation loss and the cold loss resulting from the pumps. Research shows that the transportation cold loss can be controlled within 1% if the insulation and construction of pipes is good. The main cold loss is caused by the secondary chilled water pumps (Kang and Zuo 2009). To reduce the energy consumption of the chilled water pumps, available methods are classified as follows:

1) *To reduce the resistance of the pipelines*. Specific surfactants in DCHSs could reduce the friction attributed to a formation of an additional viscous sub-layer along the pipe internal surfaces (Chou 1991). Some additives were tested and could be used in the DCHS without serious technical problems. However, slight toxicity limited the application and they could only be used in primary systems.

2) *To increase the thermal capacity of the fluid in the chilled water network.* A DCHS coupled with dynamic-type ice storage system was proposed (Kozawa et al. 2005; Hamaoka et al. 1996; Torikoshi et al. 1992). The ice-slurry is transported to the substations from the ice storage tanks at the central plant. The aim is to reduce the transportation power and the costs of pipelines. By adding 25% volume of pentadecane into the chilled water, the volumetric thermal capacity of heat transfer fluid undergoing at the temperature difference of 15℃ is increased by almost 40%. With a larger thermal capacity, the flow rate and pump energy consumption can be decreased significantly (Choi et al. 1992).

3) *To limit the pipe distance and enlarge the difference between the supply and return chilled water temperatures.* Shou and Chen (2003) suggested that the load density (average cooling load carried by one meter of pipeline) should be over 14 kW/m for DCSs. The difference between the supply and return chilled water temperatures

should be about 8~10℃ and 10℃ for the system with thermal storage system. The chilled water network radius should be around 1~2 km considering the heat transportation loss. Kang et al. (2010) also studied the optimal distance using DCSs considering the cooling load density and differential temperature between the supply and return chilled water. Results show that the distance for economic cooling could be longer for areas with higher cooling load density. The supply and return differential temperature should not be less than 5℃.

In most of the operation studies, the central plants and the users (cooling systems in buildings) are operated separately, which is the result of separate management. The coordinated operation of users and central plants will benefit both sides. In the operation optimization of chilled water system, the dynamic performance is usually neglected such as the response delay caused by the chilled water network of long distance. Control optimization of the entire chilled water systems including DCSs and users, considering the dynamic character and interactions, needs to be studied.

2.2.4 Conclusive remarks

DCSs have been widely used due to outstanding advantages compared with the traditional cooling systems. However, there is still much work to be done for the systems to achieve the expected or optimal performance.

Various uncertainties exist in the data used at planning and design stages. These uncertainties will cause the system performance to deviate from the expected. For example, the capital cost of one DCS project in Hong Kong has to be increased again and again because the installation cost of chilled water pipelines is much higher than that of the original budget. There are also some DCSs that are oversized too much

caused by the large difference of actual cooling load and estimated cooling load. All these are caused by the uncertainties existing in information and data used at planning and design stages. How to handle these uncertainties and ensure the system to perform well is vital.

2.3 Uncertainty and sensitivity analysis in building energy systems

Uncertainty can be defined as being any departure from the unachievable ideal of complete determinism (Walker et al. 2003). It is often divided into two categories: aleatory and epistemic (Paté-Cornell 1996). Aleatory uncertainty arises due to natural unpredictable variation in the system. It stems from variability in known populations, which cannot be reduced by the knowledge of experts although the knowledge can help quantify the uncertainty. Therefore, aleatory uncertainty sometimes is regarded as irreducible uncertainty. Epistemic uncertainty is because of a lack of knowledge about the system. It can be eliminated with sufficient study (Hora 1996).

Uncertainty exists generally in building energy systems. The sources of uncertainty in building energy systems were grouped into five levels, including meteorology, urban, building, systems, and occupants (Sun 2014). When the study is conducted based on the simulation, uncertainties exist in both the inputs and the processing methods or platforms. Uncertainty study can be used to address issues including the model accuracy, the accuracy of the input variables, effects of assumptions on the outputs, the performance of different options, etc. (Macdonald 2002). By considering and quantifying the uncertainty, the decision can be made with confidence. Plenty of research has been done regarding the uncertainty and sensitivity analysis of building energy systems, which is reviewed in this section.

2.3.1 Performance assessment of building energy systems

Uncertainties in building physical parameters are recommended to be taken into consideration when designing building energy systems or assessing the performance of the systems (Brohus et al. 2012; Eisenhower et al. 2011; Heiselberg et al. 2009; Hopfe et al. 2013; Zhang et al. 2013). The most important factors were identified. Performance distributions of buildings with uncertainty were obtained in terms of energy consumption, thermal comfort, and monetary cost. Uncertainty and sensitivity analysis method was adopted to rate the energy performance of a family house in Italy (Corrado and Mechri 2009). The 129 input data were identified and grouped into three sets, including climatic data, envelope data, and building use data. Less than 10 input data were proved to have a significant influence on the energy rating uncertainties. Energy consumption of dwellings considering uncertainties in the climate, building construction and inhabitants was studied by Pettersen (1994). Results show that the energy consumption can be varied with an uncertainty of $\pm$ 25-40%. The source of uncertainties in a housing stock model was studied and method to handle the uncertainties was proposed (Booth et al. 2012).

Uncertainty analysis can be used to assess the performance of retrofit of building energy systems. Lee et al. (2013) proposed a method to conduct probabilistic risk assessment of the energy saving in energy performance contracting projects. Uncertainties in weather conditions, occupancy, operating hours, thermostat set-point, etc. were considered. Possible energy saving was obtained with quantified confidence. Menassa (2011) presented a quantitative approach to determine the investment value in sustainable retrofits for existing buildings considering different uncertainties associated with the life cycle costs and perceived benefits of the investment. The

proposed methodology provided the decision maker with managerial flexibility to determine, prioritize and evaluate the required retrofits over time. Uncertainty analysis was conducted by Eisenhower et al. (2011) in the energy consumption of one normal building and one high performance building, which was similar to the normal building but with better envelopes and equipment. It involved uncertainties in the heating/cooling source and equipment, primary movers of air loop and water loop, terminal units, external and internal parameters of buildings, zone set-points and sizing parameters. Sensitivity analysis was implemented to find important parameters. Results show that the high performance building is more robust to uncertainty.

2.3.2 Uncertainty in modelling of building energy systems

When a study is conducted based on simulation, uncertainties exist in both the inputs and embodied methods or sub-processes. Eisenhower et al. (2011) conducted uncertainty study in the intermediate process by performing decomposition, which aimed to find the most important subsystem in modelling. O'Neill and Eisenhower (2013) used measured data to conduct model calibration and the uncertainty study was implemented to tune the models. The necessity to decouple uncertainties in HVAC systems and building models was investigated by Augenbroe et al (2013). The coupled simulation method usually requires a higher level of expertise of system modeling and can be computationally intensive. Results show that for a given building the monthly energy difference using two methods was seldom more than 20%, which was acceptable for most of purposes.

2.3.3 Design of building energy systems

Uncertainty can be involved in the design optimization of building energy systems. Uncertainties in the peak load prediction are investigated (Huang et al. 2015), which

is the basis of capacity selection for the heating, ventilation and air conditioning (HVAC) system. Multi-criteria optimization is conducted including the energy consumption, initial cost and failure time. The uncertainties in the building performance evaluations were addressed by De Wit and Augenbroe (2002) and their potential impact on design decisions was assessed. Results show that considering the uncertainties can change the decision maker's choice for the same project. Zhang and Augenbroe (2014) investigated that how to right-size a photovoltaic system. Uncertainties in the building's physical properties, solar irradiance, efficiency and degradation rates of PV panels are considered. A method was proposed to estimate building energy performance in early design decisions (Rezaee et al. 2014). Design evolution uncertainties in early design were quantified and their impact on design decisions was examined. Results using different models or software indicate different solutions. It indicates that uncertainties in the models have to be fully addressed. Sun et al. (2014) proposed a new design method considering uncertainty in the cooling/heating load. Results recommend that using actual weather data in the load calculation helps to alleviate the oversize problem in the cooling/heating system design.

2.3.4 Cooling/heating load prediction

Many variables are used in the cooling load prediction and most of them contain uncertainties (Li et al. 2003; Prada et al. 2014; Sun et al. 2014; Yıldız and Arsan 2011). The impact that furniture and contents (i.e. internal mass) have on zone peak cooling loads is investigated (Raftery et al. 2014), which is not accounted in traditional simulations. Results show that involving internal mass can change the peak cooling load by a median value of −2.28% (−5.45% and −0.67% lower and upper quartiles

respectively). Climatic effect on cooling loads in subtropical regions was studied by Li et al. (2003). Weather data from 1979 to 2000 were used in the cooling load calculation and results were compared with that using the design conditions recommended by local building design practice. It showed that the common method can oversize the air conditioning plant due to larger peak cooling load prediction. The weather data should be examined closely so that appropriate external design conditions can be selected according to different applications and acceptable risk levels. Weather data, which represent the boundary conditions in energy simulation, can affect the model outcomes significantly. Uncertainty of the meteorological conditions therefore should be involved in the design process. Lee et al. (2012) developed a framework which generated stochastic meteorological years using historical meteorological data for any given location. This was realized by stochastic modeling of meteorological data as a Vector Auto-Regressive process with seasonal non-stationarity. The annual cooling and heating load considering the physical, design and scenario uncertainties was investigated by Hopfe (2009). The distribution of the annual heating/cooling load, weighted overheating and under-heating hours related to the thermal comfort was analyzed. The peak cooling load considering the uncertainties of design parameters was studied (Dom ínguez-Mu ñoz et al. 2010). Influential factors for the peak cooling load were identified.

2.3.5 Conclusive remarks

From the above review it can be found that research on building energy systems considering uncertainty mainly aims to present the result distribution, compare with the deterministic results, find the most important factors, and calibrate models. Even for the design of building energy systems, studies are mainly about the energy systems

in buildings. For large centralized cooling plants or DCSs, the design considering uncertainties is rarely studied.

2.4 Reliability assessment of building energy systems

Reliability can be defined as the probability of successful operation or performance of systems and their related equipment, with minimum risk of loss or disaster (Stapelberg 2009). Reliability design has been widely used and studied in the fields such as structure, industrial manufacture, power system, computer science, etc. (Frangopoulos and Dimopoulos 2004; Heising 1991). Redundancy is usually adopted to improve the reliability of systems. Redundancy can be active where the additional components may also work under normal conditions, or passive where these components only are switched on during abnormal conditions or failure occurrence (Aguilar et al. 2008). Usually passive redundancy is used in building cooling systems. For example, four chillers may be installed for a cooling system, of which three chillers are the basic chillers to meet the cooling demand and another one serves as a backup and keeps off under normal operation conditions.

Reliability analysis or assessment is necessary to avoid/reduce losses caused by the failure of components/systems. It is also used in building energy systems. Chinese et al. (2011) used a multi-criteria approach to select the space heating system for an industrial building, where the criteria included reliability, operation cost, comfort, etc. Kwak et al. (2004) proposed a method to predict an optimal inspection period for condition-based preventive maintenance based on reliability assessment of air-conditioning facilities in office buildings. The expected profit produced by the method was also analyzed. Myrefelt (2004) used actual data collected from buildings belonging to seven large real estate operators to analyze the reliability of the HVAC

system. Reliability assessment is usually used to improve the system design, which has been reported in fields such as power system, chemical process, etc. However, its application in building energy systems (especially the large centralized cooling systems) is very limited.

From the above review, it shows that very limited studies are done considering reliability of equipment/systems in the design process of HVAC systems. Comprehensive design optimization considering both demand uncertainty and equipment reliability is far from sufficient.

2.5 Summary

This chapter presents a review on the application of DCSs, uncertainty study and reliability assessment in building energy systems. From the above review, the following gaps can be summarized:

i. Performance assessment of DCSs compared with ICSs in subtropical areas needs further study. Performance of DCSs with different sustainable energy technologies needs to be estimated;

ii. Studies are not sufficient yet on the design optimization of the central cooling plant in both DCSs and ICSs considering uncertainty. Uncertainties in the cooling load of DCSs are not studied yet, which can affect the design optimization of DCSs.

iii. Reliability assessment is rarely considered in the design optimization of both DCSs and ICSs;

Therefore, this study attempts to improve the design of DCSs and ICSs after performance assessment and comparison. Improved design methods will be proposed for both DCSs and ICSs by involving uncertainty and reliability.

CHAPTER 3 DCS FOR A NEW DEVELOPMENT AREA AND PRELIMINARY PERFORMANCE ANALYSIS

This chapter introduces a DCS project for a new development area in Hong Kong. The planning information from the government is presented. The DCS is designed based on the planning and hypothesis. A feasibility study is conducted to investigate the performance of the DCS with different technologies, which aims to deal with the excessive peak electricity demand after adding the new district. Three technologies are studied, including the thermal storage system, PHES and CCHP system.

3.1 New development areas of North East New Territories

Developing new areas is one of the ten major infrastructure projects in Hong Kong, which aims to address the long-term housing demand and provide employment opportunities. The new development area in the district of North East New Territories includes Kwu Tung North, Fanling North and Ping Che/Ta Kwu Ling (CEDD 2015), as shown in Fig. 3.1. The new development area locates at the border between Hong Kong and another city, Shenzhen.

The new development area concerned covers a total area of 787 ha (1ha=10000m^2) and is proposed to accommodate a population of about 152,000 and to provide new job opportunities of more than 52,000 after full development. The development is intended to address the long-term housing demand and provide employment for the next 20 to 30 years. The new development area will be developed for multiple purposes, including housing, education and community facilities, improvement of the rural environment, better protection of resources of high conservation value and timely

development of land for special industries with clean industrial processes (ARUP 2015). The district of Kwu Tung North is investigated in this study. The DCS is planned to supply cooling for this new area.

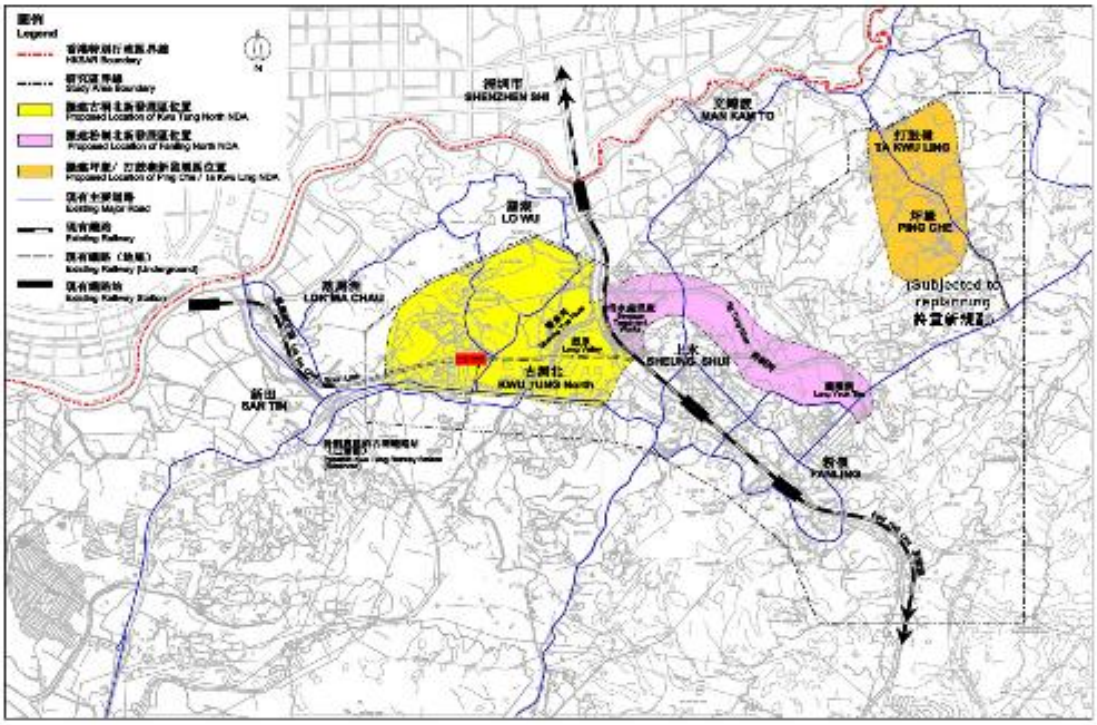

Fig. 3.1 Location of the new development areas (colored areas)

The initial planning from the government is shown in Fig. 3.2. It shows that various buildings will be planned, including:

1) Residential zones and public rental housing;
2) Public facilities such as the green belt, petrol filling station, refuse collection point, hospitals, schools, metro stations, post offices;
3) Commercial buildings like hotels, commercial centers, shops, administration buildings, immigration buildings, banks, etc.

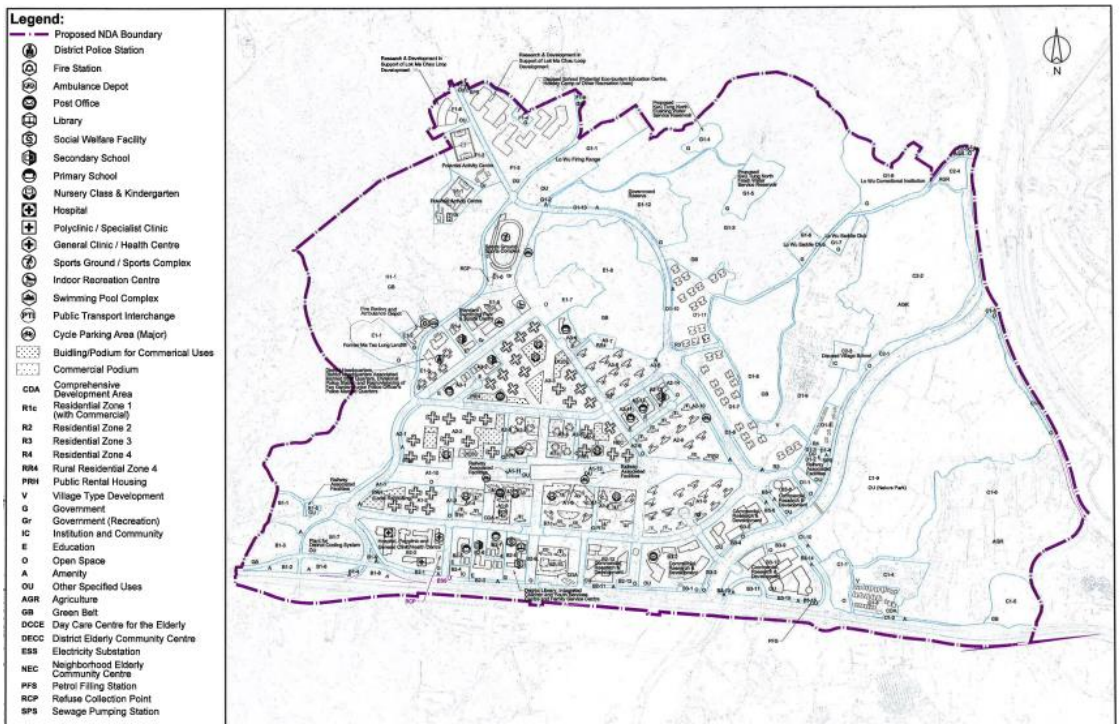

Fig. 3.2 District plan of Kwu Tung North

3.2 Users and cooling load prediction of the DCS

Although both residential and commercial buildings are to be constructed in this area, only public and commercial buildings will be connected to the DCS. Users of the DCS include hospitals, schools, metro stations, hotels, research centers, shops, post offices, administration buildings, immigration buildings, banks, commercial centers, etc. Totally 37 buildings are involved. The cooling loads of all these buildings are estimated using a Transient System Simulation program (TRNSYS). The cooling load index for each building is shown in Table 3.1, which is calculated by dividing the peak cooling load with the floor area of each building.

Table 3.1 Cooling load indices for 37 buildings connected to the DCS in the district

No.	Building Name	Building Area (m^2)	Cooling Load Index (W/m^2)	No.	Building Name	Building Area (m^2)	Cooling Load Index (W/m^2)
1	Sickroom Building	38100	127.45	20	Shops	5032	256.57
2	Doctor's Building	18900	200.38	21	Research Building	17136	147.74
3	Operation Building	21600	211.51	22	Hotel	26180	174.95
4	Sickroom Building	12240	189.96	23	Research Building	25056	226.85
5	Health Center	27360	321.63	24	Post Office	4160	139.63
6	Primary School	12672	194.93	25	Bank Building	9216	140.13
7	Teacher's Office	1248	221.72	26	Office Building	17664	148.61
8	Library	2496	300.01	27	Office Building	65600	141.57
9	Classroom	9984	136.96	28	Gym	11000	317.31
10	Teacher's Office	1872	182.81	29	Immigration Building	10176	163.32
11	Library	1872	345.02				
12	Secondary School	12528	194.84	30	Commercial Building	24964	329.60
13	Teacher's Office	2808	149.71				
14	Library	2106	210.27	31	Office building	35616	144.28
15	Children and Youth Center	9720	257.74	32	Commercial Building	24696	281.96
16	District Library	15540	237.59	33	Research Building	26000	137.76
17	Family Center	15080	199.40	34	Hotel	117552	153.79
18	Commercial Building	64800	237.51	35	Administrative Building	62496	164.79
19	Commercial Building	25200	306.27	36	Railway Station	8400	310.77
				37	Railway Station	6800	307.16

For a typical week in summer, the cooling loads for typical buildings are shown in Fig. 3.3. It shows that the cooling loads of office buildings during weekends are lower than that during weekdays. However, for hotels and commercial centers, the cooling loads during weekends are larger due to higher occupant density. For most of the buildings, the cooling loads at night are lower than that at daytime while the hotels have higher loads during night time because they have more occupants at night.

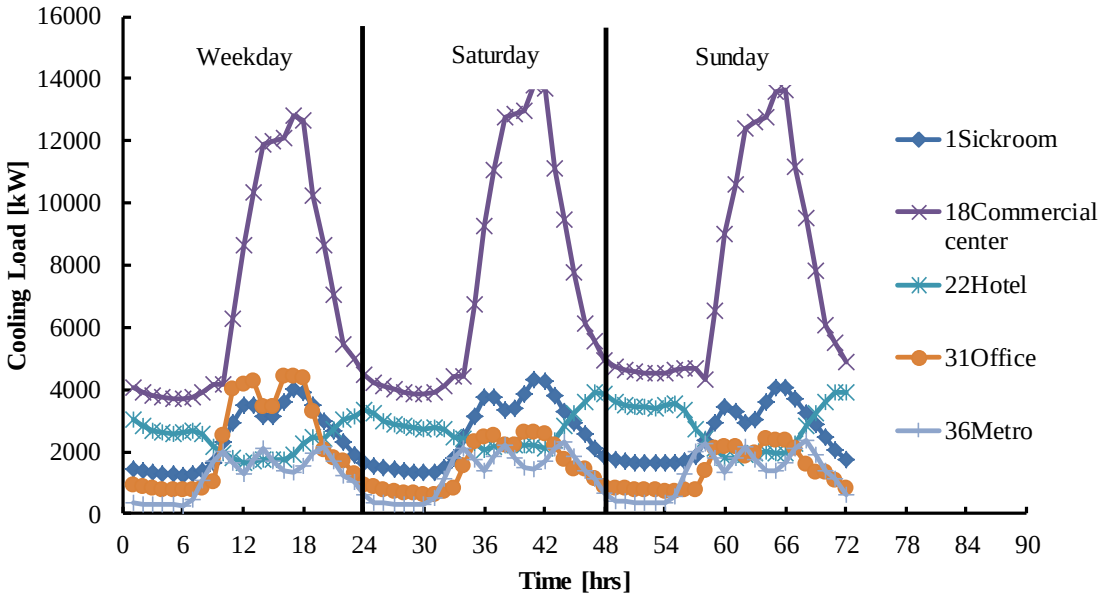

Fig. 3.3 Cooling loads of typical buildings in a typical week in summer

The cooling load of the entire new development district is shown in Fig. 3.4. It shows that buildings need cooling almost all the year because of the subtropical climate. The maximum cooling load is 107224 kW. Based on the peak cooling load, a DCS can be designed. The electricity load is also calculated and shown in Fig. 3.5. Performance of the DCS with different technologies can be obtained.

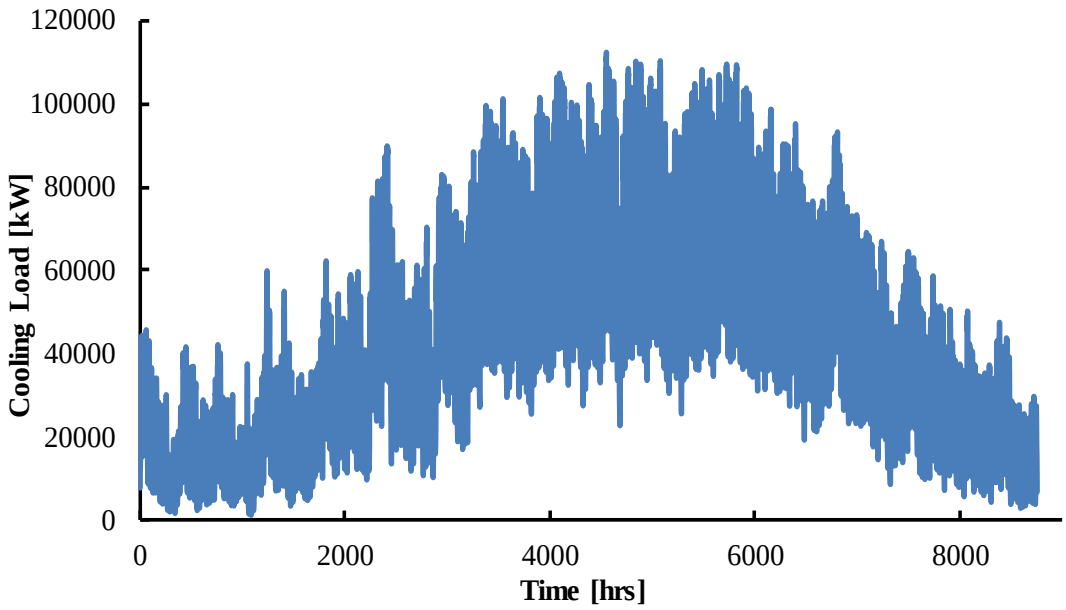

Fig. 3.4 Annual hourly cooling load of Kwu Tung North district

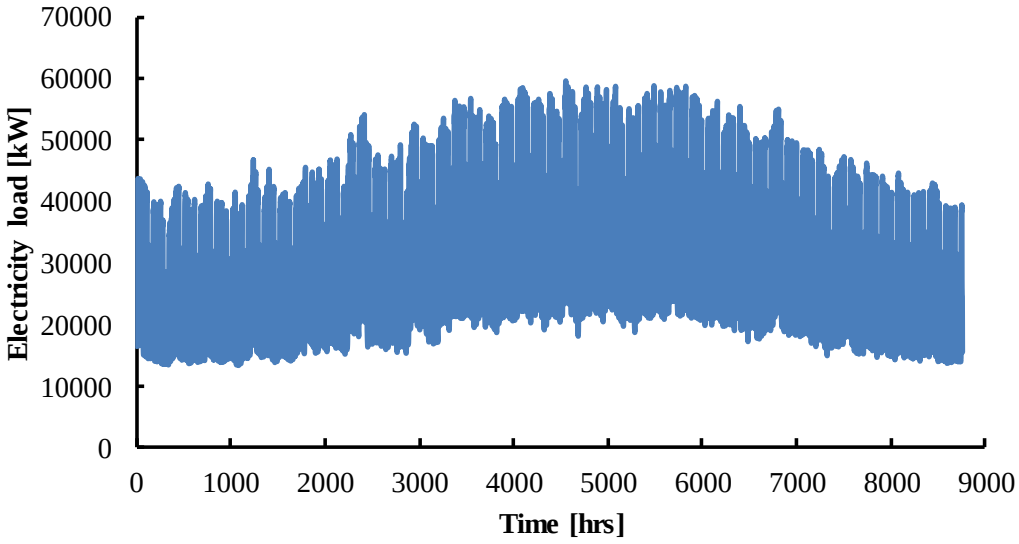

Fig. 3.5 Annual hourly total electricity load of the 37 buildings in the new development area

3.3 Performance analysis of the DCS with multiple energy technologies

By adding a new district accompanying with increasing population, the electricity demand of the entire city will be largely increased due to new buildings and facilities. It definitely will result in the increased load to the existing power station. Three ways can be used to deal with the peak demand of the grid, including thermal storage system, PHES and CCHP system. Performance assessment and comparison of the DCS with different technologies are shown in Fig. 3.6. Parameters used are shown in Table 3.2.

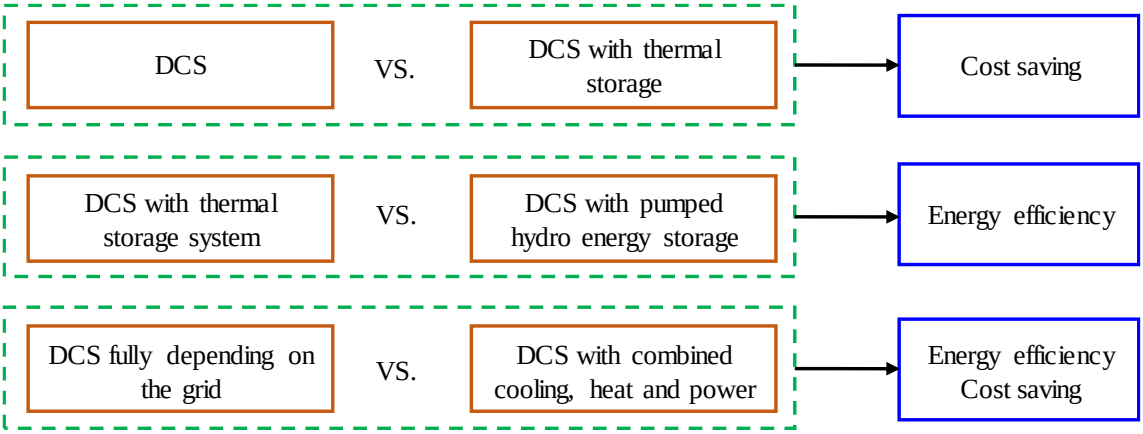

Fig. 3.6 Feasibility study of DCSs with different technologies

1) DCS with and without thermal storage systems

Using thermal storage system can help users to reduce the operation costs and the utility company will benefit from obtaining a more leveling demand profile. For the central cooling system, energy can be stored using ice or chilled water. Chilled water storage system requires much more space than the ice storage system. Thus, the ice storage system is used in this study.

Three methods can be used to design the ice storage system (ASHRAE 1993). One is full storage, which means all the cooling load during peak time is fully met by the ice storage system. The second is partial storage for load leveling. The basic chillers run

with a full capacity for 24 hours on the design day and the excessive cooling load is met by the ice storage system. The third one is partial storage for demand limiting. In such a system, the basic chillers work at a reduced capacity during the peak time. In this section, two methods are evaluated: full storage and partial storage for demand limiting.

2) DCS with pumped hydro energy storage vs. DCS with thermal storage system

PHES helps the power plant to generate electricity during the peak time while thermal storage system helps transfer the thermal demand during peak time to the off-peak time. Both are very effective in addressing the peak load issues. The one with higher efficiency should be preferred if the government wants to reduce the primary energy consumption or achieve low carbon district/city. Primary energy consumptions of the PHES and thermal storage system are compared and analyzed. A sensitivity study on the efficiencies of both systems is conducted.

3) DCS with and without combined cooling, heat and power system

DCS with CCHP supplies the district cooling, heat and electricity simultaneously. Two ways can be used to size the CCHP system, both of which are considered in this study. One is based on the thermal demand, where the plant should supply sufficient heating/cooling to the users. In this study, the cooling demand should be met firstly. If there is surplus electricity, CCHP system can send to the grid. If the electricity cannot meet the demand of the district, electricity should be drawn from the grid. The other is based on the electricity demand, where the system is sized to meet the electricity demand of the district. If the cooling produced by absorption chillers cannot meet the cooling demand, electricity-driven chillers should be started.

The efficiencies of the DCS with and without CCHP system used in the cooling dominated areas are compared. Primary energy consumptions of both systems to supply the same amount of cooling, heat and power are compared. Costs of the DCS with CCHP system at different prices of the primary energy are assessed and the payback periods are calculated.

Table 3.2 Parameters for models used in the simulation

Parameters	Values
Thermal storage system	
COP of the ice storage system COP_{ice}	3
PHES	
Electricity generation efficiency η_{ele}	0.38
Transportation efficiency of electricity from power plants to users η_{tran}	0.93
Electricity distribution efficiency η_{PHES}	0.95
CCHP	
Efficiency for electricity generation E_{ele}	0.3
Percentage of heat used for absorption chillers E_{cool}	0.4
Percentage of heat used for heating/hot water E_{heat}	0.2
Percentage of heat loss E_{loss}	0.1
COP for absorption chillers COP_{abs}	1.1
Electricity generation efficiency for DCS without CCHP E_{grid}	3.5

3.4 DCS with thermal storage system

Two tariffs are used in the economic performance assessment of the DCS with thermal storage system. One is a tariff in Hong Kong (CLP 2014), where the utility company gives special incentive for users using ice storage system, as shown Table 3.3. It can be seen that the total charge (EC_{total}) includes the demand charge (EC_{demand}), energy

usage charge (EC_{energy}) and fuel clause (EC_{fuel}), as shown in Eq. (3-1). The second is a tariff in Guangzhou, which is a city of similar climate and close to Hong Kong. The utility company in Guangzhou (China Southern Power Grid, 2015) also has a special tariff to reduce the peak load of the grid, as shown in Table 3.4. For commercial buildings with ice storage system, the tariff of residential buildings is used. Here the tariff for commercial and residential users is listed. It can be seen that the cost is determined by the energy usage and the time of the day. Costs under the tariff in Guangzhou are also calculated to investigate the effects of tariffs.

$$EC_{total} = EC_{demand} + EC_{energy} + EC_{fuel} \quad (3\text{-}1)$$

Table 3.3 Tariff for different users in Hong Kong

Tariff type	**Item**				
	Demand charge ($/kVA)		**Energy charge ($/kWh)**		**Fuel clause($/kWh)**
	peak period	**off-peak period**	**peak period**	**off-peak period**	**all the time**
General Service Tariff	0	0	0.124 (first 5000 kWh) 0.123 (exceeding part)	0	0.029
Bulk Tariff (monthly no less than 20,000 kWh)	8.41 (first 650)	0 (less than the on-peak peak)	0.086 (first 200,000)	0.077	0. 029
	8.03 (exceeding part)	3.29 (larger than the on-peak peak)	0.084 (exceeding part)		
Large Power Tariff(monthly no less than 3000 kVA)	14.79 (first 5000)	0.0 (less than the on-peak peak)	0.065(first 200 kWh/kVA)	0.053	0. 029
	14.17 (exceeding part)	4.17 (exceeding part)	0.0625 (exceeding part)		
Ice-Storage Air-Conditioning Tariff	8.41 (first 650)	0 (less than the on-peak peak)	0.086 (first 200,000)	0.077	0. 029
	8.03 (exceeding part)	3.29 (larger than the on-peak peak)	0.084 (exceeding part)		

Note: *Off-peak time: Monday-Saturday: 9:00 pm-9:00 am next day, Sunday and Public Holiday*

Peak time: Rest time excluding off-peak time

Table 3.4 Tariff for different users in Guangzhou

Users	Limitation		Price(Cent/kWh) Base price	Renewable energy surcharge	City construction surcharge	Large water conservation project fund	Reservoir tranfer fund	Total
Commercial user	<1000kv		15.7	0.2	0.24	0.1	0.1	16.4
	1-10kv		15.3	0.2	0.24	0.1	0.1	16.0
	20kv		15.2	0.2	0.24	0.1	0.1	15.9
	>=35kv		14.9	0.2	0.24	0.1	0.1	15.6
Residential user	Multi-step	First step	9.4	-	0.24	0.1	0.1	9.8
		Second step	10.2	-	0.24	0.1	0.1	10.6
		Thrid step	14.2	-	0.24	0.1	0.1	14.7
	Time of use	Peak time	15.5	-	0.24	0.1	0.1	15.9
		Intermediate-peak time	9.4	-	0.24	0.1	0.1	9.8
		Off-peak time	4.7	-	0.24	0.1	0.1	5.2

Note: *Peak time: 14:00-17:00, 19:0-22:00; Intermediate-peak time: 8:00-14:00, 17:00-19:00, 22:00-24:00; Off-peak time: 0:00-8:00*

3.4.1 Costs of DCS with full ice storage system

In the DCS with full ice storage system, chilled water pumps are the only components that consume electricity during the peak time. Costs of the system under Hong Kong tariff are shown in Table 3.5. It can be seen that the demand charge decreases significantly while the energy charge increases largely for the DCS with full ice storage system. The unitary cost decreases from 0.13 to 0.12 ($/kWh) due to the lower electricity price during the off-peak time. The total annual operation cost increases by 27.4%. It indicates that the full ice storage system is not economic efficient under the current tariff in Hong Kong. The investment on the full ice storage system cannot be paid back.

Table 3.5 Annual operation costs of the DCS with and without full ice storage system under Hong Kong tariff

	Demand ($\times 10^6$\$)	**Energy ($\times 10^6$\$)**	**Fuel ($\times 10^6$\$)**	**Total ($\times 10^6$\$)**	**Average cost ($/kWh)**
DCS without ice storage	3.25	5.09	2.46	10.81	0.13
DCS with full ice storage	1.49	8.93	3.35	13.77	0.12

The operation costs under Guangzhou tariff are shown in Table 3.6. It can be seen that the operation cost for DCS with ice storage system is largely reduced. When the cooling during the peak time is met by the ice storage system, the operation cost is about 18% less than that without ice storage system. If the cooling at both peak time and intermediate-peak time is met by the ice storage system, the annual cost is about 22% less than that without ice storage system. It shows that the DCS with ice storage system under Guangzhou tariff is very beneficial. The incentive is not so attractive for using ice storage system in Hong Kong. If the utility company wants to reduce the

peak load of the power plant significantly, current tariff should be revised and the difference between electricity prices during the peak time and the off-peak time should be enlarged.

Table 3.6 Annual operation costs for the DCS with and without ice storage system under Guangzhou tariff

	Peak time ($\times 10^6$\$)	**Intermediate –peak time ($\times 10^6$\$)**	**Off-peak time ($\times 10^6$\$)**	**Total ($\times 10^6$\$)**	**Average cost (\$/kWh)**
No storage	0.80	3.85	4.17	8.82	0.10
Ice storage for peak time	2.65	3.85	0.75	7.25	0.07
Ice storage for peak and intermediate-peak time	5.43	0.69	0.75	6.87	0.05

3.4.2 Costs of DCS with partial ice storage system for demand limiting

The charge for electricity consumption is calculated monthly in Hong Kong. The aim of using ice storage system therefore is to reduce the monthly operation cost. Firstly the cooling load profile of next month is predicted based on modelling. The maximum operation chillers can be obtained based on the predicted cooling load. Several chillers will be switched off during the peak time to reduce the peak electricity demand. Exact number of chillers to be off is determined by checking the load profile of the month, which can be taken as the profile of numbers of operating chillers. The best is to reduce the peak electricity demand largely without consuming too much extra energy. Results of the DCS with ice storage system for demand limiting are shown in Fig. 3.7.

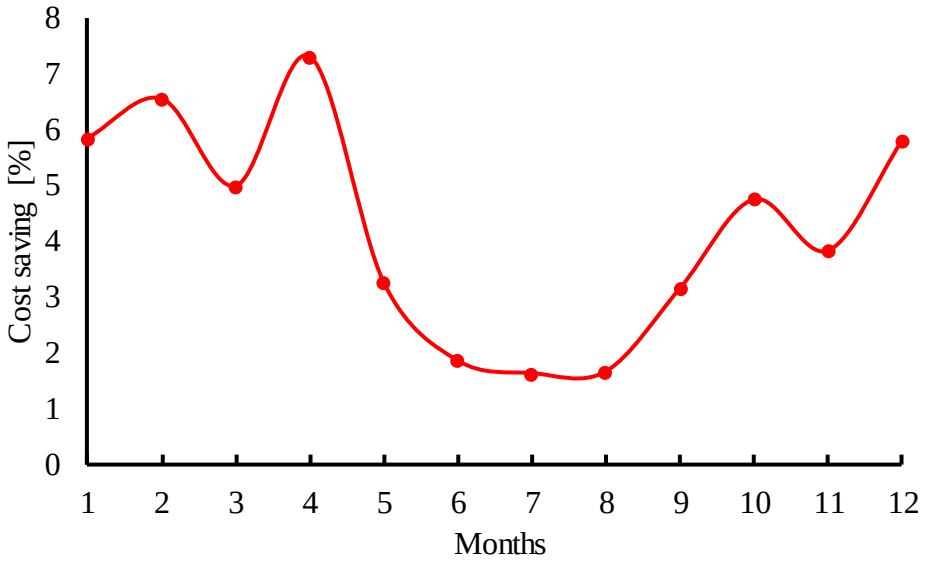

Fig. 3.7 Monthly operation cost saving of the DCS with partial ice storage system for demand limiting

Fig. 3.7 shows that more cost saving is achieved during January, February, March, April, October and December. All these months are in the mild seasons of a year when the cooling load is relatively low. During the hot summer, the cost saving is not very high. It is because the cooling load keeps high in the summer. The duration requiring more running chillers is long. Much more energy is consumed to store cooling during the off-peak time to meet the cooling need during the peak time. The saving is compensated by the extra energy charge. The annual cost saving of the DCS with partial ice storage for demand limiting is about 4%, which is much more promising compared with the DCS with full ice storage system.

3.5 DCS with PHES *vs.* DCS with thermal storage system

Part of electricity in Hong Kong is supplied from a nuclear power station. The PHES plant locating in a nearby city helps coordinate the mismatch of the electricity demand and supply. The schematic diagram of a PHES is shown in Fig. 3.8 (Wikipedia 2015). The energy flow for a typical PHES can be illustrated in Fig. 3.9. The primary energy

is transferred into electricity with an efficiency of η_{ele}. During the off-peak time, water is pumped from a lower reservoir and to the higher one. During the peak time, water is released to drive the turbines. The PHES can generate electricity with an efficiency of η_{PHES}. Then the electricity is transported and distributed to users from the power plant with a transportation efficiency η_{tran} and a distribution efficiency η_{dist}. After that, electricity is used to produce cooling by driving normal electrical chillers with a COP COP_b. For the thermal storage system, the processes are similar excluding the PHES part. The COP of thermal storage system COP_{tes} differs from that of normal cooling systems. Parameters used in this study are listed in Table 3.2. The η_{PHES} and COP_{tes} play an important role in determining the priority of both systems so sensitivity study is conducted on both parameters.

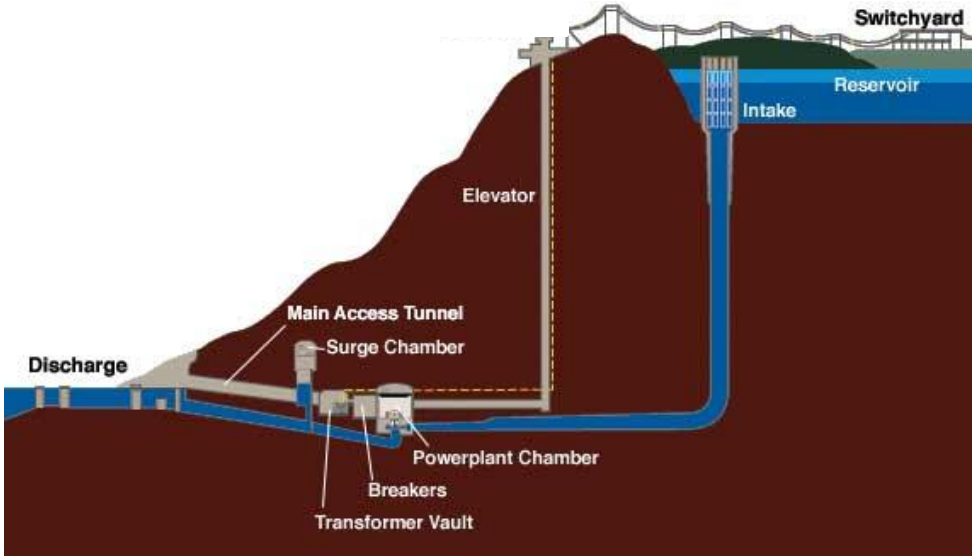

Fig. 3.8 Schematic diagram of a PHES

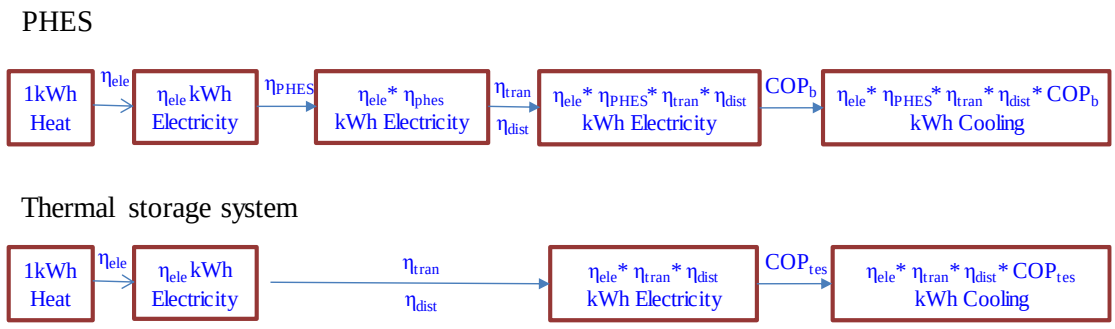

Fig. 3.9 Energy flow for PHES and thermal storage system

The performance of DCS with PHES and thermal storage system is obtained based on the energy flow in Fig. 3.9 and parameters in Table 3.2. Previous research shows that the system with thermal storage is much more efficient than the system with PHES and it can produce more cooling (MacCracken 2010). When the efficiency of PHES is 70% and the overall COP of the thermal storage system is 3.5, the system with thermal storage produced 1.24 kWh cooling while the system with PHES produced 0.91 kWh cooling, using 1 kWh heat from the primary energy. The efficiency of the system with PHES and that with thermal storage are important to determine priority of both systems. Sensitivity study on the performance of the systems using PHES and thermal storage is conducted by changing the efficiencies of both systems.

The difference between cooling energy produced by DCS with PHES and DCS with thermal storage using unitary primary energy is shown in Table 3.7. The negative values mean that the DCS with thermal storage system can produce more cooling than that with PHES. The positive value means that the DCS with PHES can produce more cooling. It shows that if the COP of the DCS with thermal storage is lower than 2.3, the DCS with PHES will always be more efficient. When such a COP is 3 (which is often used in literature) and the efficiency of PHES is 0.75 (which is also often used in literature), the system with thermal storage is hardly efficient compared with the

system with PHES. This conclusion is significantly different from that of previous research.

With such a table, the choice between PHES and thermal storage can be made if the primary aim is to reduce the energy consumption. For the PHES, the capital cost is very high and the project can be very large. However, once it is constructed, it will be very beneficial for users. For thermal storage system, its scale is much smaller and it can be installed very flexibly.

Table 3.7 Cooling prodcution difference between the systems using PHES and thermal storage system using unitary primary energy

		COP of ice storage system															
		2	2.1	2.2	2.3	2.4	2.5	2.6	2.7	2.8	2.9	3	3.1	3.2	3.3	3.4	3.5
Efficiency of PHES	0.6	0.098	0.063	0.027	**-0.008**	**-0.044**	**-0.079**	**-0.114**	**-0.150**	**-0.185**	**-0.220**	**-0.256**	**-0.291**	**-0.327**	**-0.362**	**-0.397**	**-0.433**
	0.62	0.125	0.090	0.054	0.019	**-0.017**	**-0.052**	**-0.087**	**-0.123**	**-0.158**	**-0.194**	**-0.229**	**-0.264**	**-0.300**	**-0.335**	**-0.371**	**-0.406**
	0.64	0.152	0.116	0.081	0.046	0.010	**-0.025**	**-0.061**	**-0.096**	**-0.131**	**-0.167**	**-0.202**	**-0.237**	**-0.273**	**-0.308**	**-0.344**	**-0.379**
	0.66	0.179	0.143	0.108	0.072	0.037	0.002	**-0.034**	**-0.069**	**-0.104**	**-0.140**	**-0.175**	**-0.211**	**-0.246**	**-0.281**	**-0.317**	**-0.352**
	0.68	0.205	0.170	0.135	0.099	0.064	0.029	**-0.007**	**-0.042**	**-0.078**	**-0.113**	**-0.148**	**-0.184**	**-0.219**	**-0.255**	**-0.290**	**-0.325**
	0.7	0.232	0.197	0.162	0.126	0.091	0.055	0.020	**-0.015**	**-0.051**	**-0.086**	**-0.122**	**-0.157**	**-0.192**	**-0.228**	**-0.263**	**-0.298**
	0.72	0.259	0.224	0.188	0.153	0.118	0.082	0.047	0.011	**-0.024**	**-0.059**	**-0.095**	**-0.130**	**-0.165**	**-0.201**	**-0.236**	**-0.272**
	0.74	0.286	0.251	0.215	0.180	0.145	0.109	0.074	0.038	0.003	**-0.032**	**-0.068**	**-0.103**	**-0.139**	**-0.174**	**-0.209**	**-0.245**
	0.76	0.313	0.278	0.242	0.207	0.171	0.136	0.101	0.065	0.030	**-0.006**	**-0.041**	**-0.076**	**-0.112**	**-0.147**	**-0.182**	**-0.218**
	0.78	0.340	0.304	0.269	0.234	0.198	0.163	0.127	0.092	0.057	0.021	**-0.014**	**-0.049**	**-0.085**	**-0.120**	**-0.156**	**-0.191**
	0.8	0.367	0.331	0.296	0.260	0.225	0.190	0.154	0.119	0.084	0.048	0.013	**-0.023**	**-0.058**	**-0.093**	**-0.129**	**-0.164**
	0.82	0.393	0.358	0.323	0.287	0.252	0.217	0.181	0.146	0.110	0.075	0.040	0.004	**-0.031**	**-0.067**	**-0.102**	**-0.137**
	0.84	0.420	0.385	0.350	0.314	0.279	0.243	0.208	0.173	0.137	0.102	0.066	0.031	**-0.004**	**-0.040**	**-0.075**	**-0.110**
	0.86	0.447	0.412	0.376	0.341	0.306	0.270	0.235	0.200	0.164	0.129	0.093	0.058	0.023	**-0.013**	**-0.048**	**-0.084**
	0.88	0.474	0.439	0.403	0.368	0.333	0.297	0.262	0.226	0.191	0.156	0.120	0.085	0.049	0.014	**-0.021**	**-0.057**
	0.9	0.501	0.466	0.430	0.395	0.359	0.324	0.289	0.253	0.218	0.182	0.147	0.112	0.076	0.041	0.006	**-0.030**

3.6 DCS with CCHP system

DCS with CCHP system supplies cooling, heat and power to the users in the district. Heat produced by the primary energy is used in four means, as shown in Eq. (3-2~5). The actual values of coefficients used in this study are shown in Table 3.2 and they meet the constraint given by Eq. (3-6). Absorption chillers are used to generate cooling with waste heat after electricity generation. The COP of absorption chillers (Eq. (3-7)) is assumed to be 1.1.

$$E_{ele}=\frac{Heat\ for\ generating\ electricity}{Total\ heat\ of\ the\ primary\ energy} \tag{3-2}$$

$$E_{cool}=\frac{Heat\ for\ absorption\ chillers}{Total\ heat\ of\ the\ primary\ energy} \tag{3-3}$$

$$E_{heat}=\frac{Heat\ for\ heating\ or\ hot\ water}{Total\ heat\ of\ the\ primary\ energy} \tag{3-4}$$

$$E_{loss}=\frac{Heat\ loss\ of\ the\ CCHP\ system}{Total\ heat\ of\ the\ primary\ energy} \tag{3-5}$$

$$E_{ele} + E_{cool} + E_{heat} + E_{loss} = 1 \tag{3-6}$$

$$COP_{abs}=\frac{Cooling\ energy\ produced}{Heat\ used\ by\ absorption\ chillers} \tag{3-7}$$

The comparison of DCS with and without CCHP system is conducted on two aspects: energy efficiency and cost. Therefore, the electricity generation efficiency of DCS without CCHP system (E_{grid}) is required and assumed to be 3.5. Primary energy consumptions of both systems to supply the same amount of cooling, heating and electricity are evaluated. The operation costs for DCS with and without CCHP system ($Cost_{CCHP}$, $Cost_{grid}$) are determined by the prices of primary energy (P_{gas}) (which is natural gas in this study). Costs for electricity from the grid are calculated based on primary energy used by the power plant when generating the electricity. The payback

period (*Pb*) of the DCS with CCHP system can be obtained using Eq. (3-8), where $Cost_{CAP}$ is the capital cost of the CCHP system.

$$Pb=\frac{Cost_{CAP}}{Cost_{grid} - Cost_{CCHP}} \tag{3-8}$$

3.6.1 Energy performance analysis

Performance of DCS with CCHP system compared with the DCS fully depending on the grid is shown in Table 3.8. It can be seen that when the DCS integrated with CCHP system is designed based on thermal demand, the integrated system saves 8.5% of the primary energy, if no hot water is required in this district. 8.1% of primary energy is saved if the integrated system is designed based on the electricity demand. When the DCS integrated with CCHP system and the DCS fully depending on the grid produce the same amount of cooling, hot water and electricity, the primary energy saving for the integrated system can be more than 17%. It indicates that the CCHP system is very energy efficient when it is used in the cooling dominated areas.

Table 3.8 shows that the energy saving changes largely when the use of hot water changes. A sensitivity study therefore is conducted to investigate the effects of hot water use on the energy saving potential of DCS with CCHP. The annual energy of hot water produced by the DCS with CCHP system designed based on thermal demand is 83(10^6 kWh). The actual required heat for water can be lower or higher than that. Energy saving of the integrated system is investigated when the required amount of hot water changes and the results are shown in Fig. 3.10. For the DCS without CCHP system, the hot water is obtained directly using water heater with a primary energy efficiency of 0.8. Fig. 3.10 shows that the energy saving of the DCS with CCHP

system increases with the increased hot water demand. The saving is up to 18%. If the hot water demand is higher than that produced from the CCHP, the saving decreases.

Table 3.8 Energy consumption for the DCS with and without CCHP system

	DCS with CCHP		**DCS fully depending on grid**	
	Thermal demand based	*Electricity demand based*	*Thermal demand based*	*Electricity demand based*
Electricity generated by CCHP (10^6 kWh)	250	202	/	/
Surplus electricity (10^6 kWh)	47	/	/	/
Electricity from grid (10^6 kWh)	0	13		271
Hot water (10^6 kWh)	83	67	/	/
Gas used by CCHP to meet the cooling and electricity demand (10^6 m^3)	83	67	/	/
Gas used by grid to meet the cooling and electricity demand (10^6 m^3)	/	3.7	77	77
Gas used by grid to supply the same amount of cooling and electricity (10^6m^3)			91	77
Gas used by CCHP to produce equivalent cooling, hot water and electricity (10^6m^3)	83	71	/	/
Gas used by the grid to produce equivalent cooling, hot water and electricity (10^6m^3)	/	/	101	86
Primary energy saving to meet the cooling and electricity demand	8.5%	8.1%	/	/
Primary energy saving to produce equivalent cooling, hot water and electricity	18%	17%	/	/

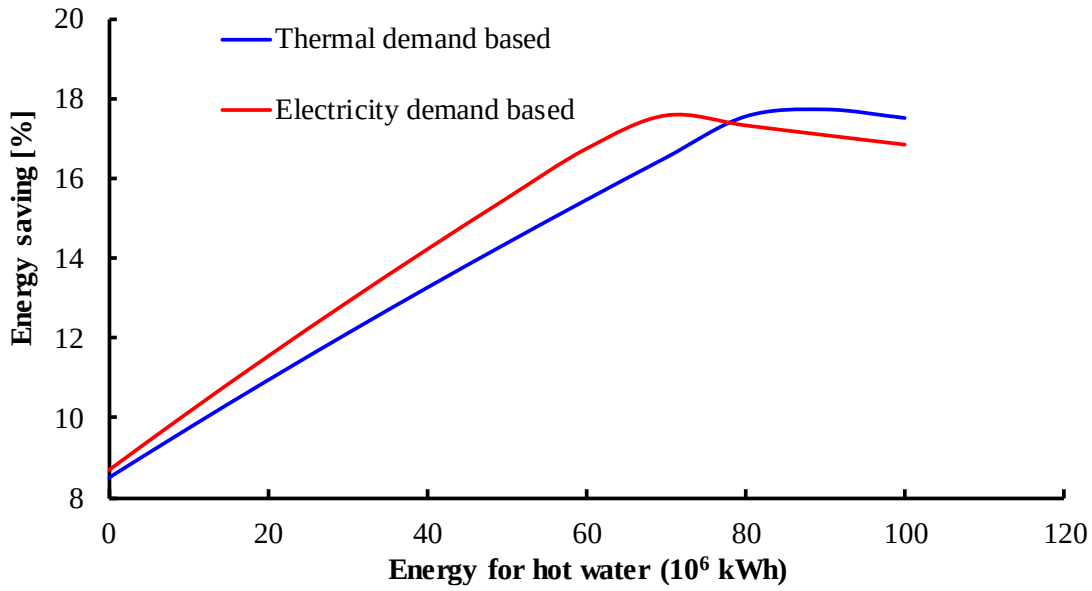

Fig. 3.10 Energy saving of DCS with CCHP system under different hot water demands

3.6.2 Economic performance analysis

The economic performance of the DCS with CCHP system is evaluated and compared with the DCS without CCHP, as shown in Table 3.9. The capital cost of CCHP ($Cost_{CAP}$), is calculated using a price of 1600 $/kW. The capital cost of the CCHP for the district designed based on thermal energy demand is much larger than that designed based on electricity demand. When hot water is not used in the district (which is the most unfavorable scenario), operation costs and payback periods are calculated. When the cost is evaluated under the natural gas price in Hong Kong, the investment costs on the integrated system designed based on electricity demand and thermal energy demand are paid back in 9.7 and 14.7 years respectively. The economic performance of the integrated system under the lower natural gas price in Guangzhou is also assessed. The investment costs are paid back in 18.1 years and 27.5 years respectively for the DCS with CCHP system designed based on electricity demand and thermal demand respectively.

Table 3.9 Economic analysis of the DCSs with and without CCHP system

Items		No hot water		Equivalent hot water for DCS with and without CCHP	
		Electricity demand based	Thermal demand based	Electricity demand based	Thermal demand based
Capital cost of CCHP $Cost_{CAP}$ *(10^6\$)*		65.4	122.6	65.4	123.0
Capital cost of extra power plant (10^6\$)		24.5	46.4	24.5	46.4
Hong Kong	*Gas price* P_{gas} *(\$/MJ)*	*0.03*	*0.03*	*0.03*	*0.03*
	Annual operation cost of DCS with CCHP $Cost_{CCHP}$ *(10^6\$)*	76.9	84.2	76.9	84.2
	Annual operation cost of DCS without CCHP $Cost_{grid}$ *(10^6\$)*	83.6	83.6	92.7	109.4
	Payback period Pb (year)	9.7	14.7	4.1	6.3
	Payback period concerning power plant cost (year)	6.0	9.2	2.6	3.9
Guangzhou	*Gas price ($/MJ)*	0.016	0.016	0.016	0.016
	Annual operation cost of DCS with CCHP $Cost_{CCHP}$ *(10^6\$)*	40.9	40.3	40.9	40.3
	Annual operation cost of DCS without CCHP $Cost_{grid}$ *((10^6\$)*	44.6	44.6	49.5	58.4
	Payback period Pb (year)	18.1	27.5	7.7	11.7
	Payback period concerning power plant cost (year)	11.3	17.2	4.8	7.3

When the hot water produced by the CCHP system is fully used by the district (which is the most favorable scenario), under the price in Hong Kong, the investment costs of DCS with CCHP system are paid back in 4.1 and 6.3 years based on electricity demand and thermal demand respectively. Under the price in Guangzhou, the investment costs of DCS with CCHP are paid back in 7.7 and 11.7 years for the same systems

respectively. The payback periods are much shorter than that with no hot water demand.

One extra advantage of using CCHP system is that the need of power plant expansion is avoided. It can save the utility company considerable capital investment on power plant expansion. Further economic assessment is made by assuming the capital cost for the power plant of the utility as 600 $/kW. The capital cost of extra power plant for the district is obtained and the payback periods of the CCHP system when capital costs of extra power plant are concerned are shown in Table 3.9 as well. Under the natural gas price in Hong Kong, the payback period ranges from 2.6 to 6 years for the system design based on electricity demand. It ranges from 3.9 to 9.2 years for the system designed based on thermal demand. Under the natural gas price in Guangzhou, the payback period ranges from 4.8 to 11.3 years for the system design based on electricity demand. It ranges from 7.3 to 17.2 years for the system designed based on thermal demand.

The above analysis shows that the DCS with CCHP system is also economic feasible under the current natural gas price in Hong Kong. The DCS with CCHP designed based on electricity demand is recommended due to its shorter payback period. It should be noticed that, when estimating the payback period for DCS with CCHP system, the operation costs of both the CCHP system and utility power plant are calculated using the consumptions of the same primary energy (i.e. natural gas) in this study. It is practically reasonable in Hong Kong as the utility companies are requested to use more natural gas for electricity generation. In fact, if coal is used by the power plant for electricity generation, which is very cheap now, the investment for CCHP system (using natural gas) is very hard to be paid back.

3.7 Summary

The performance of DCS is assessed in this chapter on the basis of a DCS project in Hong Kong. The DCS is designed based on the planning information from the government. Performance of the DCS with three technologies is evaluated when the peak demand by adding a new district is of concern. Thermal storage system is introduced to reduce the peak demand during the peak time. PHES can also be used to meet the peak demand of the entire city by producing electricity at the supply side. Results are compared with the thermal storage system. The results are very sensitive to the efficiency of both storage systems. Performance of the DCS with CCHP system is calculated and compared with the DCS fully depending on the grid. The following conclusions can be made:

i. Full ice storage system is not beneficial under current Hong Kong tariff because of much higher annual operation cost. It is very beneficial under Guangzhou's tariff The Hong Kong tariff should be revised and the difference of electricity prices at peak time and off peak time should be increased to promote the use of full ice storage system.

ii. The DCS with partial ice storage system for demand limiting can save around 4% of the annual operation cost, which is recommended in the application.

iii. The priority of the PHES and thermal storage system depends on the efficiencies of both systems. It is hard to conclude which one is better, which is different from the conclusion of former researchers. Detailed comparison and assessment are strongly recommended before the decision is made.

iv. The DCS integrated with CCHP system is more efficient than that fully depending on the power grid. The energy saving ranges between 8% and 18%. Hot water demand affects the energy saving and payback periods significantly. The integrated system designed based on electricity demand is recommended due to its short payback period.

CHAPTER 4 MODELING AND PERFORMANCE ASSESSMENT OF DCS AND ICS

This chapter aims to assess the performance of DCSs by comparing with ICSs for the new development area. Models used to simulate the DCS and ICS are introduced. Three types of DCSs and ICSs with different chilled water systems are studied. The performance of DCSs and ICSs is analyzed under different load ratios and weather conditions. Energy consumption and operation costs of two systems are compared on the basis of the local electricity tariff. Furthermore, the energy saving potential of DCSs at different partial loads during night time is also studied.

4.1 Performance assessment and comparison approaches

The DCS performance assessment method and steps are illustrated by the flowchart shown in Fig. 4.1. The assessment involves three major tasks, including system design, system modeling and result analysis. The detailed steps are listed as follows.

System design

- Collect the district plan information, including the building numbers, building heights and floors, building functions, envelop materials, etc.
- Plan the DCS based on the geography and geology of the district, including the numbers and locations of the central plants.
- Calculate the cooling loads of the buildings. Various types of buildings are involved and the cooling loads should reflect the typical characters of different buildings. Differences are introduced for the settings of buildings with similar functions. The DCSs and ICSs are designed based on common design practice.

The numbers and capacities of the cooling equipment are selected based on the cooling load.

System modelling:

- Each DCS and ICS consists of chillers, pumps, air handling units (AHU), cooling towers, etc. Models for main components are built based on the physical models or by fitting with data from manufactures. Models for the supplemental equipment are from the TRNSYS toolkit.
- Models of the entire systems are built by connecting and integrating all the components. Many sets of cooling equipment are selected in the ICSs. The parameters may vary for different buildings, like the nominal coefficient of performance (COP) of the chillers, the pump heads, the efficiencies of the pumps and the nominal powers of the cooling towers. The models in this study contain and embody such divergence.

Result analysis

- Analyze the results from the local and global views. Annual operation performance data are obtained from the virtual system. Global analysis is conducted including the energy and economic performance of the entire year and whole system.
- Local analysis is carried out by decomposing the data into several categories at the seasonal level, cooling load level and component level.

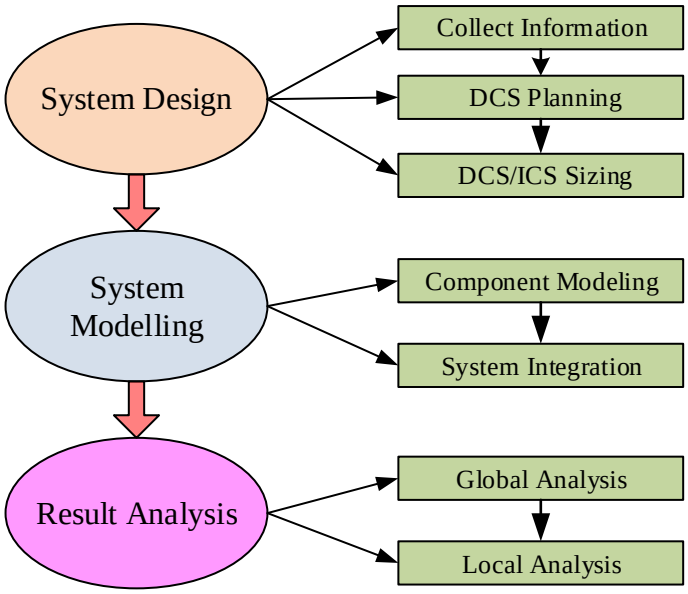

Fig. 4.1 Flowchart of the method used to assess the performance of a DCS

4.2 Preliminary design of the DCS and ICSs for a new development area

Three kinds of systems with different chilled water pump schemes are simulated and compared: constant primary flow chilled water system (CP), constant primary & variable secondary flow chilled water system (CPVS) and variable primary flow chilled water system (VP). The schematic diagram is shown in Fig. 4.2. The three different types of DCSs and ICSs are marked as DCS-CP, ICS-CP, DCS-CPVS, ICS-CPVS, DCS-VP, and ICS-VP for short.

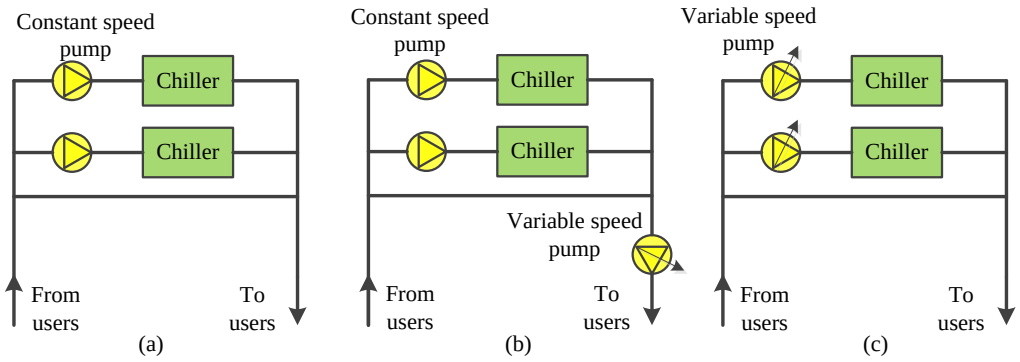

Fig. 4.2 Schematic diagram of systems with different chilled water systems

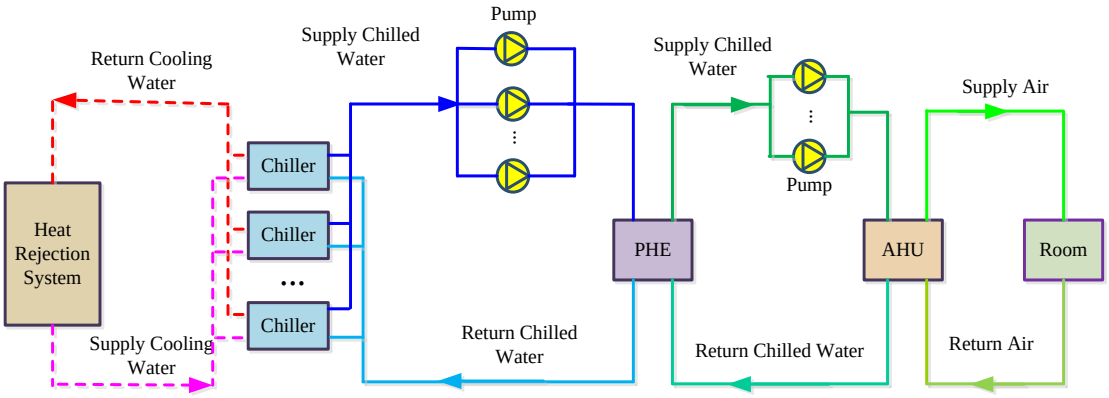

Fig. 4.3 Schematic diagram of a DCS with indirect connection with the end users

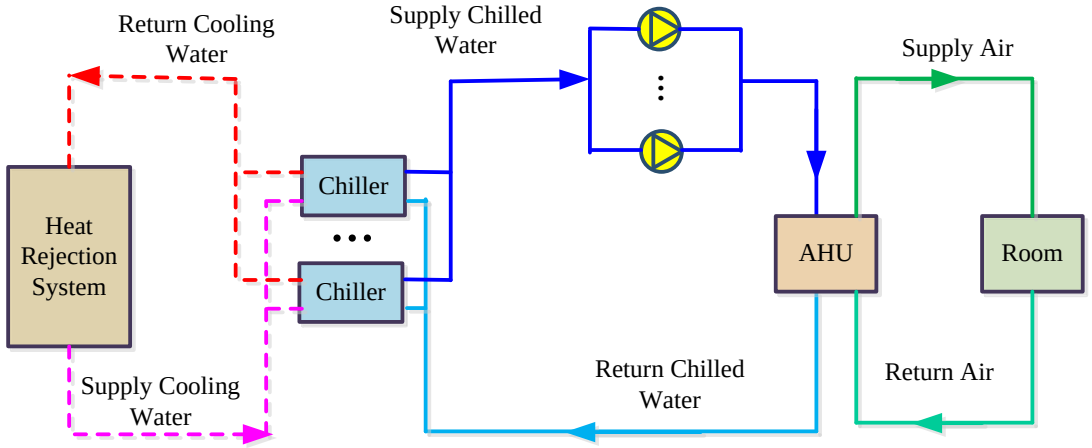

Fig. 4.4 Schematic diagram of an ICS with primary only chilled water system

According to the preliminary plan, cooling towers are adopted for heat rejection. In this study, all the DCSs and ICSs use water cooled chillers with cooling towers. The chillers are sized based on the maximum of the cooling load sum of all buildings in the district multiplied by a factor of 1.2 considering uncertainty in the climate and system design. For the DCS, 10 chillers with an individual capacity of 3400 tons are selected, together with 10 cooling water pumps, 10 cooling towers and 10 sets of chilled water pumps. For the ICSs, the chiller number ranges from 2 to 4 and one chiller corresponds to one cooling water pump, one cooling tower and one set of chilled water pumps. The chiller capacity ranges from 432 kW to 4900 kW. Constant speed cooling water pumps are selected. For the chilled water network, the buildings

in the new district are organized in tree shaped networks. The distance from the remote user to the central plant is about 1.2 km. The design supply and return temperatures are 7 ℃/12℃. Based on the location of buildings, the cooling load, the design temperature, the size of the pipes and resistance of the network can be determined. The pump head is selected based on the manual (ASHRAE 2012) and the detailed calculations details can be found in the manual. The detailed parameters for the pumps selected are shown in Table 4.1. The schematic diagram of the DCS and ICS is shown in Fig. 4.3 and Fig. 4.4.

Table 4.1 Cooling water pumps and chilled water pumps for different systems

System	Pump	CP	VP	CPVS
DCS	Primary chilled water pump head	55m	55m	15m
	Secondary chilled water pump head	N/A	N/A	45m
	Cooling water pump head	23m	23m	23m
ICS	Primary chilled water pump head	40~45	40~45	12~15m
	Secondary chilled water pump head	N/A	N/A	30~35m
	Cooling water pump head	18~20m	18~20m	18~20m

4.3 Models for the DCS and ICS

4.3.1 Chiller model

Centrifugal chillers are used in the systems. Their performance is simulated under different working conditions based on impeller tip speed, impeller exhaust area, impeller blade angle and other coefficients/constants, which are available from chiller technical data or identified using chiller performance data. Detailed modeling processes can be found in the reference (Wang 1998). Chillers with different capacities are selected and modelled. All the chillers are selected based on the given data from a major manufacturer. The nominal coefficient of performance (COP) may differ. For chillers with the capacity of over 1400 kW, the nominal COP is between 5.0 and 6.0. For chillers with medium capacity (between 500 kW and 1400 kW), the nominal COP is between 4.5 and 5.0. For small chillers with a capacity of below 500 kW, the nominal COP is about 4. Detailed parameters are not introduced one by one. The performance curve of the chillers in DCS is presented here as an example, as shown in Fig. 4.5. It can be found that the COP increases gradually with the increase of part load ratio and it reaches the maximum of 6.0 at around 80%.

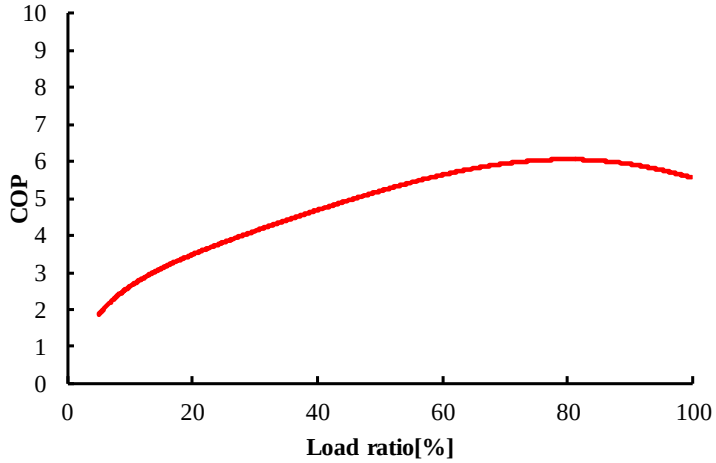

Fig. 4.5 Performance curve of chillers

4.3.2 AHU model

The model here is to simulate the performance of AHUs in the buildings as the end-users. The inputs of the AHU model are the chilled water supply temperature, water flow rate, inlet air temperature and air flow rate. The outputs of the AHU model are the outlet chilled water temperature and the outlet air temperature. The model was developed by an author (Wang 1998). A first-order differential equation, as shown in Eq. (4-1), is used to represent the dynamics of a coil with lumped thermal mass. The dynamic equation ensures that the energy is conserved. The supply air temperature and return water temperature ($t_{a,out}$, $t_{w,out}$) is computed using Eq. (4-2) and Eq. (4-3), respectively, based on the energy balance in both the air side and the water side. The heat transfer calculation is based on the classical number of transfer units and heat transfer effectiveness methods. The classical method to calculate the effect of the fins in the air side on the thermal resistance is used.

$$C_c \frac{dt_c}{d\tau} = \frac{t_{a,in} - t_c}{R_1} - \frac{t_c - t_{w,in}}{R_2} \tag{4-1}$$

$$t_{a,out} = t_{a,in} - \frac{SHR(t_{a,in} - t_c)}{R_1 C_a} \tag{4-2}$$

$$t_{w,out} = t_{w,in} - \frac{t_c - t_{w,in}}{R_2 C_w} \tag{4-3}$$

4.3.3 Pump model

Both constant and variable speed pumps are used in the systems. For the constant speed pump it is easy to get the energy consumption. For the variable speed pumps, performance curves are fit based on the data from a manufacturer. The pump size

changes to match the capacity of chillers. The equation of pump power is shown as Eq. (4-4) (Bernier and Bourret 1999).

$$N=H*Q*\rho*g/(1000*\eta) \quad (4\text{-}4)$$

4.3.4 Models of supplementary components

Cooling towers are used in DCSs and ICSs. The capacity of the cooling towers corresponds to that of the chillers. The model for cooling towers is Type 51b in TRNSYS. Indirect connection between the central plants and the users is adopted to clear the management delineation and avoid cross influence between different users. Plate heat exchangers (PHEs) are used to isolate the central chiller plant equipment and the users. The model for PHEs used in the simulation is Type91 in TRNSYS, which needs to set the heat exchanger efficiency.

4.3.5 Control strategies for pumps and chillers

As shown in the schematic diagrams of the DCS and ICS (Fig. 4.3 and Fig. 4.4), the DCS has at least one more group of chilled water pumps compared with the ICS. For each system, the following control strategies are adopted.

I. *DCS-CP and ICS-CP:* The chillers are controlled based on the cooling load and the chiller capacity. When the cooling load is larger than the capacity of all the running chillers, turn on one more chiller including its associated chilled water pump and cooling water pump. When one running chiller is turned off and the capacity of remaining chillers is still not less than the current cooling load, turn off one chiller including its associated chilled water pump and cooling water pump.

II. *DCS-VP and ICS-VP*: The control strategy for chillers and cooling pumps is the same as that in CP system. For the chilled water pump in DCSs, the frequency of the pump is controlled by a proportional-integral-derivative (PID) controller to keep the differential pressure across the most remote PHE as constant. For the chilled water pump in ICSs, the frequency of the pump is controlled by a PID controller to keep the pressure drop across the remote branch of the AHU as constant.

III. *DCS-CPVS and ICS-CPVS*: The control strategy for the chillers, cooling pumps and primary chilled water pumps is the same as that in CP system. The control strategy for the variable speed secondary chilled water pumps is similar to that in the VP systems.

All the systems are simulated on the TRNSYS platform. The TRNSYS building model is used for the annual cooling load calculation. Models of the primary components are developed and used on the TRNSYS platform. Outlines of the primary component models are given here below.

4.4 Performance analysis of the DCS and ICS

4.4.1 Comparisons between the DCS and ICS — constant primary-only (CP)

The results of DCS-CP and ICS-CP are shown in Table 4.2. It can be observed that the DCS-CP consumes 9.7% less energy compared with ICS-CP. Almost all the subsystems of DCS-CP consume less energy except the chilled water pumps. It is because the DCS has one more group of chilled water pumps compared with the ICS. Chillers in the DCS-CP are the main subsystem that consumes less energy compared

with ICS-CP. Therefore, it is very important to reduce the energy consumption of the chilled water system in order to enhance the advantages of DCS-CP.

Table 4.2 Annual energy consumption of DCS-CP and ICS-CP

	Chiller	Chilled water pump	Cooling water pump	Cooling tower	Total
DCS ($\times 10^6$ kWh)	61.50	32.12	7.68	2.32	103.61
ICS ($\times 10^6$ kWh)	85.05	18.50	8.65	3.90	116.11
Energy saving (%)	26.7	-73.6	11.2	40.5	9.7

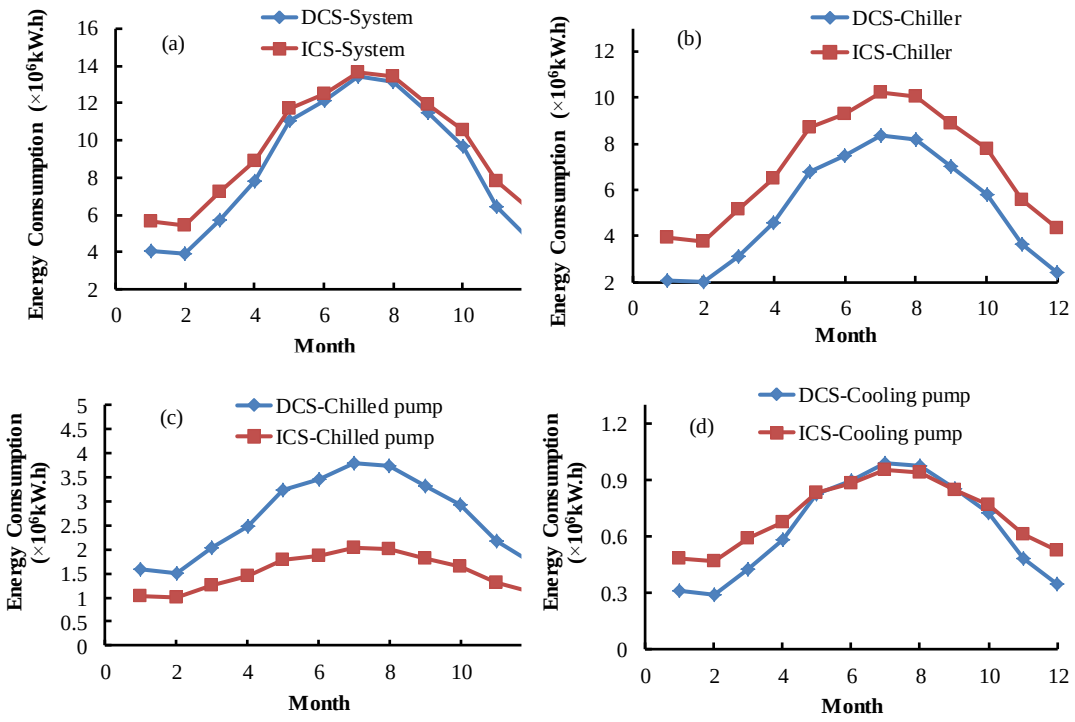

Fig. 4.6 DCS and ICS monthly energy consumptions — CP system

The monthly energy consumptions of main subsystems of DCS-CP and ICS-CP are shown in Fig. 4.6. It can be found that DCS-CP can hardly save energy in June, July and August while it consumes much less energy during other months in the year. The chillers of DCS-CP consume less energy throughout the year. Although the absolute differences between the energy consumptions of the chillers in DCS and ICS are rather

constant, the relative values are much higher in the cold months when the buildings have lower cooling demand. The chilled water system energy consumption of DCS-CP is higher throughout the year and the difference is very large in the summer time. It is because more chilled water pumps work in summer and the difference due to operating one extra group of chilled water pumps is large. The cooling water pumps of DCS-CP consume less energy compared with ICS-CP only in the winter period. In summer, the energy consumptions are almost the same.

To further understand the energy performance of DCS-CP and ICS-CP, their energy consumptions and the savings at different load ratios are shown in Fig. 4.7. The value of the energy consumption stands for the sum of the energy consumption corresponding to a cooling load ratio with an interval of 5% (e.g. 15% stands for the range between 10% and 15%). The saving stands for the percentage of energy saved by the DCS compared with the ICS. Fig. 4.7 shows that the percentage of energy saving is lower when load ratio is higher. It indicates that the energy saving potential of DCS-CP becomes lower with the increased load ratio. The energy saving of the chillers is over 10% and up to 60%. It indicates that the chillers in DCS-CP always save energy. For the chilled water pumps, all the energy ratios are negative which indicates that the chilled water pumps in the DCS-CP consume more energy than that in the ICS-CP at all load ratios. The absolute difference between chilled water system energy consumptions in the DCS-CP and ICS-CP is very large when the load ratio is between 30% and 80%. It is because most of the time in the year the load ratio is within the range between 30% and 80%. The relative energy saving of chilled water pumps is low when the load ratio is large. It indicates that more extra energy is consumed by the chilled water system in DCS-CP. The cooling water pumps in the DCS-CP consume less energy only when the load ratio is below 50%.

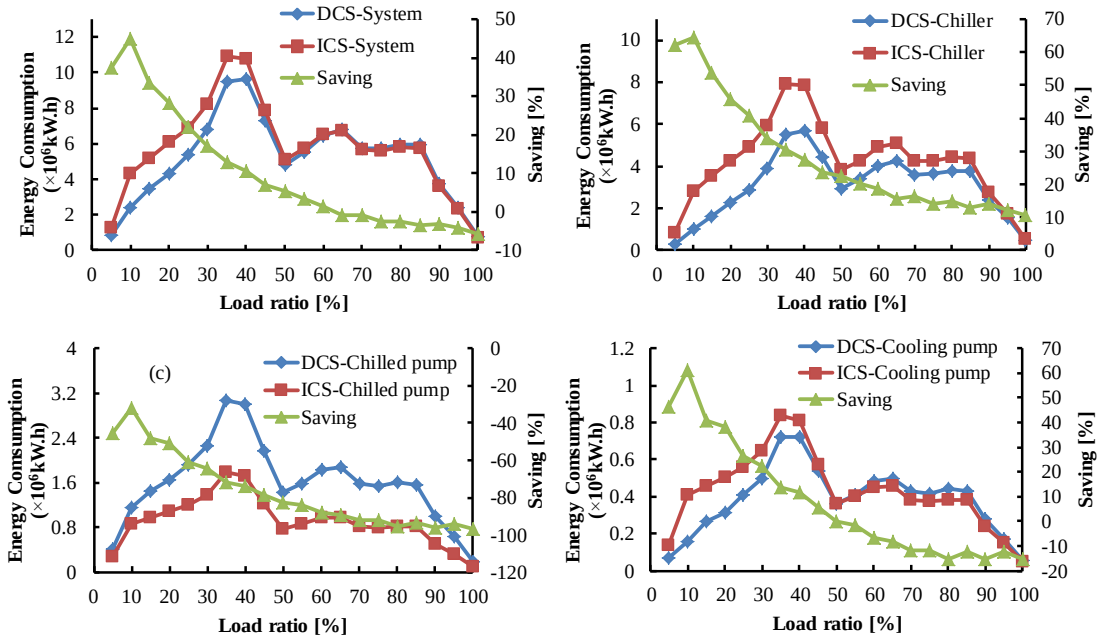

Fig. 4.7 DCS and ICS energy consumptions *vs.* cooling load ratio — CP system

The system energy is actually saved by the DCS (i.e., saving is positive) only when the load ratio is below 60%. It is because when the load ratio is low, chillers have to run to meet the cooling demand with low COPs in ICS-CP. Particularly during night time, it is very common that one chiller runs with low partial load, together with one chilled water pump and one cooling water pump. However, this can be avoided in the DCS-CP. Even if cooling loads of all the buildings are very low, the total cooling load of all buildings may be suitable for one or two chillers to work with high COPs in DCS-CP. This can be considered as the load concentration effect (Shimoda et al. 2008). When the load ratio is very high, the chillers in the ICS-CP also have high COPs in spite of the capacity of chillers. At this condition, although chillers of DCS-CP work at high COPs, it is very hard for DCS-CP to compensate the energy consumption of the extra group of chilled water pumps. Thus, it is reasonable that energy saving of DCS mainly appears at low load ratio.

4.4.2 Comparison between the DCS and ICS — constant primary and variable secondary (CPVS)

The results of DCS-CPVS and ICS-CPVS are summarized in Table 4.3. Table 4.3 shows that the DCS-CPVS consumes 14% less energy compared with ICS-CPVS. Chillers of the DCS-CPVS are the main subsystem that consumes less energy compared with ICS-CPVS. Almost all the subsystems of DCS-CPVS consume less energy except the chilled water pumps. It is because the DCS-CPVS has two more groups of chilled water pumps. Therefore, it is very important to decrease the energy consumption of chilled water system to enhance the advantage of DCS-CPVS.

Table 4.3 Annual energy consumption of DCS-CPVS and ICS-CPVS

	Chiller	**Chilled water pump**	**Cooling water pump**	**Cooling tower**	**Total**
DCS ($\times 10^6$ kWh)	63.00	17.78	7.73	2.32	90.84
ICS ($\times 10^6$ kWh)	83.47	9.98	8.71	3.90	106.06
Energy Saving (%)	24.52	-78.15	11.19	40.54	14.35

The monthly energy consumptions of main subsystems in the DCS-CPVS and ICS-CPVS are shown in Fig. 4.8. It can be found that the energy consumption trend is similar to that of the CP system. For the entire system, the DCS-CPVS can save the energy all the year, which is different from the CP system. It is because the energy consumption of the extra chilled water pumps in the DCS-CPVS is much lower than that in the DCS-CP. The energy saving of other subsystems in DCS-CPVS can fully compensate the energy consumption of extra chilled water pumps. The chillers in DCS-CPVS consume less energy throughout the year. The energy saving of DCS-CPVS is high in cold months. The energy consumption of the chilled water system in DCS-CPVS is higher than that in ICS-CPVS all the year, especially in summer. The

energy consumption of the cooling water pumps in the DCS-CPVS is lower than that in the ICS-CPVS except the summer period.

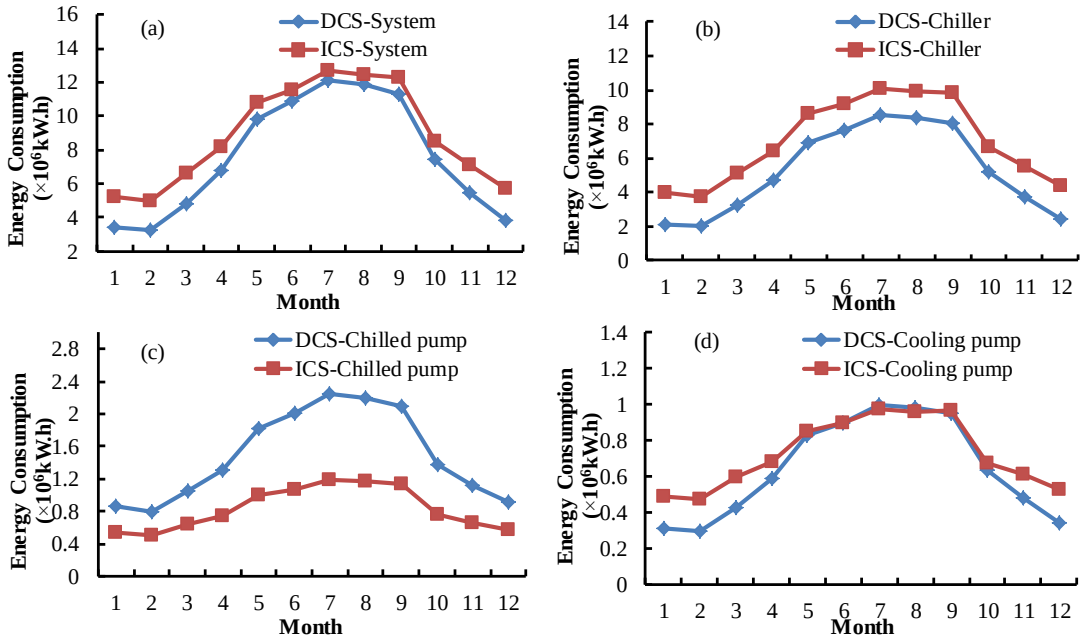

Fig. 4.8 DCS and ICS monthly energy consumptions — CPSV system

The energy consumptions of the DCS-CPVS and ICS-CPVS at different load ratios are shown in Fig. 4.9. Similar to the case of constant primary systems, the energy saving is lower when load ratio is higher. It shows that DCS-CPVS is more energy efficient compared with the ICS-CPVS most time over the year due to the load concentration effect and therefore higher COPs of chillers. The DCS-CPVS energy saving is positive only when the load ratio is below 80%. The energy savings of chillers are over 6% and up to 64% which confirms again the chillers in DCS-CPVS can always save energy. The savings of chilled water pumps are negative, indicating more energy consumption. The absolute difference between chilled water system energy consumptions in the DCS-CPVS and ICS-CPVS is also very large when the load ratio is between 30% and 80%. The cooling water pumps of the DCS-CPVS consume less energy only also when the load ratio is below 50%.

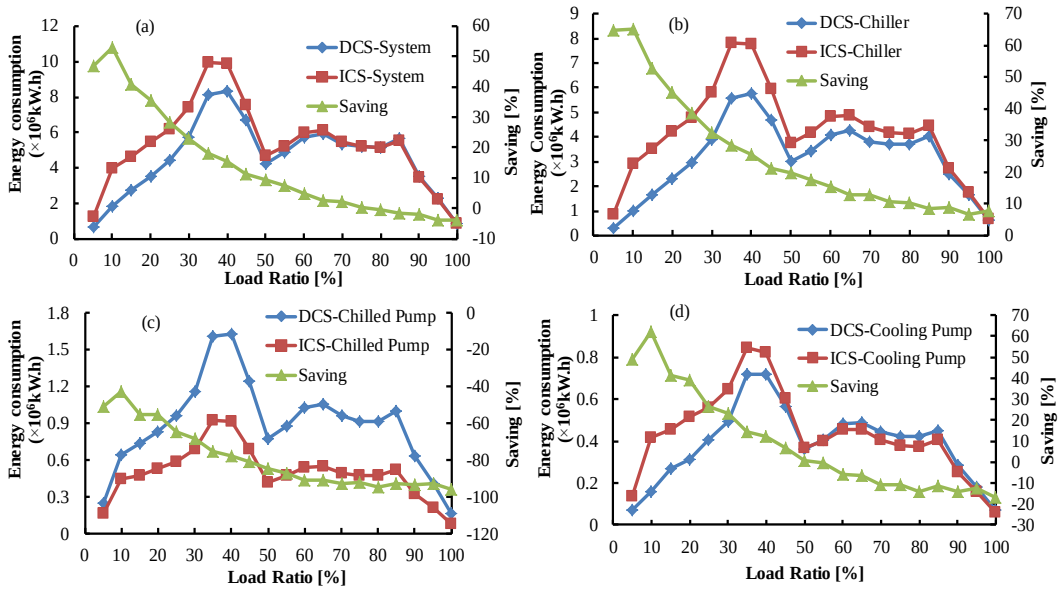

Fig. 4.9 DCS and ICS energy consumptions *vs.* cooling load ratio — CPSV system

4.4.3 Comparisons between the DCS and ICS — variable primary only (VP)

The energy consumptions of DCS-VP and ICS-VP are summarized in Table 4.4. It can be seen that the DCS-VP consumes 15% less energy compared with the ICS-VP. The chilled water pumps in the DCS-VP are also the only part that consumes more energy.

Table 4.4 Annual energy consumptions of DCS-VP and ICS-VP

	Chiller	**Chilled water pump**	**Cooling water pump**	**Cooling tower**	**System**
DCS($\times 10^6$ kWh)	61.57	15.94	7.73	2.32	87.56
ICS($\times 10^6$ kWh)	83.32	7.44	8.60	3.90	103.26
Energy Saving (%)	26	-114	10	41	15

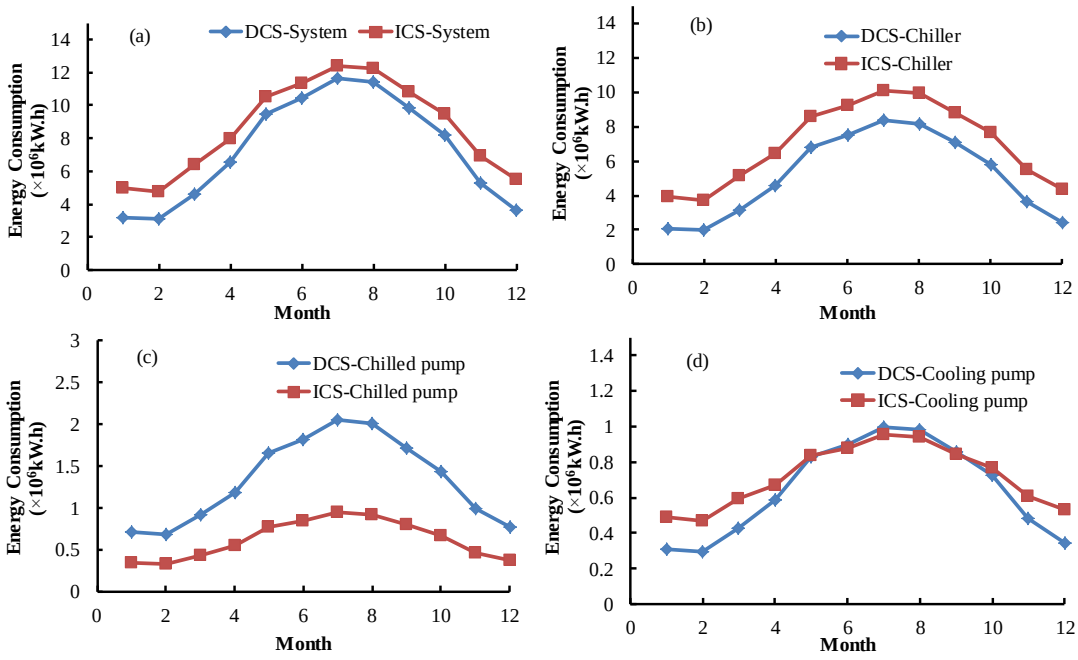

Fig. 4.10 DCS and ICS monthly energy consumptions — VP system

The monthly energy consumptions of main subsystems of the DCS-VP and ICS-VP are shown in Fig. 4.10. The trend is also similar to that in the CP system and CPVS system. For the entire system, the DCS-VP can save energy all the year, which is similar to the case of the DCS-CPVS. The chillers of the DCS-VP consume less energy than that in the ICS-VP all the year. The energy saving of DCS-VP is also larger in the cold months. The chilled water system energy consumption of the DCS-VP is higher than that of the ICS-VP all the year, particularly during the summer period. The energy consumption of cooling water pumps in the DCS-VP is lower than that in the ICS-VP almost all the year except in summer.

Energy consumptions of DCS-VP and ICS-VP at different load ratios are shown in Fig. 4.11. Similar to the previous two cases, the energy saving is lower when load ratio is higher. The DCS-VP energy saving is positive only when the load ratio is below 90%. It shows that DCS-VP is more energy efficient compared with the ICS-VP most

time over the year due to the concentration effect and therefore higher COPs of chillers. The energy savings of chillers in DCS-VP are between 10% and 64%. The savings of chilled water pumps are negative, indicating more energy consumption. The cooling water pumps of the DCS-VP consume less energy only also when the load ratio is below 50%.

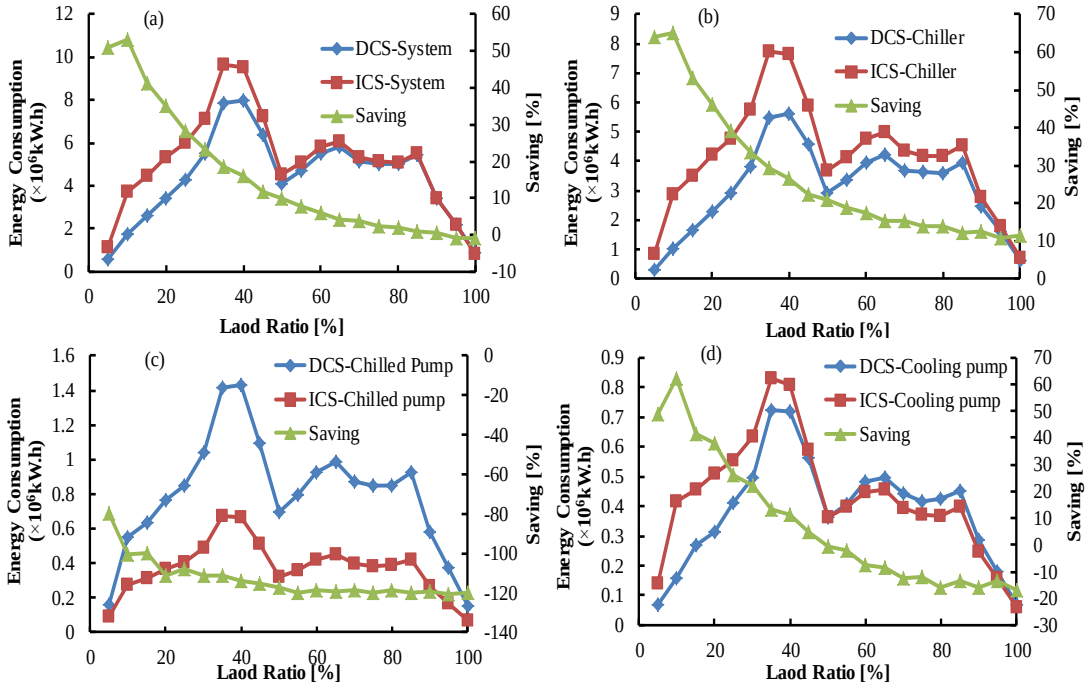

Fig. 4.11 DCS and ICS energy consumptions *vs.* cooling load ratio — VP system

4.4.4 Sensitivity study of cooling loads during night time

As discussed in the above three sections, the energy saving potential for DCS is mainly at the time when the load ratio is not very high. To assess the effect of part load ratio on the efficiency of DCS, sensitivity study is conducted by changing the cooling load percentages of buildings during night time. The chilled water pump scheme used in the test is VP. Results are shown in Fig. 4.12.

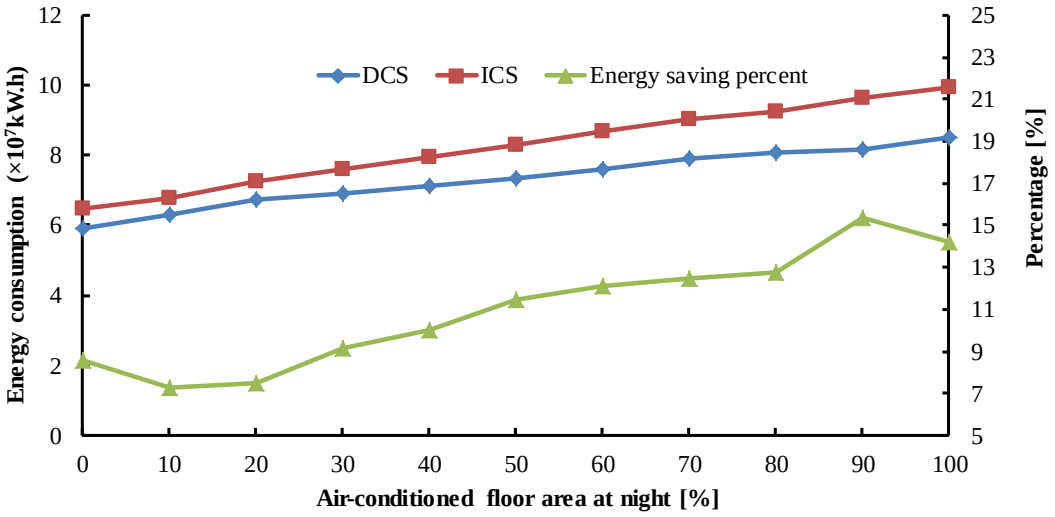

Fig. 4.12 Comparison between the DCS and ICS energy consumptions under different percentages of building floor area air-conditioned during night time

It can be found that with the increase of the cooling need during night time, the difference between energy consumptions of the DCS and the ICS increases gradually. At the same time the energy saving percentage of the DCS is also increased and can be as high as 15%. However, the lowest saving of the DCS occurs when there is only 10% (instead of 0%) of buildings with cooling load during night time. It is because when most buildings do not have cooling demand during night time, all the cooling equipment in these buildings is shut down. However, in the case of the DCS, at least one set of central cooling equipment has to work even if only one building needs cooling. If the energy saving of the DCS, due to system efficiency and concentration effect, cannot compensate the energy reduction of the ICS due to shutting down cooling plants, the energy saving of the DCS decreases. When all the buildings do not have cooling load at night, the DCS is also shut down. This avoids the DCS to work at low partial loads and COPs. Thus, it is reasonable that the DCS shows a little higher saving potential at 0% compared with the cases of 10% and 20% air-conditioned floor

area at night. In the test, at least 7% of energy can be saved by the DCS, no matter how much percent of buildings have cooling demand during night time.

4.4.5 Economic analysis of the DCS and ICS

The operation costs of the DCS and ICS were calculated based on electricity tariffs in Hong Kong (Table 3.3). Both the "large power tariff" and the "bulk tariff" are applicable for the DCS and ICS. These two tariffs are used to calculate the electricity bill of the DCS and ICS.

Only the electricity bills for the DCS-VP and ICS-VP are calculated. Detailed cost items under "Bulk Tariff" and "Large Power Tariff" are shown in Table 4.5. It can be observed that even for one identical system, the difference between costs under different tariffs is very large. Operators or managers should select the proper one in practice. The energy cost of the DCS is over 10% lower than that of the ICS, indicating that DCS is very efficient economically. The cost saving mainly lies in the energy charge part.

Table 4.5 Costs of the DCS and ICS under different tariffs

System	Tariff	Demand charge ($\times 10^6$\$)	Energy charge ($\times 10^6$\$)	Fuel clause ($\times 10^6$\$)	Total ($\times 10^6$\$)
DCS	Bulk tariff	1.83	6.90	2.46	11.19
	Large power tariff	3.25	5.10	2.46	10.81
ICS	Bulk tariff	1.85	12.83	2.88	12.72
	Large power tariff	3.29	5.88	2.88	12.04

4.5 Discussions on factors affecting energy and economic performance

By comparing the three systems we find that the CP system consumes more energy than the other two systems. The VP system is the most energy efficient. The main difference lies in the chilled water pumps. However, the control strategy for the chilled water system is not optimized.

In the simulation tests, the cold losses of the DCS chilled water network, due to DCS chilled water pumps and heat exchange with the surrounding environment, are not taken into consideration. Previous research shows that the cold loss caused by the heat exchange with the environment is only about 1%, which can be ignorable. Both the DCS and ICS experience the cold loss due to the pumps in the chilled water system. The DCS has at least one more group of pumps which may cause more cold loss compared with the ICS. However, the pump efficiency can be high to 90%. That means only less than 10% of the pump energy is released into the chilled water. As the chilled water pumps occupy about 20% of the overall system energy consumption, it can be predicted that around 2% of extra cold loss will be rejected into the chilled water in the DCS. From the above results it can be seen that about 15% of energy can be saved by the DCS. Consequently, the DCS can still achieve energy saving of about 13% even after counting the cold losses.

4.6 Summary

Performance of the DCS in the new district of Hong Kong is assessed and compared with conventional ICSs. Models for the systems are presented. Performance of DCSs and ICSs with different chilled water system configurations is studied and compared. After detailed analysis and comparison, the following conclusions can be made:

i. The DCS is an energy efficient cooling system for the new development area in the subtropical area. It consumes around 15% less energy compared with traditional ICS.

ii. The DCS shows energy saving potential all the year, especially in the cold months when the buildings have low cooling demands. The DCS shows high energy saving at partial loads, especially when the load ratio is below 50%.

iii. Chillers are the main subsystem that saves energy in the DCS. It is due to the load concentration effect which allows the chillers to work at high COPs, especially when the load ratio for individual building is low.

iv. The chilled water system is the only subsystem that consumes more energy in the DCS because the DCS has at least one extra group of pumps compared with the ICS. Thus, reducing the energy consumption of chilled water system in the central plant is the important to enhance the advantage of DCSs.

v. The DCS can save at least 7% of energy comparing with the ICS, no matter how much percent of buildings have cooling loads during night time.

vi. The annual operation cost of the DCS is 10% lower compared with the ICS under the electrical tariffs of Hong Kong.

CHAPTER 5 DESIGN OPTIMIZATION METHODS

Design optimization methods for DCSs and ICSs are presented in this chapter. The concepts of robust optimal design methods considering uncertainty, and concerning both uncertainty and reliability are explained respectively. The expected performance of the cooling systems designed using proposed methods is illustrated by comparison. The strategies and steps for implementing the robust optimal design methods are introduced.

5.1 Concept and performance of robust optimal design for cooling systems

The concept of robust design is defined as "*A product or process is said to be robust when it is insensitive to the effects of sources of variability, even though the sources themselves have not been eliminated"* (Fowlkes and Creveling 1995; Zang et al. 2005). It is widely used to improve the quality and reliability of products in industrial engineering. Methods to realize the robust optimal design are reviewed by Park et al. (2006). However, studies and applications of the robust optimal design in cooling and air-conditioning systems are still not sufficient. The concept and expected outputs of robust optimal design, proposed in this study, for cooling systems are explained in this section.

5.1.1 Robust optimal design considering uncertainty only - uncertainty-based optimal design

When only uncertainty is involved, the robust optimal design is regarded as uncertainty-based optimal design in this thesis. The main purpose is to distinguish it

with the design method considering both uncertainty and reliability. The performance of uncertainty-based optimal design is illustrated in Fig. 5.1. The performance indices shown by the Y-axis may refer to the thermal comfort, the energy consumption or the total monetary cost of the design.

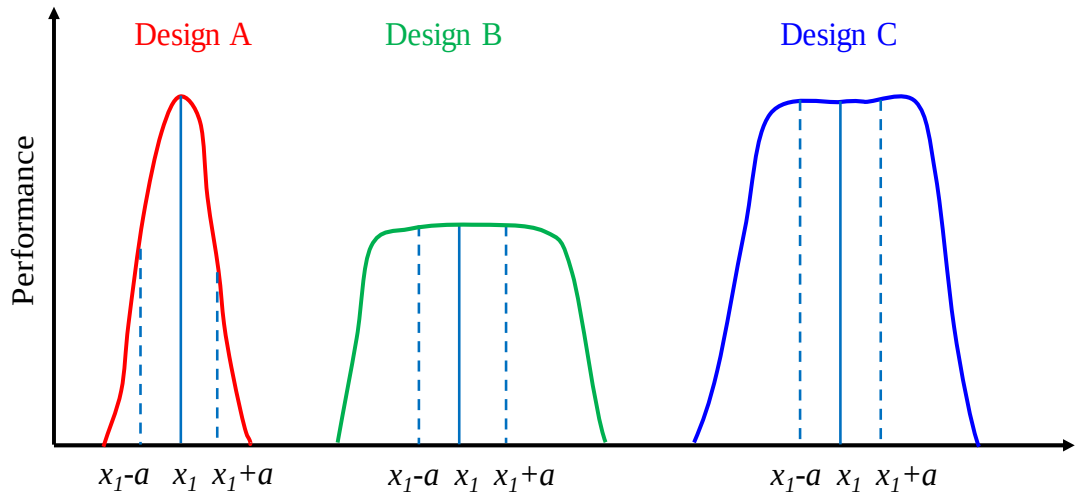

Fig. 5.1 Illustration of the performance of uncertainty-based optimal design
(x_1 is the pre-assumed design condition; a is the noise for x_1)

For *Design A*, the performance is very good at the design condition x_1 but the design is not robust. When the inputs or conditions change due to the uncertainties or noises, the performance of *Design A* will decrease sharply. For *Design B*, its performance may not be as good as *Design A* but it is robust. Even when the inputs or conditions change, the performance of *Design B* keeps stable and insensitive to uncertainty. For *Design C*, the performance is good and it can keep stable even though the inputs deviate from the pre-assumed value. That is the uncertainty-based optimal design, which is the targeted design of this method.

5.1.2 Robust optimal design considering uncertainty and reliability

When both uncertainty and reliability are concerned, the performance of robust optimal design compared with other methods is illustrated by Fig. 5.2.

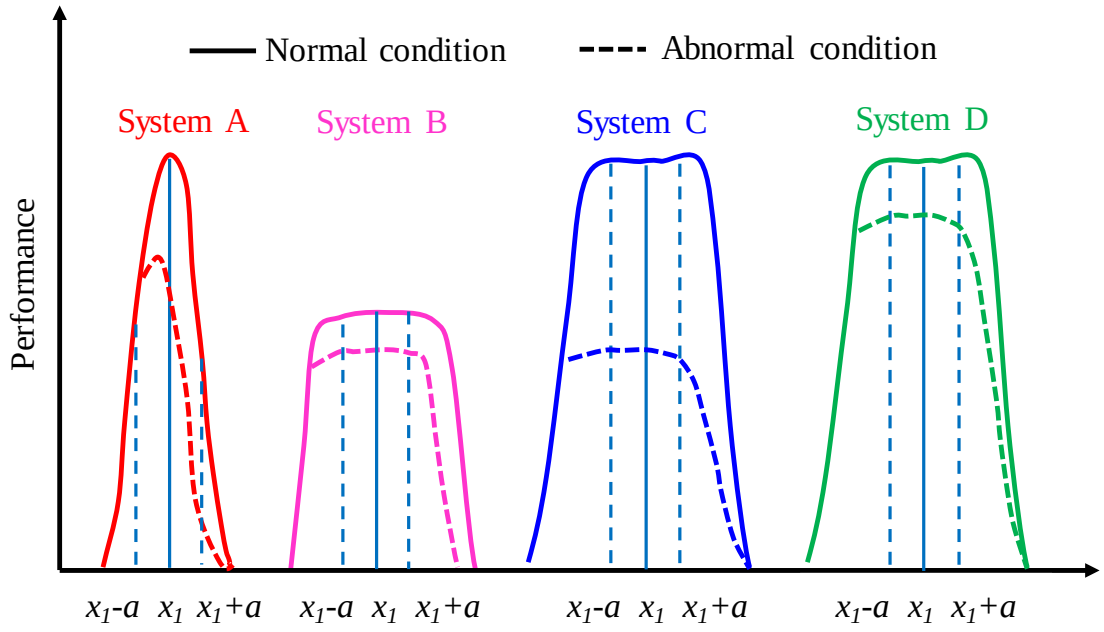

Fig. 5.2 Illustration of the performance of robust optimal design

(x_1 is the pre-assumed design condition; a is the noise for x_1. The solid line refers the performance of systems under normal working conditions; The dotted line refers the performance of systems when failures or faults arise.)

Under normal condition (solid line): *System A* using the conventional method can achieve good performance at the pre-assumed condition but the performance may drop abruptly in the presence of uncertainty (*optimal but not robust*); *System B* is insensitive to uncertainty while its performance is not good (*robust but not optimal*); Performance of *System C* and *System D* keeps good and stable even when uncertainty appears (*robust and optimal*). Under abnormal condition when damage or failure happens (dotted line): Performances of all these designs may drop while *System D* can still

achieve good and stable performance. *System D* is the final robust optimal system, which is the target system of this method.

5.2 Uncertainty-based optimal design based on mini-max regret theory

Many methods can be used to achieve the robust design (Park et al. 2006; Zang et al. 2005). Considering uncertainty, the probability distribution is required while it is not easy to obtain accurate distribution. In addition, the time can be very limited for designers to conduct a considerable amount of repeat calculations to get the probability distribution of outputs. A simple but effective method is necessary to get the uncertainty-based optimal design considering uncertainty. Therefore, the uncertainty-based optimal design method based on mini-max regret theory is developed.

Mini-max theory is used in this study due to its simplicity and efficiency. The mini-max theory was originated by Wald (1949). The uncertainty in the social, economic, environmental, technical and political factors was considered. It is regarded as a reasonable solution for the problem when the priori-distribution of the uncertainty factors is unknown. It is widely used in many fields to select the robust optimal decision considering uncertainty or risks (Aissi et al. 2009; Averbakh 2000; Nguyen et al. 2014; Pascoal and Resende 2014). In the energy field, it was used to get the robust optimal design of a cogeneration system under the uncertainty of energy demand (Yokoyama and Ito 2002; Yokoyama et al. 2014). The mini-max regret method was also coupled with interval parameter programming to support long-term planning of greenhouse gas mitigation in an energy supply system (Li et al. 2011).

The proposed uncertainty-based optimal design method and the conventional design method are illustrated in Fig. 5.3. The conventional method usually determines the optimal design scheme under certain conditions. The steps are introduced as follows:

i. List the available design schemes or plans $P(P_1,P_2,....P_i)$. Regarding the design of building cooling systems, many plans are available. For example, the system can use the surface water, air or the underground soil as the cooling source. After the cooling source is determined, the numbers and capacities of chillers can be organized in many ways. The chilled water systems can also be primary only variable flow system, primary constant & secondary variable flow system and so on.

ii. Estimate the performance of each plan under certain or pre-assumed conditions. The performance can be energy consumption, cost and/or thermal comfort. It can be obtained with the predicted cooling load of the buildings, the performance of chillers and pumps, etc.

iii. Compare the performance of each plan and the optimal cooling system can be selected with the lowest energy consumption/cost, the shortest payback period or the best thermal comfort.

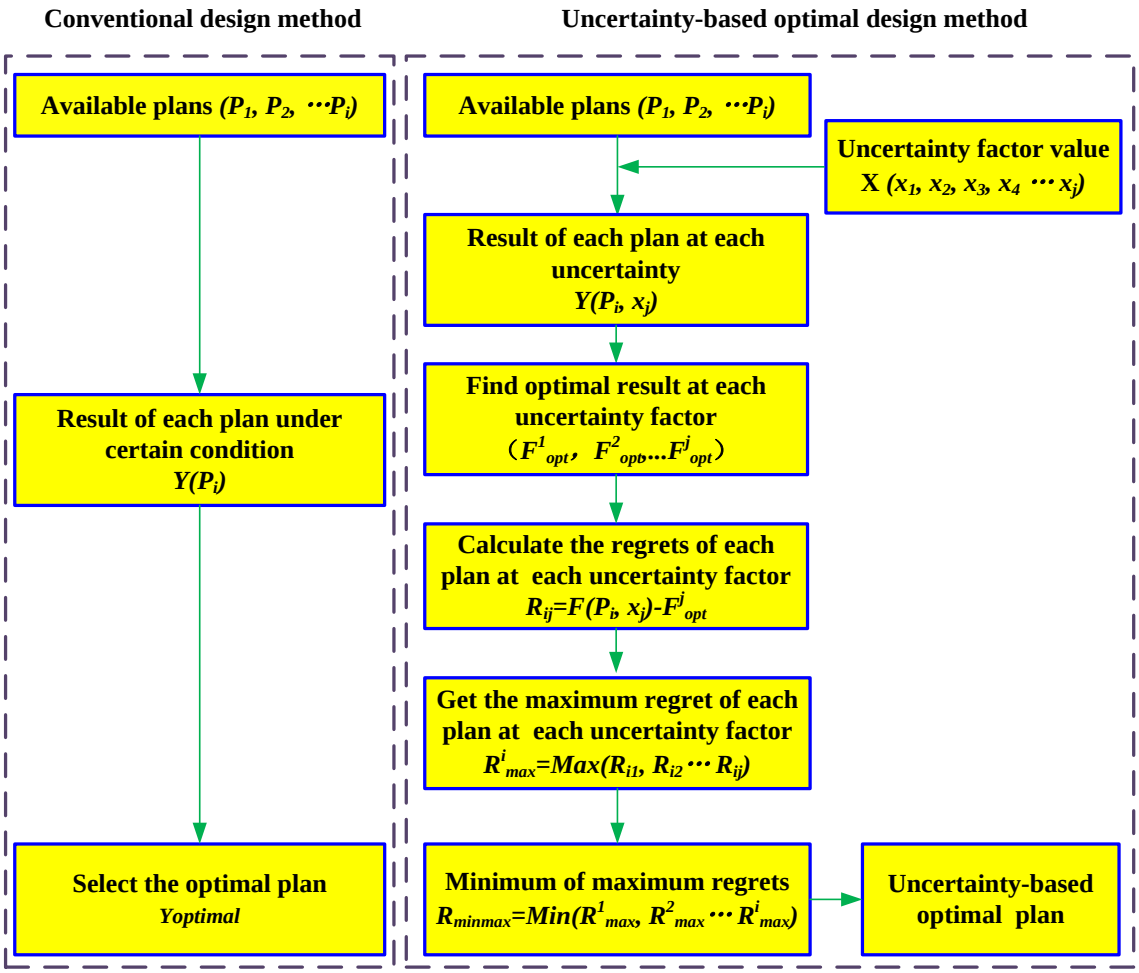

Fig. 5.3 Conventional design method vs. uncertainty-based optimal design method based on mini-max regret theory

The mini-max regret theory is used to get the uncertainty-based optimal design of the cooling system in this study. Steps to realize the method are explained bellow in detail, including:

i. List all the available design schemes or plans $P(P_1,P_2,....P_i)$, which is similar to that in the conventional method.

ii. Determine the uncertainty factor and its possible values $X(x_1, x_2... x_j)$. One apparent advantage of the mini-max regret method is that no detailed prior-distribution is required for the factors containing uncertainties. Only the range is needed, which can be divided into several intervals. Actually it is almost

impossible to get accurate distributions for the factors containing uncertainties. The assumed distribution may also bring variations to the outcomes. Such variations can be avoided in the optimal method based on mini-max regret theory.

iii. Estimate the performance of each available plan at each value of the uncertainty factor $Y(P_i, x_j)$. For the design of the cooling system, the performance can be energy consumption, thermal comfort or cost.

iv. Compare the performances of all the plans at each value of the uncertainty factor and select the optimal plan (F^1_{opt}， F^2_{opt},...F^j_{opt}). The optimal option with the lowest energy consumption/cost may change at different values of the uncertainty factor. .

v. Calculate the regrets R_{ij} between other plans and the optimal plan at each value of the uncertainty factor. Here the regret means the difference between the result of the optimal plan and that of all the left plans. It can be the energy consumption difference or cost difference.

vi. Find the maximum regret R^i_{max} for each plan at all the values of the uncertainty factor. The maximum regret for each plan refers to the maximum difference of the plan compared with the optimal ones at all the uncertainty values. To some extent, it can be regarded as a metric of robustness of the system. The smaller the maximum regret of the system is, the higher the robustness of the system is. Therefore, the aim is to get the system with the highest robustness with the smallest maximum regret.

vii. Compare all the maximum regrets of each plan and select the minimum one R_{minmax}.

viii. Determine the uncertainty-based optimal plan based on the result from step 7, which has the mini-max regrets. The mini-max regret indicates that the sensitivity of the plan is the lowest to all the possible uncertainty factors.

From the above explanation, it can be seen that the method is easy to be implemented and no new models or complicated methods are involved. This makes the method convenient to be used by the engineers or designers.

5.3 Uncertainty-based optimal design based on uncertainty quantification

The method based on mini-max regret theory described above can obtain the uncertainty-based optimal cooling system very quickly. It is very effective but cannot provide decision makers quantified risks about certain design option. The method in this section is therefore further developed to fill the gap by quantifying uncertainties at planning and design stages. With performance distribution at different probabilities, the design can be determined with quantified confidence.

5.3.1 Outline of the method

The proposed new design method considering uncertainty is illustrated in Fig. 5.4, in comparison with traditional design methods. Compared with conventional design method, uncertainties in the cooling load are considered in the new method. Instead of deterministic results, performance of different cooling system designs and corresponding possibility distributions are presented.

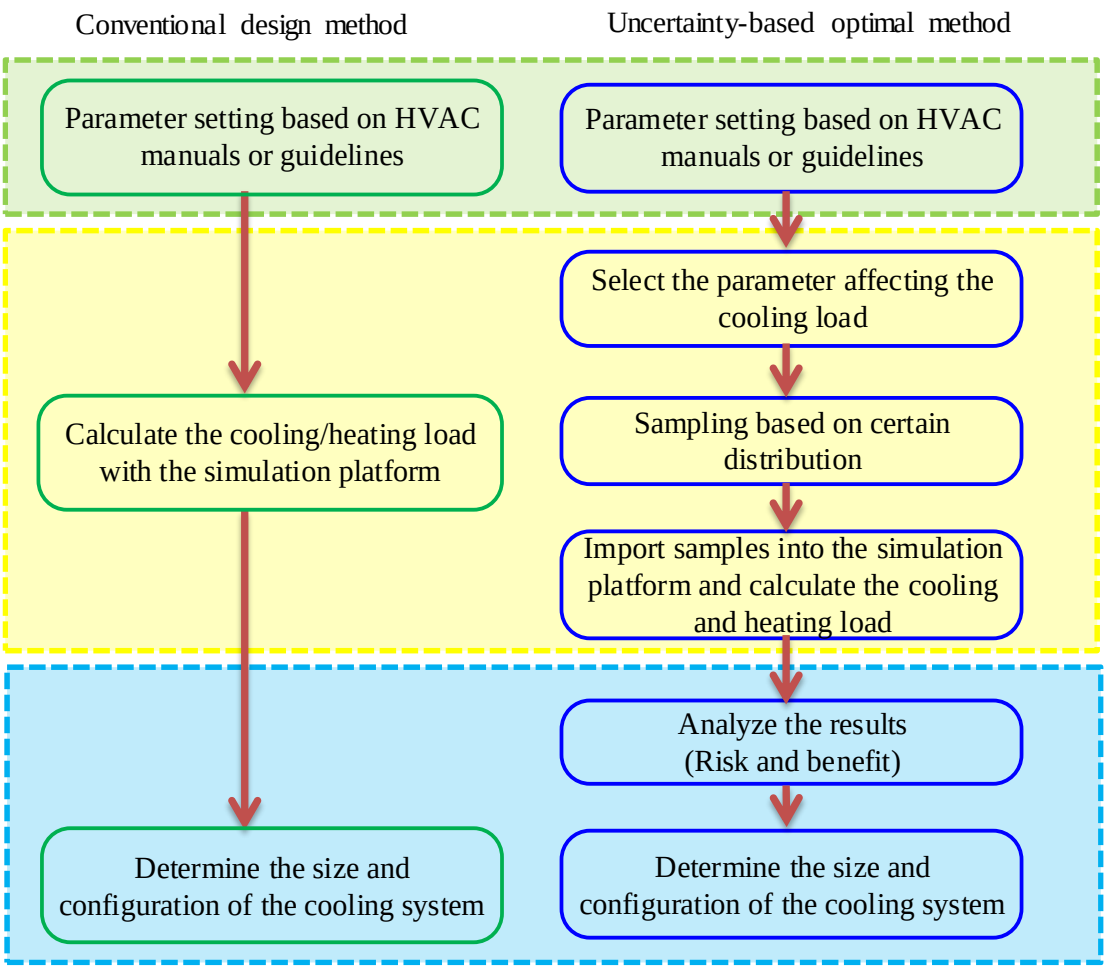

Fig. 5.4 Conventional design method *vs.* uncertainty-based optimal design method

For the conventional method, the inputs $x_1, x_2, x_3 \ldots x_n$ (such as the outdoor temperature, ventilation rate…) are imported into the models with specified or certain values. Then the output *y* (such as cooling load, energy consumption, cost, etc.) can be obtained as shown in Eq. (5-1). With this only value, the cooling system can be designed. For the proposed method, uncertainties in the inputs are considered. The calculation is expressed with Eq. (5-2). Each variable considering uncertainties can be expressed with Eq. (5-3). The uncertainty of one variable may fit some distribution function *G*, as shown in Eq. (5-4). By importing these samples into the models, the output *Y* can be obtained. By analyzing the distribution of *Y*, appropriate cooling scheme can be obtained.

$$y = f(x_1, x_2, x_3 \dots x_n) \tag{5-1}$$

$$Y = (y_1, y_2 \dots y_k)^T = f(X_1, X_2 \dots X_n) \tag{5-2}$$

$$X_i = [x_{i1}, x_{i2} \dots x_{ik}]^T \tag{5-3}$$

$$X_i \sim G_i \tag{5-4}$$

5.3.2 Classification of variables with uncertainties

Many variables used in the cooling load calculation contain uncertainties. All these uncertainties can be classified into three groups based on the physical location of these variables.

1) Outdoor weather

In the traditional method, weather data of the typical meteorological year (TMY) are used in the cooling/heating load calculation. However, the actual weather data can be very different. That is regarded as uncertainties in the weather data. Cooling/heating loads can be over-estimated or under-estimated by using the TMY data.

2) Building design/construction

At planning stage, limited information about buildings is available, such as the gross floor area, the number of floors or the orientation. Even for these parameters, data used at planning stage are very hard to be the same with that actually used when the buildings are constructed. By meeting the requirements of developers or governments, the building designs are hard to be the same for different architects. For example, the shape of the buildings or the material used for building envelopes can vary for different designers or architects. All these differences will affect the cooling loads and then

cause energy consumption deviation. These are regarded as uncertainties in the building design/construction.

3) Indoor conditions

Internal heat gain from occupants, lighting and plug-in equipment is a primary source of the cooling load. In the design calculation, variables representing the internal heat gain sources are usually determined according to design guidelines or manuals. However, actual values of these variables will vary from that used at planning and design stages. In addition, the indoor temperature and relative humidity set-points keep constant in the conventional cooling load calculation method. Actually the set-points may differ randomly from room to room, based on the users' preferences. All these differences are regarded as uncertainties in the indoor conditions.

5.3.3 Detailed steps of the proposed method

Steps to implement the new design method are illustrated in Fig. 5.5. Detailed explanations are introduced as follows.

1) The input variables that have uncertainties are selected and samples are generated for these variables. Many distributions can be used when conducting uncertainty study in building energy systems.
2) Samples are imported into the cooling load calculation software. For a DCS, many buildings with different functions are involved. Each building needs to be simulated. For each building, uncertainties of the cooling loads result from the uncertainties in the three groups of input variables.
3) The cooling load profile of the DCS and ICS can be obtained. The cooling loads of ICSs can be calculated by importing samples into the cooling load calculation

platform. By summing the cooling loads of all individual buildings in a DCS, the cooling load distribution of DCSs can be obtained.

4) The distribution of peak cooling load and annual cooling load profile are analyzed.

5) Based on the peak cooling load distribution, the optimal capacity of the DCS and ICS can be determined considering quantified risks. Based on the annual cooling load distribution, the performance of the DCS and ICS options with different configurations is obtained and the optimal system configuration therefore can be determined.

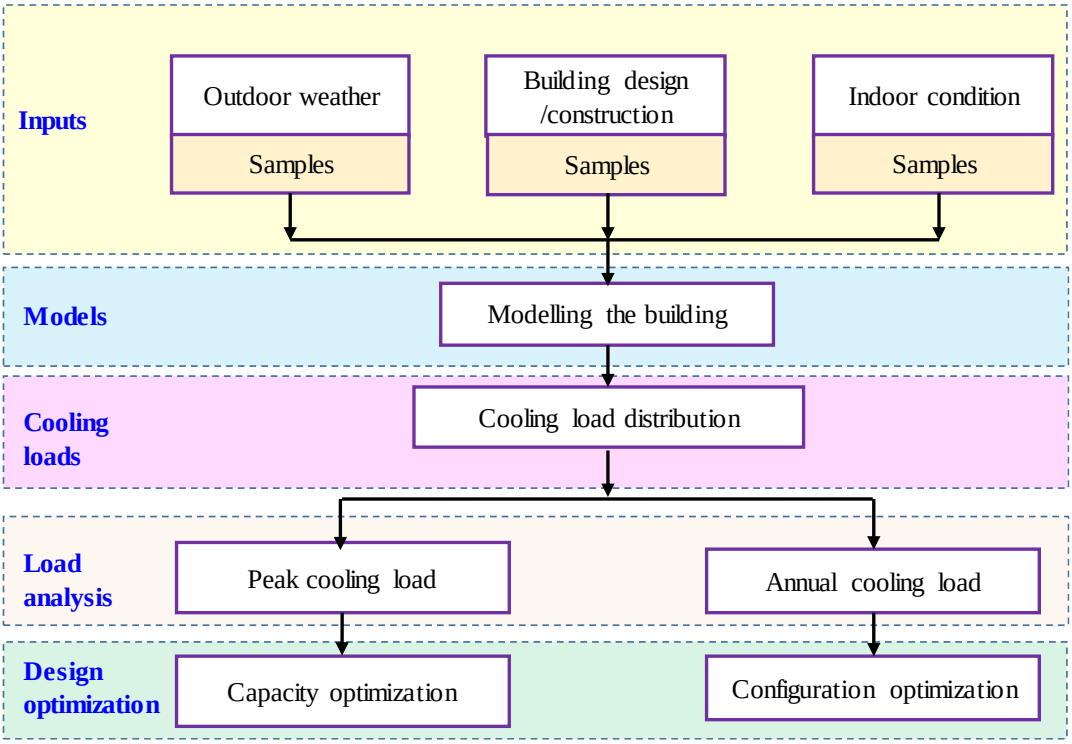

Fig. 5.5 Steps of the uncertainty-based optimal design method

5.4 Robust optimal design considering uncertainty and reliability

5.4.1 Overview of the robust optimal design method

The processes and steps of the robust optimal design method are illustrated in Fig. 5.6. The method to quantify the uncertainties is similar to that used in the uncertainty-based

optimal design method in Section 5.3. It will be not repeated here. Uncertainties in cooling load calculation are considered. By importing the samples of related parameters into the calculation, the distribution of the cooling load can be obtained.

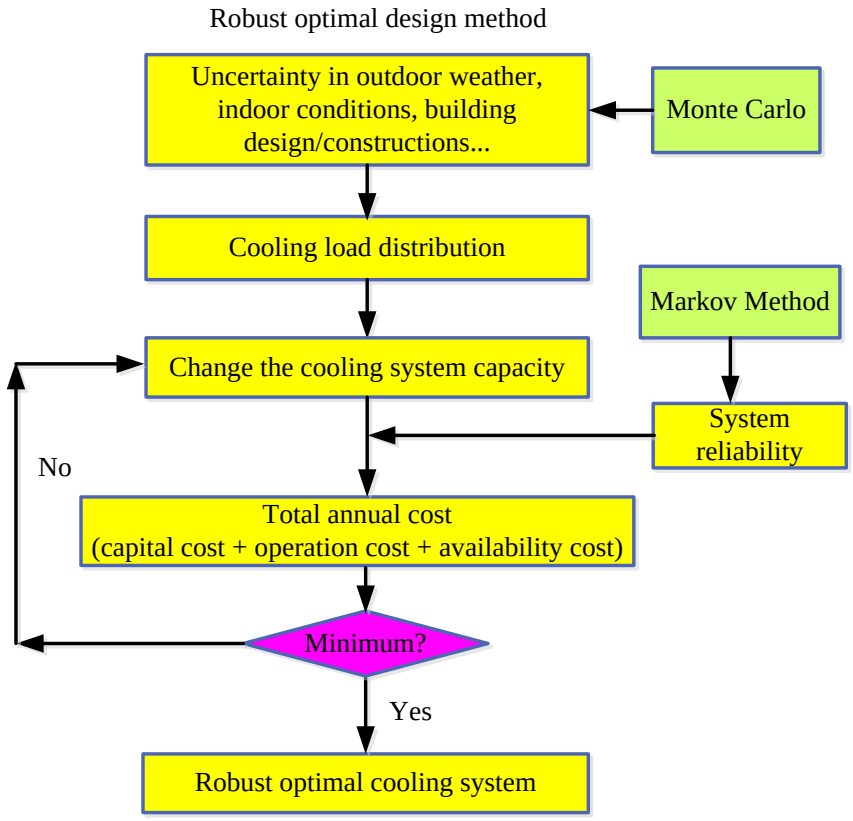

Fig. 5.6 Steps of robust optimal design method

The difference between the robust optimal method and the uncertainty-based optimal method lies in the reliability assessment of components or subsystems. Reliability assessment in the design optimization is conducted using Markov method. By assessing the reliability of the cooling system, the expected performance of the system can be obtained. By taking the total annual cost as the objective, the robust optimal cooling system can be achieved.

5.4.2 Quantification of component reliability in operation

A cooling system can be comprised by many components or sub-systems in parallel/serial, which can be regarded as a multi-state system. These components and subsystems are connected with multiple interactions and functional dependencies. Failure of one component may result in malfunction or damage of other components and bring losses to users. Therefore, reliability has to be in consideration at the design stage. Both qualitative and quantitative methods can be used to conduct the reliability analysis. One common method for qualitative analysis is failure modes and effects analysis. For quantitative reliability analysis, three methods are widely used including fault tree analysis, reliability block diagrams and Markov analysis. The Markov method is selected for its wide application in reliability analysis of multi-state systems (Lisnianski and Levitin 2003).

The aim of Markov method is to obtain the probability of each state of a multi-state system at a specific period and then the system performance can be estimated. The basic theory for the Markov method is that the state at the next time point only relates to that of current time point. The system either keeps current state or transfers to other states at the next time point. Several steps are required using the Markov method, including:

I. List all the possible states of the cooling system;
II. Determine the state transition density matrix;
III. Obtain the probability of each state of the cooling system;
IV. Calculate the mean steady-state performance of the cooling system.

The detained processes are explained using an example of a three-chiller cooling system as follows.

Totally the cooling system may have eight states considering the reliability of chillers, as shown in Fig. 5.7. It is assumed that the chiller only has two states: normal (1) and failure (0). The cooling system may transfer from one state to another due to failure and repair actions at a given period. The transfer is determined by a state transition density matrix *A* (Eq. (5-5)), which only relates to the repair rate and failure rate of chillers (Lisnianski and Levitin 2003). Probability distribution of the system at each state at time *t* can be expressed with a vector *PR(t)* (Eq. (5-6)). It can be deduced from the initial state by Eq. (5-7) and Eq. (5-8). When the time approaches infinity, $PR(\infty)$ will keep stable (Eq. (5-9)). Then the steady-state state probabilities can be obtained by solving the linear algebraic equations (Eq. (5-10) and Eq. (5-11)). The mean steady-state performance thus can be obtained (Eq. (5-12)) and the deficiency caused by failures can also be calculated. The mean steady-state system performance represents the average performance of the system considering failures.

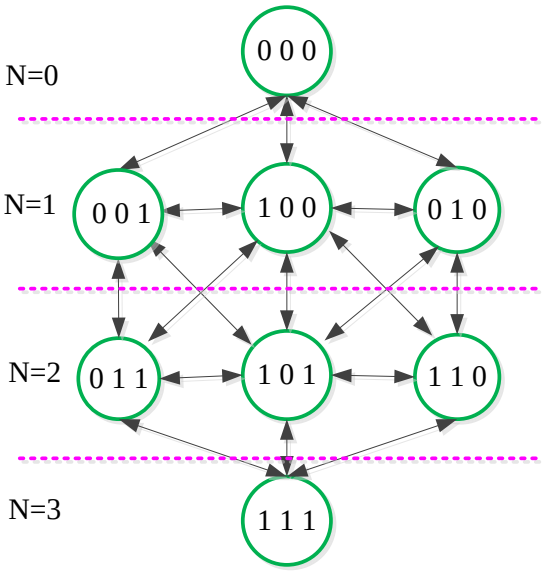

Fig. 5.7 States of a three-chiller cooling system and possible transitions

$$A=\begin{bmatrix} a_{11} & a_{12} & \cdots & a_{1k} \\ a_{21} & a_{22} & \cdots & a_{2k} \\ \vdots & \vdots & \ddots & \vdots \\ a_{k1} & a_{k2} & \cdots & a_{kk} \end{bmatrix} \quad (5\text{-}5)$$

$$PR(t)=[pr_1(t), pr_2(t)...pr_k(t)]^T \quad (5\text{-}6)$$

$$PR(1)=PR(0)A \quad (5\text{-}7)$$

$$PR(m)=PR(m\text{-}1)A = PR(0)A^m \quad (5\text{-}8)$$

$$PR(\infty)=PR(\infty\text{-}1)A = PR(\infty)A \quad (5\text{-}9)$$

$$PR(\infty)(A\text{-}I)=0 \quad (5\text{-}10)$$

$$\sum_{i=1}^{k} pr_i(\infty) = 1 \quad (5\text{-}11)$$

$$E_\infty = \sum_{i=1}^{k} y_i pr_i \quad (5\text{-}12)$$

The key issue for using the Markov method is to determine the transition density matrix *A*. As mentioned above, it only relates to the failure rate and repair rate of the component. When the repair rate and failure rate are regarded as time-independent, these two variables can be obtained by Eq. (5-13) and Eq. (5-14) (Lisnianski and Levitin 2003).

$$\lambda = 1/MTTF \quad (5\text{-}13)$$

$$\mu = 1/MTTR \quad (5\text{-}14)$$

5.4.3 Optimization objectives

For sizing the cooling systems, higher reliability usually corresponds to larger capacity, accompanying with larger capital cost and operation cost, as shown in Fig. 5.8. The

robust optimal design method balances the reliability and cost by minimizing the total annual cost (Eq. (5-15)).

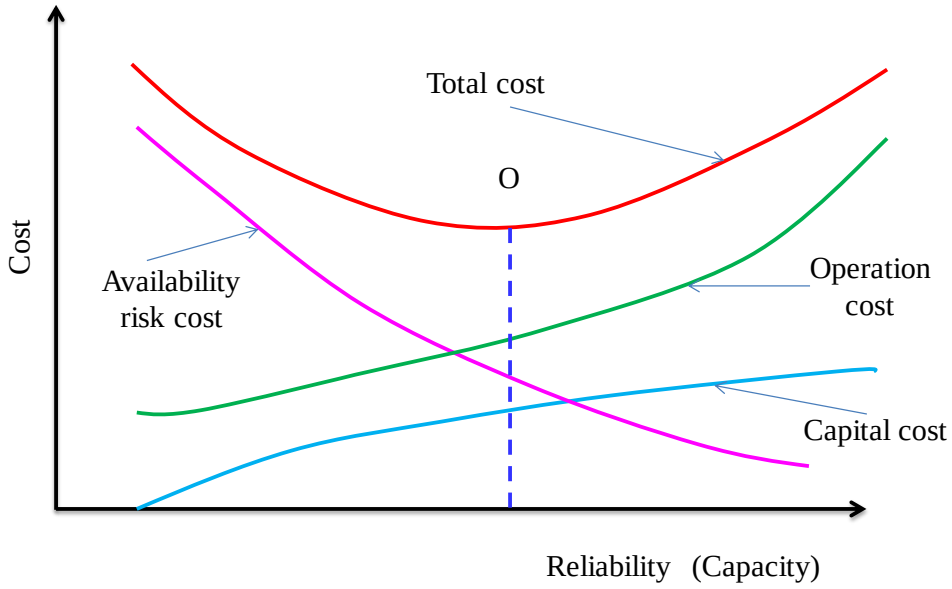

Fig. 5.8 Cost of the cooling system vs. system reliability

The total annual cost (C_{toal}) is the sum of the annual capital cost, operation cost (C_{op}) and availability risk cost (C_{ar}). The capital cost (C_{cpt}) is determined by the system capacity (CAP). The operation cost (C_{op}) is estimated based on the annual energy consumption of the cooling system. Availability risk cost is introduced to account for the loss caused by the cooling demand that the system does not satisfy, which is called penalty cost in other field (Stapelberg 2009). It is calculated based on the cooling load and the available capacity (CAP_a) of the cooling system at specific time, as shown in Eq. (5-16). If the cooling demand is met, the availability risk cost will be zero. From Fig. 5.8 it can be found that with the increase of system reliability (capacity), the availability risk cost decreases. The total annual cost decreases firstly and then increases after it reaches the minimum at point O, which is the target system. Eq. (5-15) indicates that the total annual cost is determined by the cooling system capacity

(*CAP*). Therefore, the aim is transferred to obtain the optimal capacity of the cooling system with the lowest annual total cost.

$$C_{toal}(CAP,Load)=C_{cpt}(CAP)/yr+C_{op}(CAP,Load)+C_{ar}(CAP,Load) \quad (5\text{-}15)$$

$$C_{ar}=\sum_{i=1}^{8760}(P_{ar}\times max\left(0,\ Load(i)\text{-}CAP_a(i)\right)) \quad (5\text{-}16)$$

5.5 Summary

Design optimization methods considering uncertainty, both uncertainty and reliability are developed for DCSs and ICSs. Processes for uncertainty quantification and reliability assessment are described and the steps to implement the methods are explained. The optimal design method based on mini-max regret theory is introduced, which determines the robust cooling systems in a simple and effective way. By quantifying uncertainties, the uncertainty-based optimal design method is realized and the optimized design can be achieved. By quantifying uncertainty and reliability, the robust optimal design with the lowest total annual cost can be achieved.

CHAPTER 6 OPTIMAL DESIGN BASED ON MINI-MAX REGRET THEORY CONSIDERING UNCERTAINTY

Considering the uncertainty at planning and design stages, the optimal cooling system can be achieved based on mini-max regret theory without probability assumptions. The method is demonstrated in this chapter through a case study. Chillers and chilled water pumps of cooling systems are two primary energy consuming sub-systems. Appropriate design of these two components is very important for achieving high system efficiency. Therefore, the optimal design method based on mini-max regret theory is implemented in the design optimization of chiller combination and chilled water pump configuration in this chapter.

6.1 System introduction

The cooling system of an office building in the new district described in Chapter 4 is selected to test and evaluate the new method. The annual hourly cooling load is calculated with the weather data of TMY in Hong Kong by TRNSYS, which is shown in Fig. 6.1. It shows that the cooling is required almost all the year due to the subtropical climate. The maximum cooling load is 5746 kW, which is the basis for sizing the cooling system. The design scheme of the cooling system using the conventional method is taken as the reference case.

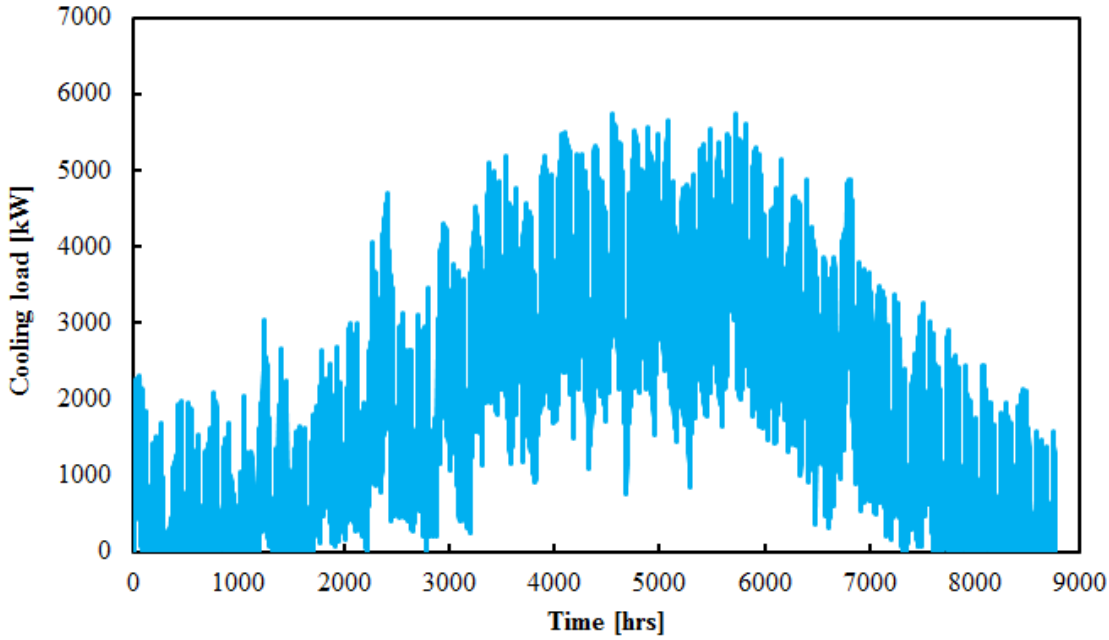

Fig. 6.1 Annual hourly cooling load of the building in the reference case

The aim of the proposed optimal design method is to obtain the optimal design of the cooling system considering uncertainty during the design process. It is implemented in the two major aspects of the cooling system: the combinations of chillers with different numbers and capacities, and the configurations of chilled water pumps. For the design optimization of chiller combinations, uncertainty in the cooling load calculation is concerned. For the design optimization of chilled water pump configurations, uncertainty in the resistance of the chilled water pipeline is concerned.

A) Combination of chillers

When determining the numbers and capacities of chillers, the conventional approach is to select several identical chillers because of simplicity, easy control and convenient maintenance. However, this may not be the efficient way considering the partial load. Even though the optimal combination can be selected based on the cooling load in the reference case, it may not be the uncertainty-based optimal one in consideration of

uncertainty. Here the mini-max regret method is used to obtain the uncertainty-based optimal combination of chillers considering uncertainty in the cooling load calculation.

To obtain the uncertainty-based optimal cooling system based on the mini-max regret theory, the following assumptions are made:

- The uncertainty in the cooling load is quantified by multiplying the cooling load by a factor ranging from 0.5~1.5 with an interval of 0.1.
- The chiller number ranges from 2 to 4. For each number, many combinations are available. The chiller capacity is discrete with an interval of 10% of the total capacity of the cooling systems.
- The performance curve of all the chillers with different capacities is assumed to be the same, which aims to avoid the deviation caused by the performance uncertainty of the chillers.
- All the cooling water pumps and chilled water pumps are constant speed pumps.

Cooling systems with different numbers of chillers are designed using the maximum cooling load. For each option of chillers, the available combinations are listed in Table 6.1. The value in the table is the ratio of each individual chiller capacity to the total capacity of the cooling plant. The performance curve of the chillers is shown in Fig. 4.5. The hydraulic heads are 20m (1m equals to 10^4 Pa) and 40m for the cooling water pumps and the chilled water pumps respectively. The power of the pumps is calculated with Eq. (4-4).

Table 6.1 Combinations of chillers for the cooling system

2 chillers		3 chillers		4 chillers	
No.	**Combinations**	**No.**	**Combinations**	**No.**	**Combinations**
C2-1	2 identical chillers	C3-1	3 identical chillers	C4-1	4 identical chillers
C2-2	0.1+0.9	C3-2	0.1+0.45+0.45	C4-2	0.1+0.1+0.1+0.7
C2-3	0.2+0.8	C3-3	0.2+0.4+0.4	C4-3	0.1+0.1+0.2+0.6
C2-4	0.3+0.7	C3-4	0.3+0.35+0.35	C4-4	0.1+0.1+0.3+0.5
C2-5	0.4+0.6	C3-5	0.4+0.3+0.3	C4-5	0.1+0.1+0.4+0.4
		C3-6	0.5+0.25+0.25	C4-6	0.1+0.2+0.2+0.5
		C3-7	0.6+0.2+0.2	C4-7	0.1+0.3+0.3+0.3
		C3-8	0.7+0.15+0.15	C4-8	0.2+0.2+0.2+0.4
		C3-9	0.8+0.1+0.1	C4-9	0.2+0.2+0.3+0.3

2) Configurations of chilled water pumps

The chilled water system can be organized in different configurations. In this case study, chilled water systems with five different configurations are considered. The resistance of the chilled water pipeline is the main factor affecting the energy consumption of pumps in operation. Therefore, uncertainty in the chilled water pipeline resistance is concerned. The resistance is expressed as the required hydraulic head (m). The parameters of these five chilled water systems used in the reference cases and the uncertainty-based cases considering uncertainty are shown in Table 6.2.

Table 6.2 Parameters of the chilled water pumps for the reference case and uncertainty-based cases

	Pump configuration	Pump head (m)			
		Reference case		Uncertainty-based case	
		Primary pumps	Secondary pumps	Primary pumps	Secondary pumps
CP3	3 constant-speed primary pumps	45	N/A	35~55	N/A
CP3VS3	3 constant-speed primary pumps & 3 variable-speed secondary pumps	15	30	15	20~40
VP3	3 variable speed primary pumps	45	N/A	35~55	N/A
CP3VS4	3 constant-speed primary pumps &4 variable-speed secondary pumps	15	30	15	20~40
VP4	4 variable speed primary pumps	45	N/A	35~55	N/A

The cooling systems with three identical chillers are selected to study the configurations of the chilled water systems considering the uncertainty of the pipeline resistance. Therefore, three constant speed pumps are designed for the primary pumps. The primary pumps operate following the sequence of the chillers they serve. The variable speed pumps (in the primary constant & secondary variable flow chilled water systems and primary only variable flow chilled water systems) are controlled by PID controllers. The controller is used to maintain the pressure drop across the most remote terminal user as a constant. The efficiency of the pumps for all the constant speed pumps is assumed to be the same as a constant.

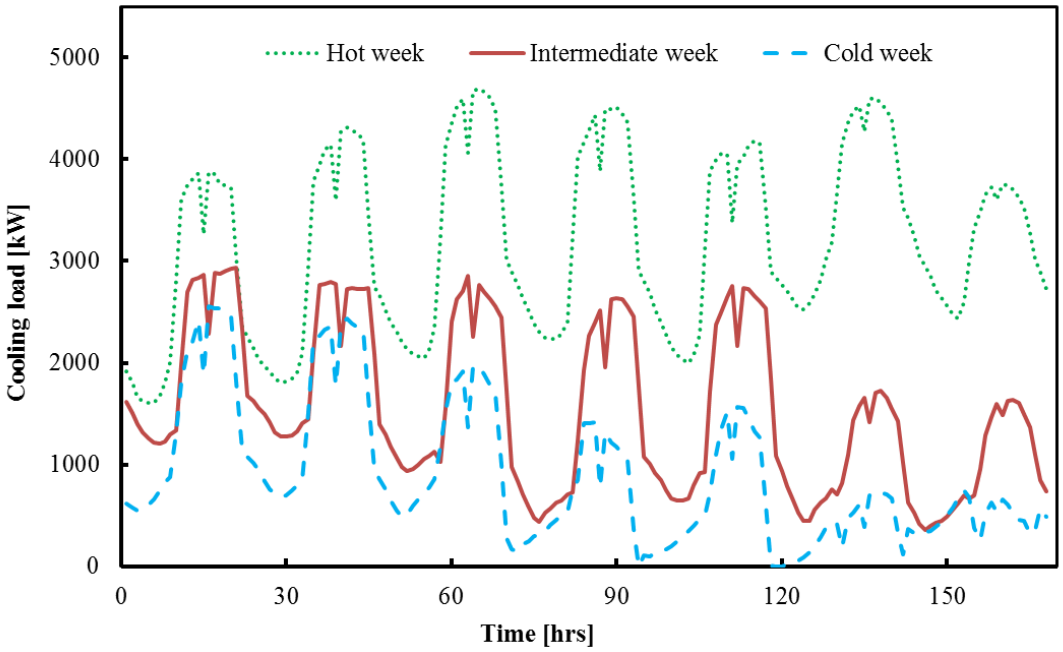

Fig. 6.2 Cooling loads of typical weeks in three different seasons

To simplify the calculation and reduce the tuning work of the PID controller, the energy consumptions of the cooling systems under the cooling loads of three typical weeks (instead of the whole year) are calculated. The cooling loads of these three weeks are taken from the hot season, the intermediate season and the cold season respectively, as shown in Fig. 6.2. It shows that the cooling load in the hot week is much higher than that in other two weeks. The cooling load in the cold week is very low and sometimes the cooling system will be shut down. The performances of the cooling systems with different combinations of chillers and configurations of chilled water pumps is presented in the following section. The energy consumption is used as the criterion to select the uncertainty-based optimal cooling system.

6.2 Performance of systems with different combinations of chillers

6.2.1 Combinations of two chillers

The energy performance of cooling systems with different combinations of two chillers is shown in Table 6.3. It shows that, for all the systems, the energy consumption increases with the increase of the uncertainty factor. For different systems under the same uncertainty factor, the energy consumption can be very different. With the energy consumption of each system at each uncertainty factor, the optimal systems with the lowest energy consumption at different uncertainty factors can be obtained. The regrets for each system can be calculated.

The regrets for the cooling systems with two chillers at different uncertainty factors are shown in Fig. 6.3. It shows that the System C2-2 has the largest regrets at all the different uncertainty factors, indicating that it has the largest deviation from the optimal design. System C2-4 and C2-5 have smaller regrets. The maximum regrets for each system at different uncertainty factors can be determined. The mini-max regret can also be determined. It is 0.0095 kWh which is from System C2-4. Therefore, System C2-4 is the uncertainty-based optimal cooling system when two chillers are selected. The capacities of the two chillers are 0.3 and 0.7 of the total capacity of the cooling system respectively.

Table 6.3 Energy consumption (10^6 kWh) of the cooling systems under different uncertainty factors of the cooling load - *Two chillers*

System / Uncertainty factor	C2-1	C2-2	C2-3	C2-4	C2-5
0.50	2.48	3.08	2.41	2.16	2.25
0.60	2.83	3.40	2.84	2.51	2.56
0.70	3.18	3.69	3.20	2.87	2.91
0.80	3.50	3.98	3.53	3.24	3.26
0.90	3.83	4.29	3.85	3.61	3.61
1.00	4.16	4.60	4.16	3.96	3.95
1.10	4.51	4.91	4.48	4.30	4.30
1.20	4.84	5.21	4.78	4.62	4.63
1.30	5.14	5.48	5.05	4.90	4.93
1.40	5.41	5.72	5.29	5.16	5.20
1.50	5.65	5.94	5.52	5.40	5.46

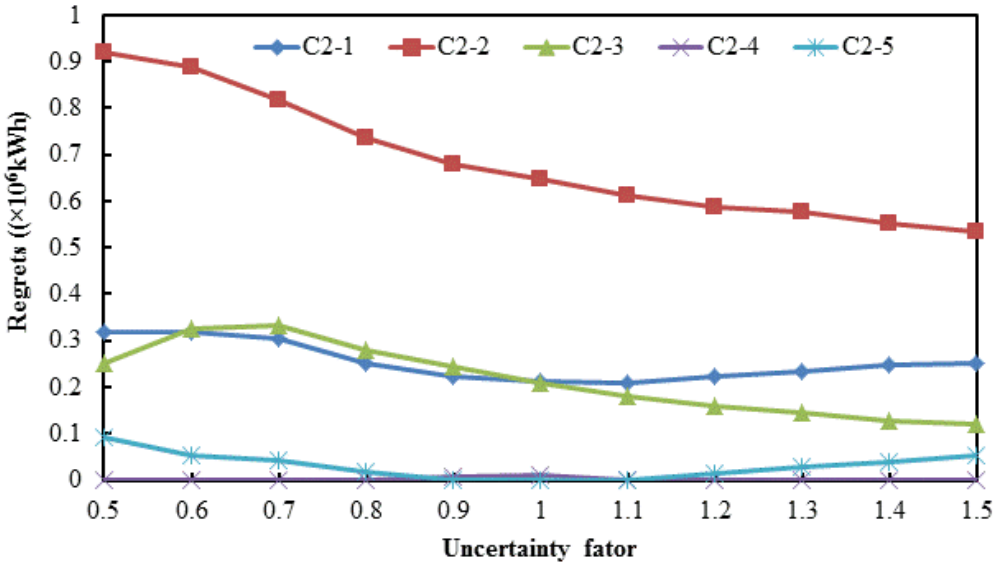

Fig. 6.3 Regrets for the cooling systems with different combinations of two chillers

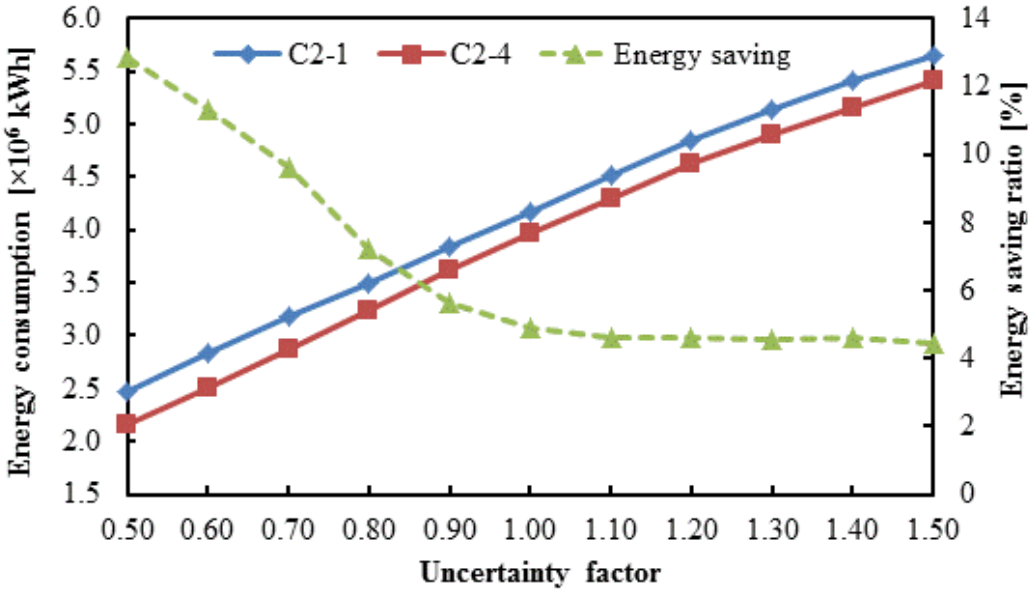

Fig. 6.4 Comparison between energy consumptions of System C2-1 and C2-4

The comparison between the energy consumptions of System C2-4 and C2-1 is shown in Fig. 6.4. The energy saving of System C2-4 is also shown in the figure. It can be found that the uncertainty-based optimal system always consumes less energy compared with System C2-1. The energy saving is up to 13%. The saving increases with the decrease of the cooling load uncertainty factors. It indicates that if the cooling load of the building decreases in the future, the advantage of the uncertainty-based optimal cooling system will become more apparent.

6.2.2 Combinations of three chillers

The energy performance of cooling systems with different combinations of three chillers is shown in Table 6.4. It shows similar trend as the cases of two chillers (Table 6.3). The energy consumption of all the systems increases with the increase of the uncertainty factors. For different systems under the same uncertainty factor, the energy consumption is also very different. The energy consumption of System C3-3 and System C3-7 is lower at each cooling load uncertainty factor. Actually the energy

consumptions of System C3-3 and System C3-7 are similar. That is due to the identical cooling load interval that can be used by the sequence control of the chillers in these two systems (i.e. 0.2 of the cooling system capacity). The optimal cooling system with the lowest energy consumption at each uncertainty factor can be obtained based on the data shown in Table 6.4.

Table 6.4 Energy consumption (10^6 kWh) of the cooling systems under different uncertainty factors of the cooling load - *Three chillers*

System / Uncer-tainty factor	C3-1	C3-2	C3-3	C3-4	C3-5	C3-6	C3-7	C3-8	C3-9
0.50	2.17	2.13	1.95	2.08	2.05	2.01	1.95	2.00	2.34
0.60	2.50	2.45	2.31	2.42	2.38	2.38	2.31	2.37	2.77
0.70	2.85	2.80	2.67	2.77	2.73	2.74	2.67	2.74	3.14
0.80	3.22	3.14	3.02	3.13	3.09	3.10	3.02	3.11	3.47
0.90	3.58	3.48	3.37	3.50	3.45	3.45	3.37	3.48	3.80
1.00	3.93	3.84	3.73	3.86	3.80	3.80	3.73	3.84	4.11
1.10	4.28	4.19	4.08	4.21	4.16	4.15	4.08	4.18	4.44
1.20	4.60	4.53	4.42	4.54	4.49	4.48	4.42	4.50	4.74
1.30	4.89	4.84	4.72	4.83	4.79	4.78	4.72	4.79	5.01
1.40	5.16	5.12	4.99	5.10	5.06	5.05	4.99	5.06	5.26
1.50	5.40	5.38	5.25	5.35	5.31	5.30	5.25	5.31	5.49

The regrets for all the systems at different uncertainty factors are shown in Fig 6.5. It can be found that the System C3-9 has the largest regrets at all uncertainty factors, indicating that it has the largest deviation from the optimal system. System C3-3 and C3-7 has the lowest deviation, which is 0. That is because the energy consumptions of

the System C3-3 and C3-7 are the lowest at every uncertainty factor. Having the regrets, the maximum regrets for each system at all the uncertainty factors can be determined. Accordingly, the mini-max regret can also be obtained. In this study, the mini-max regret is 0 which is from the System C3-3 and C3-7. It indicates that the System C3-3 and C3-7 are the uncertainty-based optimal cooling systems among all the design options. The capacity of three chillers is 0.2, 0.2, 0.6 or 0.4, 0.4, 0.2 of the total cooling system capacity.

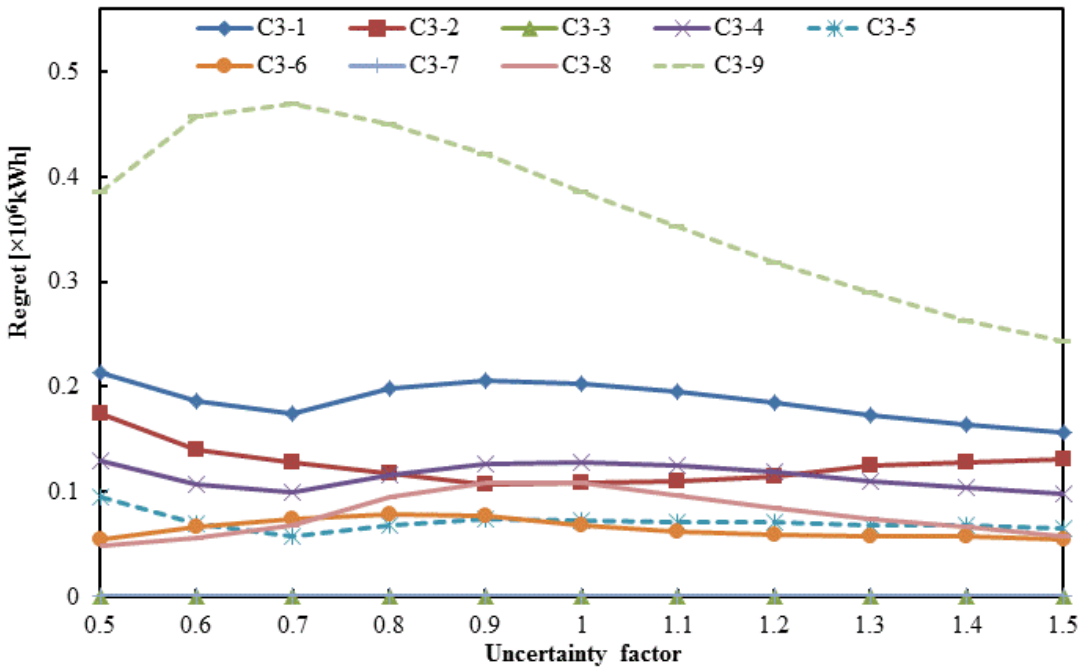

Fig. 6.5 Regrets for the cooling systems with different combinations of three chillers

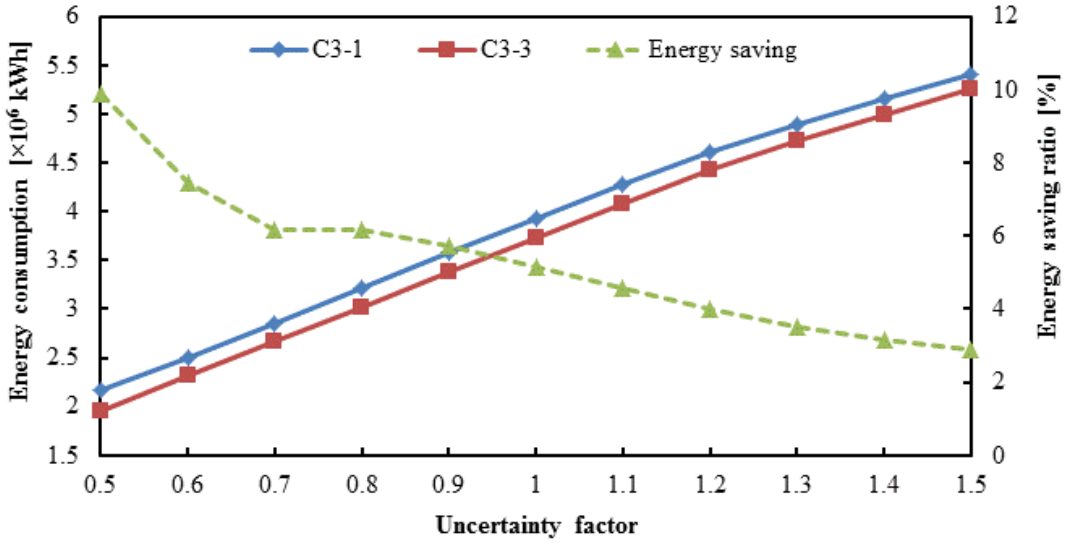

Fig. 6.6 Comparison between energy consumptions of System C3-1 and C3-3

The energy consumption comparison of System C3-1 and C3-3 is illustrated in Fig. 6.6. The energy saving of System C3-3 is also shown in the figure. It can be seen that the uncertainty-based optimal system can always consume less energy compared with System C3-1. At least 2.8% of energy can be saved by the uncertainty-based optimal cooling system. The energy saving ratio can be up to 10%. The saving increases with the decrease of the cooling load uncertainty factors. It indicates that if the cooling load of the building decreases in the future, the advantage of the uncertainty-based optimal cooling system will become more apparent.

6.2.3 Combinations of four chillers

The energy performances of the cooling systems with combinations of four chillers are shown in Table 6.5. It has the similar trend as that for the previous two cases shown in Table 6.3 and Table 6.4. The energy consumptions of all the systems increase with the increase of the uncertainty factors. For different systems under the same uncertainty factor, the energy consumption is very different. Having the energy

consumption of each system at each uncertainty factor, the optimal systems with the lowest energy consumption at different uncertainty factors can be obtained. The regrets can also be calculated.

Table 6.5 Energy consumption (10^6 kWh) of the cooling systems under different uncertainty factors of the cooling load - *Four chillers*

System / Uncerta-inty factor	C4-1	C4-2	C4-3	C4-4	C4-5	C4-6	C4-7	C4-8	C4-9
0.50	2.01	1.95	1.84	1.82	1.87	1.82	1.91	1.95	1.89
0.60	2.38	2.32	2.20	2.19	2.24	2.19	2.25	2.31	2.25
0.70	2.74	2.70	2.56	2.55	2.60	2.55	2.60	2.67	2.61
0.80	3.10	3.08	2.92	2.91	2.95	2.91	2.96	3.02	2.97
0.90	3.45	3.45	3.29	3.28	3.31	3.27	3.33	3.37	3.33
1.00	3.80	3.81	3.65	3.64	3.66	3.64	3.69	3.73	3.68
1.10	4.15	4.17	4.02	4.01	4.03	4.00	4.06	4.09	4.05
1.20	4.48	4.52	4.39	4.38	4.40	4.37	4.43	4.46	4.42
1.30	4.78	4.87	4.76	4.75	4.76	4.74	4.80	4.82	4.78
1.40	5.05	5.22	5.11	5.11	5.12	5.10	5.16	5.17	5.14
1.50	5.30	5.56	5.47	5.47	5.48	5.46	5.51	5.53	5.49

The regrets for the cooling systems with combinations of four chillers at different uncertainty factors are shown in Fig. 6.7. It can be seen that the energy consumptions of System C4-3, C4-4 and C4-6 are lower than that of other systems. System C4-1, which is commonly used, has lower energy consumption when the uncertainty factor is large. However, the regrets are the largest when the uncertainty factor is less than 1, indicating that it has the largest deviation from the optimal design. The maximum regrets for each system at different uncertainty factors can be determined. The mini-

max regret can also be determined. It is 0.16 (10^6 kWh), which is from System C4-6. Therefore, System C4-6 is the uncertainty-based optimal cooling system when four chillers are selected. The capacity of four chillers in System C4-6 is 0.1, 02, 0.2 and 0.5 times the cooling system capacity.

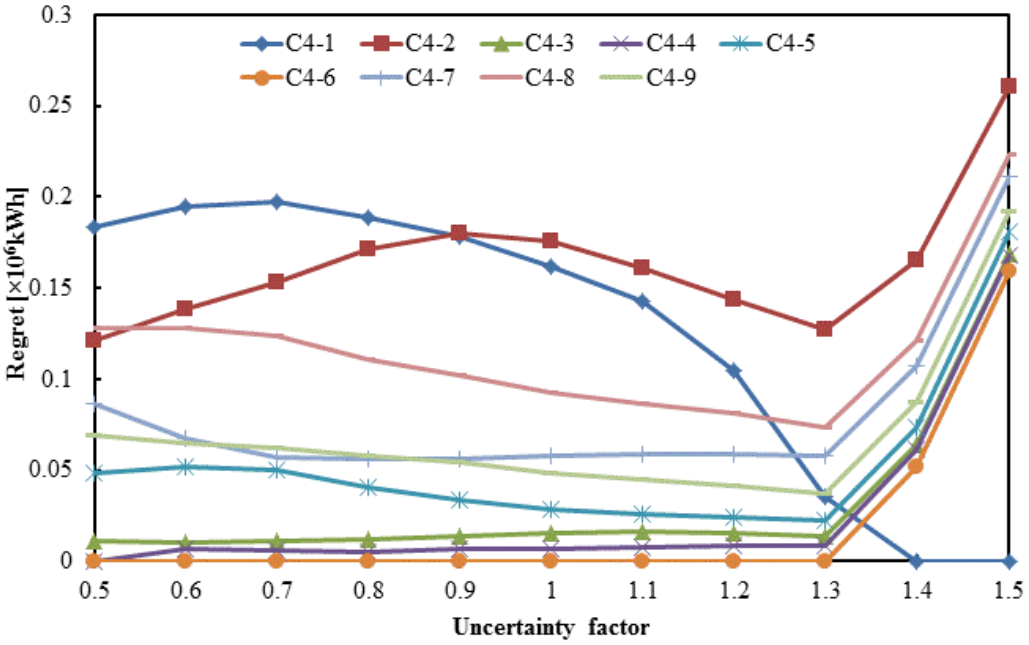

Fig. 6.7 Regrets for the cooling systems with different combinations of four chillers

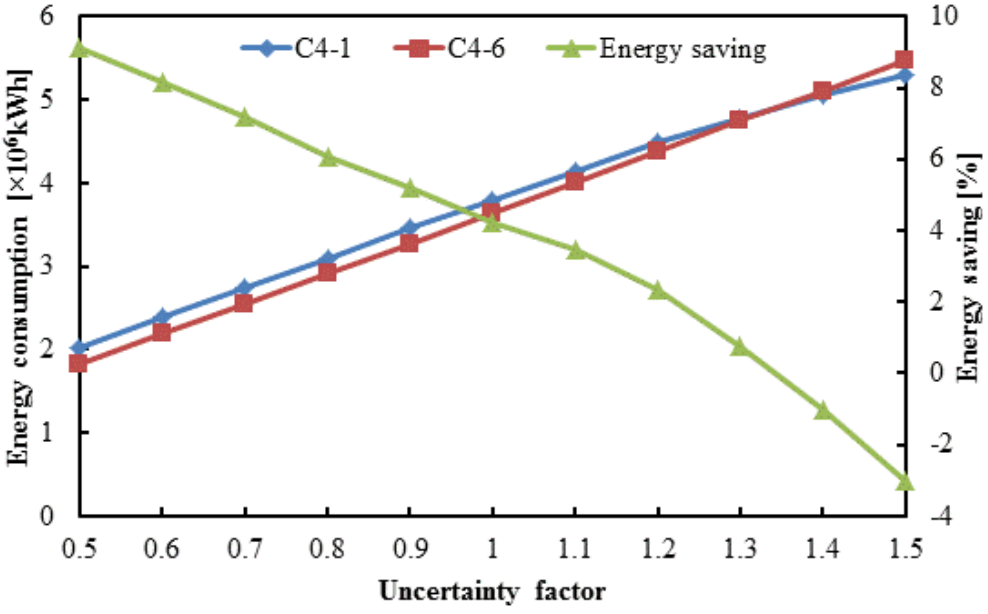

Fig. 6.8 Comparison between energy consumptions of System C4-1 and C4-6

The comparison between energy consumptions of System C4-1 and C4-6 is shown in Fig. 6.8. The energy saving of System C4-6 is also shown in the figure. The trend is different from the other two previous cases. The cooling system selected using the uncertainty-based optimal design method is not always the most efficient. When the uncertainty factor is more than 1.2, the energy consumption of System C4-6 is larger than that of System C4-1. System C4-6 can save up to 8% of energy compared with System C4-1. The saving increases with the decrease of the uncertainty factor. It indicates that, if the cooling load of the building decreases in the future, the advantage of the uncertainty-based optimal cooling system will become more apparent.

The cooling system designed using the uncertainty-based optimal method can be more energy efficient among most of the cases when the cooling load varies. The energy saving can be high to 12% compared to the system determined by the commonly used method. The designer can use this method to determine the uncertainty-based optimal combinations of chillers.

6.3 Systems with different configurations of chilled water pumps

The results for different configurations of chilled water pumps considering uncertainty in the pipeline resistance are presented in this section. The energy consumptions of the chilled water pumps in three typical weeks at different resistances are summarized in Table 6.6.

Table 6.6 Energy consumption (10^3 kWh) of chilled water pumps at different pipeline resistances in the three typical weeks

	Head (m) / **Config-uration**	**35**	**37**	**39**	**41**	**43**	**45**	**47**	**49**	**51**	**53**	**55**
Hot week	CP3	12.51	13.22	13.94	14.65	15.37	16.08	16.80	17.51	18.23	18.94	19.66
	CPVS3	10.51	10.69	10.89	11.11	11.36	11.59	11.83	12.09	12.37	12.68	13.09
	CPVS4	10.25	10.37	10.51	10.67	10.84	11.02	11.26	11.45	11.66	11.88	12.21
	VP3	6.49	6.65	6.82	6.98	7.16	7.33	7.55	7.76	7.95	8.15	8.36
	VP4	6.15	6.27	6.40	6.52	6.66	6.81	6.96	7.13	7.28	7.45	7.63
Intermediate week	CP3	5.65	5.97	6.29	6.62	6.94	7.26	7.58	7.91	8.23	8.55	8.88
	CPVS3	4.54	4.57	4.59	4.62	4.64	4.67	4.69	4.72	4.74	4.77	4.80
	CPVS4	4.31	4.33	4.34	4.37	4.39	4.41	4.43	4.46	4.48	4.50	4.52
	VP3	2.45	2.47	2.50	2.52	2.54	2.57	2.59	2.62	2.64	2.66	2.69
	VP4	2.12	2.12	2.13	2.14	2.15	2.17	2.18	2.20	2.21	2.23	2.25
Cold week	CP3	2.61	2.76	2.91	3.05	3.20	3.35	3.50	3.65	3.80	3.95	4.10
	CPVS3	2.35	2.37	2.39	2.40	2.42	2.43	2.45	2.47	2.48	2.50	2.52
	CPVS4	2.19	2.21	2.22	2.23	2.25	2.26	2.27	2.28	2.29	2.30	2.31
	VP3	1.54	1.55	1.56	1.57	1.58	1.59	1.59	1.61	1.62	1.63	1.64
	VP4	1.25	1.26	1.27	1.27	1.28	1.27	1.27	1.27	1.28	1.29	1.30

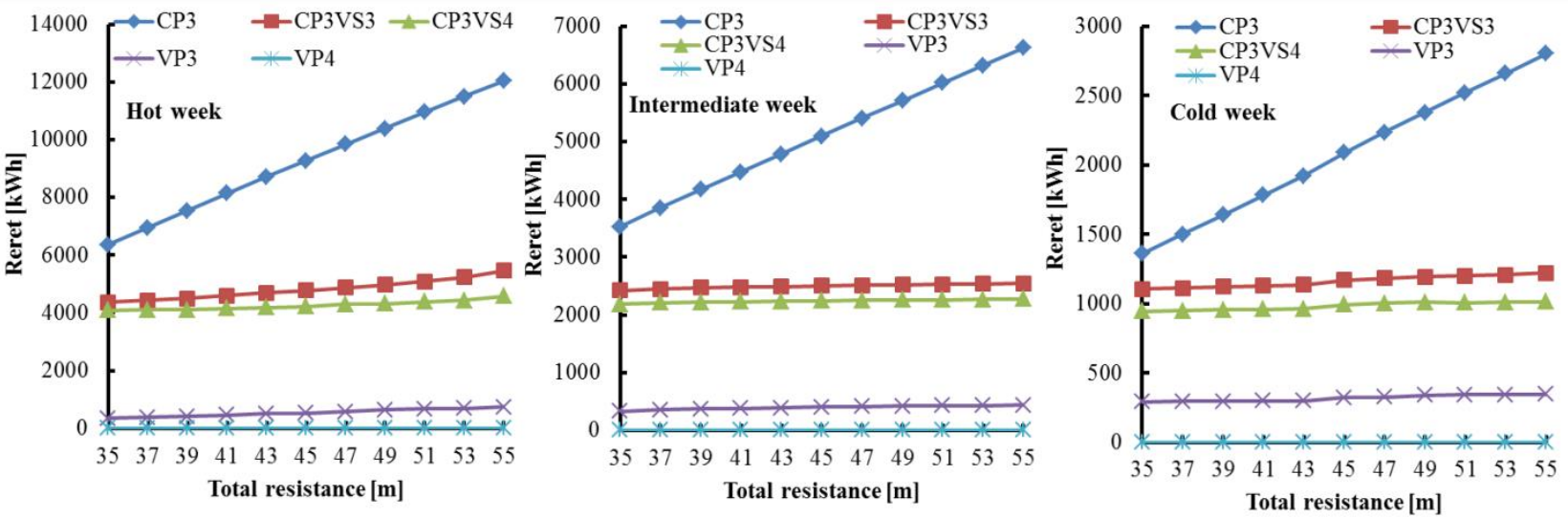

Fig. 6.9 Regrets of five chilled water pump configurations at different resistances

From Table 6.6, it can be observed that the energy consumption of the chilled water systems increases with the increase of the total resistance of the chilled water network. For each chilled water pump configuration, the energy consumption is the largest in the hot week and the lowest in the cold week, due to the cooling load difference. At the same cooling load and the pipeline resistance, the energy consumption of the configuration with constant speed primary pumps is much higher than that of the other two types of configurations. The configuration with variable speed primary pumps has the lowest energy consumption. It indicates that the chilled water system with variable speed primary pumps is more efficient than other systems. Compared with the configuration with constant speed primary only pumps, the configuration with variable speed primary only pumps can save 50%~60% of energy in the hot week at different resistances. In the intermediate week, the configuration with variable speed primary only pumps can save 62%~75% of energy, which is higher than that in the hot week. The advantage of the configuration with variable speed primary only pumps is more apparent when the cooling load is low. In the cold weeks, the chillers and pumps are shut down when the cooling load is too low. The energy saving for the configuration with variable speed primary only pumps is about 52%~68%. In all these three weeks, the energy saving for the configuration with variable speed primary only pumps increases with the increase of resistance.

The regrets for each chilled water pump configuration at different resistances in the three typical weeks are shown in Fig. 6.9. It can be seen that the trend is similar for the five different chilled water pump configurations in different weeks. The absolute regrets are the highest in the hot week and the lowest in the cold week. The regrets for VP4 system are 0 at all the resistances in the three weeks. It means that VP4 system is always the optimal system, no matter how the resistance changes in the range between

35m and 55m. The regrets for CP3 system are always higher than other systems at different resistances. It means that the configuration with constant speed primary-only pumps is always energy consuming, which should be avoided during the cooling system design. The configuration with constant primary & variable secondary pumps is better than that with constant speed primary-only pumps but worse than that with variable speed primary-only pumps. In addition, the system with more pumps has lower regrets when the means of pump connection is the same. It shows that the cooling system with more pumps in a given means of pump connection is more efficient.

The maximum regrets of the five chilled water pump configurations at all the resistances can be obtained. From Fig. 6.9 it can be seen that the maximum regrets locate at the end of each curve. The mini-max regret can be calculated by comparing the maximum regrets. It is 0 kWh in this case, which is from the VP4 system. It indicates that the VP4 system is the uncertainty-based optimal system among all the chilled water pump system options.

6.4 Discussions

The uncertainty-based optimal design of the cooling system can be obtained using the proposed method. The advantage of this method is that it is easy to realize the design optimization. No additional complex methods or models are introduced when selecting the uncertainty-based optimal cooling system. The uncertainty-based optimal design is determined by repeating the original methods a few more times. This is very beneficial for practical applications as it is usually difficult or impossible for consultants or designers to optimize the design by learning new and complicated methods due to limited time and efforts. Such a method will help them to obtain the uncertainty-based optimal design effectively.

Usually there are many factors that have uncertainty in the design of cooling systems, only two of which are studied in this section. Uncertainty-based optimal design of the cooling systems considering other uncertainty factors is worth to be investigated in further study. More efforts are needed on optimizing the cooling system design by considering uncertainty at both design and operation stages.

The chiller capacity changes with an interval of 10% of the cooling system capacity in this paper. In actual applications, the interval may be smaller and more cases can be obtained and compared. The uncertainty-based optimal chiller combinations are selected without considering backup system. The decision is just made based on energy performance of cooling systems. For practical applications, uncertainty-based optimal design of cooling systems needs to consider the reliability of components and backup system.

The annual energy consumption of the chilled water pumps is not estimated in this study. However, three typical weeks are selected from the hot season, intermediate season and cold season. The trend of pump energy consumption in these three weeks keeps consistent. Thus, the conclusions can be made based on the performance of five chilled water pump configurations in these three weeks.

The mini-max regret of the uncertainty-based optimal chilled water pump configuration is 0 kWh in this study. It means that the configuration of VP4 is always the best considering uncertainty in the pipeline resistance. Even without considering the uncertainty, Configuration VP4 may also be selected due to lower energy consumption. Coincidentally the optimal design is also the uncertainty-based optimal design. However, this may not be the general case when optimizing the cooling system design. Usually the mini-max regret is not 0, as shown in the study of chiller

combinations. A trade-off may exist in the robustness and performance. The proposed method mainly contributes at such situation. It helps to select the uncertainty-based optimal system by compromising the robustness and optimum.

6.5 Summary

An improved design method for cooling systems is proposed based on mini-max regret theory. The method is easy to be implemented and no complicated models or computation are involved. It is very beneficial for practical applications.

The uncertainty-based optimal cooling system with different numbers of chillers can be obtained using the proposed method. If two chillers are selected, the uncertainty-based optimal combination of chillers is the option with individual chiller capacities of 0.3 and 0.7 of the total cooling system capacity. It can save up to 12% of energy compared with the commonly used system (equally sized). If three chillers are selected, the uncertainty-based optimal chiller combination is the option with 0.2, 0.2 and 0.6 or 0.4, 0.4 and 0.2 of the total cooling system capacity. The energy saving can be up to 10%. The uncertainty-based optimal combination of four chillers is the option with individual capacities of 0.1, 0.2, 0.2 and 0.5 of the total cooling system capacity. The energy saving can be up to 10%.

The results of the study on five types of chilled water pump systems show similar energy consumption trend under different cooling loads. The configuration with constant speed primary-only pumps is always the most energy-consuming, which is recommended to be avoided in practical applications. The chilled water configuration with variable speed primary-only pumps is the uncertainty-based optimal one, considering uncertainty in the resistance of the pipeline. The energy consumption can be reduced by 50% in the case of the uncertainty-based optimal configuration. For the

configurations with similar connection way of chilled water pumps, the option with smaller pumps is more efficient.

The probability distribution of uncertainty factors is not considered in this uncertainty-based optimal design method based on mini-max regret theory. Design optimization with uncertainty quantification is investigated in the following section.

CHAPTER 7 OPTIMIZED DESIGNS OF ICS AND THEIR PERFORMANCE CONSIDERING UNCERTAINTY AND RELIABILITY

Optimal design methods for ICSs are investigated based on uncertainty quantification at planning and design stages. Results of the uncertainty-based optimal design are analyzed and compared with that using the conventional design method. Then the performance of ICSs designed using the robust optimal design, considering both uncertainty and reliability, is analyzed and compared with that using the conventional method, uncertainty-based optimal design method and reliability-based optimal design method.

7.1. Introduction of the ICS

An office building of eight floors is selected to test the use of the new design methods. The surface to volume ratio is about 0.1. The envelope material is concrete blocks. The total floor area is about 36,000 m^2. The building is simulated using TRNSYS, and the cooling loads with and without uncertainty are calculated with a time step of one hour. The calculated cooling load without uncertainty is shown in Fig. 7.1 and taken as the reference case. The peak cooling load is 5,014 kW (140W/m^2). It appears at the 4,554th hour of the whole year. Therefore, the 4554th hour is marked as the peak hour. In the conventional design process, the capacity of the cooling system will be determined based on this peak cooling load.

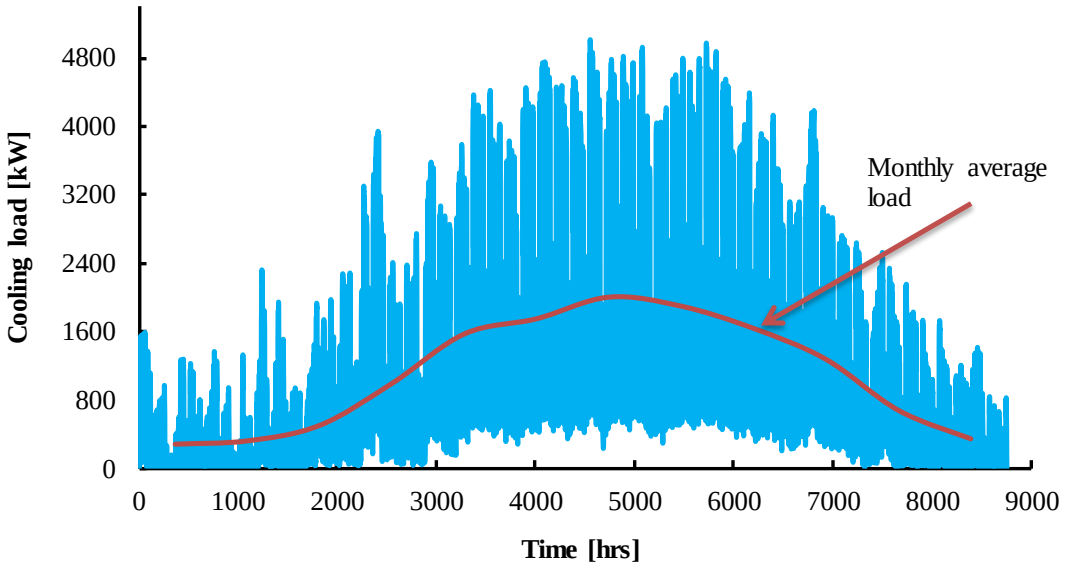

Fig. 7.1 Annual hourly cooling loads of the office building without uncertainty

Table 7.1 Factors and their distributions concerned in uncertainty analysis of ICS

Factor	Reference Case	Uncertainty analysis	
		Distribution	Value
Outdoor temperature (℃)	TMY	Normal distribution	u: TMY; σ: 1
Outdoor relative humidity (%)	TMY		u: TMY; σ: 4
Radiation (W/m^2)	TMY		u: TMY; σ: 40
Indoor air temperature(℃)	25		u: 25; σ: 0.6
Indoor relative humidity (%)	55		u: 55; σ:4
Ventilation rate (1/h)	1.5	Triangular distribution	1.5* triangular (0.3, 1.2, 0.9)
Occupant (m^2/person)	6		6* triangular (0.3, 1.2, 0.9)
Lighting (W/m^2)	12		12* triangular (0.3, 1.2, 0.9)
Equipment (W/m^2)	19		19* triangular (0.3, 1.2, 0.9)

Note: In the normal distribution, u refers to the mean value and σ refers to the standard deviation. For a triangular (a,b,c), a, b and c refer to the lower limit, upper limit and mode respectively.

Uncertainties of nine factors are considered in this chapter, as shown in Table 7.1. Uncertainties in the building design/construction are not considered. The sampling

methods are explained as follows. 1020 trials are conducted for the uncertainty analysis of the cooling load.

- For the outdoor weather condition, three most important factors affecting the cooling load are concerned, including the outdoor dry-bulb temperature, relative humidity and solar radiation. The samples of these three factors are assumed to fit normal distributions. The weather data of TMY are taken as the mean of these factors at each time step.
- For the internal heat sources, the parameter settings in the simulation are usually the possible maximum values. The most important factors regarding the internal heat gain sources include the occupant density, ventilation rate, lighting density and equipment density. The actual values for these four factors are most likely lower than that. Coefficients are assigned to the values used in the reference case and assumed to fit triangular distributions. The mode, upper limit and lower limit of these coefficients are chosen as 0.9, 1.2 and 0.3 respectively.
- The indoor temperature and relative humidity set-points keep constant in the reference case. Actually the set-points may differ randomly from room to room, based on the preferences of users. It can range from 22℃ to 28℃ actually, instead of 25℃ in the reference case. The indoor relative humidity is not controlled in many projects. Therefore, uncertainties of the indoor temperature and relative humidity set-points are assumed to fit normal distributions.

7.2 Uncertainty quantification of cooling loads

7.2.1 Peak cooling load distribution of a building

By considering uncertainties of nine operation factors used in design, the cooling load distribution at the peak hour (4554th hour) can be obtained. To check whether the

cooling load of a building fits a normal distribution, the commonly-used Q-Q plot is used to compare the cooling load distribution at the peak hour with the standard normal distribution, as shown in Fig. 7.2. Note, if all the data locate closely along the solid line, the data are proven to fit a normal distribution.

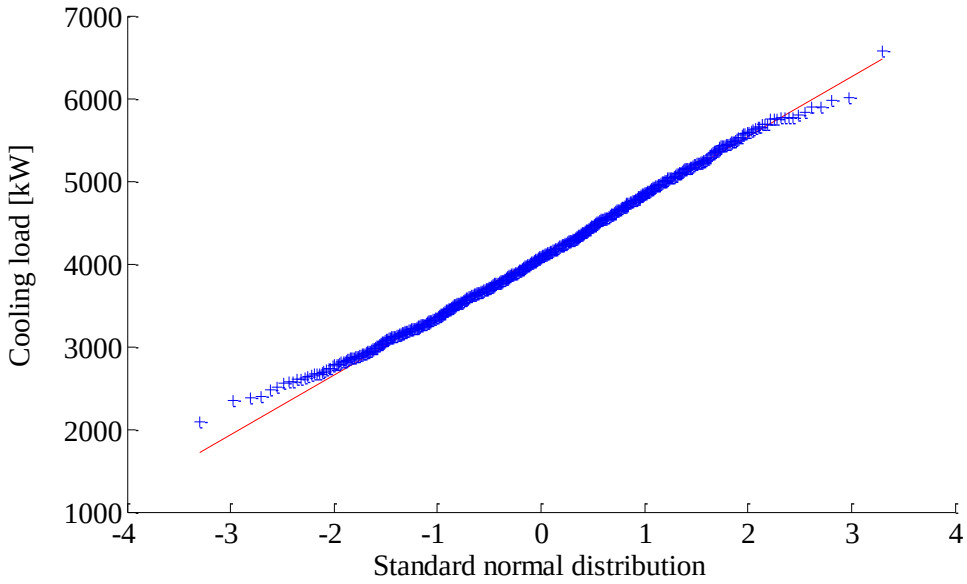

Fig. 7.2 Q-Q plot of the cooling loads at the peak hour vs. standard normal distribution

Fig. 7.2 shows that the cooling loads at the middle are very close to the solid line while data at two ends deviate significantly from the solid line. It indicates that the cooling loads do not exactly fit a normal distribution. The frequency and cumulative distribution function (CDF) of the cooling loads at the peak hour are illustrated in Fig. 7.3. The peak cooling load in the reference case and that times 1.2 are also marked in the figure as dotted lines. The mean cooling load at the peak hour is 4103 kW, which is about 24% lower than the peak cooling load of the reference case. Fig. 7.3 shows that the peak cooling load of the reference case locates at the cumulative probability of 90%. It means that the cooling load at the peak hour has a probability of 90% to be

lower than the peak cooling load of the reference case, which also indicates that the cooling system designed using the conventional method is very possible to be oversized. If a safety factor of 1.2 is used (which is often used in current design practice), the cumulative probability is about 99.5%. It means that the cooling load at the peak hour has a probability of 99.5% to be less than the peak cooling load times 1.2. The cooling system sized based on this load has a probability of 99.5% to be oversized. The value around 4200 kW has high frequency and the most possible peak cooling load is around 4200 kW. From the analysis, it shows that the cooling system designed based on the peak cooling load without considering uncertainty has strong probability to be oversized. The probability will be much stronger if a safety factor is assigned.

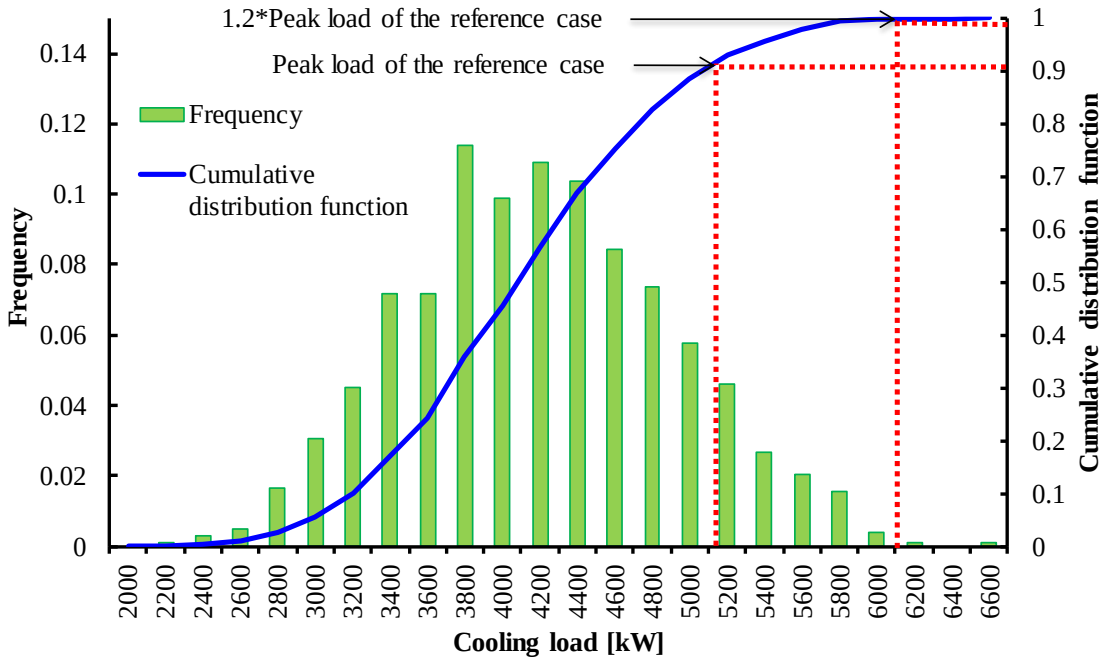

Fig. 7.3 Distribution of cooling loads at the peak hour

7.2.2 Annual cooling load distribution of a building

The annual cooling loads play a key role in the selection of the system configuration, such as the chiller combinations. The distribution of the annual average cooling load is shown in Fig. 7.4, considering uncertainties of inputs in the design calculation. The annual average cooling load in the reference case is also presented in the figure with dotted line. It shows that the annual average cooling load has a possibility of over 80% to be lower than that of the reference case. Without considering uncertainties, it may lead to overestimate the energy consumption when assessing the building performance. The most possible annual average cooling load is around 900kW, which is about 18% lower than that of the reference case.

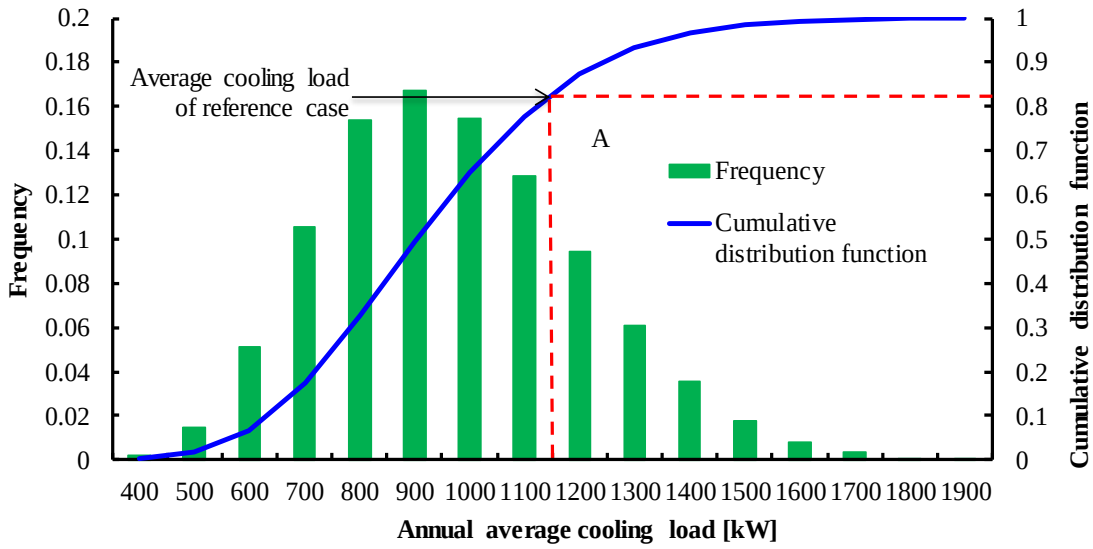

Fig. 7.4 Annual average cooling load distribution

The annual cumulative proportions of the cooling loads in these 1020 trials are shown in Fig. 7.5. Each curve shows the proportions of time corresponding to different cooling load intervals in a year. It can be seen that, when the cumulative proportion is 1, the range of the cooling loads is very large. It varies from 2000 kW to 7000 kW. Both the maximum and minimum values are from the extreme cases in the uncertainty

study, which may happen but the probability is very low. Several representative curves are extracted as shown in Fig. 7.6.

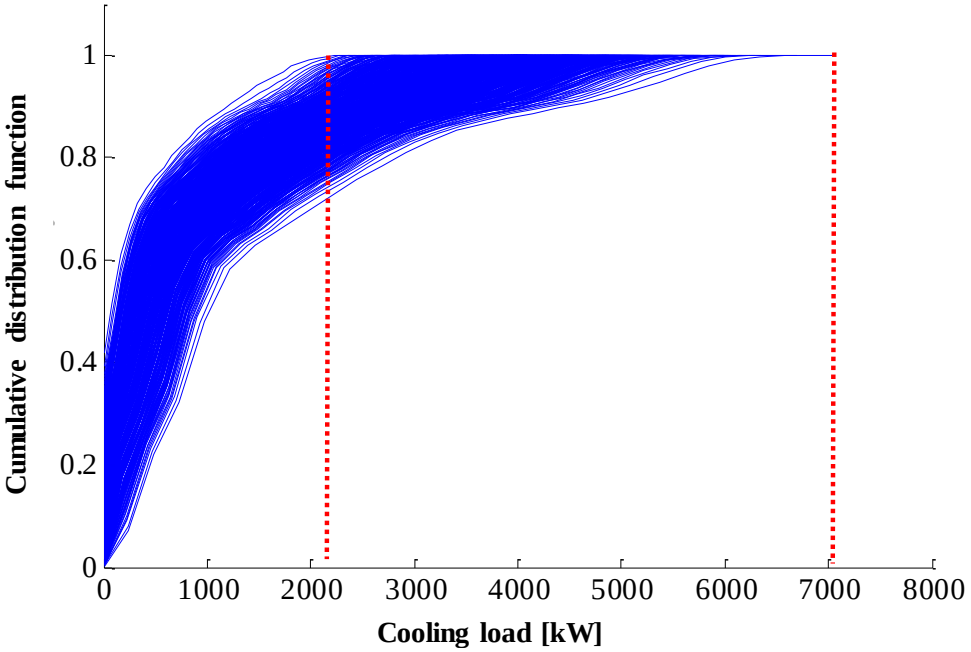

Fig. 7.5 Annual cooling load distribution considering uncertainty

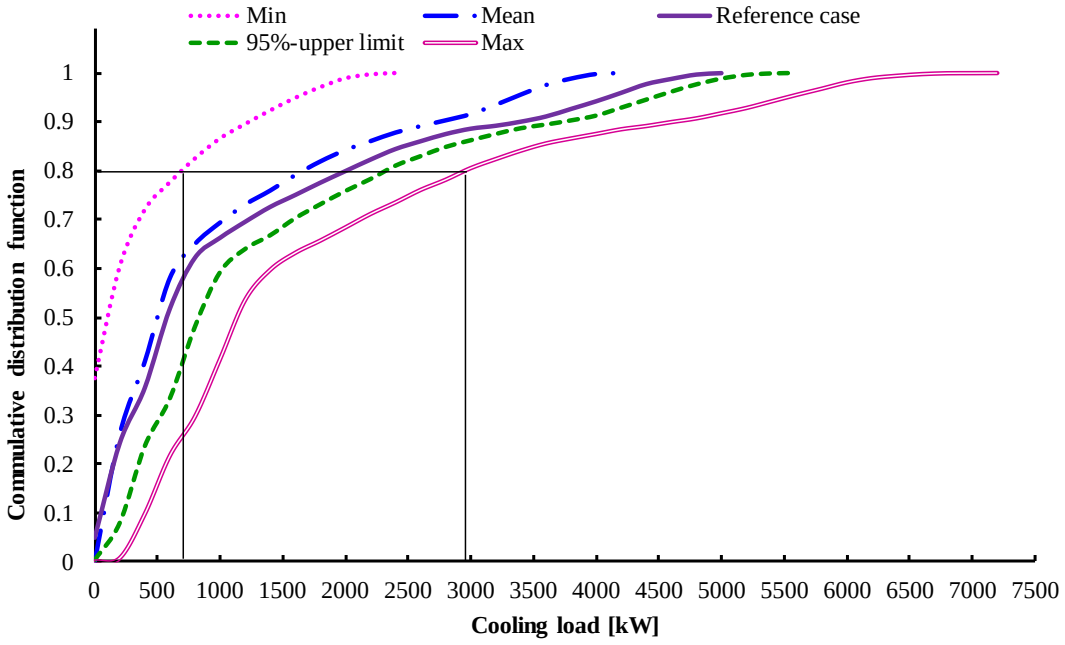

Fig. 7.6 Cumulative distribution profiles of representative annual cooling loads

The curves marked as *min*, *max* and *mean* refer to the load distribution profiles of the lowest, the highest and average cooling loads respectively among the 1020 trials at each hour in a year. The data on the *95%-upper limit* curves refer to the loads of the upper limit of the 95% confidence interval among 1020 trials at each hour in a year. Fig. 7.6 shows that the cooling load varies in a big range between the *min* and *max* curves at the same cumulative proportion. It indicates that for any value of the cumulative proportion, the cooling load varies largely when uncertainties of these nine factors are concerned. The mean values still represent the most possible cooling loads at each hour in the year. It can be seen that, at the same value of cumulative probability, the cooling load of the reference case is larger than that the mean value. It confirms again that the cooling systems sized using the cooling loads of the reference case have strong probability to be oversized.

7.3 Uncertainty-based optimal design of the ICS

Based on the uncertainty quantification, the design of the ICS can be optimized. The capacity and optimal configuration of the ICS can be determined based on the performance distribution at different risks.

7.3.1 Optimal sizing of the ICS

As mentioned in the literature, annual 0.4% cooling design day can be used to size the cooling systems. The hourly dry bulb temperatures of several years are sorted in descending order. The value of dry-bulb temperature at the 0.4% percentile corresponds to the 0.4% cooling design day. It locates at the 35th hour when scaled to one year. The cooling load distribution at the 35th hour is shown in Fig. 7.7. The cooling load at the 35th hour of the reference case is also illustrated in the figure and highlighted with dotted line. It can be seen that by considering uncertainty, the most

possible cooling load at the 35th hour is around 4660 kW while in the reference case the cooling load is 4770 kW. The difference is not as large as that for the peak cooling load. It indicates that, if the ICS is designed based on the annual 0.4% cooling design day, the probability of oversizing is much lower than that designed based on the exact peak cooling load.

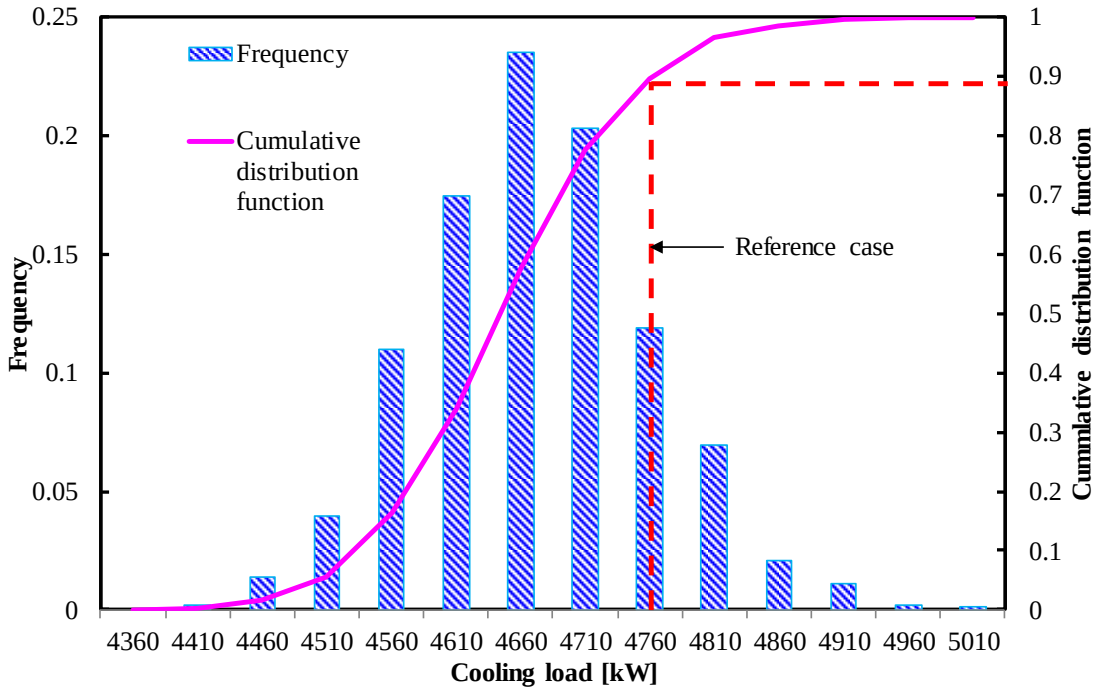

Fig. 7.7 Distribution of cooling loads at the 35th hour in each year (descending sort order of the cooling loads)

The distribution of cooling loads with the numbers of hours when the cooling demand cannot be met (marked as unmet hours) is presented in Fig. 7.8. The mean cooling loads of the 1020 trials are calculated and shown in the figure. Although the mean cooling loads do not exactly equal to that with the highest frequency but the differentials are very small. To certain extent, the mean value can represent the most possible value. Among these 1020 trials, the upper limit of the 95% confidence interval at each number of hours is also calculated and shown in the figure (marked as 95%

upper limit). It is apparent that all these three types of cooling loads decrease with the increase of unmet hours. The mean cooling load of cases with uncertainty is much lower compared with the cooling load of the reference case. The ratio (mean cooling load divided by the cooling load of the reference case) increases with the increase of the number of unmet hours. The decision makers can size the ICS based on their specific requirement. For example, if the number of unmet hours should be no more than 50, the ICS can be sized based on the load of 4730 kW, 5155 kW and 3890 kW. Larger cooling load can be selected (such as 5155 kW) if the requirement is very strict. Otherwise, lower ones can be used.

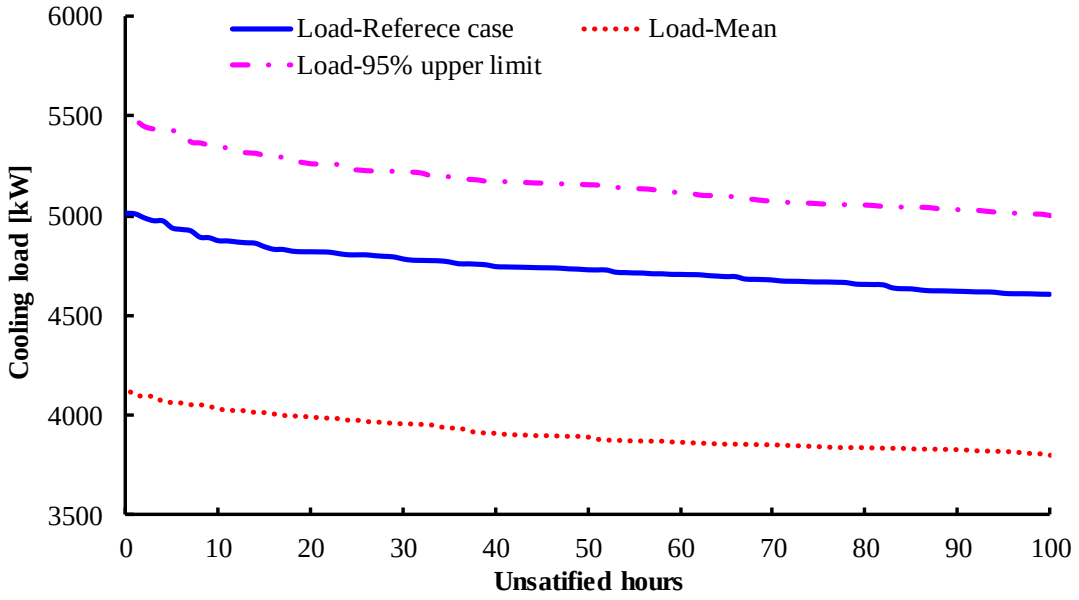

Fig. 7.8 Cooling load distribution vs. the number of annual unmet hours

The corresponding capital cost for the chillers with the number of unmet hours is illustrated in Fig. 7.9. The cost is calculated based on data practically offered by one manufacturer. With the increase of unmet hours, the capital cost decreases gradually. Fig. 7.9 shows that the capital cost of the ICS sized based on the mean cooling load can be 20% lower than that sized based on the load from the upper limit of 95% confidence interval. With the curves and results in Fig. 7.8 and Fig. 7.9, designers can

select the corresponding cooling load with quantified risk and potential cost. If the primary objective is to meet the cooling demand, the cooling load on the 95% upper limit curve can be used to determine the capacity of the ICS. If the requirement for thermal comfort is not very strict and the budget is quite limited, lower cooling load can be used such as that on the mean cooling load curve. No matter which is selected as the capacity of the cooling system, the decision can be made with quantified confidence and cost.

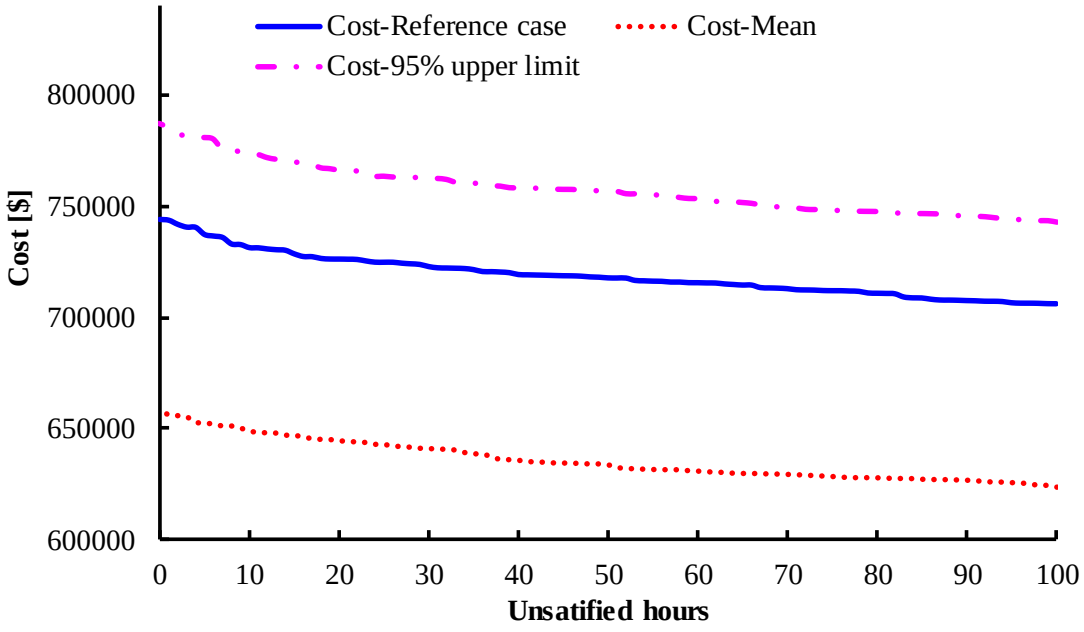

Fig. 7.9 Capital cost distribution vs. number of annual unmet hours

7.3.2 Optimal configuration of the ICS

The study on chiller configurations is presented as an example to illustrate the necessity to consider the uncertainties of the input variables for cooling load calculation in selecting the configurations of ICSs. Energy consumption of the ICS with different configurations is compared. The model for centrifugal chillers developed in Section 4.3 is used in the ICS.

The peak cooling load of the reference case is 5040 kW, which is used as the design capacity of the ICS as an example. Three chillers are selected with a total capacity of 5100kW. Chillers with two common configurations are compared: three identical chillers with an individual capacity of 1700kW (marked as S_{ics1}) and two chillers with an individual capacity of 2000kW & one chiller with a capacity of 1100kW (marked as S_{ics2}). Energy consumptions of S_{ics1} and S_{ics2} are 1,732,736 kWh and 1,672,506 kWh in the reference case. The energy consumption of S_{ics2} is 3.5% lower than that of S_{ics1}. Considering the difference of energy consumptions without concerning uncertainty, the decision maker may easily choose S_{ics2} due to lower energy consumption. However, at practical operation, the chosen configuration in the reference case may not be as efficient as expected. By considering uncertainty in the cooling load, the relative energy consumption difference of both configurations is shown in Fig. 7.10.

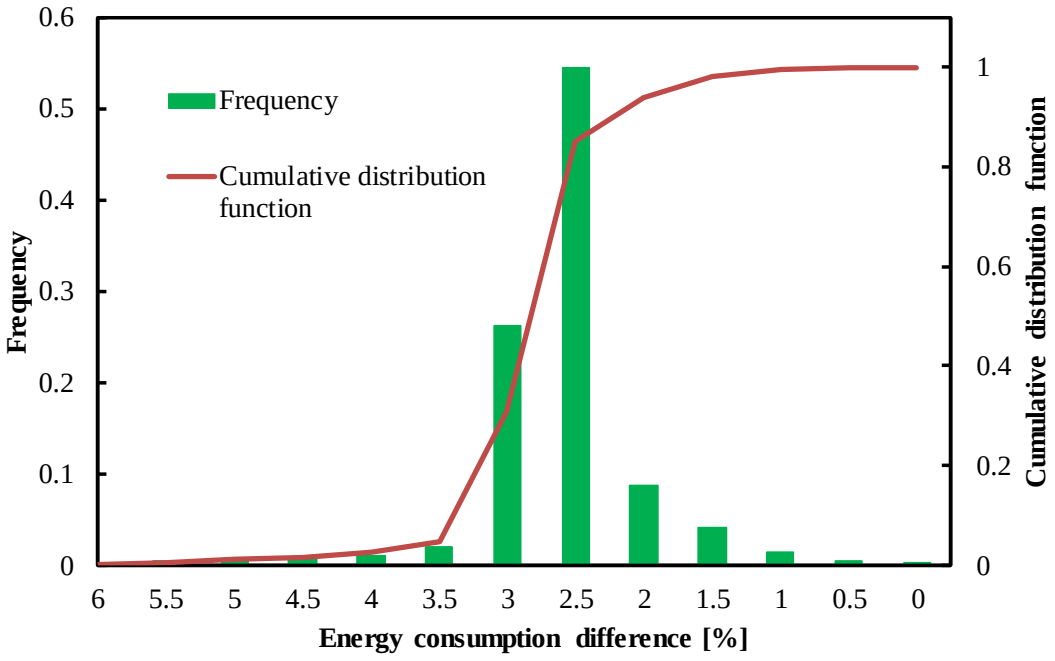

Fig. 7.10 Distribution of relative difference between energy consumptions of two ICSs

Fig. 7.10 shows that such difference varies from 0 to 6%. It means that sometimes the energy consumptions of both configurations show large difference and sometimes the difference can be ignorable. It can be therefore risky to make the decision without considering uncertainty. The cumulative probability of the difference at 3.5% is less than 0.1. It means that the difference has over 90% probability to be lower than that. Values around 2.5% have the highest frequency, indicating that it is very possible to be around 2~2.5%. Although S_{ics2} is still more efficient, its advantage is not as apparent as that in the reference case. In addition, the purchase, installation, operation and management of S_{ics2} are more complicated compared with S_{ics1}. If the efficiency difference of both configurations is not very large, the decision maker may change his mind and choose S_{ics2}. No matter which configuration is selected, the decision can be made with quantified risk and benefit as shown in the figure. That is the main contribution by considering uncertainty in the design process.

7.3.3 Conclusive remarks

In this section, a new method to optimize the ICS design is proposed by considering uncertainties of operation factors affecting the cooling load design calculation. The impacts of the operation factors including the outdoor weather, internal heat sources and indoor set-points are studied. A case study is given as an example to demonstrate the use of proposed method. The oversizing problem is explained from the viewpoint of uncertainty. The sizing and configuration of the ICS based on the risk and benefit analysis are presented. Conclusions can be made as follows:

i. The peak cooling load varies largely by considering uncertainties of operation factors. If the capacity of an ICS is based on the cooling load without considering

uncertainty, it has high probability to be oversized. If a safety factor is assigned, the oversize probability will be greatly increased.

ii. By showing the distribution of unmet hours and capital costs, the proposed design optimization method offers decision makers quantified risk and benefit. The decision makers can size the ICS based their specific concerns with more confidence.

iii. The annual average cooling loads varies largely considering uncertainty. The annual cumulative cooling load is usually over estimated using the conventional method. That may affect the building performance assessment.

iv. The configuration of the ICS can be selected according to quantified risk and benefit when considering uncertainty. The selected configuration may not perform as well as expected and its efficiency is most likely overqualified.

7.4 Robust optimal design of the ICS considering uncertainty and reliability

Both uncertainty of design inputs and reliability of components are quantified and used in enhancing the optimal design. The method of uncertainty quantification is similar to that described in Section 7.2. The performance of the ICS designed using the robust optimal method is presented in the following section compared with other design methods.

7.4.1 System description

The system design is different from that in Section 7.2 since the reliability of the ICS is considered. In the conventional method, backup systems are used to consider the possible system failures or faults. The peak cooling load of the ICS, shown in Fig. 7.1,

is 5014 kW (140 W/m^2). With a safety factor of 1.2 and one more group of backup systems, three identical chillers with an individual capacity of 2000 kW are selected as basic working chillers and another identical chiller is selected as the standby. Totally four identical chillers are selected, together with four groups of chilled water pumps and cooling water pumps, which is taken as the reference case.

The reliability of the ICS is considered in this section besides uncertainty. The following assumptions are therefore made to quantify the system reliability and achieve the robust optimal ICS:

- The chillers of the ICS are repairable;
- The repair rate and failure rate of the chillers is time-independent;
- The COP of the chillers of different capacities is identical and follow similar performance curves.

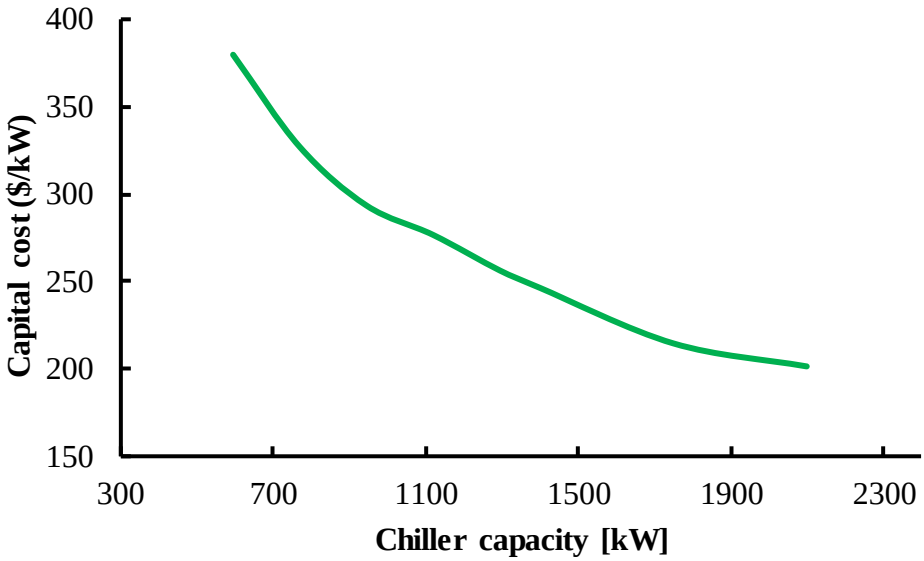

Fig. 7.11 Capital cost of chillers of different capacities

The reliability of chillers is concerned when evaluating the reliability and performance of the ICS. All the chillers are assumed to have the same failure rate and repair rate.

The failure rate of 0.0001 (1/hour) and repair rate of 0.002 (1/hour) are used. Annual total cost is taken as the objective for optimization. The capital cost including the purchase and installation of chillers and pumps is calculated with a derivative equation based on data from manufacturers, as shown in Fig. 7.11. It can be seen that the price (per kW) of chillers decreases with the increase of the capacity. The life cycle of the ICS is assumed to be 20 years. Therefore, the annual capital cost is obtained by dividing the capital cost with 20. The operation cost is calculated with the annual electricity consumption times the electricity price, which is 0.15$/kWh. The availability risk cost is calculated based on the unmet cooling demand that is the difference between the actual cooling load and available system capacity. The availability risk "price" will affect the final optimal result, which depends very much on the preference of stakeholders and the business/clients served. A sensitivity study is conducted on the availability risk price to show its effect on the optimal capacity of the ICS.

7.4.2 Performance of the ICS designed based on different methods

Considering the reliability of chillers, the mean steady-state capacity (see the description in Section 5.4.2) of the four-chiller ICS with a total capacity of 8000 kW can be calculated. It depends on the failure rate and repair rate of chillers. Actually it only correlates with the ratio of the failure rate divided by the repair rate. The mean steady-state capacities at different ratios are shown in Fig. 7.12. It shows that the mean steady-state capacity of the ICS reduces if the ratio increases. It decreases from 7960 kW to 4000 kW when the ratio increases from 0.005 to 1. When the ratio changes from 0.005 to 0.05, the mean steady-state capacity is reduced by 341 kW, which is about 4.3% of the nominal cooling system capacity. When the chiller has the equal failure

rate and repair rate (where the ratio is 1), the mean steady-state capacity of the ICS is almost half of the nominal capacity. Larger mean steady-state capacity corresponds to stronger ability to meet the cooling demand. It shows that the ratio of failure rate and repair rate plays an important role in determining the mean steady-state capacity of the ICS.

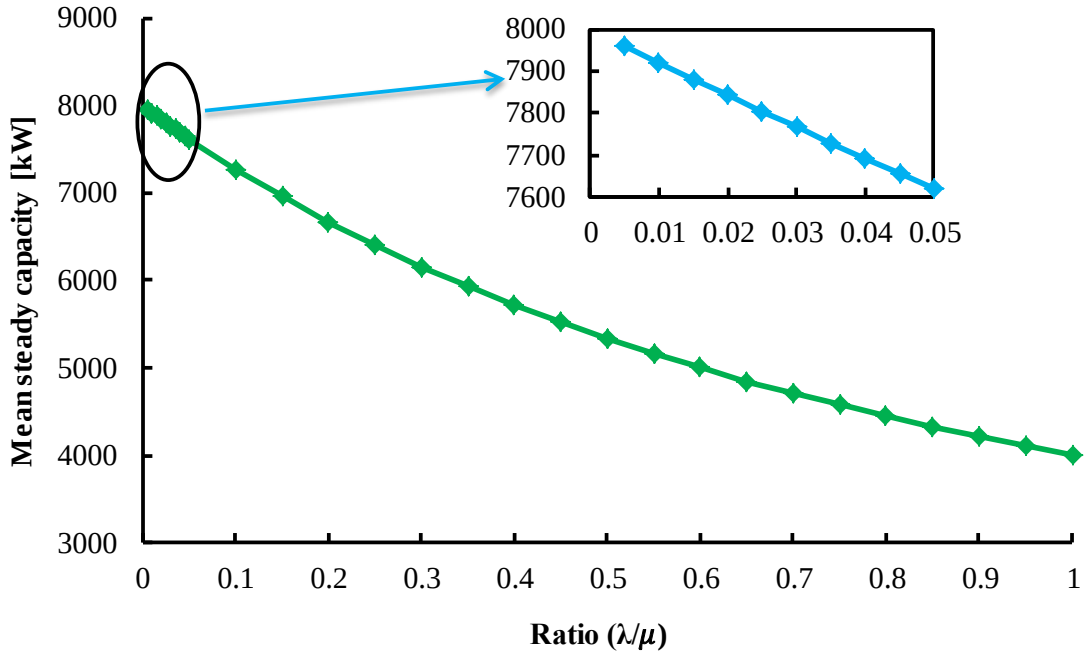

Fig. 7.12 Mean steady-state (expected) capacities of the ICS at different ratios (failure rate/repair rate)

Usually the failure rate is much lower than the repair rate and the ratio can be very low. However, the failure rate will rise with the working time due to aging or wearing problems. In such situation, the deficiency problem caused by the failure of chillers will become more serious and the design optimization considering reliability is more important. Therefore, a large ratio of 0.05 is selected in this case study to investigate the design optimization of the ICS. The availability risk price will affect the results. Before a sensitivity study of the price is conducted, the optimization results based on

an availability risk price of 1.5 $/kWh (10 times of the electricity price) are shown in Fig. 7.13.

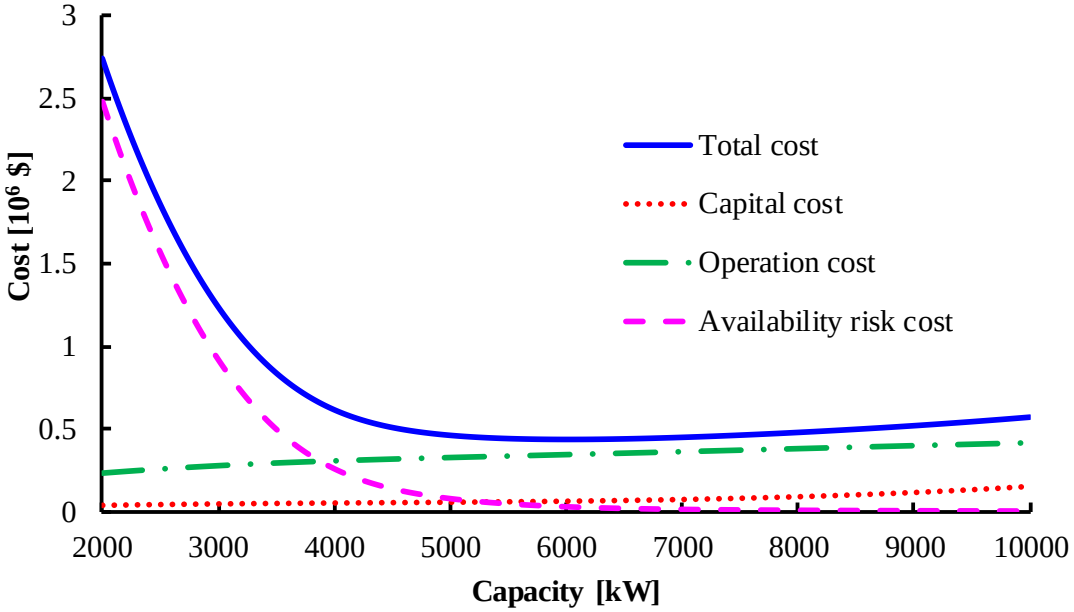

Fig. 7.13 Annual costs of the ICS of different capacities

From Fig. 7.13, it can be seen that the total annual cost of the ICS decreases firstly and then increases with the capacity increase. The decrease mainly results from the rapidly reduced availability risk cost caused by the unmet cooling demand at the low capacity. Both the operation cost and capital cost keep increasing with the increase of the ICS capacity. The capital cost contributes the least percentage among the three types of costs, especially at low capacity. The total cost decreases rapidly when the capacity is below 3000 kW and further decreases gradually before it reaches the minimum. It increases gradually afterwards. The minimum cost appears at the capacity of 5972 kW. It means that the optimal capacity of the ICS is 5972 kW considering both the uncertainty of the cooling load and reliability of chillers. Compared with the capacity of 8000 kW in the reference case, around 25% of the installation capacity can be reduced.

The optimal capacity of the ICS depends on the difference between the electricity price and the availability risk price. Therefore, a sensitivity study is conducted to show the effect of the availability risk price on the optimal capacity of the ICS and the results are shown in Fig. 7.14. The horizontal axis is the availability risk price ratio (ARPR), which is the availability risk price divided by the electricity price. The capacities of the ICS obtained from four different methods are presented, including the conventional method (marked as reference-case), the method only considering the reliability of chillers (marked as reliability-only), the method only considering the uncertainty of the cooling load (marked as uncertainty-only) and the robust optimal method considering both uncertainty and reliability (marked as robust optimal method).

From Fig. 7.14, it can be seen that the ICS capacity based on the conventional design method is not affected by the availability risk price and it keeps constant. For the ICS based on other three methods, the optimal capacity increases with the increase of the ARPRs. The optimal capacities of the ICS designed using the uncertainty-only method are the lowest. The capacities of the ICS designed using the robust optimal method are larger than that designed using the uncertainty-only method and smaller than that designed using the reliability-only method. That is because the cooling load has high probability to be overestimated considering uncertainties in the inputs used in the calculation, as proven in Section 7.2. When the ARPR approaches 20, the capacities of the ICS based on the robust optimal method and the reliability-only method are very close. Fig.7.14 also shows that even when the ARPR is 20, the capacity of the ICS using the conventional method is still 19% higher than that using the robust optimal method. By quantifying the uncertainty of the cooling load and the reliability of

chillers, the proposed method can reduce the installation capacity of the ICS. That also means that the robust optimal method helps to moderate the oversizing problem.

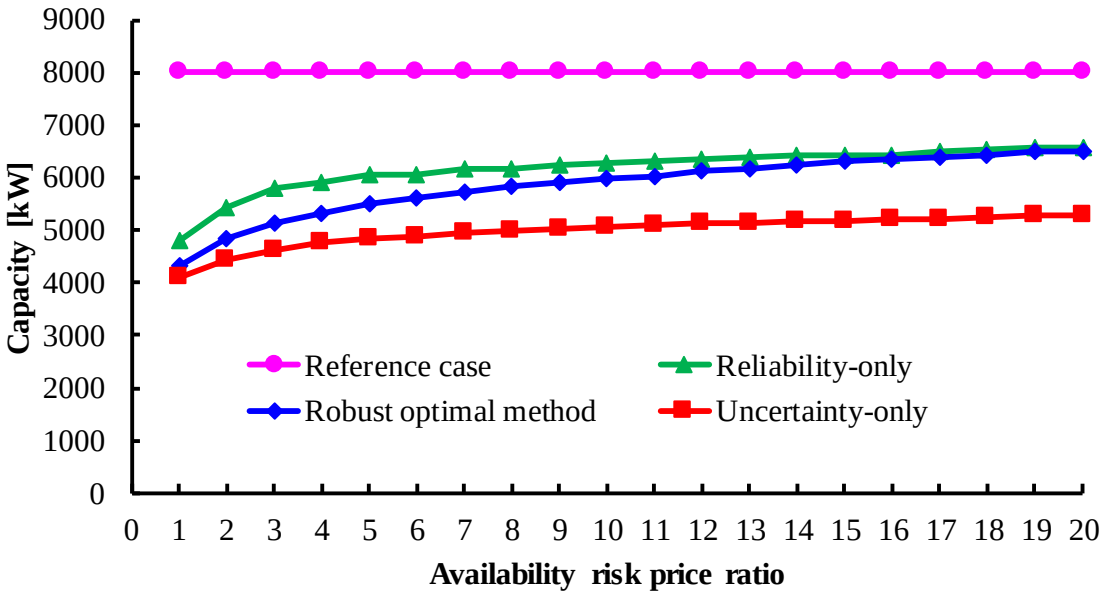

Fig. 7.14 Capacities of the ICS under different availability risk price ratios

The total annual costs of the ICS with different capacities using the four methods are shown in Fig. 7.15. It can be seen that the costs of the reference case almost keep constant at different ARPRs. The total annual costs of the ICS designed using the other three methods increase with the increases of the ARPRs. Costs of the ICS using the uncertainty-only method rise rapidly. The ICS designed using the robust optimal method can always have the lowest cost under different ARPRs. Compared with the conventional method, the proposed robust optimal method can save about 4%~15% of the total annual cost. It shows that the ICS designed using the proposed robust optimal method has high robustness and can always be cost efficient. When the ARPR approaches 20, the costs of the ICS based on the robust optimal method and reliability-only method are very close. It indicates that the availability risk price is very high in this case and the importance of system reliability already dominates over that of uncertainty. The trend is consistent to that shown in Fig. 7.14.

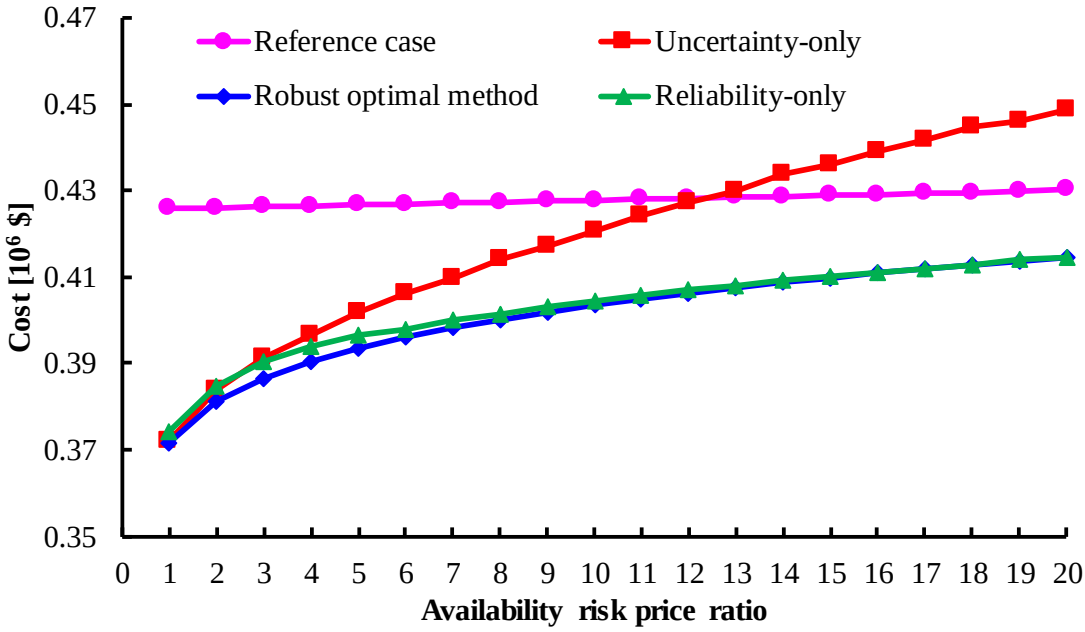

Fig. 7.15 Total annual costs of ICS under different availability risk price ratios

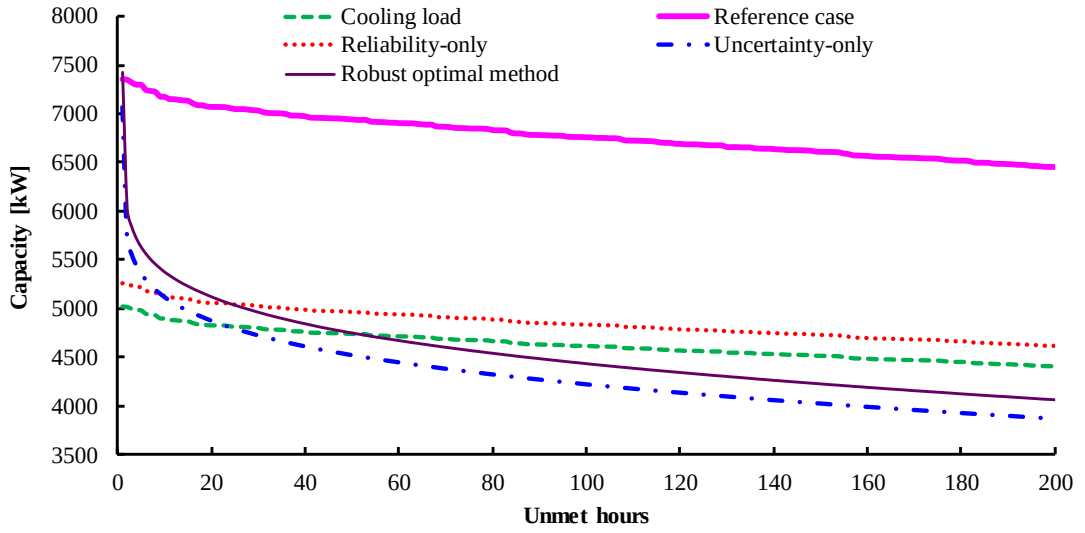

Fig. 7.16 Capacities of the ICS under different unmet hours

In practice, the capacity of the ICS is sometimes determined based on the number of unmet hours. Capacities of the ICS designed using four methods at different numbers of unmet hours are shown in Fig. 7.16. It can be seen that all the capacities from the four methods decrease with the increase of unmet hours. When the number of unmet hours is very small, the capacities of the ICS designed using the uncertainty-only

method and robust optimal method are much larger than that of the systems designed using the other two methods. When the number unmet hours is 0, the capacity of the ICS designed using the robust optimal method is even higher than that of the reference case. It indicates that the capacity obtained using the conventional method may fail to meet the need if the thermal comfort requirement is extremely high. When the number of unmet hours increases, the capacities of the ICS designed using both the reliability-only method and the robust optimal method decrease dramatically and are lower than that designed using the conventional method. When the number of unmet hours exceeds 25, the capacity of the ICS designed using the robust optimal method will be larger than that designed using the uncertainty-only method and smaller than that designed using both the reliability-only method and the conventional method. The trend is similar to that in Fig. 7.14. Having the capacity distribution in Fig. 7.16, users can determine the capacity of the ICS based on their specific requirement and priority.

7.4.3 Discussions

The reliability of the ICS is concerned in the design optimization in this study. The repair rate and failure rate of the chiller are assumed to be constant. However, it is obvious that the failure rate usually is not constant. It may follow the bathtub curve, as shown in Fig. 7.17. The failure rate is large at the beginning of its life cycle due to installation and commissioning errors. At the late phase of its life cycle, the failure rate increases due to aging and wearing problems. It keeps almost constant during the middle of its life cycle. Design optimization considering reliability is more valuable and necessary when the failure rate is high. Therefore, higher failure rate is selected in this study. In the future study, time-dependent failure rates could be considered to get more practically meaningful results.

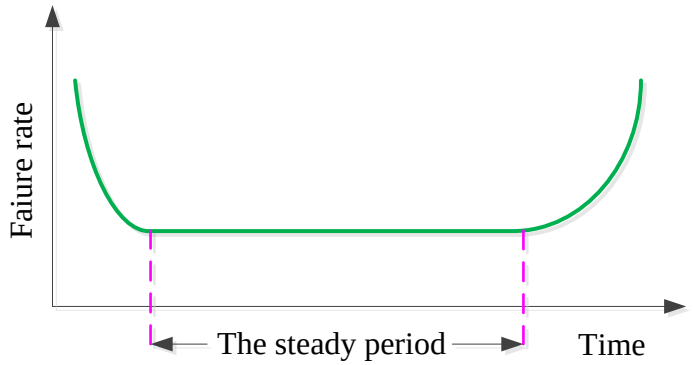

Fig. 7.17 Typical failure rate distribution with time

Availability risk cost is introduced in this study for the design optimization. It is calculated based on the cooling load that the ICS cannot meet due to cooling load calculation deviation and failure of chillers. It is used to quantify the loss and compensation caused by the unmet cooling load. Actually the availability risk price represents the importance of the thermal comfort in practical cases. A high availability risk price corresponds to stricter requirement on the thermal comfort. When the price reaches 18 $/kWh (120 times of the electricity price) the optimal capacity of the ICS designed using the robust optimal method will exceed 8000 kW in this study. It inversely proves that when the requirement on the thermal comfort is extremely strict, the conventional design method might also fail to meet the requirement and the robust optimal method can make the guarantee. The concept of the availability risk cost is widely used in the electricity field. How to use it in the HVAC field might need more careful and throughout study.

Only two states of the chiller are considered in this section. Actually a chiller may have different stages considering its efficiency and capacity. In addition, other components in the ICS also have the reliability issues such as pumps, cooling towers, etc. Comprehensive design optimization study including all these aspects needs to be conducted.

7.4.4 Conclusive remarks

A robust optimal design is developed considering both the uncertainty of the cooling load and reliability of primary components in ICSs. With the objective of the total annual cost including the capital cost, operation cost and availability risk cost, the optimal capacity of the ICS can be obtained. Performance of the ICS using the new method is analyzed. The following conclusions can be summarized:

i. The proposed method can properly determine the optimal capacity of the ICS by quantifying cooling load uncertainty and assessing the reliability of the ICS. The optimal capacity is affected by the availability risk price. The optimal capacity becomes larger at a higher price. When the price is 20 times of the electricity price, the capacity is still about 20% lower than that designed using the conventional method.
ii. The optimal capacity of the ICS determined using the proposed method is lower than that designed only considering the reliability of chillers, and higher than that designed considering the uncertainty of the cooling load only.
iii. The total annual cost of the ICS designed based on the robust optimal method can be reduced by 4%~15% compared with the conventional method.

7.5 Summary

This chapter presents results of ICSs designed using the uncertainty-based optimal design method and robust optimal design method. When the uncertainty at planning and design stages is quantified, the cooling loads of the ICS can be obtained at different probabilities. Through the comparison and analysis, it shows that the cooling

load using the conventional calculation method has high probability to be over-estimated.

By quantifying the uncertainty of cooling loads of the ICS, the system can be designed with quantified risks. According to the peak cooling load distribution, the capacity of the ICS can be determined based on the number of unmet hours and the risks. According to the energy saving distribution of different design options, the optimal configuration of the ICS is determined and its performance can be estimated with quantified confidence.

By concerning both uncertainty and reliability, the robust optimal cooling system can be achieved with the lowest total annual cost. By introducing the availability risk cost, the losses caused by unmet cooling demands can be evaluated. By minimizing the total annual cost (including the capital cost, operation cost and availability risk cost), the robust optimal ICS can be achieved. The capacities and costs of the ICS at different availability risk prices are presented. A larger capacity is required under a higher availability risk price, which corresponds to the relative importance of the thermal comfort requirement to users.

CHAPTER 8 OPTIMIZED DESIGNS OF DCS AND THEIR PERFORMANCE CONSIDERING UNCERTAINTY AND RELIABILITY

The DCSs obtained using two design optimization methods and their performance are presented in this chapter. The cooling loads of the DCS are quantified considering uncertainty at planning and design stages. Different strategies are used to address the uncertainties of the three groups of variables used in the design calculation. The uncertainty-based optimal design method is applied in the DCS and the performance of the DCS delivered is compared with that using the conventional design method. Concerning both uncertainty and reliability, the robust optimal DCS is achieved and its performance is evaluated.

8.1 Introduction of the DCS

A new building energy simulation tool EPC (Energy Performance Coefficient Calculator) (Quan et al. 2015) is used to predict the cooling load of the DCS. The tool is developed by the High Performance Building Group in Georgia Institute of Technology. It is a modified version of a reduced-order building energy model, which is based on ISO 13790:2008 standard. The underlying model of the EPC is much smaller than other tools such as EnergyPlus, offering a faster computational speed. The assumptions and simplifications in EPC were calibrated on a large collection of different buildings. It is very useful when there are many buildings involved and the information for individual buildings is limited. Therefore, it is very suitable to be used in this study. In addition, it can involve the uncertainties in building

design/construction such as the overall heat transfer coefficient of the building envelope, window wall ratio, shape of the building, etc.

The way to address the uncertainties is different from that used in Chapter 7. For the outdoor weather data, the actual measured data of Hong Kong from 1979 to 2007 are used, which is proved to be a better way to account for uncertainties in the weather. For the building design/construction, the number of floors and the building size are based on the initial plan. The range of the thermal properties of building materials can be found in the design manual for hot summer and warm winter area of China (which is the climate of Hong Kong). Uniform distributions in the ranges are adopted to account for uncertainties in the building materials. For the indoor conditions, relative normal distributions are assigned to those values obtained from the design manuals or guidelines. Detailed information for inputs used in the reference case and the uncertainty study is shown Table 8.1.

Table 8.1 Factors and their distributions concerned in uncertainty analysis of the DCS

Group	Abbreviation	Parameter	Reference case	Uncertainty study	
				Distribution	Value (Mean, St.)
Outdoor weather	*Drybulb temp*	Dry-bulb temperature of outdoor air	TMY	Actual data:1979~2007	
	Humidity	Humidity of outdoor air			
	Radiation	Global radiation			
Building design/ construction	*Building floor*	Building floor	Based on the plan	Relative normal	(1,0.04)
	Building length	Building length	Based on the plan	Relative normal	(1,0.04)
	WWR	Window wall ratio	0.5	Uniform	(0.3,0.7)
	Uwall	Conductivity of wall ($W/(m^2.K)$	1.5	Uniform	(1,1.5)
	Uwindow	Conductivity of window ($W/(m^2.K)$	3	Uniform	(1.5,3)
	Uroof	Conductivity of roof ($W/(m^2.K)$	0.9	Uniform	(0.4~0.9)
	Wallabsp	Wall absorption coefficient	0.9	Uniform	(0.4~0.9)
	Roofabs	Roof absorption coefficient	0.8	Uniform	(0.4~0.8)
	Wintran	Window solar transmittance	0.8	Uniform	(0.4~0.8)
Indoor condition	*Occupant*	Occupant density	Ranging from 4~15 m^2/person for different buildings	Relative normal	(1,0.04)
	Lighting	Lighting density	Ranging from 10~20 W/m^2 for different buildings	Relative normal	(1,0.04)
	Equipment	Plug-in equipment power density	Ranging from 8~20 W/m^2 for different buildings	Relative normal	(1,0.04)
	Ventilation rate	Ventilation rate	Ranging from 1~4 ACH for different buildings	Relative normal	(1,0.04)

The steps to implement the new design method are illustrated in Fig. 8.1. Totally 580 trials are conducted for the uncertainty study. Detailed explanations are introduced as follows:

i. The input variables that have uncertainties are selected and samples are generated for these variables. For the normal distributions, Latin Hypercube Sampling (LHS) method is used to improve the calculation efficiency (Iman 2008).

ii. Samples are imported into the cooling load calculation program. For a DCS, many buildings with different functions are involved. Each building is simulated.

iii. The cooling load profile of the DCS is obtained, by summing the cooling loads of all individual buildings.

iv. The distributions of the peak cooling load and annual cooling load of the DCS are analyzed.

v. Based on the peak cooling load distribution, the optimized capacity of the DCS is determined considering the quantified risks. Based on the annual cooling load distribution, the performance of the DCS options of different configurations (different chiller combinations, with or without thermal storage systems, etc.) is obtained and the optimized DCS configuration is therefore determined.

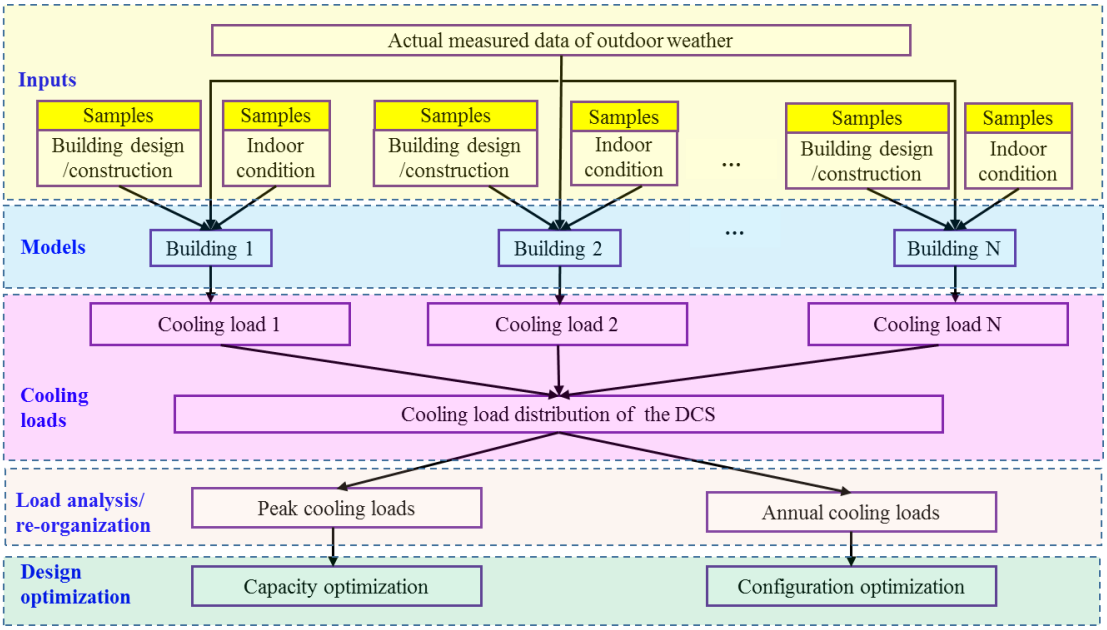

Fig. 8.1 Steps of the DCS design method considering uncertainty

8.2 Uncertainty quantification of cooling loads

Strategies to quantify the uncertainties in DCS design are different from that used in Chapter 7 for the ICS design. By importing samples into EPC, the cooling load distributions considering uncertainty are obtained. Energy performance of DCSs at different probability levels is then calculated. The performance of DCSs at different capacities and configurations is also estimated. Before the cooling load and design results are presented, actual weather data from 1979 to 2007 are compared with that of TMY, as shown in Fig. 8.2. It can be seen that the actual data of some periods distribute evenly around the TMY data and the TMY data can be taken as the mean. During the left periods (most of the time), the actual data can be much larger or smaller than the TMY data. If the cooling loads are calculated based on the weather data of TMY, the cooling load can be estimated inaccurately. The comparison shows again that it is necessary to consider uncertainty in the DCS design optimization.

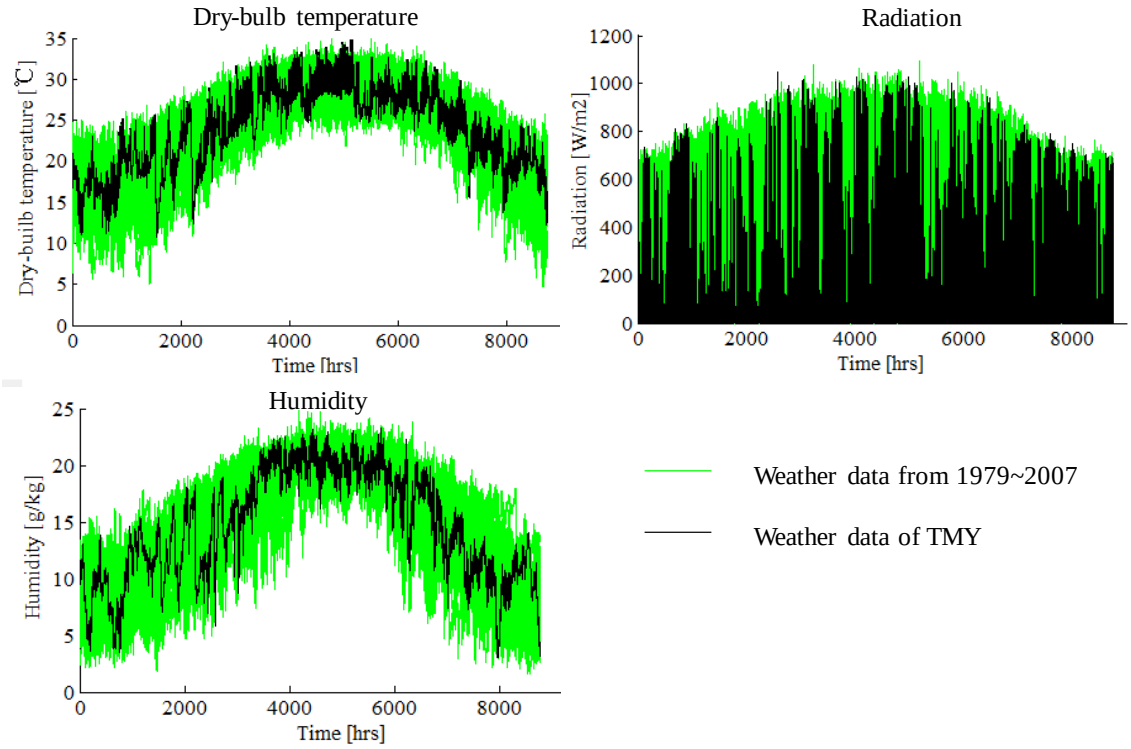

Fig. 8.2 Actual weather data in Hong Kong from 1979 to 2007 vs. data of TMY

8.2.1 Peak cooling load distribution of the district

The peak cooling load distribution of the district (described in Section 3.2) is shown in Fig. 8.3. It shows the peak cooling load varies between 86 MW and 119MW. The frequency of the peak load is high between 98 MW and 104 MW, which indicates that it has high probability to fall in such a range. The peak cooling load of the reference case is 109 MW, with a CDF of over 90%. It indicates that, in consideration of uncertainty, the peak cooling load has a probability of 90% to be less that of the reference case.

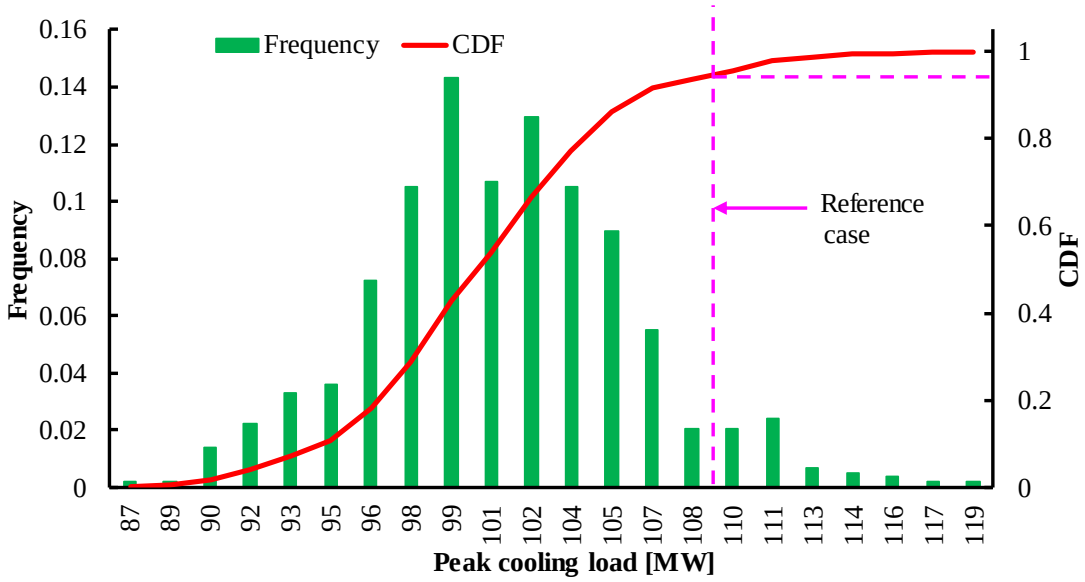

Fig. 8.3 Distribution of the peak cooling load of the DCS

8.2.2 Annual cooling load distribution of the district

The annual cooling loads are the basis for energy consumption estimation of DCSs. Considering uncertainty at planning and design stage, the annual average cooling loads are obtained. To check whether the annual average cooling loads fit a normal distribution, the Q-Q plot is used and results are shown in Fig. 8.4. If all the data are on or very close to the red line, the data fit a normal distribution. Fig. 8.4 shows that almost all the data are on the red line. The annual average cooling loads therefore almost fit a normal distribution.

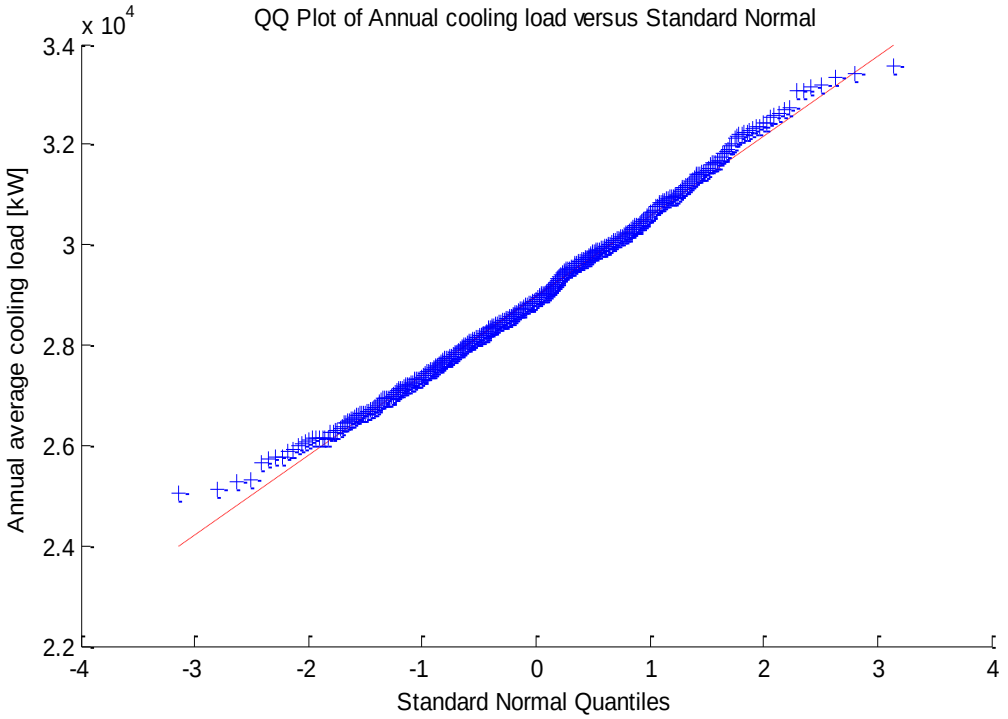

Fig. 8.4 Q-Q plot of annual average cooling loads

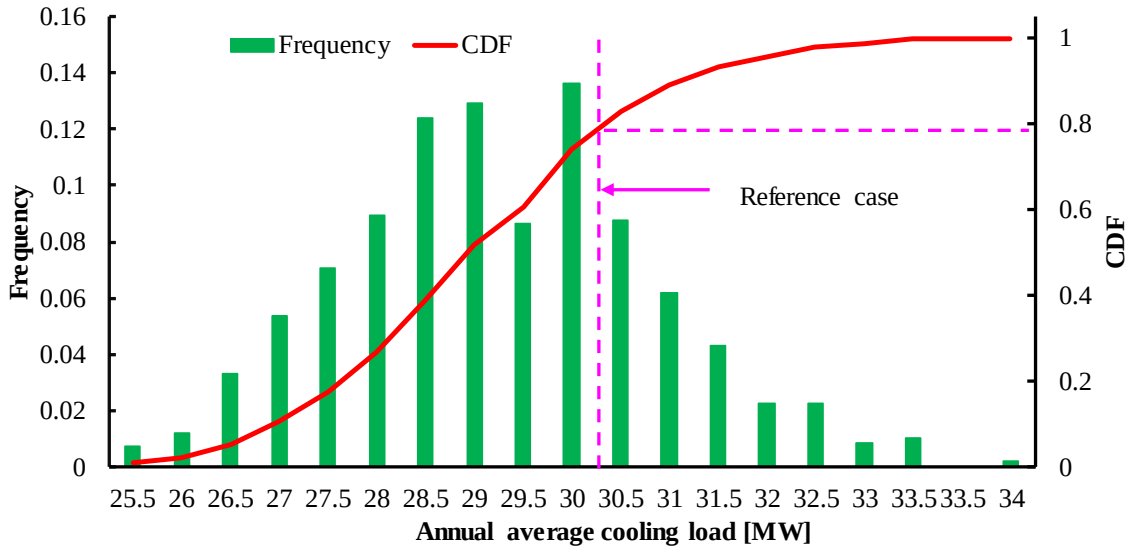

Fig. 8.5 Distribution of annual average cooling loads of the DCS

The distribution of the annual average cooling loads of the DCS are shown in Fig. 8.5. The annual average cooling load of the reference case is also presented for comparison. It can be seen that the annual average cooling load varies between 25.5 MW and 34MW, which is 0.84 and 1.12 times of that in the reference case. The frequency for

the load between 28.5 MW and 30 MW is high, which indicates that the annual average cooling load has high probability to fall into such a range. The annual average cooling load of the reference case is 30.4 MW, which responds to about 80% of the CDF. It indicates that the annual average cooling loads involving uncertainty have a probability of 80% to be less that of the reference case if the cooling load is calculated using the similar settings. At the same time, the annual average cooling loads can also be larger than that of the reference case, with a chance of less than 20%.

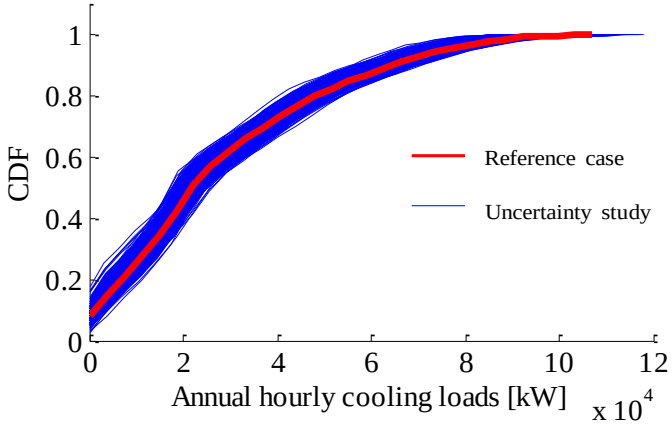

Fig. 8.6 Annual hourly cooling load distribution

The distribution of annual hourly cooling load for each trial is shown in Fig. 8.6. The cooling loads of the reference case are highlighted in red. It can be seen that at the same CDF, the cooling loads of the reference case are larger than the mean of cases with uncertainty. This is consistent to the results in Fig. 8.5.

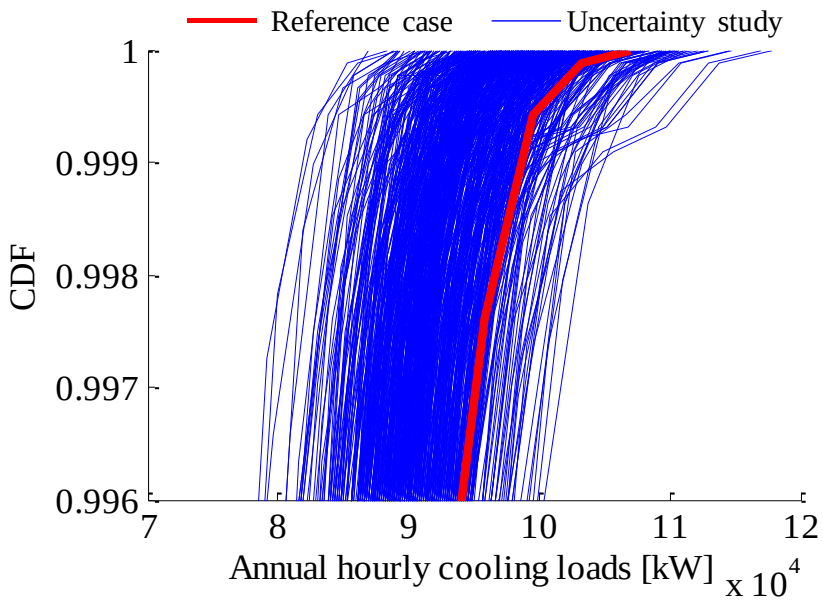

Fig. 8.7 Peak cooling load distribution

Usually the larger cooling loads are used for sizing the DCS. The cooling load distributions with a CDF of over 99.6% are shown in Fig. 8.7. It shows that the cooling loads vary significantly. If the DCS is sized based on the load of the reference case, no quantified risks can be obtained. In addition, Fig. 8.7 shows that it has strong probability to oversize the DCS without quantifying uncertainty at planning and design stage.

8.3 Uncertainty-based optimal design of the DCS

With the cooling load distribution, performance assessment and design optimization of the DCS can be conducted. The results are presented in the following sections.

8.3.1 Performance assessment of the DCS

With the annual cooling load distribution, the performance of DCSs is obtained. Accurate estimation of the energy consumption of DCSs is important for the government, investors and users. The government needs to know how much more

electricity will be required by building this new district and whether the existing grid has enough capability. The investors need to know how long the investment can be paid back. For users, the annual energy consumption relates closely to the bills to pay.

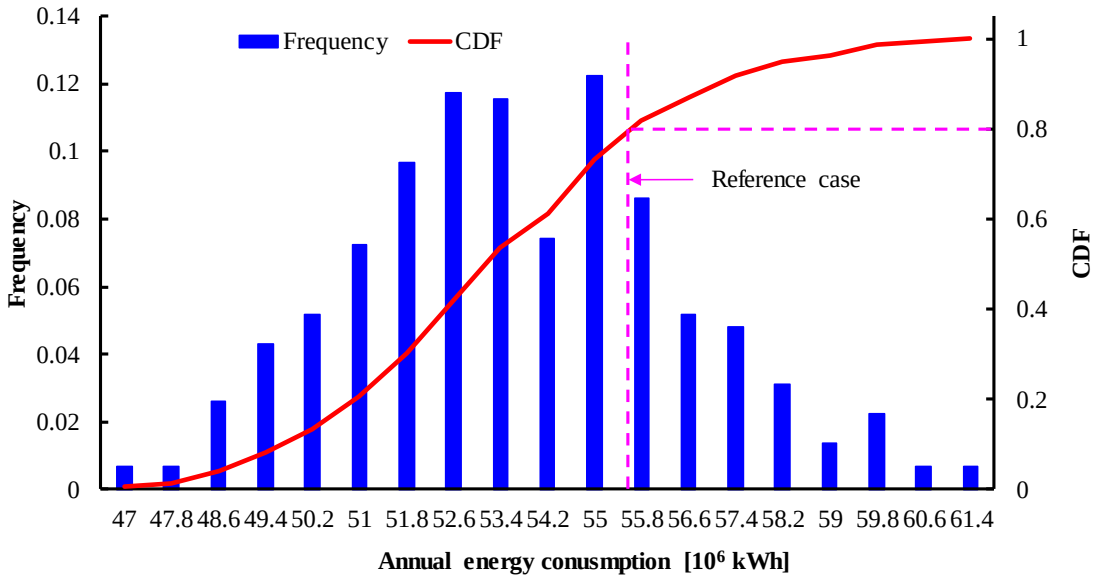

Fig. 8.8 Distributions of the energy consumption of the DCS considering uncertainty

By quantifying the uncertainty in the annual cooling load calculation, the distribution of energy consumption of the DCS at different risks is obtained and shown in Fig. 8.8. It can be seen that the energy consumption of the DCS varies between 47×10^6 (kWh) and $\times 10^6$ (kWh). Frequency of the energy consumption between 51.8×10^6 (kWh) and 55×10^6 (kWh) is high, which means it has strong probability to be in this range. The energy consumption of the reference case is also marked in Fig. 8.8 for comparison, which corresponds to the CDF of about 80%. It shows that the annual energy consumption of the DCS considering uncertainty has a probability of 80% to be lower than that of the reference case. In other words, the energy consumption of the DCS can also be under-estimated with a chance of 20%. By quantifying the uncertainties, the stake holders can make decisions using the energy consumption distribution and corresponding quantified risks.

8.3.2 Optimal sizing of the DCS

One important task of the DCS design is to obtain the system capacity. The capacity is determined by the peak cooling loads. By involving the uncertainties into the design, the DCS is sized with quantified confidence. The distribution of the peak cooling load at different quantified risks is shown in Fig. 8.9.

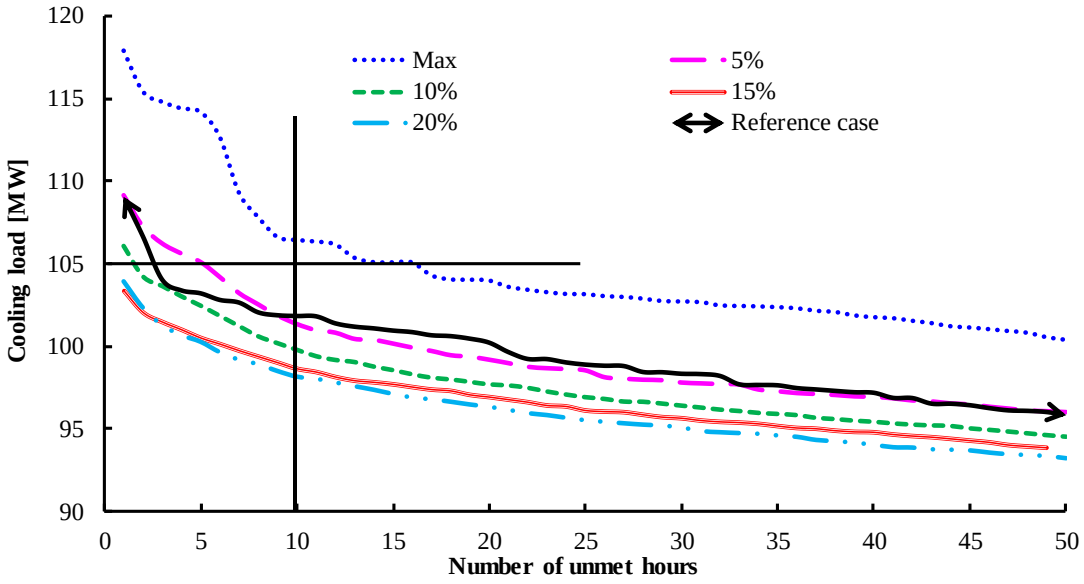

Fig. 8.9 Design cooling loads of DCS at different risks *vs.* the number of unmet hours

Fig. 8.9 shows that the design cooling load of the DCS reduces with the increase of the number of unmet hours. For a given number of unmet hours, the design cooling load increases with the decrease of the allowed risks. With such quantified data, the DCS can be sized with quantified risks. For a given capacity, the design method considering uncertainty can provide the quantified risks for certain numbers of unmet hours. For example, if the DCS in the district has a capacity of 105 MW, the number of unmet hours can hardly be over 16 per year and has a chance of 5% to be over 5 per year (or a chance of 95% to be less than 5). For a specific number of unmet hours, the capacity can be obtained at different risk requirements. For example, if the number of

unmet hours is set to 10, the risk that the number exceeds 10 can be reduce to 0 if the capacity of the DCS is no less than107MW. If designers want to keep the risk to be lower than 10%, the capacity should be not less than 101 MW. By involving the uncertainty in the design process, the DCS is sized based on specified and quantified risk/comfort requirements. In contrast, the conventional method can tell nothing more except giving the certain design capacities.

8.3.3 Optimal configuration of the DCS

Another important task of the design optimization is to select the configuration of the DCS. The configuration relates to the operation cost of the DCS in the life cycle. In this section, two types of configurations are studied, aiming to answer two questions:

- Is it necessary to install chillers of different capacities in the DCS?
- Is it cost effective to install an ice storage system in the DCS?

A. DCSs with different configurations of chillers

It is often suggested to install chillers of different capacities in ICSs, which aims to improve the energy efficiency of the system at partial load. The capacity of DCSs can be much larger than that of ICSs and much more chillers will be installed. By considering uncertainty, the necessity to use chillers of different capacities in the DCS is investigated by comparing with the conventional design method. In the DCS of this study, totally seven chillers are selected. This is referred to a DCS project in Hong Kong, which has a similar capacity. For comparison, performance of this DCS using seven identical chillers with an individual capacity of 15000 kW is also investigated, marked as S_{dcs1}. Five chillers with an individual capacity of 17500 kW and two chillers with an individual capacity of 8750 kW are selected, which is marked as S_{dcs2}. The

energy consumption ratios (annual energy consumption of S_{dcs1} divided by that of S_{dcs2}) are shown in Fig. 8.10.

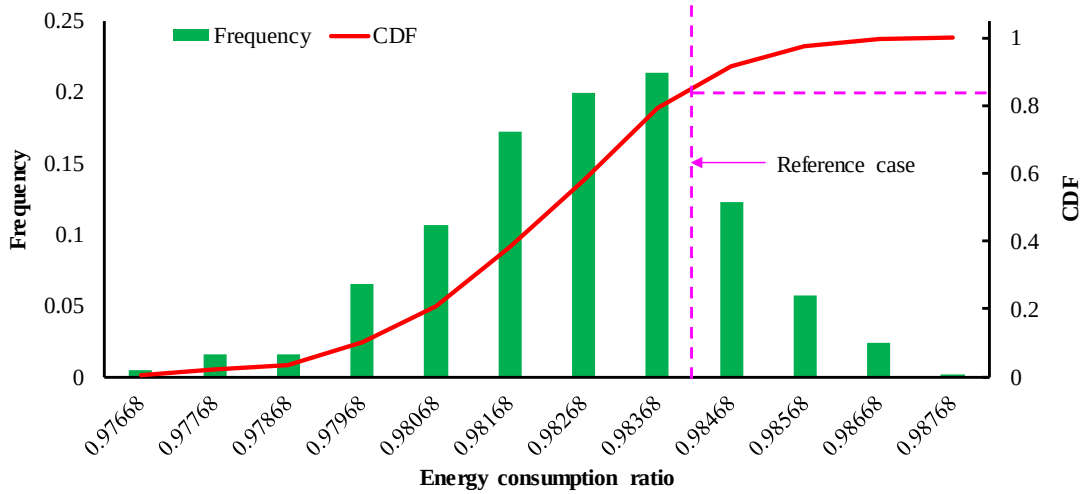

Fig. 8.10 Energy consumption ratio of two DCS designs with different chiller configurations

From Fig. 8.10, it can be seen that the ratio is 0.984 in the reference case and S_{dcs2} consumes 1.6% less energy than S_{dcs1}. No further information can be obtained from the conventional design method. However, by considering uncertainty, the distribution of the energy consumption ratios at different risks can be obtained. Fig. 8.10 shows that the ratio varies between 0.975 and 0.988. The energy saving by S_{dcs2} is between 1.2% and 2.5%, which is not very promising and it is hard to be over 2.5%. Considering more complicated control and maintenance, S_{dcs2} may be not preferable in the DCS. The curve of CDF shows that the energy consumption ratio can be higher than that of the reference case with a chance of about 20%. By using the design method considering uncertainty and results in Fig. 8.10, the decision makers can select appropriate design schemes with quantified risks.

B. DCS with ice storage system

DCSs are often integrated with ice storage systems to reduce the operation cost and the peak electricity load of the local grid. Accurate estimation on the cost saving of the integrated system is very important for investors, which determines the payback period of the investment. By using the conventional design method, the cost saving is estimated without quantitative risks. The cost can be under-estimated or over-estimated. The improved design method can avoid such problems by offering the cost distribution at different risk levels. The performance of the DCS integrated with the ice storage system is investigated to illustrate the new design method. The COP of the ice storage system is assumed to be 3. The peak period is between 8 a.m. and 8 p.m. from Monday to Friday and the rest of time is off-peak period. A simplified tariff based on the tariff in Guangzhou (Table 3.4) is used. The electricity price is 0.16 $/kWh for the peak time and 0.08 $/kWh for the off-peak period. The distribution of the annual operation cost of the DCS with the ice storage system is shown in Fig. 8.11.

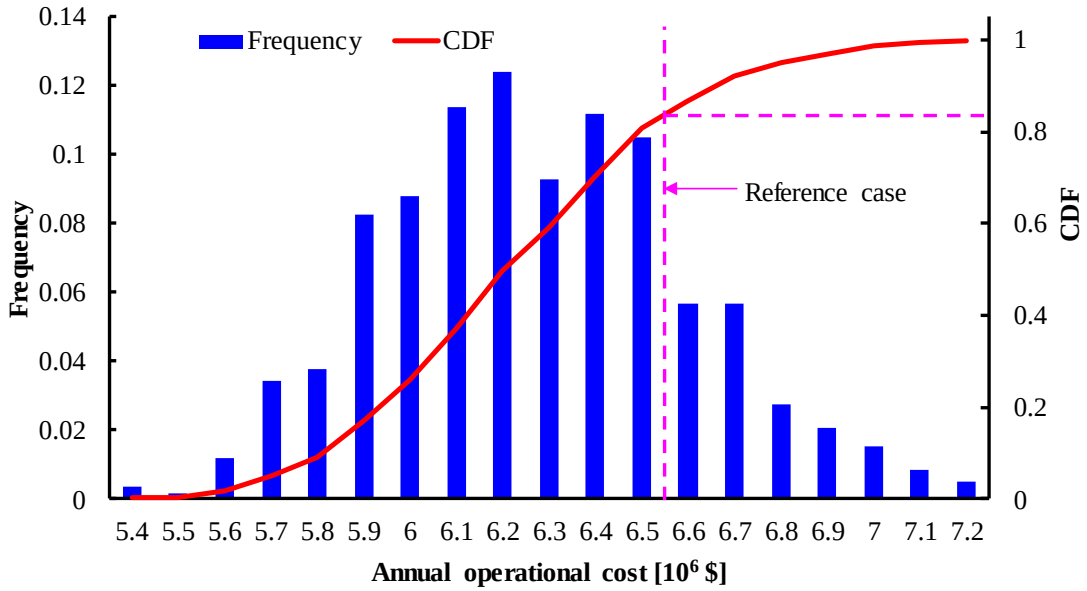

Fig. 8.11 Distribution of the annual operation cost of the DCS integrated with ice storage system considering uncertainty

From Fig. 8.11 it can be seen that the annual operation cost of the DCS with the ice storage systems varies in a quite large range, i.e. between 5.4×10^6 ($) and 7.2×10^6 ($). The frequency of the cost between 6×10^6 ($) and 6.5×10^6 ($) is high, which means that the annual operation cost of the DCS has strong probability to be in this range. The annual operation cost of the reference case is also illustrated in Fig. 8.11, corresponding to the CDF of about 80%. It means that the annual operation cost of the DCS with the ice storage system has a probability of 80% to be lower than that of the reference case. Without quantifying the uncertainty at the design stage, the annual operation cost has high possibility to be over-estimated.

8.4 Robust optimal design of the DCS considering uncertainty and reliability

Performance of the DCS designed using the robust optimal design method is evaluated in this section. It is compared with that obtained using the conventional method, uncertainty-only method, reliability-only method. As proved in Section 8.3, using chillers of different capacities in the DCS makes no big impact on energy or cost efficiency so the DCS with identical chillers is investigated here.

The capacities of the DCS determined using different design methods are shown in Fig. 8.12. The capacity obtained using the conventional method is determined by multiplying the peak cooling load of the reference case by 1.1. It can be seen that the optimal capacity of the DCS increases with the increase of ARPRs when the design of DCS is optimized using the uncertainty-only method, reliability-only method and robust optimal method. The capacity of the DCS using robust optimal method is larger than that using uncertainty-only method, and smaller than that using reliability-only method. When the ARPR exceeds 10, the capacity of the DCS using the robust optimal

method is larger than that using the conventional method. It demonstrates that if the availability risk price is very high, or the requirement for the thermal comfort is very strict, the capacity of the DCS determined using the conventional method is still not enough.

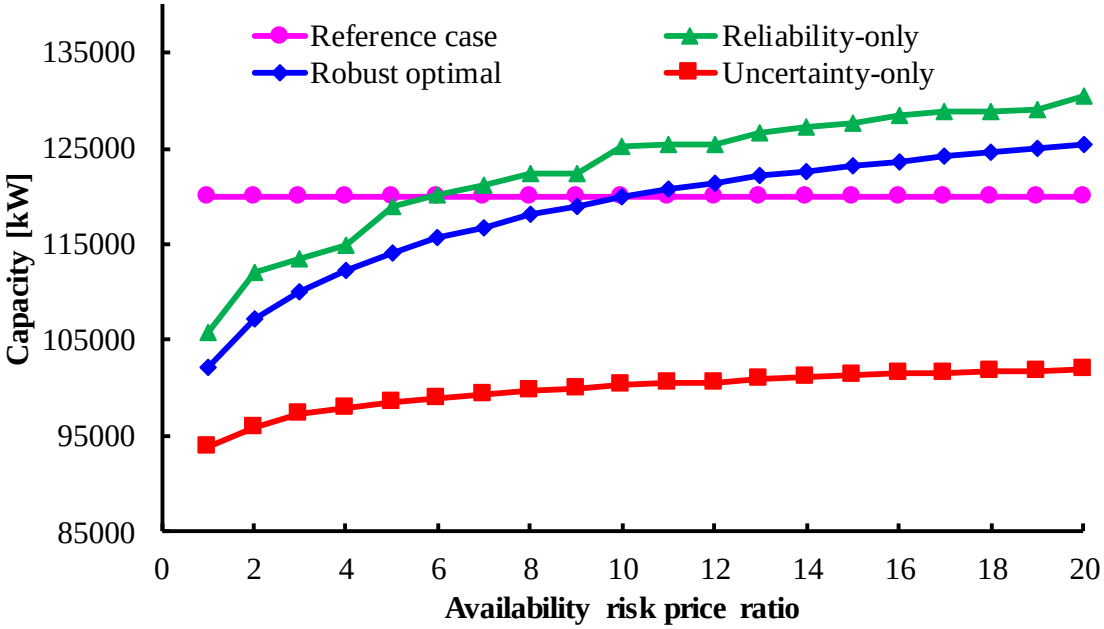

Fig. 8.12 Optimal capacity of the DCS using different methods

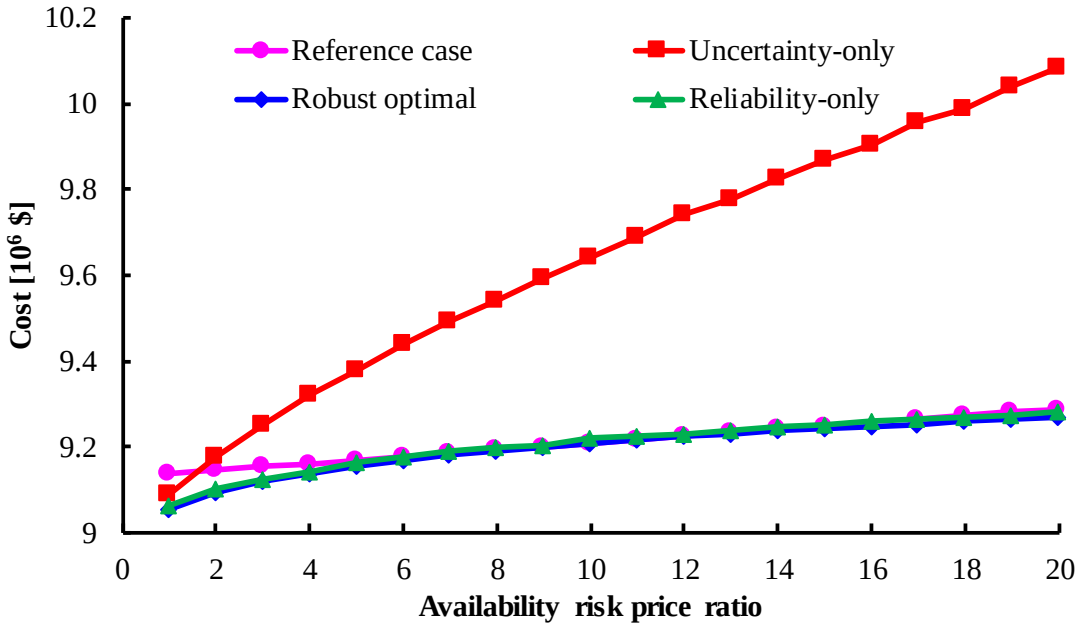

Fig. 8.13 Optimal total annual cost of the DCS using different methods

The total annual costs of the DCS designed using four methods are shown in Fig. 8.13. It can be seen that the cost of the DCS designed using the uncertainty-only method increases largely. It results from the lower capacity obtained at the design stage and the higher insufficient capacity in operation. For the other three methods, the total annual costs are close to each other. That is because that the capital cost contributes a very small portion of the total annual cost. Even if a larger capacity is used, the total annual cost increase is not obvious.

8.5 Summary

In this chapter, the uncertainty in the cooling load calculation of the DCS is quantified. Actual measured weather data are used to account for uncertainties in the outdoor weather. By involving uncertainty into system design and assessment processes, the performance of the DCS at different risks is obtained and analyzed. The robust optimal DCS can be obtained by quantifying uncertainty and reliability. After the above study, the following conclusions can be made:

i. The annual average cooling load of the DCS varies between 0.84 and 1.12 times of that of the case without considering uncertainty. It almost fits the normal distribution. With the distribution of the annual cooling load, the energy performance of different DCS options and their corresponding risks can be obtained. The stake holders can make decisions and choices with quantified confidence by considering uncertainty.
ii. The peak cooling loads of the DCS at different risk levels are obtained using the proposed design method. With the distribution of the number of unmet hours and cooling loads at different risks, the DCS can be properly sized based on specific risks (which a designer would like to take) and the indoor comfort requirements.

iii. The configuration of DCSs can be selected based on quantified risks and benefits using the improved design method. The energy saving potential of the DCS using chillers of different capacities is not very promising, which is not recommended considering control and maintenance issues. Annual cost saving of the DCS with ice storage system varies significantly when considering uncertainty in the cooling load. Appropriate designs of DCSs and the corresponding performance can be ensured by using the new design method.

iv. The robust optimal design of the DCS with the lowest total annual cost is obtained. With the increase of the availability risk price ratio, the optimal capacity increases. When the ratio is high enough, the capacity using the robust optimal design method is larger than that using the conventional method.

v. The capacities of the DCS, based on the robust optimal method considering both uncertainty and reliability, are smaller than that based on the reliability-only method. Systems that designed using the uncertainty-only method have the smallest capacities and the largest total annual cost.

CHAPTER 9 IMPACTS OF UNCERTAINTY AND RELIABILITY ON THE DESIGN OF DCS AND ICS

In this chapter, the impacts of uncertainty and reliability on the design optimization of DCSs and ICSs are assessed and compared. Firstly the cooling load distributions of the DCS and the ICS are analyzed when uncertainties of variables fit similar distributions. Sensitivity analysis is conducted to identify the influential factors for the actual cooling loads of the DCS and ICS. Then the impacts of uncertainty on the design of the DCS and ICS are evaluated and compared. When both uncertainty and reliability are concerned in the design process, the performance of the DCS and ICS is analyzed and compared. The impacts of implementing the robust optimal design method on the two systems are then summarized.

9.1 Introduction

The cooling loads of the DCS used here are based on the results in Chapter 8. For comparison, one office building with eight floors is selected from the district and the ICS for this building is designed. Annual hourly cooling loads of the DCS and ICS without considering uncertainty (marked as the reference case) are shown in Fig. 9.1.

For both DCS and ICS, chilled water systems with primary constant speed pumps are designed. Chillers of different capacities are used in both systems. Chillers with larger capacities usually have higher nominal COPs. Fig. 9.2 shows the nominal COPs used in this study for chillers with different capacities in the DCS and ICS. The COP of a chiller at different part load ratios is shown in Fig. 4.5. The nominal COP may be different for different chillers and the same curve then moves vertically.

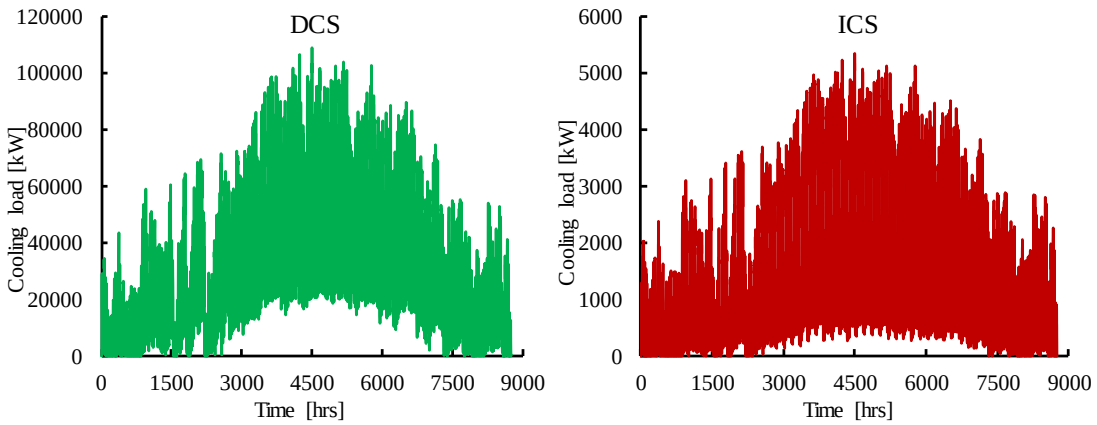

Fig. 9.1 Annual hourly cooling load of the DCS and ICS in the reference case

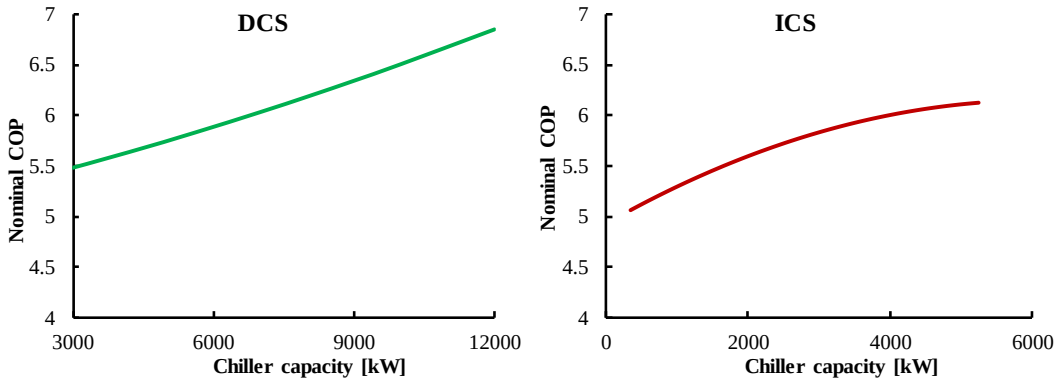

Fig. 9.2 Nominal COPs of chillers of different capacities for the DCS and ICS

Capital costs of the DCS and ICS of different capacities can be estimated based on the empirical relation shown in Fig. 9.3, which is obtained based on the cost information of major suppliers in the market. It shows that the unitary cost decreases with the increase of the system capacity. The operation cost is estimated based on the local electricity price, which is about 0.15 $/kWh in Hong Kong. The availability risk cost is estimated using the introduced availability risk price, which is up to the preference of the actual stakeholders of a project. The difference between the availability risk price and the electricity price affects the optimization results. Therefore, the total annual costs for the DCS and ICS at different availability risk prices are estimated and analyzed.

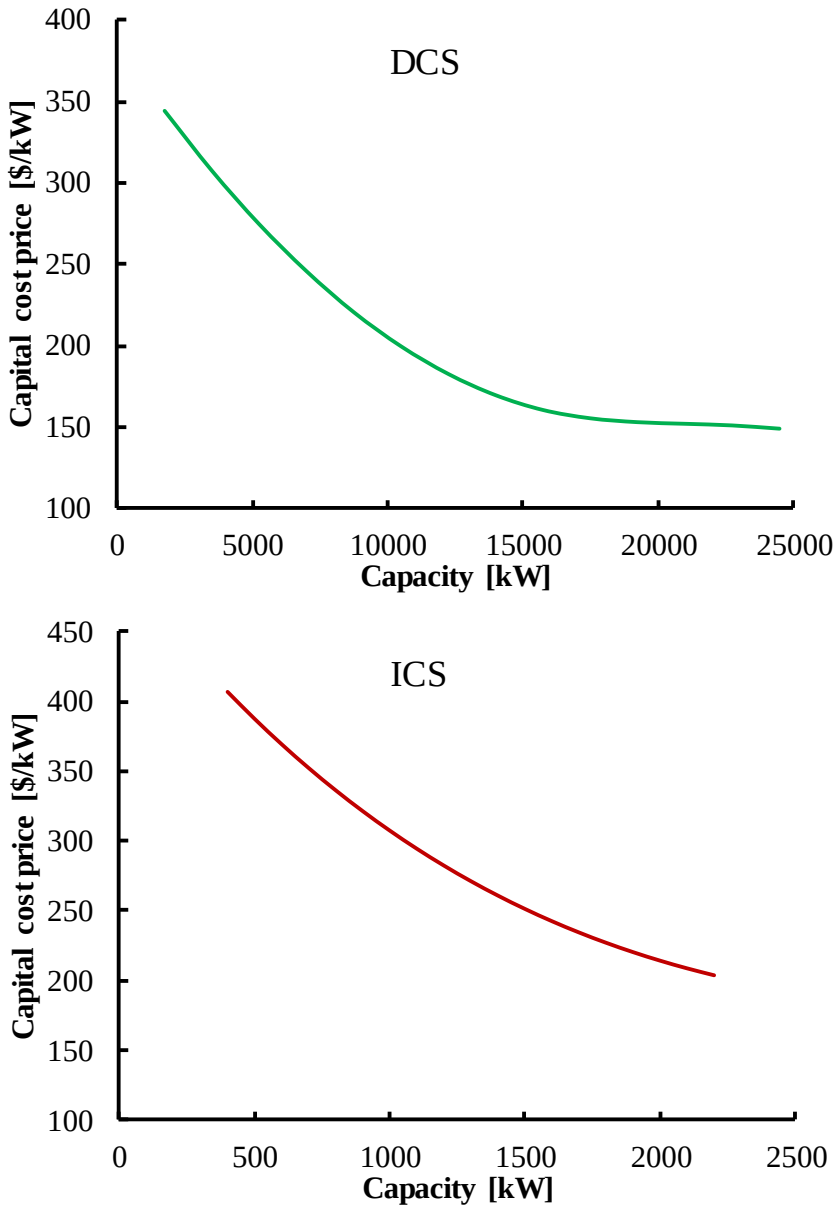

Fig. 9.3 Capital costs for the ICS and DCS of different capacities

9.2 Impacts of uncertainty on cooling loads of the DCS and ICS

The peak cooling load is used to determine the capacity of cooling systems. The annual average cooling load is the basis for energy consumption estimation. Distributions of the peak cooling load and annual average cooling load of the DCS considering uncertainty are analyzed and compared with that of the ICS in this section.

The distribution of the peak cooling load of the DCS is shown in Fig. 9.4a. The peak cooling load of the DCS varies between 87 MW and 120 MW. It corresponds to a relative difference between -21% and 9% compared with the peak cooling load in the reference case. The peak cooling load has high frequency between 98 MW and 105 MW. The peak cooling load of the reference case locates at over 90% of the CDF. It shows that, if the cooling load is calculated using data in the reference case and without considering uncertainty, the peak cooling load can be over-estimated with a probability of 90%.

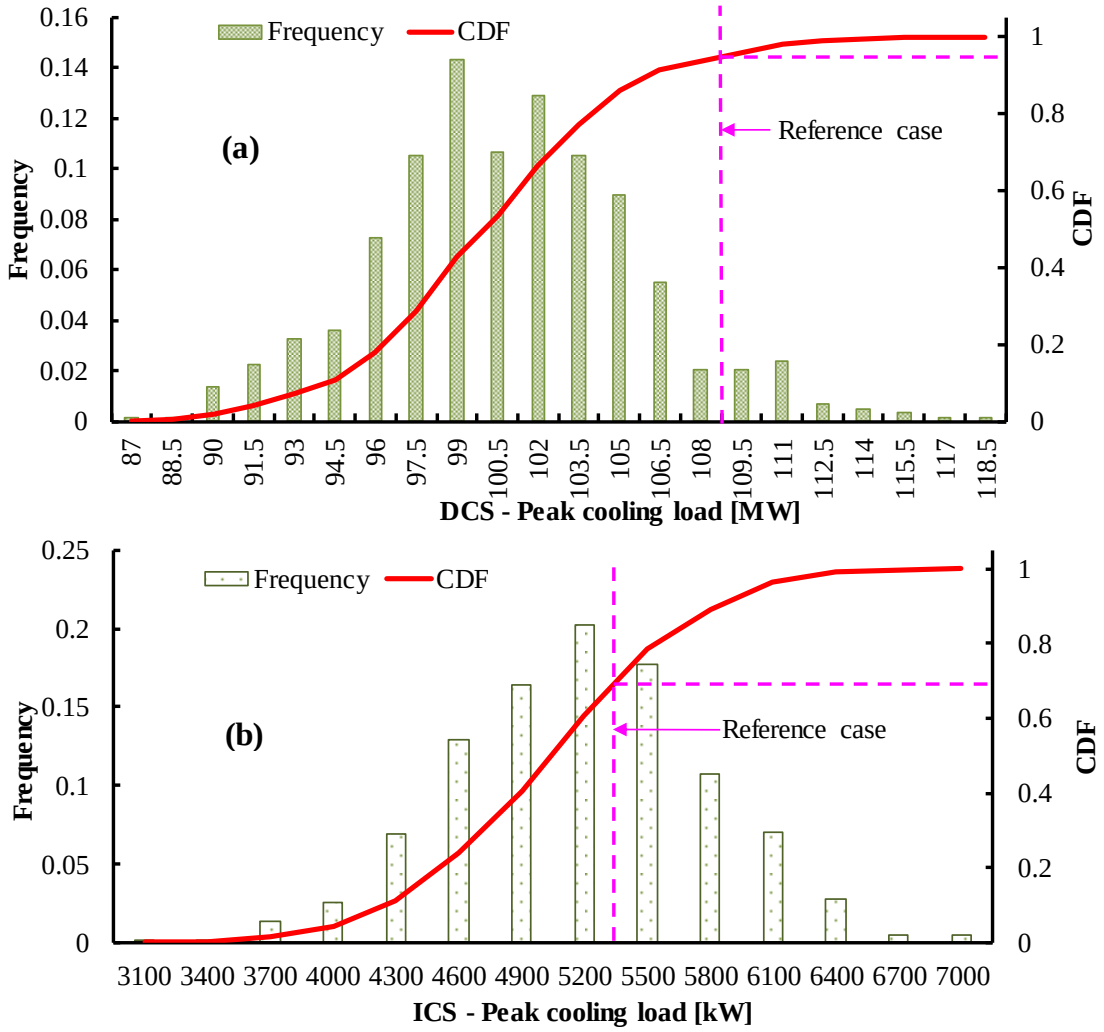

Fig. 9.4 Peak cooling load distribution of the DCS and ICS

As shown in Fig. 9.4b, the peak cooling load of the ICS varies between 3100 kW and 7000 kW. It corresponds to a relative difference between -44% and 30% compared with the peak cooling load in the reference case. The peak cooling load has high frequency between 4600 kW and 5500 kW. Fig. 9.4 shows that the peak cooling load of the ICS varies much more significantly than that of the DCS when uncertainties of input variables have similar distributions. It means that the uncertainty has even larger impacts on the cooling load of the ICS. Involving uncertainty in the design of ICSs is therefore more important. It also demonstrates that DCSs have higher capability to accommodate uncertainties compared with ICSs. That is because multiple buildings are connected to a DCS and the cooling load of the DCS is the sum of all individual buildings. The variation caused by uncertainty is reduced by summing cooling loads of all the buildings due to averaging facts. It can be expected that, if the number of buildings keeps increasing, uncertainty will have limited impact on the cooling loads of DCSs.

The distribution of the annual average cooling load of the DCS is shown in Fig. 9.5a. It can be seen that the annual average cooling load of the DCS varies between 25.5 MW and 34 MW. It corresponds to a relative difference between -16% and 12% compared with the annual average cooling load in the reference case. The cooling load has high frequency between 28 MW and 30.5 MW. The annual average cooling load of the reference case locates at around 80% of the CDF. It can be over-estimated with a probability of 80% when uncertainty is not considered.

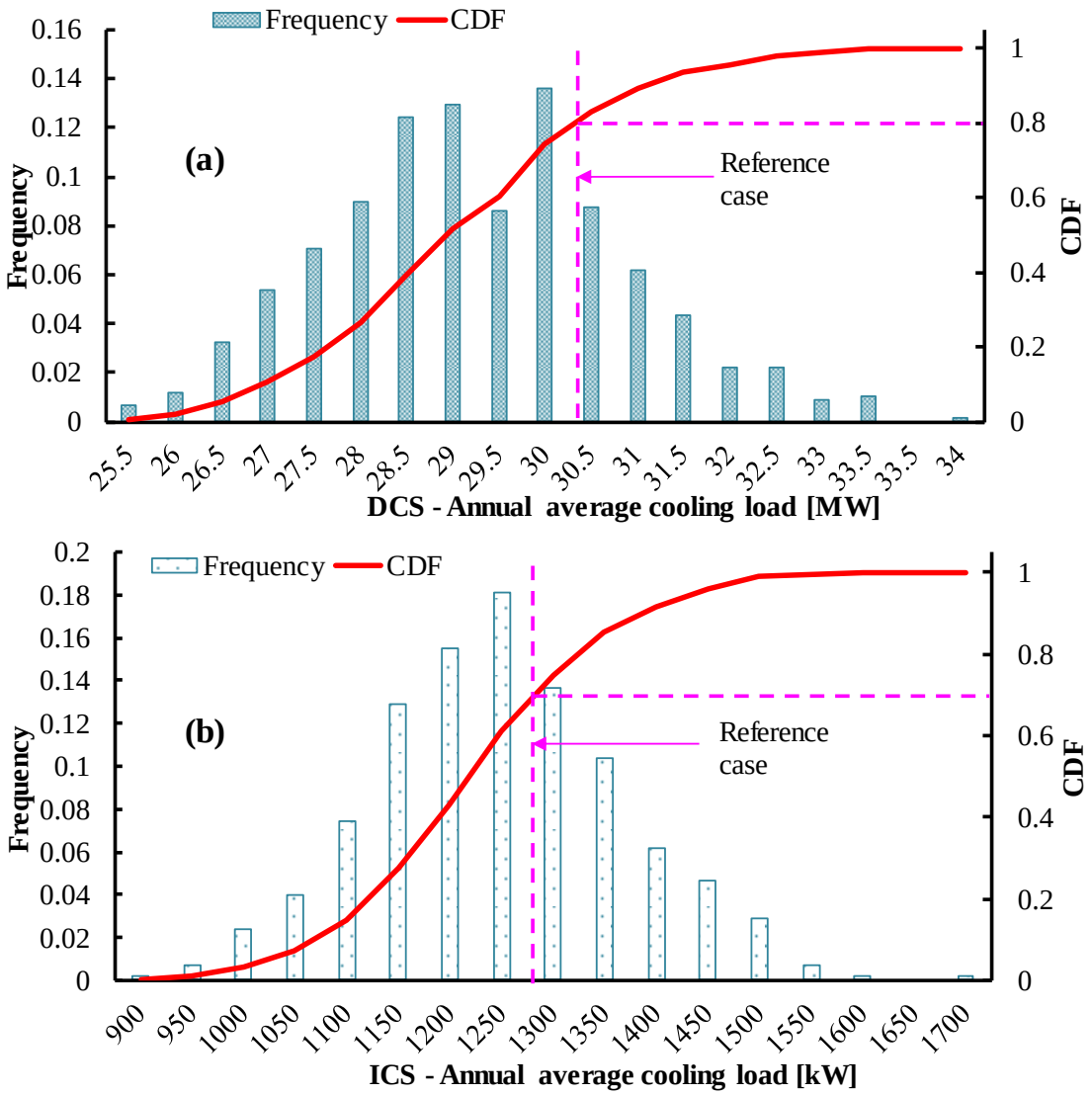

Fig. 9.5 Annual average cooling loads of the DCS and ICS

Fig. 9.5b shows that the annual average cooling load of the ICS varies between 900 kW and 1700 kW. It corresponds to a relative difference between -36% and 30% compared with the annual average cooling load in the reference case. The annual average cooling load has high frequency between 1150 kW and 1300 kW, indicating high probability in this range. Fig. 9.5 shows that the annual average cooling load of the ICS varies more significantly than that of the DCS when uncertainties of input variables have similar distributions. It proves again that the uncertainty has larger impacts on ICSs and involving uncertainty in the design of ICSs is more important.

9.3 Sensitivity analysis for identification of influential factors

The primary purpose of sensitivity analysis is to find the most important input factors for outputs such as the energy consumption, the cooling/heating load, etc. By ranking the importance of input factors, important variables can be obtained and measures can be followed up to reduce the variation of the design outcomes. Many methods can be used to conduct sensitivity analysis, which can be grouped into local and global methods. Global method is adopted in this study due to its ability to handle the interaction of inputs (Tian 2013).

The sensitivity analysis contains three primary steps: 1) To obtain the regression model representing the relationship of all the inputs and outputs; 2) To select significant input variables out of all the inputs using parameter screening methods; 3) To rank the sensitivity of selected variables based on some reasonable sensitivity index (SI). The regression model can be expressed with Eq. (9-1). Parameter screening is necessary to remove insignificant input variables. This is especially important when the samples or trials are limited while the number of input variables is large. The "Lasso" method is used (Tibshirani 1996), which is regarded as a very effective screening method. It can always choose the most correlated parameters to enter the model. Where, y is the output. x_1, x_2 ...x_n are the input variables. a_1, a_2 ... a_n are the regression coefficients.

$$y_1 = a_1 x_{i1} + a_2 x_{i2} \ldots\ldots + a_n x_{in} \tag{9-1}$$

The importance or sensitivity index are calculated using ANalysis of VAriance (ANOVA) as shown in Eq. (9-2) and Eq. (9-3). The sum of squared total (*SST*) indicates the uncertainty associated with the outputs. SST is consisted with two parts:

the sum of squared regression (SSR) and the sum of squared error (SSE). The ratio of *SSR* to *SST* (R^2) indicates the accuracy of regression model. The uncertainty in the outputs caused by variable *j* can be calculated by decomposing SSR, which is expressed as SS_j. The SI can be obtained using Eq. (9-3). A larger SI indicates higher sensitivity of a parameter for the output. Detailed processes and explanations can be found in the reference (Sun et al. 2014).

$$R^2 = \frac{SSR}{SST} \tag{9-2}$$

$$SI_j = \frac{SS_j}{SST} \times 100\% \tag{9-3}$$

For the purpose of comparison, another method *random forest* is also used, which is frequently used to rank the importance of variables. Random forests are a very popular and efficient ensemble learning method for classification, regression and other tasks based on model aggregation ideas, which is introduced by Breiman (2001). A multitude of decision trees are constructed considering two randomization processes, i.e., random selection of training samples and features for tree development. A certain unification scheme will be used to generate the final outcome, e.g., the majority votes for classification tasks and mean aggregation for regression tasks. One advantage of random forests is that it can avoid over-fitting by using the out-of-bag observations for validation. The quantification of the variable importance is one of the common applications of random forests. The principle is to test the increase of the mean error or mean square error when input variables are randomly permuted. Detailed processes and explanations can be found in (Breiman 2001).

Results of the sensitivity analysis on the annual average cooling loads are shown in Fig. 9.6. Fig. 9.6a indicates that variables representing the indoor conditions (the occupant density, lighting density, plug-in load density and ventilation rate) are the

most important for the annual average cooling load of the DCS. Uncertainties in building design/construction are the least important compared with the other two groups of variables. Among the variables of building design/construction, the most important ones are the window wall ratio (WWR) and transmittance of windows. It shows that windows have to be designed carefully if one wants to get green buildings or low energy buildings in Hong Kong climate. For the annual average cooling load of the ICS, the ranking is similar. Variables based on the descending sequence of importance are also that representing the indoor conditions, outdoor weather and building design/construction.

The ranking of variables for the peak cooling load calculation can also be obtained using the similar method, as shown in Fig. 9.7. It can be seen that, for the peak cooling load of the DCS and ICS, the most important variable is the ventilation rate of the outdoor fresh air. The uncertainties in the weather play a more important role in the peak cooling load of the DCS than that of the ICS. The rankings of the outdoor dry-bulb temperature and humidity are very high concerning that impacts on the peak cooling load calculation of the DCS, which is very different for that of the ICS. That is because the outdoor weather data are identical at one trial (i.e. one year) for each building, which is the same in the cooling load calculation of the ICS. However, variables representing the building design/construction and indoor conditions are random for all the 37 buildings in the district. The cooling load of the DCS is the sum of the cooling loads of all individual buildings, which may average the random values for individual variables. The uncertainties in variables representing the building design/construction are also not important for the cooling loads compared with that representing the indoor and outdoor environment.

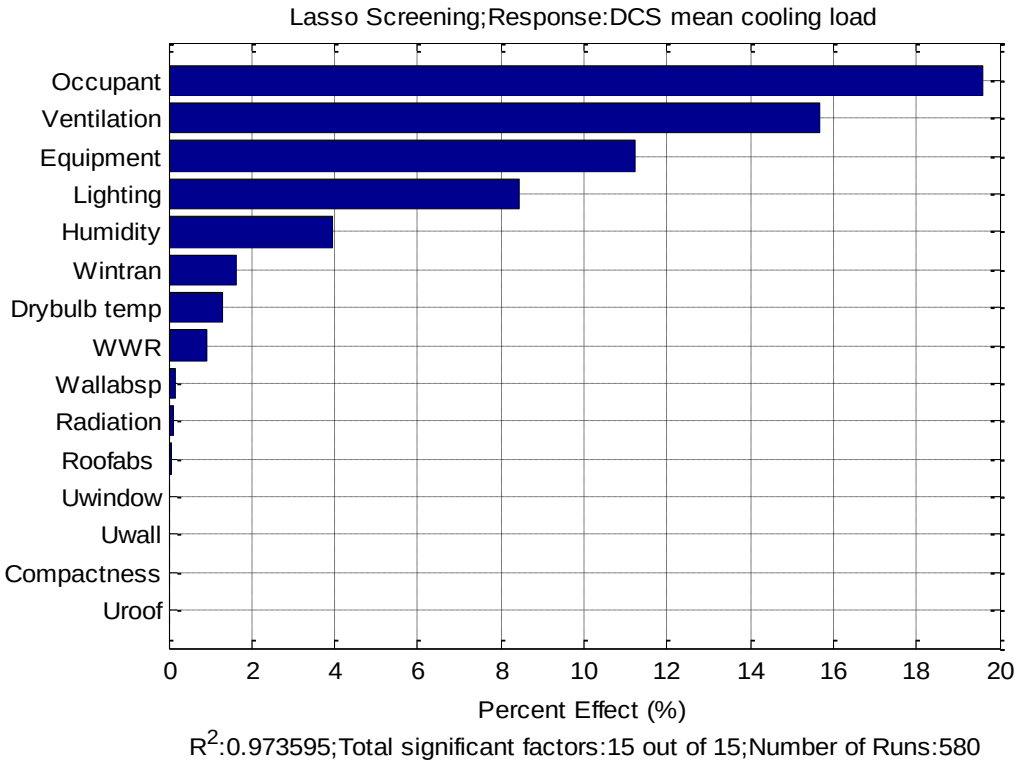

(a) *Annual average cooling load of the DCS*

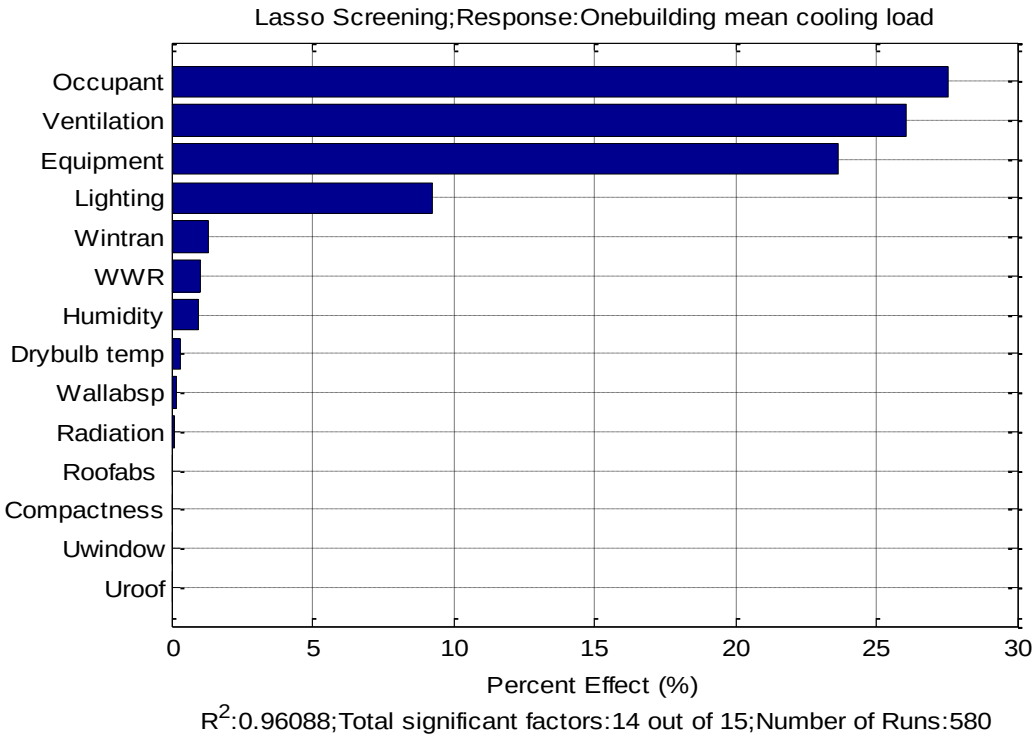

(b) *Annual average cooling load of the ICS*

Fig. 9.6 Ranking of impacts of input variables on the annual average cooling load

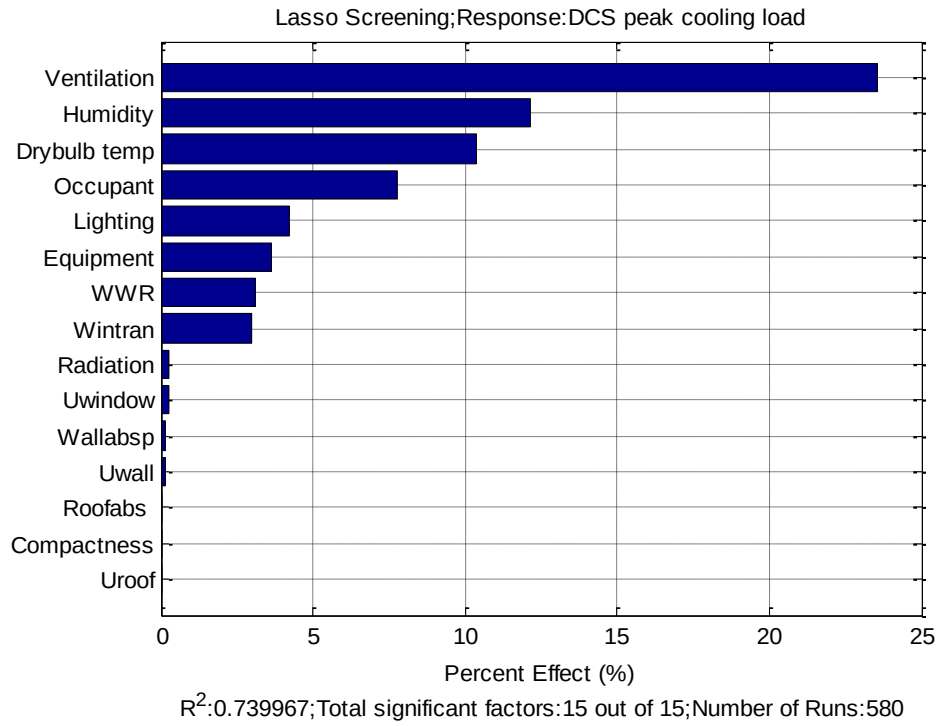

(a) *Peak cooling load of the DCS*

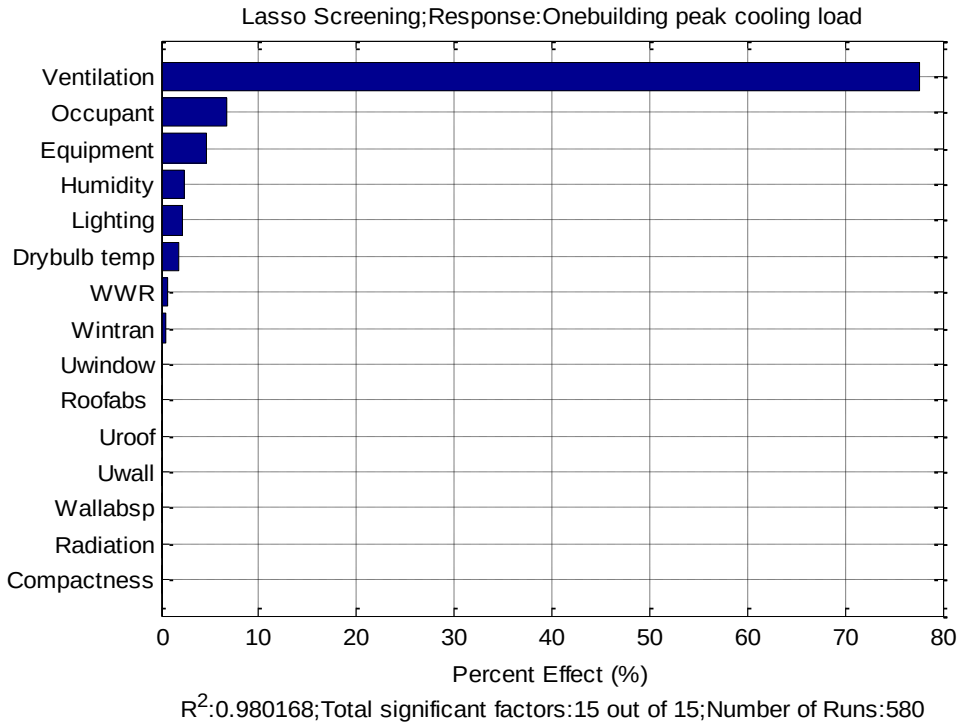

(b) *Peak cooling load of the ICS*

Fig. 9.7 Ranking of impacts of input variables on the peak cooling load

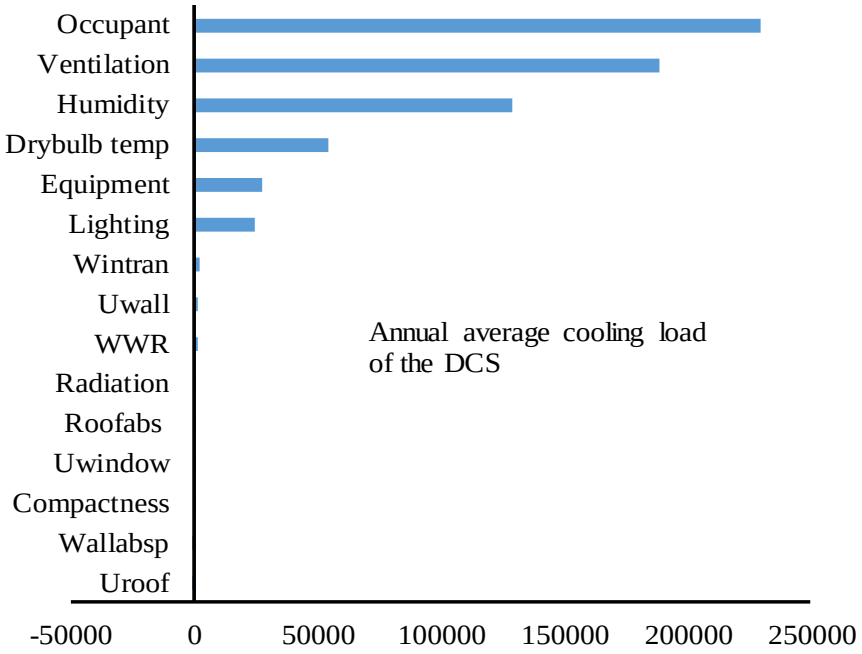

(a) *Annual average cooling load of the DCS*

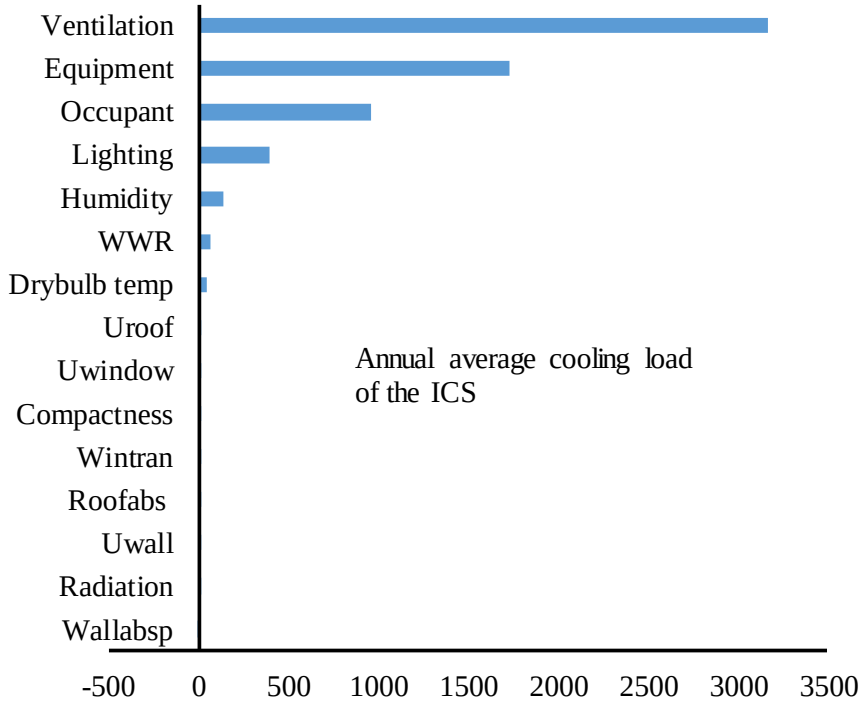

(b) *Annual average cooling load of the ICS*

Fig. 9.8 Ranking of impacts of input variables on annual average cooling loads using random forests

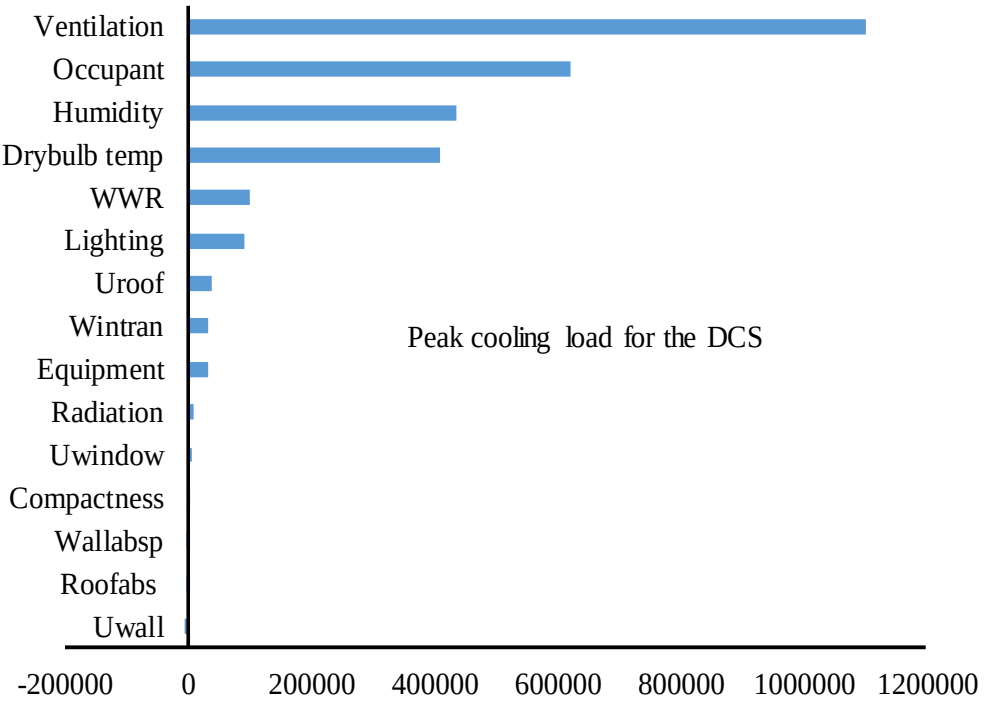

(a) *Peak cooling load of the DCS*

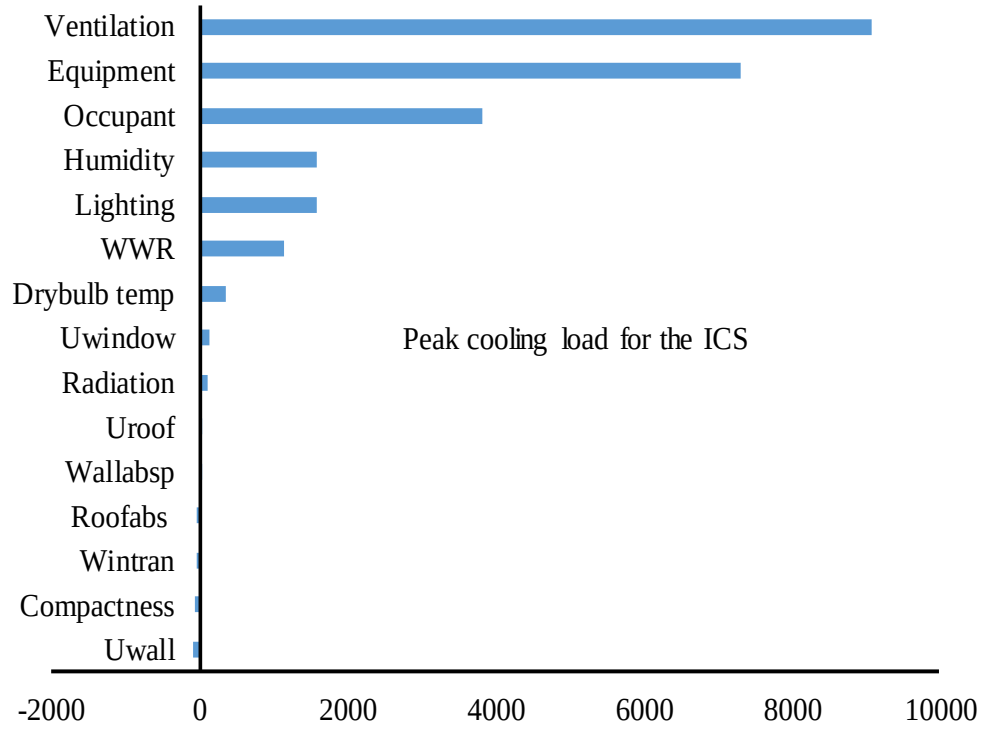

(b) *Peak cooling load of the ICS*

Fig. 9.9 Ranking of impacts of input variables on peak cooling loads using random forests

Results of the sensitivity analysis using random forests are shown in Fig. 9.8 and Fig. 9.9. The values of the horizontal axis are the increase in mean squared errors when the variables are permuted randomly. Variables with larger values mean the greater importance for the outputs. In general, uncertainties in the outdoor weather and indoor conditions have more impacts in both the annual average cooling load and peak cooling load, compared with that in building design/construction. Uncertainties in the weather play a more important role in the cooling load of the DCS compared with that of the ICS. All these results are similar to that using ANOVA method. Detailed ranking for an individual variable may be different due to working mechanisms of these two methods.

9.4 Impacts of uncertainty on the design optimization of the DCS and ICS

The impacts of the uncertainty on the design optimization of the DCS and ICS are assessed and compared.

Performance of the DCS and ICS using chillers of different capacities is compared. The capacities of the DCS and ICS are determined by limiting the unmet hours to 35 with a probability of 100%. It is 10,500 kW for the DCS and 6,300 kW for the ICS. For the DCS, 7 chillers are selected which is referred to a real DCS project with a similar capacity. The DCS with 7 identical chillers is named as S_{dcs1}. The system with 6 large chillers and one small chiller is named as S_{dcs2} (the capacity of the small one is half of that of the large one). For the ICS, the system with 3 identical chillers is named as S_{ics1}. The system with 2 large chillers and 1 small chiller is named as S_{ics2} (the capacity of the small one is half of that of the large one). Considering uncertainty, energy saving by systems using chillers of different capacities in both the DCS and ICS is shown in Fig. 9.10.

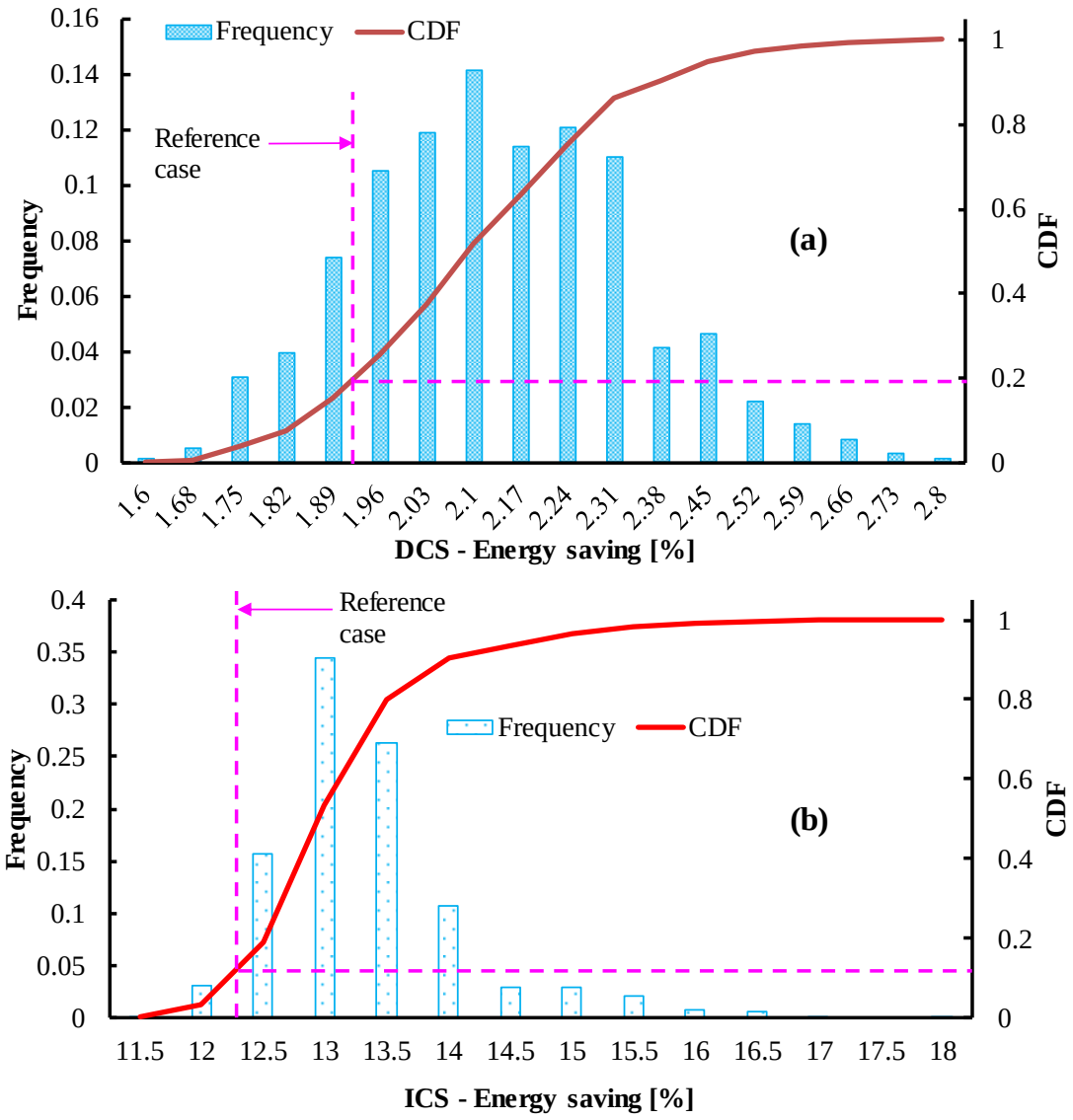

Fig. 9.10 Energy saving distributions of the DCS and ICS using chillers of different capacities

Fig. 9.10a shows that the energy saving of S_{dcs2} varies between 1.6% and 2.8%, which is not very promising. Energy saving has high frequency between 1.96% and 2.31%, which indicates that it has high possibility to fall in such a range. For the ICS in Fig. 9.10b, the energy saving of S_{ics2} is between 11.5% and 18%. The energy consumption difference is quite large. Energy saving has high frequency between 12.5% and 14%. Energy saving of S_{dcs2} is not as large as that of S_{ics2}. It shows that using chillers of

different capacities in DCSs makes no big difference from the viewpoint of energy saving.

9.5 Impacts of uncertainty and reliability on the design optimization of the DCS and ICS

When both uncertainty and reliability are considered in the design stage, cost saving of the DCS and ICS using chillers of different capacities is shown in Fig. 9.11. The availability risk price (see Chapter 7) is assumed as 1.5 $/kWh, which is 10 times of the electricity price. It shows that the cost saving of S_{dcs2} varies between 0.8 % and 2.2%. The percentage is less than that of energy saving. It indicates that, considering reliability, the advantage of systems using chillers of different capacities becomes less. Cost saving of S_{ics2} ranges from 3% to 12.5%, which is also lower than the percentage of energy saving.

The difference between the electricity price and availability risk price affects the results. Therefore, capacities and total annual costs at different availability risk prices are calculated as shown in Fig. 9.12 and Fig. 9.13. It can be seen that, with the increase of ARPRs, the optimal capacity and the annual total cost of the DCS increase. At the same ARPR, the optimal capacity of S_{dcs1} is about 3% less than that of S_{dcs2} while the cost is 2% higher. The relative cost saving decreases with the increase of ARPRs. The optimal capacity and the annual total cost for the ICS are shown in Fig. 9.13. The trend is similar to that of the DCS. Both the capacity and cost increase with the increase of ARPRs. At the same ARPR, the capacity of S_{ics2} is about 9% higher than that of S_{ics1} while the cost is about 7% lower. It proves that, even considering reliability, using chillers of different capacities in ICSs is still preferred due to the lower cost. Fig. 9.12

and Fig. 9.13 shows that the impacts of uncertainty and reliability on the design of DCSs are much smaller compared with ICSs.

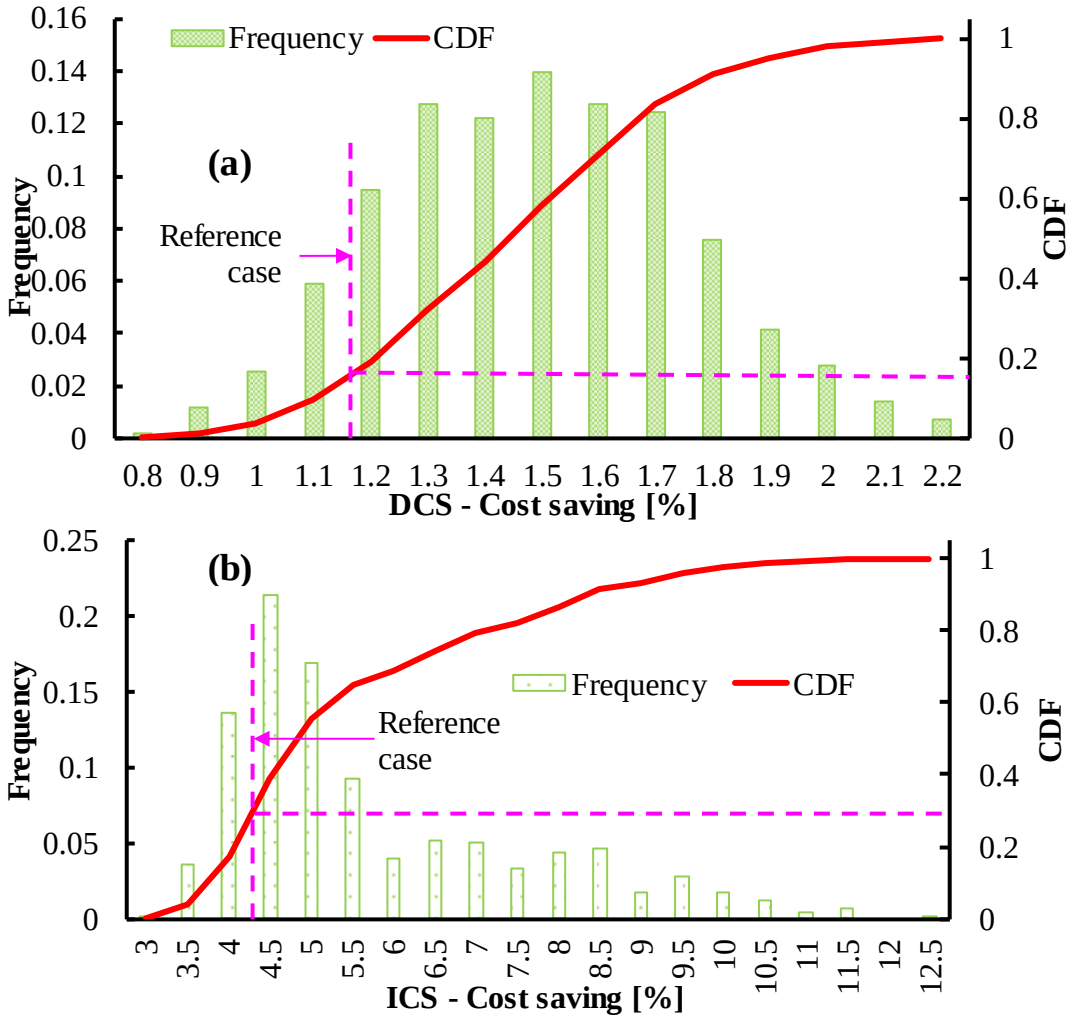

Fig. 9.11 Cost savings of DCS and ICS using chillers of different capacities

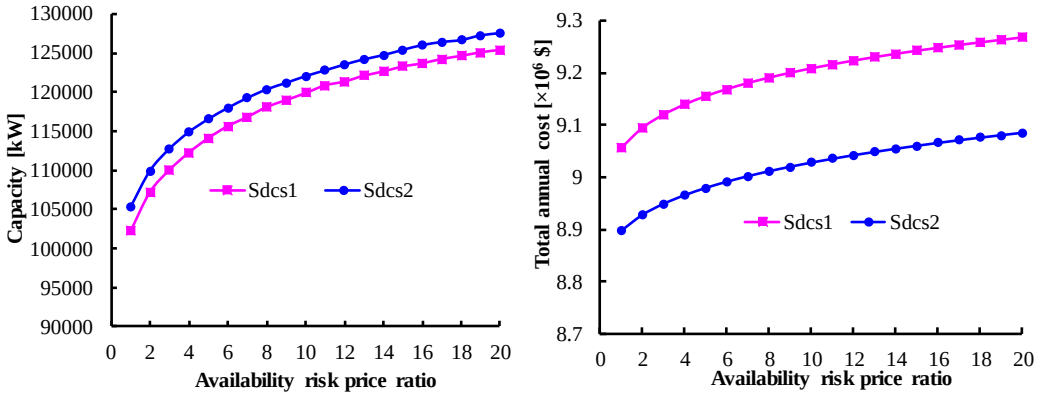

Fig. 9.12 Optimal capacities and total annual costs at different ARPRs - *DCS*

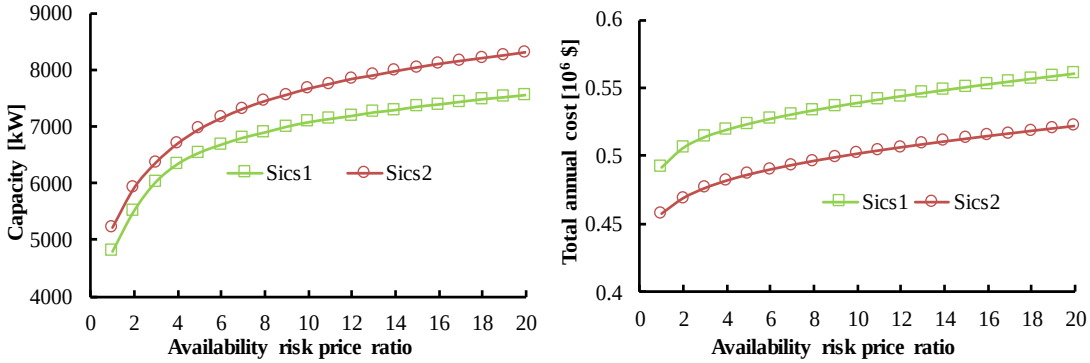

Fig. 9.13 Optimal capacities and total annual costs at different ARPRs - *ICS*

9.6 Summary

Impacts of uncertainty and reliability on the design of DCSs and ICSs are compared. The following conclusions can be made through the analysis and discussions:

i. Uncertainty at the design stage affects the cooling load prediction of DCSs and ICSs significantly. The cooling load variation of DCSs is much smaller than that of ICSs when the uncertainties of input variables fit similar distributions. It is therefore more important to consider uncertainty in the design of ICSs. DCSs have higher capability to accommodate uncertainty.

ii. Uncertainties in the indoor conditions are the most influential for both the annual cooling load and peak cooling load of the DCS and ICS. Uncertainties in building design/construction have the least impact on the cooling loads of the DCS and ICS, among which the uncertainties in windows are the most influential. Uncertainties in the weather condition are more important for the cooling load of the DCS compared with that of the ICS.

iii. DCSs and ICSs using chillers of different capacities are more energy and cost efficient. Energy saving of DCSs using chillers of different capacities is not as

large as that of ICSs at the same arrangement. It is not recommended to use chillers of different capacities in DCSs.

iv. Considering reliability, systems using chillers of different capacities are still preferred for both the DCS and ICS but the advantage in the DCS is less significant. The cost saving is smaller than energy saving.

v. The impact of uncertainty and reliability on the design of DCSs is smaller than that on the design of ICSs.

CHAPTER 10 CONCLUSIONS AND FUTURE WORK

In this chapter, main contributions of this thesis are summarized. Conclusions are made based on the above studies. Recommendations for future work are presented.

10.1 Main Contributions of this study

This study investigates the performance of DCSs and conducts design optimization for DCSs and ICSs considering uncertainty of cooling loads and system reliability. Main contributions are summarized as follows:

i. Detailed performance assessment of the DCS in the subtropical area is conducted by comparing it with ICSs. Energy performance of the DCS under different seasons and part load ratios is analyzed. Energy and economic performance of the DCS coupled with different technologies to handle the peak electricity load is quantified and analyzed in the subtropical area.

ii. Detailed literature review on the studies of DCSs and their applications is presented. Studies involving uncertainty and reliability quantification in building energy systems are summarized and classified.

iii. Uncertainties at planning and design stages of DCSs and ICSs are quantified. The uncertainty-based optimal design methods for DCSs and ICSs are developed. Performance of the cooling systems using the proposed methods is analyzed and compared with that using the conventional design method.

iv. The robust optimal design methods considering both uncertainty and reliability are developed and implemented in DCSs and ICSs. Performance of the cooling

systems using the robust optimal design method is evaluated and compared with that using the conventional method, uncertainty-only method and reliability-only method.

v. The impacts of uncertainty and reliability on the design optimization of DCSs and ICSs are evaluated and compared.

10.2 Conclusions

Conclusions from the performance assessment of the DCS compared with ICSs

i. The DCS is an energy efficient cooling system for the new development area in the subtropical area. It can save around 15% energy compared with the traditional ICS.

ii. The DCS shows high energy saving potential all the year, especially in the cold months when the buildings have low cooling demands. The DCS shows high energy saving potential when the load ratio is below 50%.

iii. Chillers are the major contributor to energy saving in DCSs compared with ICSs. It is due to the load concentration effect which allows the chillers to work at high COPs, especially when the load ratio for individual buildings is low.

iv. The chilled water system is the only subsystem that consumes more energy in the DCS compared with the ICS. It is because the DCS has at least one extra group of pumps compared with ICSs. Reducing the energy consumption of chilled water systems is important to enhance the advantage of DCSs.

v. The DCS can save at least 7% of energy compared with the ICS in the conditions studied, no matter how much percent of buildings have cooling loads during night time.

vi. The annual operation cost of the DCS is 10% lower than that of the ICS under the current tariff in Hong Kong.

Conclusions from the performance analysis of the DCS with different technologies

i. The DCS with full ice storage system is not cost-efficient under current Hong Kong tariff because of much more annual operation cost. The DCS with partial ice storage system for demand limiting can save around 4% of the annual operation cost, which is recommended in the design of the DCS.

ii. The priority of the DCS with PHES and the DCS with thermal storage system depends on the efficiency of both systems. Detailed comparison is strongly recommended before the decision is made.

iii. The DCS integrated with CCHP system is more energy efficient than that fully depending on the local grid. The energy saving ranges between 8% and 18%. Hot water demand affects the energy saving and payback periods significantly. The integrated system designed based on electricity demand is recommended due to a short payback period (2.6 to 6 years).

Conclusions from the design method based on mini-max regret theory

i. The optimal design method based on mini-max regret theory is easy to be implemented. It can achieve the uncertainty-based optimal cooling system very effectively. No complicated models or methods are involved.

ii. The uncertainty-based optimal combination of two chillers is the option with individual chiller capacities of 0.3 and 0.7 of the system capacity. It can save up to 12% of energy compared with that with equal-size chillers. The uncertainty-based optimal combination of three chiller is the option with 0.2, 0.2 and 0.6, or 0.4, 0.4 and 0.2 of the system capacity. The energy saving can be up to 10%. The uncertainty-based optimal combination of four chillers is the option with individual capacities of 0.1, 0.2, 0.2 and 0.5 of the system capacity. The energy saving can be up to 10%.

iii. Five types of chilled water pump systems are studied. The primary-only chilled water system with constant-speed pumps is always the most energy-consuming. It is recommended to avoid the use of such a system in practical applications. The primary-only chilled water configuration with variable-speed pumps is the uncertainty-based optimal, considering the uncertainty in the pipeline resistance. Such a chilled water system consumes about 50% less of energy. For the chilled water system of a similar connection way, the option with smaller pumps is more efficient.

Conclusions from the design optimization of ICSs

i. The uncertainty-based optimal design method is developed. The peak cooling load of the ICS varies largely by considering uncertainties at design stage. If the ICS is sized using the conventional method, it has a high probability to be oversized. With the distribution of unmet hours and capital costs at different risk levels, decision makers can determine an ICS based on their specific concerns with quantified confidence.

ii. The annual average cooling load varies significantly considering uncertainty. The performance of the ICS with different configurations at different risk levels is obtained when considering uncertainty. The selected configuration using the conventional method cannot perform as well as expected and the efficiency is most likely overqualified.

iii. By quantifying the cooling load uncertainty and assessing the reliability of the ICS, the robust optimal design of the ICS is achieved. The optimal capacity of the ICS determined using the robust optimal method is lower than that using the reliability-only method, and higher than that using the uncertainty-only method.

Conclusions from the design optimization of DCSs

i. The annual average cooling load of the DCS considering uncertainties varies between 0.84 and 1.12 times of that without considering uncertainty. It almost fits a normal distribution when the uncertainties of input variables are quantified using the method of this study. Based on the distribution of the annual cooling load, the energy performance of different DCS options at different risks can be obtained.

ii. The peak cooling load at different risk levels is obtained based on uncertainty quantification. With the number of unmet hours and cooling loads at different risks, the DCS can be properly sized under certain risk and thermal comfort requirement.

iii. The configuration of the DCS can be selected based on quantified risks and benefits based on the uncertainty-based optimal design. The energy saving of

the DCS using chillers of different capacities is not promising. It is not recommended considering control and maintenance issues. Annual cost saving of the DCS with ice storage system varies significantly when considering uncertainty in the cooling load.

iv. The robust optimal design of the DCS with the lowest total annual cost is achieved. With the increase of the availability risk price, the optimal capacity increases. When the availability risk price is high enough, the capacity of the DCS using the robust optimal design method is larger than that using the conventional method.

v. The capacity of the DCS obtained using the robust optimal method is smaller than that using the reliability-only method. When only uncertainty is considered, the capacity of the DCS is smaller but the total annual cost is higher.

Conclusions from the comparison of DCSs and ICSs

i. The cooling load variation of the ICS is larger than that of the DCS when the uncertainties of input variables fit similar distributions. The uncertainty has larger impact on the cooling load of ICSs and it is more essential to involve it in the design process. DCSs have a stronger capability to accommodate uncertainties.

ii. Uncertainties in the indoor conditions are the most influential for both the annual cooling load and peak cooling load of the DCS and ICS. Uncertainties in building design/construction have the least impact on the cooling loads of DCSs and ICSs, among which uncertainties in windows are the most

influential. Uncertainties in the weather condition play a more important role in DCSs compared with ICSs.

iii. Cooling systems using chillers of different capacities are more energy efficient, which is consistent in both DCSs and ICSs. However, the energy saving is larger in ICSs. There is no significant benefit to use chillers of different capacities in DCSs from the viewpoint of energy saving.

iv. Considering reliability, systems that using chillers of different capacities are still preferred for both DCSs and ICSs but the advantage is decreased. The cost saving is not as high as the energy saving.

10.3 Recommendations for future work

This thesis answers several important questions about the DCSs and ICSs but many other problems still need to be solved. Following points are recommended for further studies:

i. Uncertainties in the performance of components in the cooling systems (such as chillers, pumps, valves, etc.) are rarely considered at design stage. These uncertainties will affect the operation performance of the cooling systems. Comprehensive optimization method considering uncertainty at planning, design and operation stages needs to be developed.

ii. Effective and accessible tools are necessary to implement the proposed design methods considering uncertainty and reliability. It will be much more helpful if such tools can be integrated with popular building energy simulation tools such as EnergyPlus, TRNSYS, etc. Similar tools for building energy systems

are available such as GURA-Workbench. However, for the central cooling plant, such tools are still needed to be developed.

iii. Probability density functions to quantify uncertainties of input variables (except that representing the weather condition) in this study are mostly determined based on experiences or assumptions. It is necessary and important to develop more reliable methods to obtain probability density functions as reasonable/accurate as possible.

iv. It is usually very calculation-intensive and time-consuming to model a large DCS serving many buildings, or an energy system at urban scale. Effective and reliable tools to simulate the performance of energy systems at large scale are worth to be developed. It will be much more valuable if the tools can involve the dynamic characteristics of the energy systems.

v. One characteristic of the DCS is that it has multiple buildings as users. If taking each building as an agent, the multi-agent concept can be implemented in the DCS to optimize the operation of the DCS. Multi-agent has been widely used in the building energy system (Huberman and Clearwater 1995; Klein et al. 2012; Zhao et al. 2013). Its application in DCSs is worth to be studied.

vi. With the development of smart grid, new concepts are emerging such as smart poly-generation micro-grid, smart energy network, and smart thermal grid (Bracco et al. 2014; Chai et al. 2013; Lund et al. 2014). Buildings play an important role in the smart grid because building energy systems contribute a large percent of the total electricity consumption in urban areas (Wang et al. 2014; Xue et al. 2014). This results in the necessity to develop smart DCSs to

be integrated with smart grid. The technologies to integrate DCSs with smart grid and potential problems need to be investigated.

REFERENCES

Aguilar O., Kim J. K., Perry S., Smith R. 2008. Availability and reliability considerations in the design and optimisation of flexible utility systems. *Chemical Engineering Science* 63(14): 3569-3584.

Aissi H., Bazgan C., Vanderpooten D. 2009. Min–max and min–max regret versions of combinatorial optimization problems: A survey. *European Journal of Operational Research* 197(2): 427-438.

Ampofo F., Maidment G. G., Missenden J. F. 2006. Review of groundwater cooling systems in London. *Applied Thermal Engineering* 26(17–18): 2055-2062.

Andersson O. 2007. ATES for district cooling in Stockholm. *NATO Science Series* 234: 239-243.

ARUP. 2014. New development areas in Hong Kong. http://www.arup.com/Projects/Hong_Kong_New_Development_Areas.aspx

ASHRAE. 1993. Design guide for cool thermal storage. American Society of Heating, Refrigerating and Air-Conditioning Engineers.

ASHRAE. 2009. ASHRAE Handbook: Fundamentals. American Society of Heating, Refrigerating and Air-Conditioning Engineers.

ASHRAE. 2012. ASHRAE Handbook: HVAC Systems and Equipment. American Society of Heating, Refrigerating and Air-Conditioning Engineers.

ASHRAE. 2013. District Cooling Guide. American Society of Heating, Refrigerating and Air-Conditioning Engineers.

Augenbroe G., Zhang Y., Khazaii J., Su H., Sun Y., Lee B. D., Wu C. J. 2013. Implications of the uncoupling of building and HVAC simulation in the presence of parameter uncertainties. *Proceedings of BS2013: 13th Conference of International Building Performance Simulation Association*: 3169-3176.

Averbakh I. 2000. Minmax regret solutions for minimax optimization problems with uncertainty. *Operations Research Letters* 27(2): 57-65.

Babus'Haq R. F. 1987. Optimal heat transfer design for district-heating and cooling pipelines in air-filled cavities. PhD Dissertation, Cranfield University, United Kingdom.

Babus'Haq R. F., Probert S. D., George H. E. 1990. District heating and/or district cooling distribution pipelines: optimal configurations. *Journal of Power and Energy* 204: 57-66.

Babus'Haq R. F., Probert S. D., Shilston M. J. 1986. District-cooling distribution network: Optimal configuration of a double-pipe system in a rectangular trench. *Applied Energy* 25(4): 273-298.

Bernier M. A., Bourret B. 1999. Pumping energy and variable frequency drives. *ASHRAE Journal* 41(12): 37-40.

Bo H., Gustafsson E. M., Setterwall F. 1999. Tetradecane and hexadecane binary mixtures as phase change materials (PCMs) for cool storage in district cooling systems. *Energy* 24(12): 1015-1028.

Booth A. T., Choudhary R., Spiegelhalter D. J. 2012. Handling uncertainty in housing stock models. *Building and Environment* 48: 35-47.

Booz & Company. 2012. Unlocking the Potential of District Cooling: The Need for GCC Governments to Take Action. http://www.booz.com/me/home/thought_leadership_strategy/40007409/40007869/50737873.

Bracco S., Delfino F., Pampararo F., Robba M., Rossi M. 2014. A mathematical model for the optimal operation of the University of Genoa Smart Polygeneration Microgrid: Evaluation of technical, economic and environmental performance indicators. *Energy* 64: 912-922.

Breiman L. 2001. Random forests. *Machine learning* 45(1): 5-32.

Brohus H., Frier C., Heiselberg P., Haghighat F. 2011. Quantification of uncertainty in predicting building energy consumption: A stochastic approach. *Energy and Buildings* 55: 127-140.

Buonomano A., Calise F., Ferruzzi G., Vanoli L. 2014. A novel renewable polygeneration system for hospital buildings: Design, simulation and thermo-economic optimization. *Applied Thermal Engineering* 67(1): 43-60.

Buoro D., Pinamonti P., Reini M. 2014. Optimization of a Distributed Cogeneration System with solar district heating. *Applied Energy* 124: 298-308.

CEDD. 2015. North east new territories new development areas planning and engineering study-Investigation. http://www.nentnda.gov.hk/eng/study.html.

Chai D. S., Wen J. Z., Nathwani J. 2013. Simulation of cogeneration within the concept of smart energy networks. *Energy Conversion and Management* 75: 453-465.

Chan A. L. S., Chow T.T., Fong S. K. F., Lin J. Z. 2006. Performance evaluation of district cooling plant with ice storage. *Energy* 31(14): 2750-2762.

Chan A. L. S., Hanby V. I., Chow T. T. 2007. Optimization of Distribution Piping Network in District Cooling System Using Genetic Algorithm with Local Search. *Energy Conversion & Management* 48(10): 2522-2522.

Chinese D., Nardin G., Saro O. 2011. Multi-criteria analysis for the selection of space heating systems in an industrial building. *Energy* 36(1): 556-565.

Chiu J. N., Martin V., Setterwall F. 2009. System integration of latent heat thermal energy storage for comfort cooling integrated in district cooling network. *The 11th International Conference on Thermal Energy Storage*, June 14-17, Stockholm, Sweden.

Choi U.S., France D. M., Knodel B. D. 1992. Impact of advanced fluids on costs of district cooling systems. *Annual conference on the International District of Heating and Cooling Association*, June 14-17, Boston, MA, United States.

Chou L. 1991. Drag reducing cationic surfactant solutions for district heating and cooling systems, PhD Dissertation, The Ohio State University, United States.

Chow T. T., Au W. H., Yau R., Cheng V., Chan A., Fong K. F. 2004. Applying district-cooling technology in Hong Kong. *Applied Energy* 79(3): 275-289.

Chow T. T., Fong K. F., Chan A. L. S., Yau R., Au W. H., Cheng V. 2004. Energy modelling of district cooling system for new urban development. *Energy and Buildings* 36(11): 1153-1162.

Chow T. T., Chan A. L. S., Song C. L. 2004. Building-mix optimization in district cooling system implementation. *Applied Energy* 77(1): 1-13.

CLP. 2014. Tariffs overview. https://www.clponline.com.hk/myBusiness/CustomerService/TariffOverview/Pages/Default.aspx.

Corrado V., Mechri H. E. 2009. Uncertainty and Sensitivity Analysis for Building Energy Rating. *Journal of Building Physics* 33(2): 125-156.

De Wit S., Augenbroe G. 2002. Analysis of uncertainty in building design evaluations and its implications. *Energy and Buildings* 34(9): 951-958.

Deng J., Wang R. Z., Han G. Y. 2011. A review of thermally activated cooling technologies for combined cooling, heating and power systems. *Progress in Energy and Combustion Science* 37(2): 172-203.

DeST. 2011. http://dest.tsinghua.edu.cn/chinese/default1.asp?accessdenied=%2Fchinese%2Fdefault%2Easp#.

Dincer I. 2000. Renewable energy and sustainable development: a crucial review. *Renewable and Sustainable Energy Reviews* 4(2): 157-175.

Djunaedy E., Van Den Wymelenberg K., Acker B., Thimmana H. 2011. Oversizing of HVAC system: Signatures and penalties. *Energy and Buildings* 43(2–3): 468-475.

DOE-2. 2009. Building Energy Use and Cost Analysis Tool. http://doe2.com/doe2/index.html.

Dom ínguez-Mu ñoz F., Cejudo-L ópez J. M., Carrillo-Andr és A. 2010. Uncertainty in peak cooling load calculations. *Energy and Buildings* 42(7): 1010-1018.

Eggen G., Vangsnes G. 2006. Heat pump for district cooling and heating at OSLO Airport Gardermoen. *The IEA 8th Heat Pump Conference*, Las Vegas.USA.

Eisenhower B., O'Neill Z., Narayanan S., Fonoberov V. A., Mezic I. 2011. A comparative study on uncertainty propagation in high performance building design. *Proceedings of Building Simulation 2011*: 2785-2792.

Eisenhower B., O'Neill Z., Fonoberov V. A., Mezić I. 2011. Uncertainty and sensitivity decomposition of building energy models. *Journal of Building Performance Simulation* 5(3): 171-184.

Empower. 2014. History of District Cooling. http://www.empower.ae/php/what-is-district-cooling.php?id=2.

EMSD. 2011. Benefits of DCS. http://www.energyland.emsd.gov.hk/en/building/district_cooling_sys/dcs_benefits.html.

EMSD. Hong Kong Energy End-use Data 2014. http://www.emsd.gov.hk/emsd/e_download/pee/HKEEUD2014.pdf

EnergyPlus energy simulation software. 2015. http://apps1.eere.energy.gov/buildings/energyplus/?utm_source=EnergyPlus&utm_medium=redirect&utm_campaign=EnergyPlus%2Bredirect%2B1.

Erdem H. H., Dagdas A., Sevilgen S. H., Cetin B., Akkaya A. V., Sahin B., Teke I., Gungor C., Atas S. 2010. Thermodynamic analysis of an existing coal-fired power plant for district heating/cooling application. *Applied Thermal Engineering* 30(2–3): 181-187.

Euroheat and Power. 2007. Renewables in district heating and cooling. http://www.localpower.org/documents/reporto_ehp_renewablesandde.pdf .

Feng X., Long W. 2008. Applying Single Parent Genetic Algorithm to Optimize Piping Network Layout of District Cooling System. *The Fourth International Conference on Natural Computation, Jinan, China*: 176-180.

Fowlkes W. Y., Creveling C. M. 1995. Engineering methods for robust product design: using Taguchi methods in technology and product development. AddisonWesley Publishing Company.

Frangopoulos C. A., Dimopoulos G. G. 2004. Effect of reliability considerations on the optimal synthesis, design and operation of a cogeneration system. *Energy* 29(3): 309-329.

Fu L., Jiang Y., Yuan W. X., Qin X. Z. 2001. Influence of supply and return water temperatures on the energy consumption of a district cooling system. *Applied Thermal Engineering* 21(4): 511-521.

GNS Science. 2009. Seawater used for district cooling in Stockholm. http://www.gns.cri.nz/content/download/7826/42697/file/District%20cooling%20-%20using%20Seawater.pdf.

Hamaoka Y., Toyama Y., Kuriyama T., Morikawa H. 1996. District cooling system using slurry ice. *The Thirty-third National Heat Transfer Symposium of Japan*: 241-244.

Hart D. R., Rosen M. A. 1996. Environmental and health benefits of district cooling using utility-based cogeneration in Ontario, Canada. *Energy* 21(12): 1135-1146.

Hassine I. B., Eicker U. 2013. Impact of load structure variation and solar thermal energy integration on an existing district heating network. *Applied Thermal Engineering* 50(2): 1437-1446.

Heiselberg P., Brohus H., Hesselholt A., Rasmussen H., Seinre E., Thomas S. 2009. Application of sensitivity analysis in design of sustainable buildings. *Renewable Energy* 34(9): 2030-2036.

Heising C. 1991. IEEE recommended practice for the design of reliable industrial and commercial power systems: IEEE Inc., New York.

Hilotin J. B. 2011. District cooling: Cool discomfort. http://gulfnews.com/news/gulf/uae/general/district-cooling-cool-discomfort-1.796929.

Hopfe C. J. 2009. Uncertainty and sensitivity analysis in building performance simulation for decision support and design optimization. PhD Dissertation, Eindhoven University of Technology, the Netherlands.

Hopfe C. J., Augenbroe G. L. M., Hensen J. L. M. 2013. Multi-criteria decision making under uncertainty in building performance assessment. *Building and Environment* 69: 81-90.

Hora S. C. 1996. Aleatory and epistemic uncertainty in probability elicitation with an example from hazardous waste management. *Reliability Engineering & System Safety* 54(2): 217-223.

Huang P., Huang G., Wang Y. 2015. HVAC system design under peak load prediction uncertainty using multiple-criterion decision making technique. *Energy and Buildings* 91: 26-36.

Huberman B. A., Clearwater S. H. 1995. A Multi-Agent System for Controlling Building Environments. *Proceedings of the First International Conference on Multiagent systems*: 171-176.

IEA DHC|CHP. 2013. DHC & CHP Case Studies. http://www.iea-dhc.org/the-research/case-studies.html.

Iman R. L. 2008. *Latin hypercube sampling*. Wiley Online Library.

Kang Y.Z., Wu H., Hua B. 2010. Research on economical cooling supply distance of district cooling systems. *HV&AC* 40(8): 135-139. (In Chinese).

Kang Y.Z., Zuo Z. 2009. Cooling loss of the secondary piping network in district cooling system. *HV&AC* 39(11): 31-36. (In Chinese).

Klein L., Kwak J.Y., Kavulya G., Jazizadeh F., Becerik-Gerber B., Varakantham P., Tambe M. 2012. Coordinating occupant behavior for building energy and comfort management using multi-agent systems. *Automation in Construction* 22: 525-536.

Kozawa Y., Aizawa N., Tanino M. 2005. Study on ice storing characteristics in dynamic-type ice storage system by using supercooled water: Effects of the supplying conditions of ice-slurry at deployment to district heating and cooling system. *International Journal of Refrigeration* 28(1): 73-82.

Kwak R.Y., Takakusagi A., Sohn J.Y., Fujii S., Park B.Y. 2004. Development of an optimal preventive maintenance model based on the reliability assessment for air-conditioning facilities in office buildings. *Building and Environment* 39(10): 1141-1156.

Lee B. D., Sun Y., Hu H., Augenbroe G., Paredis C. J. J. 2012. A framework for generating stochastic meteorological years for risk-conscious design of buildings. *Proceedings of the SimBuild 2012 Conference*, Madison, Wisconsin, USA: 345-52.

Lee P., Lam P., Yik F. W., Chan E. H. 2013. Probabilistic risk assessment of the energy saving shortfall in energy performance contracting projects–A case study. *Energy and Buildings* 66: 353-363.

Li D. H.W., Wong S.L., Lam J.C. 2003. Climatic effects on cooling load determination in subtropical regions. *Energy conversion and management* 44(11): 1831-1843.

Li X.l., Duanmu L., Shu H.W. 2010. Optimal design of district heating and cooling pipe network of seawater-source heat pump. *Energy and Buildings* 42(1): 100-104.

Li Y.P., Huang G.H., Chen X. 2011. An interval-valued minimax-regret analysis approach for the identification of optimal greenhouse-gas abatement strategies under uncertainty. *Energy Policy* 39(7): 4313-4324.

Li Z., Duanmu L., Shu H.W., Jiang S., Zhu Y. X. 2007. District cooling and heating with seawater as heat source and sink in Dalian, China. *Renewable Energy* 32 (15): 2603-2616.

Lindenberger D., Bruckner T., Groscurth H.M., Kümmel R. 2000. Optimization of solar district heating systems: seasonal storage, heat pumps, and cogeneration. *Energy* 25(7): 591-608.

Lisnianski A., Levitin G. 2003. *Multi-state System Reliability: Assessment, Optimization and Applications*. World Scientific.

Liu J.P., Chen Z.Q. 2006. Optimal design for tree-shaped chilled water pipe network in district cooling systems. *HV&AC* 36(7): 18-22. (In Chinese).

Liu J.P., Du Y.G., Chen Z.Q. 2004. Optimized design of the chilled water-conveying pipeline in the district cooling system. *Journal of South China University of Technology* 32(10): 28-35. (In Chinese).

Lozano M. A., Ramos J. C., Serra L. M. 2010. Cost optimization of the design of CHCP (combined heat, cooling and power) systems under legal constraints. *Energy* 35(2): 794-805.

Lu Y.Q. 2008. Practical HVAC design manual. China Architecture & Building Press. (In Chinese).

Lund H., Werner S., Wiltshire R., Svendsen S., Thorsen J. E., Hvelplund F., Mathiesen B. V. 4th Generation District Heating (4GDH): Integrating smart thermal grids into future sustainable energy systems. *Energy* 68 (2014): 1-11.

Ma H., Long W. 2009. Present status and prospects of district cooling system. *HV&AC* 39(10): 52-59. (In Chinese).

MacCracken M. 2010. Energy Storage Providing for a Low-Carbon Future. *ASHRAE Journal* September: 1-5.

Macdonald I. A. 2002. Quantifying the effects of uncertainty in building simulation. PhD Dissertation, University of Strathclyde, United Kingdom.

Majid M. A. A., Waluyo J. 2010. Thermocline Thickness Evaluation on Stratified Thermal Energy Storage Tank of Co-generated District Cooling Plant. *Journal of Energy and Power Engineering* 4(2): 28-33.

Menassa C. C. 2011. Evaluating sustainable retrofits in existing buildings under uncertainty. *Energy and Buildings* 43(12): 3576-3583.

Myrefelt S. 2004. The reliability and availability of heating, ventilation and air conditioning systems. *Energy and Buildings* 36(10): 1035-1048.

Nagae S., Shimoda Y., Takamura S., Uno Y., Watanabe K., Shoji Y. 2011. Verification of the Energy Efficiency Advancement in District Heating and Cooling Plant by Renovation. *ASHRAE Transactions* 117(1): 139-146.

Nguyen T. H., Yadav A., An B., Tambe M., Boutilier C. 2014. Regret-based optimization and preference elicitation for stackelberg security games with uncertainty. http://teamcore.usc.edu/people/thanhhng/Papers/aaai2014_mirage.pdf.

O'Neill Z., Eisenhower B. 2013. Leveraging the analysis of parametric uncertainty for building energy model calibration. *Building Simulation* 6(4): 365-377.

Ortiga J., Bruno J. C., Coronas A. 2013. Operational optimisation of a complex trigeneration system connected to a district heating and cooling network. *Applied Thermal Engineering* 50(2): 1536-1542.

Ortiga J., Bruno J. C., Coronas A., Grossman I. E. 2007. Review of optimization models for the design of polygeneration systems in district heating and cooling networks. *Computer Aided Chemical Engineering* 24: 1121-1126.

Ortiga J., Bruno J.C., Coronas A. 2013. Operational optimisation of a complex trigeneration system connected to a district heating and cooling network. *Applied Thermal Engineering* 50(2): 1536–1542.

Ozgener L., Hepbasli A., Dincer I. 2005. Energy and exergy analysis of geothermal district heating systems: an application. *Building and Environment* 40(10): 1309-1322.

Ozgener L., Hepbasli A., Dincer I. 2006. Performance investigation of two geothermal district heating systems for building applications: Energy analysis. *Energy and Buildings* 38(4): 286-292.

Pak P. S., Suzuki Y. 1997. Exergetic evaluation of gas turbine cogeneration systems for district heating and cooling. *International Journal of Energy Research* 21(3): 209-220.

Paksoy H. O., Andersson O., Abaci S., Evliya H., Turgut B. 2000. Heating and cooling of a hospital using solar energy coupled with seasonal thermal energy storage in an aquifer. *Renewable Energy* 19(1–2): 117-122.

Panwar N.L., S.C. Kaushik, and S. Kothari. 2011. Role of renewable energy sources in environmental protection: A review. *Renewable and Sustainable Energy Reviews* 15(3): 1513-1524.

Park G.J., Lee T.H., Lee K. H., Hwang K.H. 2006. Robust design: An overview. *AIAA journal* 44(1): 181-191.

Pascoal M. M. B., Resende M. 2014. The minmax regret robust shortest path problem in a finite multi-scenario model. *Applied Mathematics and Computation* 241: 88-111.

Paté-Cornell M. E. 1996. Uncertainties in risk analysis: Six levels of treatment. *Reliability Engineering & System Safety* 54(2): 95-111.

Pettersen T. D. 1994. Variation of energy consumption in dwellings due to climate, building and inhabitants. *Energy and Buildings* 21(3): 209-218.

Poeuf P., Senejean B., Ladaurade C. 2010. District cooling system: the most efficient system for urban application. *Sustainable refrigeration and heat pump technology conference*, Sweden.

Prada A., Cappelletti F., Baggio P., Gasparella A. 2014. On the effect of material uncertainties in envelope heat transfer simulations. *Energy and Buildings* 71: 53-60.

Qatar cool. 2010. Qatar district cooling company Qatar cool. http://www.districtenergy.org/assets/pdfs/2010AnnualConference/PROCEEDINGS/Plenaries-AND-Keynote/KHATIB-QATAR-COOL-PlenaryREV1.pdf.

Quan S., Li Q., Augenbroe G., Brown J., Yang P.J. 2015. Urban Data and Building Energy Modeling: A GIS-Based Urban Building Energy Modeling System Using the Urban-EPC Engine. In *Planning Support Systems and Smart Cities*: 447-469. Springer International Publishing.

Quantile-quantile plot. 1997. http://citeseerx.ist.psu.edu/viewdoc/download?doi=10.1.1.217.7873&rep=rep1&type=pdf.

Raftery P., Lee E., Webster T., Hoyt T., Bauman F. 2014. Effects of Furniture and Contents on Peak Cooling Load. *Energy and Buildings* 85: 445-457.

Renewables in district heating and cooling. http://www.localpower.org/documents/reporto_ehp_renewablesandde.pdf.

Rentizelas A., Tatsiopoulos I., Tolis A. 2009. An optimization model for multi-biomass tri-generation energy supply. *Biomass and Bioenergy* 33(2): 223-233.

Rezaee R., Brown J., Augenbroe G. 2014. Building Energy Performance Estimation in Early Design Decisions: Quantification of Uncertainty and Assessment of Confidence. *Construction Research Congress*: 2195-2204.

Rezaie B., Rosen M. A. 2012. District heating and cooling: Review of technology and potential enhancements. *Applied Energy* 93: 2-10.

Rodriguez-Aumente P. A., Rodriguez-Hidalgo M. d. C., Nogueira J. I., Lecuona A., Venegas M. d. C. District heating and cooling for business buildings in Madrid. *Applied Thermal Engineering* 50 (2): 1496–1503.

Rosen M. A., Le M. N., Dincer I. 2005. Efficiency analysis of a cogeneration and district energy system. *Applied Thermal Engineering* 25(1): 147-159.

Rudoy W., Cuba J. F. 1979. Cooling and heating load calculation manual. American Society of Heating, Refrigerating and Air-Conditioning Engineers.

Rybach L., Sanner B. 2000. Ground source heat pump systems, the European experience. *GHC Bulletin* 21: 16-26.

Sakawa M. Matsui T. 2013. Fuzzy multiobjective nonlinear operation planning in district heating and cooling plants. *Fuzzy Sets and Systems* 231: 58-69.

Sakawa M., Kato K., Ushiro S. 2001. Cooling load prediction in a district heating and cooling system through simplified robust filter and multilayered neural network. *Applied Artificial Intelligence: An International Journal* 15(7): 633-643.

Sakawa M., Kato K., Ushiro S. 2002. Operational planning of district heating and cooling plants through genetic algorithms for mixed 0–1 linear programming. *European Journal of Operational Research* 137 (3): 677-687.

Sakawa M., Kato K., Ushiro S., Inaoka M. 2001. Operation planning of district heating and cooling plants using genetic algorithms for mixed integer programming. *Applied Soft Computing* 1(2): 139-150.

Sakawa M., Kato K., Ushiro S., Inaoka M. 2003. An Interactive Fuzzy Satisficing Method for Multiobjective Operation Planning in District Heating and Cooling Plants through Genetic Algorithms for Nonlinear 0-1 Programming. *Studies in Fuzziness and Soft Computing* 126: 235-249.

Seeley R.S. 1996. District cooling gets hot. *Mechanical Engineering* 118(7): 82-82.

Shimoda Y., Tomoji N., Naoaki I., Minoru M. 2008. Verification of energy efficiency of district heating and cooling system by simulation considering design and operation parameters. *Building and Environment* 43(4): 569-577.

Shou Q.Y, Chen R.D. 2003. Study Foreign Experience to Advance China's District Heating and Cooling. *Fluid Machinery* 31(11): 47-50. (In Chinese).

Shu H., Duanmu L., Zhang C., Zhu Y. 2010. Study on the decision-making of district cooling and heating systems by means of value engineering. *Renewable Energy* 35(9): 1929-1939.

Skagestad B., Mildenstein P. 2002. District heating and cooling connection handbook. Netherlands Agency for Energy and the Environment.

Söderman J. 2007. Optimisation of structure and operation of district cooling networks in urban regions. *Applied Thermal Engineering* 27(16): 2665-2676.

Söderman J., Pettersson F. 2006. Structural and operational optimisation of distributed energy systems. *Applied Thermal Engineering* 26(13): 1400-1408.

Stapelberg R. F. 2009. Handbook of reliability, availability, maintainability and safety in engineering design: Springer.

Sun Y. 2014. Closing the Building Energy Performance Gap by Improving Our Predictions. PhD Dissertaiton, Georgia Institute of Technology, United States.

Sun Y., Gu L., Wu C., Augenbroe G. 2014. Exploring HVAC system sizing under uncertainty. *Energy and Buildings* 81: 243-252.

Tanaka H., Tomita T., Okumiya M. 2000. Feasibility study of a district energy system with seasobal water thermal storage. *Solar Energy* 69(6): 535-547.

Tian W. 2013. A review of sensitivity analysis methods in building energy analysis. *Renewable and Sustainable Energy Reviews* 20: 411-419.

Tibshirani R. 1996. Regression shrinkage and selection via the lasso. *Journal of the Royal Statistical Society. Series B (Methodological)*: 267-288.

Torikoshi K., Nakazawa Y., Asano H. 1992. Fluid characteristics of ice–water two-phase flow in pipes. *Proceedings of 26th Japanese Joint Conference on SHASE and JSRAE:*185-188.

Transient System Simulation Tool. 2015. http://www.trnsys.com/.

Udomsri S., Martin A. R., Martin V. 2011. Thermally driven cooling coupled with municipal solid waste-fired power plant: Application of combined heat, cooling and power in tropical urban areas. *Applied Energy* 88(5): 1532-1542.

Uno Y., Shimoda Y. 2012. Energy saving potential of cooperative management between DHC plant and building HVAC system. *Energy and Buildings* 55: 631-636.

Wald A. 1949. Statistical decision functions. *The Annals of Mathematical Statistics* 20(2): 165-205.

Walker W. E., Harremo ës P., Rotmans J., van der Sluijs J. P., van Asselt M. B., Janssen P., Krayer von Krauss M. P. 2003. Defining uncertainty: a conceptual basis for uncertainty management in model-based decision support. *Integrated assessment* 4(1): 5-17.

Wang S. 1998. Dynamic simulation of a building central chilling system and evaluation of EMCS on-line control strategies. *Building and Environment* 33(1): 1-20.

Wang S., Xue X., Yan C. 2014. Building power demand response methods toward smart grid. *HVAC&R Research* 20(6): 665-687.

Wetterlund E., Söderström M. 2010. Biomass gasification in district heating systems–the effect of economic energy policies. *Applied Energy* 87(9): 2914-2922.

Wikipedia. 2015. Pumped-storage hydroelectricity. https://en.wikipedia.org/wiki/Pumped-storage_hydroelectricity.

Woradechjumroen D., Yu Y., Li H., Yu D., Yang H. 2014. Analysis of HVAC system oversizing in commercial buildings through field measurements. *Energy and Buildings* 69: 131-143.

Wu D., Wang R. 2006. Combined cooling, heating and power: a review. *Progress in Energy and Combustion Science* 32(5): 459-495.

Xue X., Wang S., Sun Y., Xiao F. 2014. An interactive building power demand management strategy for facilitating smart grid optimization. *Applied Energy* 116: 297-310.

Yik F.W.H., Burnett J., Prescott I. 2001. Predicting air-conditioning energy consumption of a group of buildings using different heat rejection methods. *Energy and Buildings* 33(2): 151-166.

Yıldız Y., Arsan Z. D. 2011. Identification of the building parameters that influence heating and cooling energy loads for apartment buildings in hot-humid climates. *Energy* 36(7): 4287-4296.

Yokoyama R., Fujiwara K., Ohkura M., Wakui T. 2014. A revised method for robust optimal design of energy supply systems based on minimax regret criterion. *Energy conversion and management* 84: 196-208.

Yokoyama R., Ito K. 2002. Optimal design of energy supply systems based on relative robustness criterion. *Energy conversion and management* 43(4): 499-514.

Zafar S. 2014. District Cooling Perspectives for the Middle East. http://www.ecomena.org/tag/integrated-district-cooling-plant/.

Zang C., Friswell M., Mottershead J. 2005. A review of robust optimal design and its application in dynamics. *Computers & Structures* 83(4): 315-326.

Zhang T.T., Tan Y.F., Bai L. 2012. Numerical simulation of a new district cooling system in cogeneration plants. *Energy Procedia* 14: 855-860.

Zhang Y., Augenbroe G. 2014. Right-sizing a residential photovoltaic system under the influence of demand response programs and in the presence of sysetm uncertainties. *2014 ASHRAE/IBPSA-USA Building Simulation Conference,* September 10-12, Atlanta, GA, United States.

Zhang Y., Oneil Z., Wagner T., Augenbroe G. 2013. An inverse model with uncertainty quantification to estimate the energy performance of an office building. *Proceedings of 13th international building performance simulation association conference*: 614-621.

Zhao P., Suryanarayanan S., Simões M. G. 2013. An energy management system for building structures using a multi-agent decision-making control methodology. *Industry Applications, IEEE Transactions* 49(1): 322-330.